Protein binding contrast agents for potential use in MRI

Nicola C. Thompson

Protein Binding Contrast Agents For Potential Use In MRI

Nicola C. Thompson

Department of Chemistry

University of Durham

A thesis submitted in part-fulfilment for the degree of Doctor of Philosophy

January 2005

Abstract

Protein Binding Contrast Agents for potential use in MRI

Heptadentate ligands form lanthanide (III) complexes, which allow an increased hydration state about the metal centre, resulting in an improvement in the relaxivity of the contrast agents administered. A series of analogues based upon the compound **(2)** was pursued, incorporating aromatic functionalised groups, consequently increasing the hydrophobicity of the complexes. The aryl moiety significantly enhances the binding to human serum albumin (HSA), consequently improving the observed relaxivity. Relaxivity enhancements were seen for each of the carboxylate complexes in the presence of increasing serum protein concentrations.

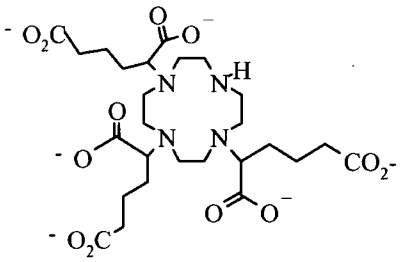

Chemical structure of the ligand aDO3A (2)

The phosphonate analogue of the aDO3A ligand **(2)** was identified as a target and synthesised as a key ligand whose lanthanide (III) complex possesses a higher peripheral negative charge, repelling the attraction towards anions, potentially maintaining higher relaxivity values in serum solutions.

A trifluoromethanesulphonamide moiety was introduced into the aDO3A moiety that exhibited a high binding affinity to human serum albumin resulting in high values for the observed relaxivity.

The solution structures of the diastereoisomers for the model albumin binding complex (S)-[Eu-(EOB)-(DTPA)]$^{2-}$ were analysed by ^{1}H NMR, CD and CPL spectroscopy. The major species observed were found to possess similar ^{1}H NMR paramagnetic shifts and emission spectra, consistent with a 9-coordinate structure involving one bound water molecule.

Declaration

The work described herein was carried out in the Department of Chemistry, University of Durham between October 2001 and December 2004. All the work is my own unless otherwise stated and no part of it has been submitted for a degree at this or any other university.

Statement of Copyright

Acknowledgments

I would like to thank my supervisor Professor David Parker, firstly, for his guidance and advice, and secondly for his insight and helpful suggestions, especially when everything seemed to go wrong.

To all my friends in the analytical department; Dr. Alan Kenwright, Ian McKeag and Catherine Heffernan, for their advice, cups of tea, tissues and making sense of my swiggly spectra; Dr. Mike Jones and Lara Turner for their assistance with mass spectrometry, source of gossip and their contribution towards my employment; Lenny Lauchlan for help with HPLC analysis; Jarka Dostal for CHN analysis and Dr. Tony Royston for NMRD work.

Special thanks to all the past and present PhD students and Post Docs of CG27; esepcailly those present in earlier times whose advice with synthetic chemistry, especially column chromatography was indispensable, to the girls for their laughs, tears and friendship; and everyone else for the fun, gossip and cakes we have shared; Paul Atkinson, Alex Badari, Gabriella Bobba, Yann Bretonnière, Aileen Congreve, Rachel Dickins, Elisa Elemento, Juan Carlos Frias, David Fulton, Filip Kielar, Mark O'Halloran, Robek Pal, Robert Poole, Horst Puschmann, Kanthi Senanayke and Simon Welsh.

To Aileen Congreve for the headaches she gave in developing something that bound so well to protein! and for all her help and assistance with submission of this thesis

Thank you to all the other people in the department who have made me smile over the last three years and making chemistry enjoyable.

The submission of this thesis was not only a personal academic mission but also a family affair, special thanks to my parents for their never failing support, love and encouragement throughout and for insisting the greatest gift I could give myself was an education.

Finally, a special thank you for Neal, for his unconditional love throughout the last four years; I thank you for keeping me sane and for never losing faith in me.

Dedicated in Loving Memory of my Brother Steven,

For never really leaving my side, you have given me the strength, courage and opportunity to persevere whilst watching down on me from Heaven.

Theres a lot of comfort in the thought
That sorrow, grief and woe
Are sent into our lives sometimes
To help our soles to grow.

Helen Steiner Rice

Abbreviations

aDO3A	1,4,7,10-tetraazacyclododecane-1,4,7-tri(adipic acid)
BOC	*tert*-butoxycarbonyl
BOM	benzyloxymethyl
CD	circular dichroism
CPL	circular polarised luminescence
CT	computed tomography
COSY	correlation spectroscopy
cyclen	1,4,7,10-tetraazacyclododecane
DCM	dichloromethane
DO3A	1,4,7,10-tetraazacyclododecane-1,4,7-triacetate
DOTA	1,4,7,10-tetraazacyclododecane-1,4,7,10-tetraacetate
DOTP	1,4,7,10-tetraazacyclododecane-1,4,7,10-tetrakis(methylene phosphonate)
DTPA	diethylenetriaminepentaacetate
DTPA-BMA	diethylenetriaminepentaacetate-bis(methylamide)
EDC	1-(3-dimethylaminopropyl)-3-ethylcarbodiimide
EOB-DTPA	ethoxybenzyl diethylenetriaminepentaacetate
EPR	electron paramagnetic resonance
Et	ethyl
EtOAc	ethyl acetate
EtOH	ethanol
Gd-BOPTA	gadobenate dimeglumine
HSA	human serum albumin
Hz	hertz
I.R.	infra red
ISC	intersystem crossing
Ln	lanthanide
m.p.	melting point
MeCN	acetonitrile
MeOH	methanol
MP-2269	4-pentyl-bicyclo[2.2.2]octan-1-carboxyl-di-L-

	aspartyllysine-DTPA
MRI	Magnetic Resonance Imaging
MS	mass spectrometry
MS-325	diphenylcyclohexyl phosphodiester-Gd-DTPA
NMR	Nuclear Magnetic Resonance
NMRD	Nuclear Magnetic Relaxation Dispersion
PCTA-[12]	3,6,9,15-tetraazabicyclo[9.3.1]pentadeca-1(15),11,13-triene-3,6,9-triacetic acid
PEG	poly(ethylene glycol)
q	number of primary coordination sphere water molecules
R_{1p}	relaxation rate caused by paramagnetic species
r_{1p}	relaxivity caused by paramagnetic species
R_f	retention factor
RIME	Receptor Induced Magnetisation Enhancement
T_1	longitudinal relaxation time
^{t}Bu	*tert*-butyl
TETA	1,4,8,11-tetraazacyclotetradecane-1,4,8,11-tetraacetate
TFA	trifluoroacetic acid
THF	tetrahydrofuran
TLC	Thin Layer Chromatography
tosyl	*p*-toluenesulfonyl
Tren Me 3,2 HOPO	*N,N',N''*-tris[(3-hydroxy-1-methyl-2-oxo-1,2-didehydro pyrid-4-yl)-carboxamidoethyl]amine
UV	ultra violet
τ_R	rotational correlation time/ reorientational correlation time

Table of Contents

Chapter 1

Introduction

Introduction

In radiology, Magnetic Resonance Imaging[1,2,3] MRI, has revolutionised the diagnosis of many diseases. As a consequence of its rapid development it has become a routine medical procedure. The technique would have been of lesser importance had it not been for the significant advances in contrast agent media, which have considerably improved the quality and utility of the images obtained. In the early days of contrast enhancement it was estimated less than 10% of all MRI procedures would require contrast agent enhancement. This figure was greatly underestimated, as realistically, it is now estimated that over 35% of examinations employ contrasting media.[4]

Gadolinium (III) is a paramagnetic metal ion commonly used in MRI contrast agents due to its unique magnetic properties. It possesses seven unpaired *f* electrons, and has a relatively slow electron spin relaxation rate, resulting in almost idyllic magnetic properties for use as a contrast agent.[5] However, the paramagnetic gadolinium (III) ion is extremely toxic at concentrations required for MRI and therefore cannot be used directly as the free aqua ion. For this reason it must be administered in the form of a stable complex, unable to release metal ions before excretion from the body.[6]

1.1 Contrast Agents

Polyaminocarboxylic ligands have proved successful in forming Gd (III) complexes with efficient relaxivity properties, high thermodynamic stability and acceptable toxicity.[6,7] There are four that are commonly used in the clinic see Figure 1.1.[1,2,4]. The ligands of these chelates belong to two different types of structure: acyclic (open chain) compounds and macrocyclic compounds. $[Gd(DTPA)]^{2-}$ (Gadopentetate, Magnevist), is an acyclic compound and was the first contrast agent permitted for clinical use. The first macrocyclic agent $[Gd(DOTA)]^{-}$ (DOTAREM), followed, which offered increased stability due to more effective capsulation of the metal ion by the ligand, resulting in a decrease in entropy upon metal complexation.[1] The ionic characteristics of both compounds caused undesirable side effects in some patients, including painful intravenous

administration and oedema.[8] The development of non-ionic open chain metal complexes was analogous to that of non-ionic macrocyclic chelates, two of which were later successfully launched in the clinic, [Gd(DTPA-BMA)] (OMNISCAN) and [GdHPDO3A] (PROHANCE). The neutral complexes offered reduced osmotic potential, resulting in fewer side effects. These compounds are the preferred choice for applications requiring larger doses. All four chelates are examples of non-specific, extravascular, extracellular compounds that are rapidly excreted by the kidneys. They are all well established and have been used to date in over 40 million scans.[9]

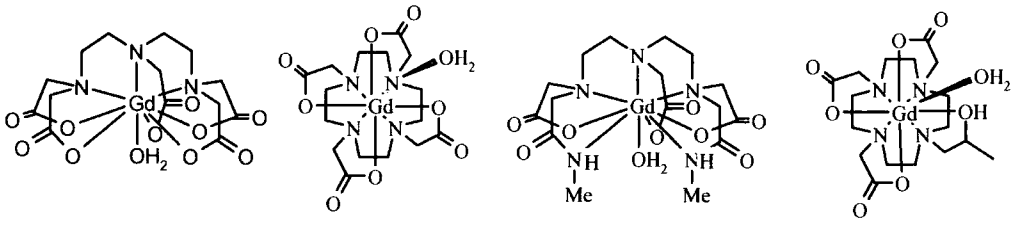

1 2 3 4

Figure 1.1: Gadolinium based contrast agents currently approved for use in MRI: (1) $[Gd(DTPA)(H_2O)]^{2-}$ (Magnevist™), (2) $[Gd(DOTA)(H_2O)]^{-}$ (Dotarem™), (3) $[Gd(DTPA\text{-}BMA)(H_2O)]$ (Omniscan™), (4) $[Gd(HP\text{-}DO3A)(H_2O)]$ (ProHance™).

1.2 Relaxation Theory

A Gd (III) complex induces an increase in the longitudinal and transverse relaxation rates, $1/T_1$ and $1/T_2$, respective of solvent nuclei. The research groups of Solomon, Bloembergen and Morgan developed the general theory regarding solvent nuclear relaxation, in the presence of paramagnetic substances.[1,2,3] The efficiency of the paramagnetic substance to enhance the relaxation rate of water protons is known as the relaxivity, r_1, of the agent. This is the proton relaxation rate enhancement in the presence of the paramagnetic agent compared to a diamagnetic environment, normalised to the concentration of the paramagnetic agent.[9] In the context of MRI contrast agents, the term relaxivity commonly refers to the longitudinal proton relaxivity, T_1.

For an aqueous solution containing a paramagnetic complex, the relaxation enhancement of the solvent water protons is propagated through the bulk solvent, following the exchange of water molecules that are directly attached to the

gadolinium centre.[10] This mechanism is depicted as the inner sphere contribution to the overall relaxivity, see Figure 1.2.

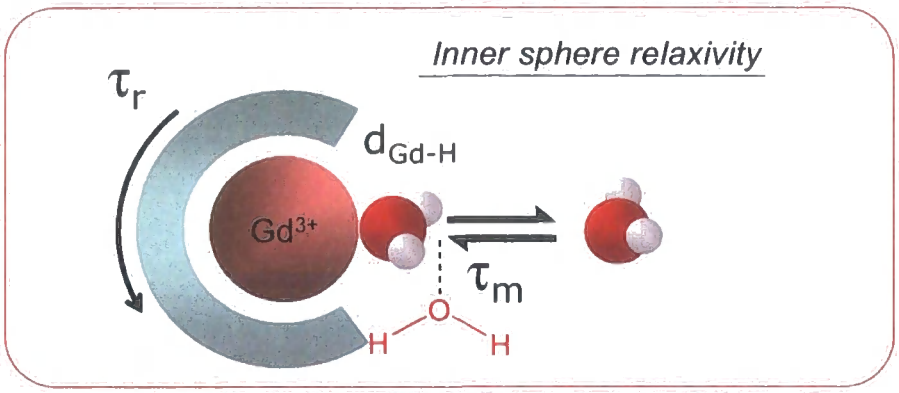

Figure 1.2: Schematic representation of a Gd (III) chelate with one inner sphere water molecule, surrounded by bulk water; τ_R refers to the rotational correlation time of the molecule, τ_m the residence time of the inner sphere water molecule and Gd-H the distance between the coordinated water proton and the Gd electron spin.

It will be seen from equations 1.2 and 1.3 below, that the inner sphere contribution is also influenced by correlation times involving rotation (τ_R), proton exchange (τ_m), and the electronic relaxation (τ_s).[1,2,10] Solvent molecules of the bulk also experience the paramagnetic effect as they diffuse in the surroundings of the paramagnetic centre. The effect of this random translational diffusion is defined as outer sphere relaxation.[7] The total paramagnetic relaxation rate enhancement due to the paramagnetic agent is therefore given in equation 1.1, where the subscripts 'IS', 'OS' and 'SS' refer to the inner, outer and second sphere respectively.

$$\left(\frac{1}{T_{1,p}}\right)=\left(\frac{1}{T_{1,p}}\right)^{IS}+\left(\frac{1}{T_{1,p}}\right)^{OS}+\left(\frac{1}{T_{1,p}}\right)^{SS} \qquad (1.1)$$

There are three different types of water (inner, second and outer sphere), these are pictorially represented in the molecular dynamic simulation (Figure 1.3), obtained for [Gd(DOTA)]$^-$ in aqueous solution.[10]

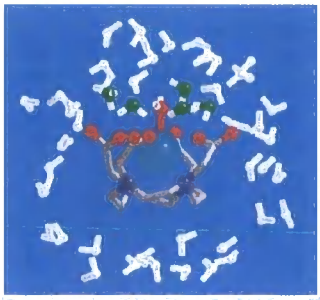

Figure 1.3: Three different types of water molecules around a Gd (III) complex as obtained by molecular dynamics simulation of $[Gd(DOTA)(H_2O)]^-$ in aqueous solution. The *inner sphere* water is directly coordinated to the metal (the oxygen is red). *Second sphere* water molecules are on the hydrophilic side of the complex, close to carboxylate groups (their oxygens represented as green balls). *Outer sphere* or *bulk water* molecules have no preferential orientation (shown in white).[10]

1.3 Inner Sphere Relaxation

The inner sphere term represents the major contribution to the overall proton relaxation rate according to the interpretations of the theory of Solomon, Bloembergen and Morgan (SBM theory). A more detailed explanation of this theory is well documented in the literature.[1,2,3,8]

For currently used monomeric gadolinium based contrast agents, the outer and inner sphere relaxation mechanisms contribute roughly the same amount to the observed proton relaxivity at the imaging fields used in MRI of 20-60 MHz.[8] The inner sphere relaxation mechanism is described in basic terms in Equations 1.2-1.3, where c is the molal concentration, q is the number of bound water nuclei per Gd ion (hydration number), $1/T_{1m}$ is the longitudinal proton relaxation rate, τ_m is the lifetime of a water molecule in the inner sphere of the complex, τ_R is the reorientational correlation time of the metal proton vector, and τ_s the longitudinal spin relaxation time of the metal ion.

$$\left(\frac{1}{T_1}\right) = \frac{cq}{55.5}\left(\frac{1}{T_{1m} + \tau_m}\right) \qquad (1.2)$$

$$\frac{1}{\tau_c} = \frac{1}{\tau_R} + \frac{1}{\tau_m} + \frac{1}{\tau_s} \qquad (1.3)$$

The equations show that through appropriate modification of the inner sphere term, the relaxivity achievable can be greatly increased, compared to the outer sphere, which is more difficult to optimise. However, increases in hydration states are often accompanied by a decrease in the thermodynamic and kinetic stability of the complex with respect to dissociation, limiting the choice of ligand to either heptadentate (q=2) or in some cases hexadentate systems (q=3). The equations show that by increasing the hydration number from one to two, it is possible to double the observed relaxivity. The Solomon-Bloembergen-Morgan theory predicts when all three influencing factors such as rotation, electron paramagnetic relaxation and water exchange are simultaneously optimised, maximum proton relaxivities for Gd (III) complexes in the order of 100 $mM^{-1}s^{-1}$ can be achieved.[1,10] These are very high compared to the measured values of relaxivity obtained for currently available agents of 4-5 $mM^{-1}s^{-1}$.

1.4 Heptadentate Ligands

1.4.1 [Gd(DO3A)]

The non-ionic complex [Gd(DO3A)][11] (Gadovist™) (Figure 1.4) is an analogue of $[Gd(DOTA)]^-$ missing one of the three carboxylates and was the first of such ligands containing an increased hydration state to be reported.[1]

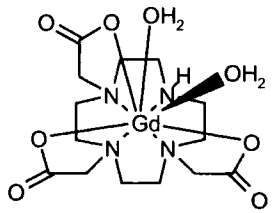

Figure 1.4: Chemical structure of [Gd(DO3A)] (Gadovist™)

The crystal structure for [Gd(DO3A)] revealed the ligand was bound around the metal in heptadentate fashion, with two solvent water molecules occupying the

remaining coordination sites.[12] Similarly to the parent complex, [Gd(DOTA)]$^-$, [Gd(DO3A)] was found to distribute rapidly into extracellular space and was then eliminated by glomerular filtration; no particular protein binding was displayed.[13] An increased hydration state led to the predicted gain in relaxivity of 4.8 $mM^{-1}s^{-1}$ (20 MHz, 313 K, pH 7.3), compared to the monomeric parent with a value of 3.5 $mM^{-1}s^{-1}$ (20 MHz, 313 K, pH 7.3).[1,8] This value was much lower than expected for such a heptadentate system. This is explained by the strong tendency of the [Gd(DO3A)] ligand to readily bind the endogenous anion, hydrogencarbonate, which *in vivo* is present in large concentrations. The carbonate anion binds in a bidentate fashion displacing two water molecules forming a ternary complex, the formation of which is clearly indicated by a reduction in the measured relaxivity. Despite the disappointing results [Gd(DO3A)], has been frequently functionalised.

1.4.2 Derivatives of [Gd(DO3A)]

The derivative [Gd(DO3MA)] (Figure 1.5)[14] incorporates three methyl acetic pendant arms, encompassing the metal ion in similar heptadentate fashion. Stability studies confirm the complex has added thermodynamic and kinetic inertness compared to the parent, resulting from the increased rigidity obtained from addition of the α-methyl groups. The water exchange time, τ_m of 68 ns is almost an optimum value for [Gd(DO3MA)]. This is much quicker than the parent analogue [Gd(DO3A)], for which τ_m is 180 ns. This should yield a greater relaxivity value, yet the measured value reported of 4.4 $mM^{-1}s^{-1}$ for [Gd(DO3MA)] was actually slightly less than for the parent complex.

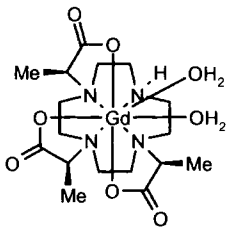

Figure 1.5: Chemical structure of [Gd(DO3MA)]

Parker *et al*[15] reported the triamide derivative, [Gd(DO3A)-Ala] and its unusual interaction with hydrogen carbonate. Under ambient conditions water was prevented from directly binding to the paramagnetic centre, whereas in acidic

media the anion is protonated and displaced by a water molecule, resulting in an increase in the observed relaxivity. This behaviour augurs well for the development of lanthanide complexes that respond to small changes in pH in biological fluids.[15,16] Ternary complexes have shown to exist between anions such as fluoride, phosphate and carbonate.[17] Reversible displacement of metal bound water molecules at a co-ordinatively unsaturated, cationic lanthanide centres is signalled by increases in luminescence intensity or emission lifetime, for the emissive lanthanide ion.[18]

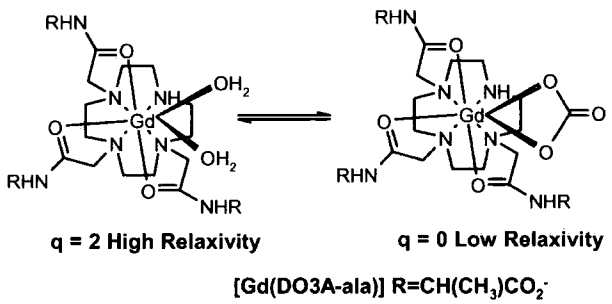

Figure 1.6: Diagram showing intramolecular binding of [Gd(DO3A-ala)].[15]

The non-covalent interaction between a metal complex and a protein can also lead to the formation of a ternary complex; this problem has been noted for some heptadentate gadolinium complexes. The displacement of ligated water molecules from the first coordination sphere of the metal ion by exogenous molecules or ions is important as it can potentially lower relaxivity. Aime, Parker and co-workers reported two novel heptadentate chelates based upon [Gd(DO3A)] that incorporated p-bromobenzyl and p-phosphonatomethylbenzanilido substituents, for the interaction with macromolecules (Figure 1.7).[19]

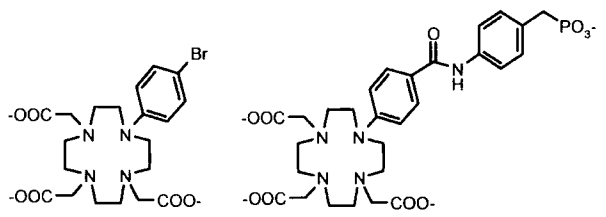

Figure 1.7: [Gd(DO3A)] incorporating p-bromobenzyl & p-phosphonatomethylbenzanilido groups[19]

Upon binding to human serum albumin the expected relaxation was not observed owing to the displacement of two water molecules from the inner sphere, by a donor atom (likely to be a carboxylate group) on the protein and possibly the phosphate anions present from the buffer solution. Moreover, it should be noted that no ternary complex formation was observed in the presence of the macromolecular substrate, poly-β-cyclodextrin.[19]

1.4.3 Pyridine - containing triaza macrocyclic ligands

In earlier work, Aime and co-workers reported the synthesis of 3,6,10-16-tetraazabicyclo[10.3.1]hexadeca-1(16),12,14-triene (PCTA), a novel heptadentate ligand involving the insertion of a pyridine moiety in the macrocyclic ring, with three carboxymethyl arms (Figure 1.8).[20] Competition experiments with the europium (III) complex confirmed the complex had good thermodynamic stability even in acidic media. The acid promoted dissociation pathway below pH 3, was found to be less rapid than for $[Gd(DTPA)]^{2-}$, suggesting the complex was suitable for use *in vivo*. This prompted the synthesis of the gadolinium (III) analogue in order to assess its use as a MRI contrast agent. The relaxivity was reported as 6.3 $mM^{-1}s^{-1}$ (20 MHz, 298 K), approximately 35% higher than $[Gd(DOTA)]^-$ and similar to the value reported for [Gd(DO3A)], resulting from increased hydration and optimised water exchange lifetimes. The structural, dynamic, thermodynamic and relaxometric properties of this novel complex provided the backbone for the research of new neutral chelates.

The pyridine-containing triaza macrocycle triacetate ligand (PCTA), and its complexation properties to alkaline earth metals and transition metal cations was first reported by Stetter *et al.*[21] The synthesis and characterisation of the PCTA ligand with various lanthanides were later investigated by Aime and co-workers[22] (Figure 1.8), involving a series of macrocyclic ligands, including 13 and 14 membered ring compounds.[22]

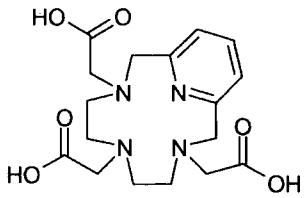

Figure 1.8: The ligand PCTA containing a pyridine moiety in the macrocyclic ring and three acetic acid arms.

The PCTA ligand acts as a heptadentate chelator towards the metal ion allowing two water molecules to complete coordination. The di-aqua hydration state was confirmed by examination of the luminescence lifetimes of the Tb (III) and Eu (III) complexes.[23] The longitudinal proton relaxivity exhibited for [Gd(PCTA)] is reported as being 5.1 $mM^{-1}s^{-1}$ (20 MHz, 313 K, pH 7), significantly higher than that of $[Gd(DOTA)]^-$. The pyridine based system is reported to have a shorter electronic relaxation time, τ_{s0} with respect to $[Gd(DOTA)]^-$, resulting in a shorter water exchange time, τ_M 70 ns (298 K), which consequently does not limit the relaxivity at low fields ($\tau_M < T_{1M}$), unlike Gd (III) chelates currently in clinical use. Stability studies showed the complex had similar thermodynamic and kinetic properties to [Gd(DO3A)], therefore the release of highly toxic gadolinium ions *in vivo* is reduced. It is expected that the pyridine moiety increases the stereochemical rigidity of the complex and also allows functionalisation towards specific targets.

Hovland *et al*[24] reported the introduction of a lipophilic moiety ($OC_{12}H_{25}$) at the 4 position of the pyridine unit of [GdPCTA]-[12], resulting in micelle aggregation, due to the amphiphilic structure of the complex in aqueous solution. Micellar formation increases the rotational correlation time, τ_R due to an increased molecular volume that should result in an increased relaxivity. As micellar formation is concentration dependent, greater relaxivity values were reported when the critical micelle concentration, (CMC) was 0.15 mM (298 K). At higher CMC values, the T_1 relaxivity reaches a plateau of 29.2 $mM^{-1}s^{-1}$, whereas at lower CMC concentrations of 0.05 mM the lowest relaxivity value measured was 11.9 $mM^{-1}s^{-1}$ (20 MHz, 298 K, pH 7). This is somewhat higher than the value reported for monomeric [Gd(PCTA)]-[12] system of 6.9 $mM^{-1}s^{-1}$ (20 MHz, 298 K, pH 7), which has a similar molecular volume.

The related complex [Gd(PCTP)]-[12] bears three bulky methylenephosphonic arms (Figure 1.9), with respect to the carboxylate compound [Gd(PCTA)]-[12]; this results in increased steric hindrance causing a reduction in the hydration state.[25]

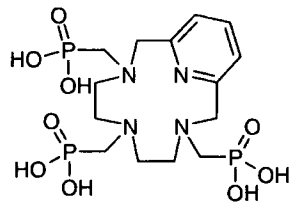

Figure 1.9: Chemical structure of ligand PCTP-[12]

However, this is not accompanied by a reduction in the observed relaxivity. The reported relaxivity value is actually slightly higher at 5.3 $mM^{-1}s^{-1}$ for [Gd(PCTP)]-[12], compared to 5.1 $mM^{-1}s^{-1}$ (20 MHz, 298 K, pH 7.5) for the carboxylate analogue. This is explained by the formation of a more well defined second coordination sphere for the phosphonate species.

The complex [Gd(PCP2A)] consists of two acetic arms and one methylenephosphonic arm, as reported by Aime *et al.*[26] Again, the ligand is arranged in heptadentate fashion allowing coordination of two inner sphere water molecules. The steric hindrance of only one phosphonate group is not so great to prevent the water molecules from coordinating to the metal centre; it also has the advantage of creating second sphere effects. These arise from the formation of hydrogen bonds between solvent molecules and the oxygens of the methylenephosphonic groups, which may contribute to an increased relaxivity. The relaxivity of [Gd(PCP2A)] was reported as 8.3 $mM^{-1}s^{-1}$ (20 MHz, 298 K, pH 7), which was independent of pH across the range 3 - 9.5. Below pH 3.0 an increase in relaxivity was observed, which was explained by the possible increase in hydration associated with protonation of the phosphonate group. Similarly to some other di-aqua complexes, ternary formation with dissolved carbonate ions was observed at basic pH, accompanied by a reduction in relaxivity. [Gd(PCP2A)] was suggested to be sufficiently stable for use *in vivo*. ^{17}O NMR determinations of water exchange revealed a fast exchange mechanism for the complex, an important pre-requisite for

coupling to macromolecular substrates.

1.4.4 Heptadentate tripodal ligands

The heptadentate tripodal ligand H_3tpaa containing three pyridinecarboxylate binding units was reported by Bretonnière *et al*[27] (Figure 1.10), with a relaxivity value of 13.3 $mM^{-1}s^{-1}$ (60 MHz, 298 K).

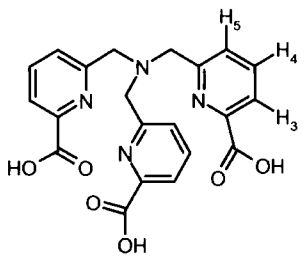

Figure 1.10: Chemical structure of the tripodal ligand H_3tpaa[27]

This was significantly higher than the value obtained for [Gd(DO3A)] or [Gd(PCTA)]-[12] of 6.1 $mM^{-1}s^{-1}$ and 6.9 $mM^{-1}s^{-1}$ respectively. Unfortunately, the complex is only partially soluble in water; the introduction of hydrophilic substituents on the pyridine rings may increase the solubility of the complex. The incorporation of hydrophobic groups on the pyridine rings may also increase the affinity of the complex towards macromolecules.

In earlier stages of contrast development, the tripodal gadolinium complex [Gd(TREN-Me-3,2-HOPO)] was reported by Xu *et al*,[28] which promised a new class of lanthanide complexes for use as contrast agents (Figure 1.11).

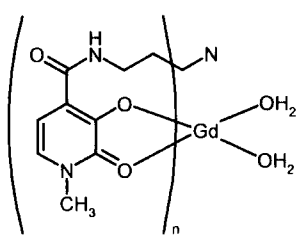

Figure 1.11: Chemical structure of [Gd(TREN-Me-3,2-HOPO)][28]

The hydroxyl-pyridinonate (HOPO) monoanions are bidentate ligands that form effective multidentate sequestering agents. The geometry imposed promotes strong chelation of metal ions in general, and of Gd (III) in particular.[28] Crystal structure analyses show the ligand binds in hexadentate fashion to the metal ion, through the hydroxypyridinone oxygens. Two inner sphere water molecules complete the octadentate coordination state of gadolinium. This is a similar state to the gadolinium aqua ion $[Gd(H_2O)_8]^{3+}$ and differs from that of the nine coordinate polyaminocarboxylate complexes.[29] Micskei *et al*[30] noted there is a relatively low energy difference between the eight and nine coordinated gadolinium energy states. As a result of octadentate binding, water exchange occurs via a rapid associative mechanism, contributing to the higher relaxivity value of the complex of 10.5 $mM^{-1}s^{-1}$ (20 MHz, 300 K). This value is approximately 2.5 times greater than $[Gd(DTPA)]^{2-}$ and can be explained due to the increased hydration state and increased molecular size, which increases the reorientational correlation time, τ_R. Ideally, the complex was reported as highly thermodynamically stable and unaffected by the presence of physiological bidentate chelators such as acetate, lactate and malonate. However, solubility problems were apparent preventing detailed magnetic characterisation and practical applicability. Consequently, there have been several reports of [Gd(TREN-Me-3,2-HOPO)] derivatives containing substituents in the TREN moiety, as well as the attachment of various HOPO chelators. Cohen and co-workers[31] synthesised and characterised three new complexes [Gd(TREN-Me-3,2-HOPOSAM)], [Gd(TREN-Me-3,2-HOPOTAM)]- and [Gd(TREN-Me-3,2-HOPOIAM)], by replacing one of the hydroxypyridinone groups with groups designed to regulate properties such as charge, solubility and stability of the resulting complex. The rapid water exchange values for complexes of [Gd(TREN-Me-3,2-HOPO)] are near optimum, ideal for obtaining maximum relaxivities from the formation of molecules with greater τ_R. Raymond and co-workers[32,33,34] reported the derivatives of [Gd(TREN-Me-3,2-HOPO)] with poly (ethyleneglycol) (PEG) groups incorporated, increasing molecular masses of the complexes to the range of 2,000 to 5,000. The polyethylene groups also had a dual purpose; they were highly water-soluble and were suggested to bind weakly to HSA across a wide pH range. However, there were concerns associated with the

rapid internal flexibility of the PEG groups.[34] The derivative [Gd(TREN-HOPO-TAM)] (Figure 1.12) has also been investigated in related work.[31]

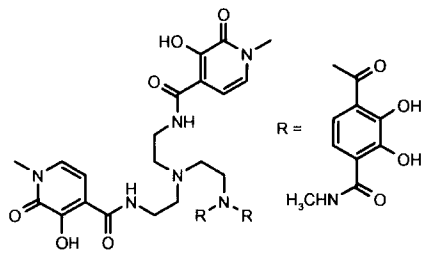

Figure 1.12: Structure of [Gd(TREN-HOPO-TAM)][31]

The complex contains two inner sphere water molecules and displays fast water exchange until PEG groups are incorporated. A reduction in the hydration number of two to one was observed for [Gd(TREN-HOPO-TAM-PEG-5000)], which is explained by partial displacement of the water molecule by the PEG oxygen donors. The longitudinal relaxivity value for [Gd(TREN-HOPO-TAM-PEG-5000)] is 9.1 $mM^{-1}s^{-1}$ (20 MHz, 298 K, pH 7.5) compared to that of the parent [Gd(TREN-HOPO-TAM)] of 8.8 $mM^{-1}s^{-1}$, which is poor considering such large increase in molecular weight and hence greater τ_R value. This is a consequence of the reduction in hydration number and the rapid internal motion of the PEG groups. In addition, it should be noted that a significant increase in water exchange rate, τ_M from 15 to 31 $\pm$ 2 ns was reported, upon addition of PEG groups.[34]

Modification of the inner sphere effect seems an obvious manner of synthesising contrast agents with increased relaxivity, yet attempts to synthesise such systems that have progressed into the clinic have failed for several reasons such as those already discussed.

In conclusion, dramatic decreases in the thermodynamic and kinetic stabilities with respect to acid or cation mediated dissociation have prevented some complexes being safe for use *in vivo*. The significant binding of the complex to endogenous anions in serum, such as phosphate or carbonate, displacing one or more of the inner sphere water molecules in ternary complexes, thus lowering relaxivity, has

been reported for many heptadentate species.[35]

According to Merbach and co-workers[8], the long water exchange lifetimes of monoaqua complexes results from the dissociative mechanism operating between the coordinated molecules and the bulk solvent. On going from octadentate ligands to heptadentate species, a different mechanism of water exchange may be expected which may result in an increased exchange rate.[36] However, for some heptadentate ligands the water exchange rates measured have been similar in magnitude to those of octadentate complexes, resulting in a quenching effect of the observed relaxivity. For some complexes designed to bind to serum albumin in a non-covalent fashion, problems associated with the removal of inner sphere waters molecules, as a result of the interaction with side chain carboxylates in Glu or Asp residues were also observed.

1. 4. 5 $[Gd(aDO3A)]^{3-}$

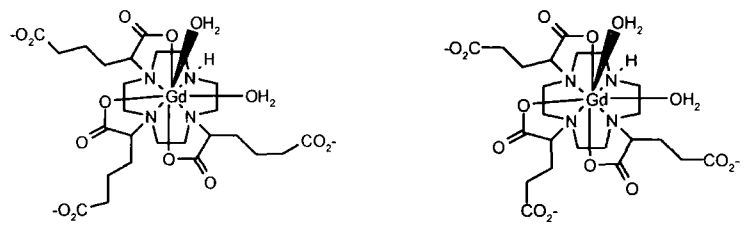

Figure 1.13: Chemical structures of $[Gd(aDO3A)]^{3-}$ and $[Gd(gDO3A)]^{3-}$ respectively

The complex [Gd(DO3MA)] was a starting point for the synthesis and characterisation of the derivatives $[Gd(aDO3A)]^{3-}$ and $[Gd(gDO3A)]^{3-}$ (Figure 1.13), reported by Parker *et al.*[37] It was hypothesised that the anionic pendant arms would inhibit the binding of bi-dentate anions such as carbonate and phosphate, retaining the two water molecules involved in the coordination of the metal ion. Luminescence studies of the europium analogues in aqueous solution at pH 7, revealed $[Gd(gDO3A)]^{3-}$ experiences intramolecular (seven ring) carboxylate ligation, displacing one of the bound waters and suppressing intramolecular binding in the pH range 4 to 7.5 (Figure 1.14).

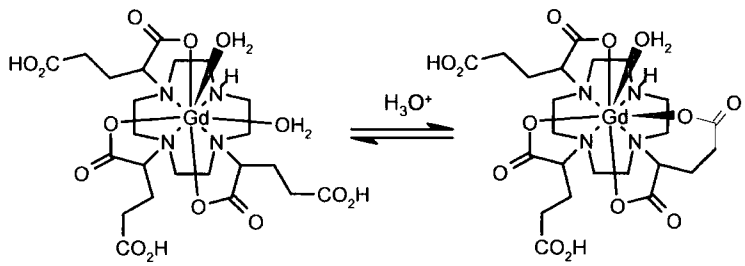

Figure 1.14: Intramolecular (seven ring) carboxylate ligation of [Gd(gDO3A)]$^{3-}$

The homologous complex [Gd(aDO3A)]$^{3-}$ exhibited very different behaviour, remaining a di-aqua species at ambient pH. Emission spectra examined in a simulated extracellular background containing various competing anions over the pH range 3.5-10.5, revealed that whilst carbonate was preferentially bound, it only formed a ternary complex above pH 7.5. Relaxometric studies revealed a limiting maximal relaxivity was reached at pH 7.3 of 10.1 $mM^{-1}s^{-1}$ (65.6 MHz, 293 K). Beyond pH 7.3 the formation of a ternary complex was observed. The complex was examined in the presence of serum, and a high relaxivity of 12.3 $mM^{-1}s^{-1}$ (65.6 MHz, 293 K) was maintained, suggesting no interaction with side chain residues of the protein molecules. An empirical screening method was used to assess kinetic stability, which involved taking several relaxivity measurements over a specific time period (pH 7, phosphate buffer). Endogenous cations such as Zn^{2+}, which may promote dissociation of the free Gd (III) ion resulting in a reduction in the relaxivity, were added. The study found that [Gd(aDO3A)]$^{3-}$ was ten times more chemically inert than clinically used [Gd(DTPA)]$^{2-}$. Therefore, [Gd(aDO3A)]$^{3-}$ offers ideal prerequisites for the introduction of hydrophobic aromatic groups that can bind strongly to proteins, increasing the τ_R effect and the overall relaxivity of the complex.[37,38]

1.5 Outer Sphere Relaxation

As previously mentioned the relaxivity due to outer sphere relaxation mechanisms contributes to about half of the overall observed relaxation for clinically used, monomeric gadolinium based contrast agents. The outer sphere relaxivity stems from modulation of dipolar proton interactions brought about by loosely diffusing water molecules from the bulk solvent and the paramagnetic centre.[39] The outer

sphere term can be estimated from the equations derived by Freed, which depend on the electronic relaxation time of the metal ion, the distance of the closest approach of the solvent and the solute (a) and the sum of the solvent and solute diffusion coefficients (D). C^{OS} is a constant ($5.8 \times 10^{-13} s^{-2} M^{-1}$) and the dependence on the electronic relaxation times is expressed in non-Lorentzian spectral density functions $J(\omega_i)$, Equation 1.4.[40]

$$R_{ip}^{OS} = C^{OS}\left(\frac{1}{aD}\right)[7J(\omega_S) + 3J(\omega_H)] \qquad \textbf{(1.4)}$$

1.5.1 Second Sphere coordination

The formation of strong hydrogen bonds between oxygen atoms on the pendant arms of the ligand and bulk water molecules increases the time experienced by the paramagnetic effect. These water molecules are found to form a second coordination shell around the metal ion and play a significant role in the overall paramagnetic contribution to the water proton relaxation rate (see Equation 1.1).

Clarkson and co-workers[41] reported that the gadolinium complex $[Gd(TTHA)]^-$ contains no inner sphere water molecules, and the second sphere contribution to the overall relaxivity was estimated to be more than 30%. The transmittance of the relaxivity from the second sphere effect to the bulk solvent is comparable to the inner sphere mechanism, where the resident lifetime and the relaxation effect play an important role.[41]

There is often no differentiation between the various types of outer sphere water molecules contributing to the overall relaxation enhancement. Direct assessments can only be determined using contrast agents that have no inner sphere water molecules and therefore no clinical interest. In the case of poly(amino carboxylate) and especially phosphonate Gd (III) complexes, (which are especially capable of tightly binding water molecules), Freed's force free model, can only roughly approximate the outer sphere contribution to relaxivity, as rotational diffusion

effects must be taken into account.

1.5.2 Nuclear Magnetic Relaxation Dispersion (NMRD) profiles

Gadolinium complexes of the ligands DOTP and TTHA contain no inner sphere water molecules and therefore their NMRD profiles directly reflect the second and outer sphere relaxivity (Figure 1.15). Measuring the relaxation rates of an abundant nuclear species as a function of the magnetic field over a wide range, typically 0.01 to 100 MHz is referred to as relaxometry. The profile is a plot of nuclear magnetic relaxation rate usually $1/T_1$, as a function of the magnetic field on a logarithmic scale, which is also referred to as a Nuclear Magnetic Relaxation Dispersion (NMRD) profile.[3, 42]

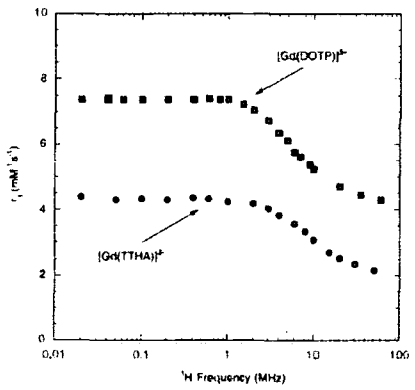

Figure 1.15: NMRD curves for two (q=0) complexes, $[Gd(DOTP)]^{5-}$ and $[Gd(TTHA)]^{3-}$ (298 K), showing that not all 'outer sphere' complexes of similar molecular volume are equivalent.[2]

Investigating a sample where certain thermodynamic properties are modified such as pressure and temperature, can influence the chemical or physical state of the species. However, variation of the magnetic field has no influence on the chemistry of the sample and is a valuable means of determining the different interaction mechanisms and dynamic processes influencing relaxation behaviour.[3]

1.5.3 $[Gd(DOTP)]^{5-}$

Attractive alternatives to the carboxylic acid donor are the phosphonic acid (PO_3H_2) and the related phosphinic acids (PRO_2H). The phosphonic acid is a stronger acid than RCO_2H, so that protonation not only of the free ligand but also of the

phosphorus double bond in the metal complex is inhibited.[43] The pentavalency of the phosphorus means an alkyl, aryl or other functionality may be introduced readily, permitting not only control over lipophilicity but also the introduction of a remote electrophilic site, which may be required if such ligands are to be used in bifunctional complexating agents in protein conjugation.[43] The tetraphosphonate, octadentate complex $[Gd(DOTP)]^{5-}$ (Figure 1.16) does not possess any water molecules in its inner coordination sphere.

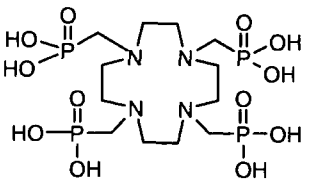

Figure 1.16: Chemical Structure of the DOTP ligand

The steric bulk of the relatively large phosphonate groups with respect to carboxylate analogues prevents access of water molecules. This was confirmed by solid and solution state studies for the complex using x-ray crsyallography and ^{17}O NMR experiments. These findings were reported by Ren and Sherry *et al.*[44] As a result of no inner sphere hydration, it was unforeseen that the relaxivity of the $[Gd(DOTP)]^{5-}$ complex of 4.7 $mM^{-1}s^{-1}$ (20 MHz, 298 K) should be the same as that of $[Gd(DOTA)]^{-}$ under the same experimental conditions at physiological pH. As mentioned this is explained by the large second sphere effect generated by the strong hydrogen bounds formed, between the uncoordinated oxygens of the phosphonate groups and the water protons. These water molecules were found to be in fast exchange inhibiting any quenching effect of the overall proton relaxation. The DOTP ligand readily forms highly charged ion-paired complexes with alkali and alkaline earth cations. This was exploited in the use of Tm (III) complexes as *in vivo* shift reagents for ^{23}Na NMR when measuring sodium gradients.[1] The complex distributes throughout all extracellular space and is filtered by the kidneys with a time constant of approximately 12 minutes. Sherry and co-workers[45] reported the synthesis and characterisation of new DOTP like ligands with extended functionality on the methylenic carbon of the phosphonate pendant arm. This was intended to increase rigidity of the ligand, hence magnifying hyperfine shifts.[43,45]

The use of $[Gd(DOTP)]^{5-}$ as a contrast agent for MRI has been unsuccessful as the complex is highly charged and despite its strong association with sodium ions is not very convenient due to osmolality problems.[46]

1.5.4 Derivatives of $[Gd(DOTP)]^{5-}$

As more conclusive evidence proved phosphonate and phosphinate moieties could result in an efficient second coordination sphere, increasing the observed relaxivity, many research groups have investigated anionic species for the basis of improving the efficacy of contrast agents. This includes attachment of hydrophobic groups to the phosphinate backbone in order to increase the rigidity, or introducing specific moieties capable of increasing the binding interaction to serum albumin.[47]

Parker and co-workers reported the synthesis and characterisation of the highly rigid, kinetically stable, eight coordinate benzylphosphinate complex, $[Gd(BzDOTP)]^-$ (Figure 1.17).[46,48,49]

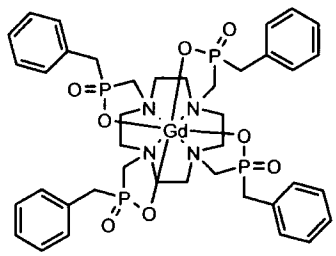

Figure 1.17: Chemical structure of $[Gd(BzDOTP)]^-$.[3]

The NMRD profile of $[Gd(BzDOTP)]^-$ was simplified due to lack of inner sphere contributions and of characteristic shape and amplitude, for a complex only affected by the translational diffusion model of pure outer sphere relaxivity. Strong binding interactions were reported for $[Gd(BzDOTP)]^-$ with bovine serum albumin (K_A = 9.1 x 10^3 M^{-1} 298 K), leading to a marked relaxivity enhancement for a (q = 0) gadolinium complex. A remarkably high efficacy of the complex in liver and bile was observed in MRI examination trials.[3] The high relaxivity enhancement upon binding is likely to result from the mobile protons of the protein that are dipolarly relaxed, by their proximity to the paramagnetic centre. In addition, the highly

organised structure and consequent reduction of the mobility of water molecules in the hydration sphere of the protein, near the binding site of the complex, allows generation of second sphere coordination interactions.[3] The complex formed between Gd (III) and the monobutyl ester of DOTP, producing [Gd(DOTPMB)]$^-$ (Figure 1.18) is also found to bind significantly to HSA, with an increase in relaxivity of 2.8 $mM^{-1}s^{-1}$ (free chelate) to 13.4 $mM^{-1}s^{-1}$ for the HSA adduct.[50]

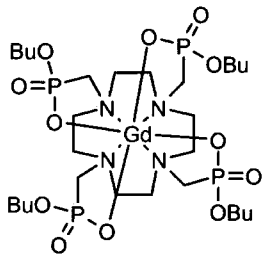

Figure 1.18: Chemical structure of [Gd(DOTPMB)]$^-$.[50]

The binding interaction with HSA (k_A = 9.3 x 10^2 M^{-1}) was much less than for the aryl methoxy substituted complex, [Gd(BzDOTP)]$^-$ resulting from the ability of the aryl methoxy groups to promote formation of a network of hydrogen bonded water molecules in the second coordination sphere of the Gd (III) chelate, near to the surface of the protein.

There is a poor understanding of the mechanism governing the relaxation enhancement of Gd (III) complexes where (q = 0). It is believed to rely on several features, including the structure and dynamics of the hydration layers of the protein and on the proton-exchange processes between the mobile protons on the protein and water molecules. The data generated to date indicate this contribution is always present and is believed to represent the largest contribution to the relaxivity of bound complexes. The contribution at present cannot be modelled preventing quantitative evaluation of their NMRD profiles. Parker and co-workers investigated the relaxometric properties for a series of methoxy-benzylphosphinate derivatives (Figure 1.19), in order to probe the effect of hydrogen bonding with respect to the aryl methoxy group.[51] The NMRD profiles for the methoxy substituted Gd (III) chelates are similar in form and nature to those reported for [Gd(BzDOTP)]$^-$. The profiles are also very similar for each of the three complexes,

consistent with Gd (III) chelates of identical molecular size, coordination polyhedron and hydration sphere. Slight differences were observed in the τ_s values; this resulted from the different substitution sites of the methoxy groups on the aromatic ring. The binding interaction of GdL^3 with bovine serum albumin of (K_d = 1.1 x 10^{-4} dm^3 mol^{-1}) was significantly higher than for the parent complex, [Gd(BzDOTP)] of (K_d = 2.8 x 10^{-4} dm^3 mol^{-1}), leading to an approximate enhancement in the relaxivity of more than 20%, as a result of more efficient hydrogen bonding in the second coordination sphere of the gadolinium ion, near to the protein surface. The derivatives showed selective biliary clearance at low concentrations of complex, a slower rate of clearance from tumour tissue and impressive proton relaxation enhancement in the presence of protein, rendering them suitable as potential MRI contrast agents.

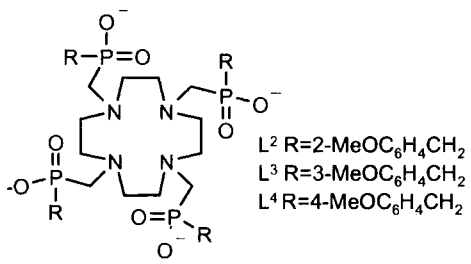

Figure 1.19: Chemical structure of methoxybenzyl ligands[51]

Macrocycles bearing pendant phosphonic or phosphinic groups exhibit excellent coordination selectivity and high thermodynamic stability. Protonation of the phosphinate or phosphonate oxygen atom is difficult to accomplish in both the free ligand and in the metal complex, resulting in metal complexes that are stable to proton catalysed dissociation pathways, required for *in vivo* imaging. Structural variations of the phosphorus substituents may effectively control the hydro-lipophilic properties of both ligand and metal complexes, which may ultimately provide a fine-tuning of the conjugation with proteins and other biologically active molecules.[52,53]

A new hexadentate macrocyclic ligand, $Me_2DO2PMe$, containing two monoethyl ester phosphonate arms has been synthesised by Bianchini *et al*[52] (Figure 1.20).

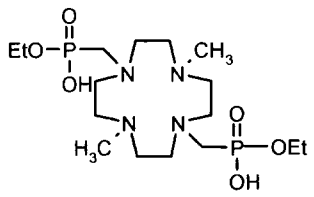

Figure 1.20: Chemical structure of the ligand $Me_2DO2PMe$[52]

The hexadentate ligand involves coordination of the four nitrogen atoms of the macrocycle and two oxygen atoms from the phosphonate groups, which allows addition of two or three water molecules to complete coordination. The data showed the stability of [Gd(Me_2DO2PMe) was very low with respect to the complexes of copper and zinc. This is a likely consequence of the strong effect of the nature and number of pendant monoethyl ester phosphonate groups. The stability results also show [Gd(Me_2DO2PMe)], is far less stable than the Gd (III) complex of the carboxylate macrocycle DO2A, consistent with the weakly basic P(O)(OEt)O- groups. However, complexation of the ligand to copper, [Cu(Me_2DO2PMe)] or zinc [Zn(Me_2DO2PMe)] shows remarkable thermodynamic stability in the pH range 2.5 to 7, since neither protonated nor hydroxylated species were apparently formed.[52]

1.6 Rotational Motion

At the magnetic field strengths used in MRI (20 - 60 MHz) the longitudinal time of bound water protons is most critically controlled by the rotational correlation time, τ_R, according to Equation 1.3. For current clinically used contrast agents, fast rotation is the limiting factor for proton relaxivity. This is demonstrated by the NMRD profile for a low molecular weight complex, in which the effect on relaxivity is considered, based upon changes in the τ_R value (see Figure 1.21).

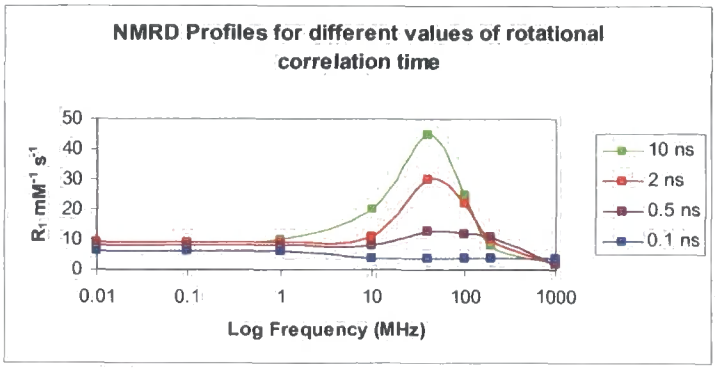

Figure 1.21: NMRD profile for a low molecular weight chelate with varying values of rotational correlation time, τ_R.

The Debye-Stokes equation can provide an estimation of τ_R for 'spherical' molecules (Equation 1.6). To obtain the "effective" radius, r_{eff}, of the molecule, a spherical shape of the complex is assumed. It is furthermore assumed that the microviscosity, η is similar to the macroviscosity of the solution, so that increasing the size of the complex should lead to an increase in τ_R. Human Serum Albumin (HSA) concentration is known to considerably affect the macroviscosity of solution and the Stokes-Einstein equation predicts τ_R, should increase linearly with viscosity.[54]

$$\tau_R = \frac{4\pi\eta r_{eff}^3}{3k_B T} \qquad (1.6)$$

It was recognised early on in contrast agent development, the critical role that rotation plays towards determining the effective correlation time. As a result, there are many strategies to slow the rate in order to increase relaxivity. These include covalent or non-covalent binding of low molecular weight complexes to macromolecules (see Figure 1.22), polymers or dendrimers. Relaxation can also be enhanced from the self assembly of monomeric complexes into micelles[57], particulates[58,59] or aggregates with low critical aggregation concentration[60], which increases the relaxation enhancement through immobilisation.[61]

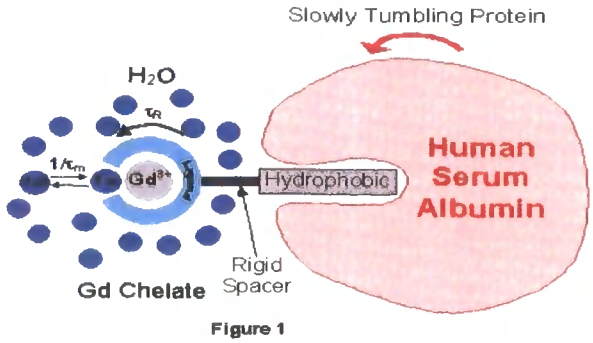

Figure 1.22: Diagram representing the non-covalent interaction of a protein and a Gd (III) chelate.

Besides increasing the reorientational time, τ_R, hence the relaxivity of such an albumin based agent the reversible interaction of the protein presents two additional advantages: a safe clearance of the agent and a longer residence time in the blood pool compared to the unbound agent. This behaviour is favourable in angiographic applications.[62]

1.6.1 Internal Flexibility of Macromolecular Gd (III) Complexes

As is expected, τ_R, values for some Gd (III) chelates are seen to increase with increasing molecular weight, however, the relationship is far from linearly predicted from the Debye-Stokes equation, resulting from the internal flexibility of some systems.[3] As some of the chelates investigated are not particularly rigid themselves, internal motion which determines relaxivity may be considerably faster than the overall tumbling motion of the whole molecule. Therefore, the Gd (III) chelate should be fixed covalently or by non-covalent binding to a macromolecule or dendrimer via a short rigid linking unit to reduce local flexibility. Linear polymers are especially susceptible and in these complexes the rotational correlation time, τ_R, is dominated by segmental motions which are independent of molecular weight. Internal flexibility effects have also been reported for non-covalently bound Gd (III) chelate- protein adducts. The complex MP-2269 has a reported τ_R value of 0.1 ns when bound to serum albumin. This value is one order of magnitude lower than the rotational correlation time of the protein molecule, consistent with inefficient rotational coupling.[8, 63]

1.7 Water Exchange

For Gd (III) chelates characterised by $q \geq 1$, the major contribution to the observed relaxation rate enhancement of the solvent water protons, arises from the exchange of bound water molecule(s) with the bulk solvent. The residence time, τ_m actually plays a dual role in determining relaxivity. It modulates the efficiency of chemical exchange from the inner sphere of the metal to the bulk (Equation 1.7) and contributes to the overall correlation time, τ_C, that governs the dipole-dipole interaction between electron and nuclear spins (Equation 1.8), where T_{1M} is longitudinal relaxation time, γ_I is the nuclear gyromagnetic ratio, g is the electron g factor, μ_B is the Bohr magneton, r_{GdH} is the electron spin – proton distance, ω_I and ω_S are the nuclear and electron Larmor frequencies, respectively; ($\omega = \gamma_B$, where B is the magnetic field).[64]

$$r_{1p}^{IS} = \frac{1.8x10^{-5}q}{T_{1M} + \tau_m} \qquad \textbf{(1.7)}$$

$$\frac{1}{T_1} = \frac{2}{15}\frac{\gamma_I^2 g^2 \mu_B^2}{r_{GdH}^6} S(S+1)\left(\frac{\mu_0}{4\pi}\right)^2 \left[7\frac{\tau_{c2}}{1+\omega_S^2\tau_{C2}^2} + 3\frac{\tau_{C1}}{1+\omega_I^2\tau_{C1}^2}\right] \qquad \textbf{(1.8)}$$

It can be seen that r_{1p}^{IS} is maximised when $T_{1M} > \tau_m$ (fast exchange conditions) and T_{1M} is as short as possible. It has already been stressed the importance rotational motion plays in relaxation theory. Fast rotation of bound water molecules leads to very short T_{1m} relaxation times according to SBM theory. If T_{1m} becomes smaller than the residence time of the protons in the first coordination sphere of Gd (III), $T_{1m} << \tau_M$, the water proton exchange will then become the limiting factor for relaxivity.[3]

The water exchange rate of metal bound water molecules for Gd (III) chelates can be conveniently determined by measuring variable temperature dependent ^{17}ONMR.[65] ^{17}O NMR is a perfect tool as the oxygen atom of the coordinated water molecule is directly bound to the paramagnetic ion and thus experiences a far more efficient relaxation enhancement than the protons, permitting observation of the

exchange rate directly.[66]

The residence lifetime is very important in relation to the relaxation of high molecular weight MRI contrast agents. Theory predicts the optimal values for water exchange, τ_m are in the range of 20-50 ns at 298 K.[58] Initially, the water exchange rates of polyaminocarboxylate complexes were believed to be faster than the Gd aqua ion ($K_{ex} \sim 10^9\ s^{-1}$), too fast to influence proton relaxivity. However, extensive studies by Merbach and co-workers reported water exchange rates determined by ^{17}O NMR for $[Gd(DTPA)(H_2O)]^{2-}$ and $[Gd(DOTA)(H_2O)]^-$ as 303 and 244 ns (298 K), which are far from optimum.[3,58] The nine coordinate Gd (III) polyaminocarboxylate complexes all have positive activation volumes, indicative of a dissociatively activated water exchange mechanism. This is expected, as there is no longer space for a second water to enter before the departure of the bound water molecule. The eight coordinate transition state is energetically unstable, requiring high activation energy, resulting in a decreased rate constant. Hence, the lower exchange rates on the lanthanide poly(aminocarboxylate) complexes differ from the faster dissociative interchange, water exchange mechanism of $[Gd(H_2O)_8]^{3+}$.[67,68]

Efforts have been devoted to optimising residence lifetimes, alleviating limitation of a complex's relaxivity. In complex design, amide linkages have tended to be avoided since it has been suggested that complexes with this structural motif may prolong residence times. It has also been noted that water exchange rates at positively charged centres are much slower than those for neutral complexes which, in turn, are slower than for negatively charged species.[69] Therefore, introduction of negative charge into the neighbourhood of the Gd (III) bound water molecule may effectively increase the observed relaxivity.[58] These empirical observations are more appropriately assessed in terms of the perturbation of the local water structure by the complex counterions or integral substituents, and the variation of the strength/length of the Gd-OH_2 bond.[70] The C_4 substitution of the ethylenic bridge of DTPA by a larger substituent such as an ethoxybenzyl group, benzyl, or a (4,4-diphenylcyclohexyl)phosphanooxymethyl group has been shown to decrease the water exchange by 25-42% as a result of increased steric crowding around the

bound water site.[71]

Merbach *et al*[72] reported the behaviour of the complex [Gd(TRITA)]$^-$, which is a derivative of the macrocyclic chelate [Gd(DOTA)]$^-$, in which one ethylene bridge is replaced by a propylene bridge. Similarly, to [Gd(DOTA)]$^-$, [Gd(TRITA)]$^-$ contains one water molecule in its inner sphere. However, the water exchange rate was found to be faster as a consequence of the increased steric compression around the bound water molecule, induced by a larger macrocycle. A slight reduction in thermodynamic stability resulted for [Gd(TRITA)(H_2O)]$^-$ but may still be stable enough for use *in vivo*. Therefore, the chelate is a potential synthon for the development of high relaxivity, macromolecular agents.[72] In addition, the distance between the plane of the carboxylate oxygens and the metal was found to be longer in the TRITA complex. This resulted in the bound water molecule being in closer proximity to the negatively charged carboxylates, facilitating the dissociative mechanism of water exchange.[58]

The nature of the second coordination sphere also has an effect on water exchange rates. The complex [Gd-DO3A-propionate(H_2O)]$^-$ has a much shorter lifetime of 8 ns, compared to that of [Gd-DO3A-alanine(H_2O)] which is significantly longer, (180 ns, 298 K).[73,74] This is explained by the hydrogen bonding interaction between the metal bound water molecule and the positively charged α-amino group of the amino acid.

Upon formation of an adduct with a macromolecule effective complex rotation is obviously slowed. However, the effect upon water exchange is often harder to quantify. Aime and co-workers reported a significant decrease in water exchange rates for two Gd (III) complexes upon albumin binding, via electrostatic or hydrophobic interactions.[75] They deduced these conclusions from the data produced by the NMRD profiles of the individual complexes. This was explained by the obstruction of the water coordination site when the complex was bound to protein. In contrast, Merbach and co-workers, used independent techniques such as ^{17}O NMR and EPR including NMRD assessments and concluded the decrease in

exchange was not as large as reported by Aime *et al.*[3,75] It can be concluded that incorporation of Gd (III) complexes into macromolecular systems may affect water exchange kinetics, therefore it is important to design a complex which displays optimal residence lifetimes prior to macromolecular formation.

1.8 Second Generation Contrast Agents

The first generation of contrast agents previously discussed are low molecular weight, highly hydrophilic gadolinium based chelates, which consequently are distributed rather unselectively throughout extracellular fluids. The inability to localize selectivity in a desired area lessens the diagnostic potential of these agents.

The development of second generation Gd (III) based systems stems from the MRI complexes endowed with higher relaxivities, or systems that are responsive or specifically targeted to certain sites *in vivo*.

Responsive or smart agents are able to report about the physiochemical environment in which they are distributed. There are a variety of complexes whose relaxivity can be modulated to changes in physiochemical environments, such as pH[76,77,78,79] metal ion concentration, partial pressure of oxygen,[7,80] degree of glycation of proteins, concentration of Ca^{2+} [81], concentration of zinc[82] and the presence of enzymes.[83, 84] A diverse range of applications has been investigated and are reported in the literature.

1.8.1 Hepatotropic Agents

A targeted or 'organ specific' contrast agent is defined as an agent that is selectively taken up by a particular type of cell (e.g. Kupffer cells of hepatocytes) and thereby only enhances organs where these cells are present either in the liver, spleen or lymph nodes.[3] The infusion of the chelate $[Gd(DTPA)]^{2-}$ in rats results in marginal hepatic uptake and negligible biliary recovery, the contrast agent is non-specific and the excretion pathway for this complex occurs by rapid glomerular filtration.[85] Markedly different from the $[Gd(DTPA)]^{2-}$ are the pharmacodynamics of gadobenate dimeglumine[86], $[Gd(BOPTA)]^{2-}$ and gadoxetic acid, $[Gd(EOB\text{-}DTPA)]^{2-}$.

These are analogues of the parent compound $[Gd(DTPA)]^{2-}$, with added hydrophobic substituents incorporated onto the DTPA backbone (see Figure 1.23)[87] These compounds are believed to be taken up by the hepatocytes and once inside or surface immobilised, the relaxivity increases because of the interactions with macromolecular structures. They therefore offer the advantages of improving detection and characterisation of liver lesions in the early extracellular distribution by fast dynamic imaging, followed by delayed imaging where the contrast is dependent upon the specificity of the agent. The complexes are excreted via the bile duct, gall bladder and intestines.[88,89] Although the compounds target the liver for $[Gd(BOPTA)]^{2-}$, only 2-4% of the injected compound is actually absorbed by the liver, whereas for $[Gd(EOB\text{-}DTPA)]^{2-}$, approximately 50% of the compound is absorbed by the organ.[88]

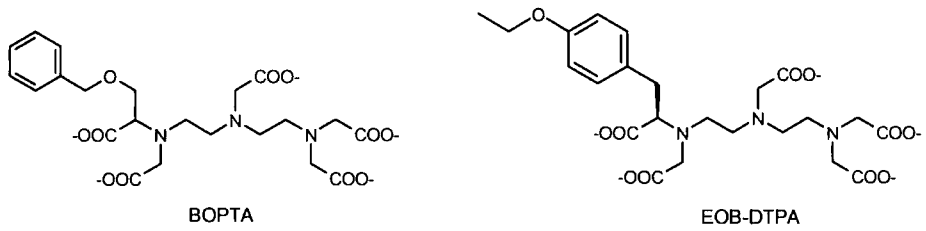

Figure 1.23: Chemical structures of the ligands BOPTA and EOB-DTPA

$[Gd(BOPTA)]^{2-}$ (MultiHance™) has been approved for use in patients in Europe but is still pending approval by the FDA. The complex has also been investigated for MR imaging in brain tumours and as a possible agent for neutron capture therapy (NCT), a growing area of research.[90] $[Gd(EOB\text{-}DTPA)]^{2-}$ (Eovist™) is presently undergoing clinical phase III studies. In addition to the promising results for MRI, $[Gd(EOB\text{-}DTPA)]^{2-}$ has also been tested successfully in patients as a potential contrast agent for computed tomography (CT).[87]

1.9 Protein Binding

The formation of adducts with HSA represents one of the major methods of increasing relaxivity of Gd (III) complexes, associated with lengthening of the molecular reorientational time, τ_R upon formation of a macromolecular adduct. This can be pursued through the formation of both covalent and non-covalent

interactions with macromolecules. Each approach has been studied in depth and several interesting systems have been developed.[3] Covalently bound complexes have proven to be more suitable for delivering the particular derivative to the site of interest, however, there are major drawbacks for *in vivo* applications such as their metabolic fate.[91] The toxicological problems associated with the use of covalently bound conjugates have prompted the search for paramagnetic chelates able to form non-covalent bonds with endogenous proteins.[3] Within this field, most of the work published focuses on the non-covalent interactions with macromolecules. This requires small molecules with suitable moieties that are organised to recognise the target protein.[91] As a result of binding the new functionalised compound may possess similar properties to covalently bound conjugates, such as providing excellent images of the blood pool, yet the excretory pathway remains that of the metal complex having a higher elimination in plasma.[91]

1.9.1 Human Serum Albumin

Human serum albumin (HSA) is present in the blood with a concentration of approximately 40 $mgml^{-1}$ (0.6 mM).[92,93] It is synthesised in the liver and exported as a non-glycosylated protein, and is the major transport protein for unesterified fatty acids. The serum protein is also capable of binding a diverse range of metabolites, drugs and organic compounds. Those compounds that bind most strongly are hydrophobic organic anions of medium size and long chain fatty acids. The remarkable binding properties of albumin account for its role in both the efficacy and delivery rate of many drugs. Anti-coagulants and general anaesthetics, are transported in the blood whilst bound to albumin (often more than 90% of drug is bound), which has stimulated a great deal of research on the nature of drug binding sites.[12] The protein is monomeric and heart shaped, consisting of 585 amino acids with a total molecular weight of 66,400 Da.[94] It is organised into three homologous α helical domains labelled (I-III), and each domain is comprised of two sub-domains, A and B, which contain six and four α helices respectively.[93]

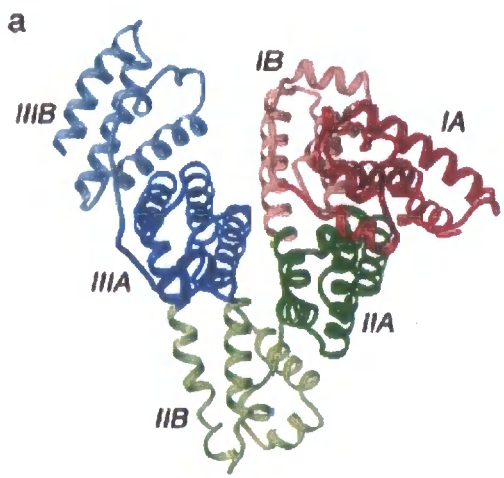

Figure 1.24: Crystal structure of un-liganded HSA. The sub-domains are colour coded as follows: IA, red: IB, light-red, IIA, green, IIB, light-green, IIIA blue, IIIB, light-blue[95]

Several studies have attempted to map the locations of fatty acid binding sites and primary drug binding sites on the protein. The fatty acid sites are distributed throughout the protein and involve all six sub-domains. By contrast many drugs bind to one of the two primary binding sites located on the protein, these are known as Sudlow's sites I and II.[96] According to Sudlow's nomenclature, bulky heterocyclic anions bind to site I (located in sub-domain IIA), whereas site II (located in sub-domain IIIA) is preferred by aromatic carboxylates with an extended conformation. The non-steroidal anti inflammatory Ibuprofen, and the anti-coagulant Warfarin, are considered stereotypical ligands for Sudlow's sites II and I respectively (see Figure 1.25).[97]

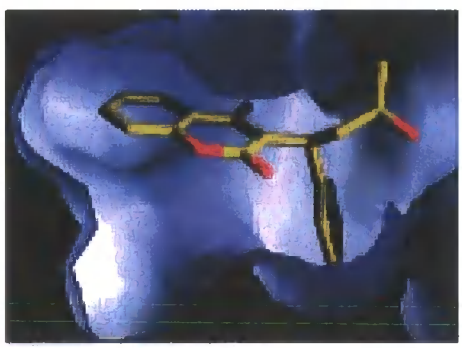

Figure 1.25: Side view of the Warfarin pocket showing a cutaway view of the surface of the binding pocket of Sudlows Site I. The coloured surface indicates electrostatic potential (blue representing basic patches)

Drug binding sites are now known to be located in sub-domains IIA and IIIA. A particularly large hydrophobic cavity is present in the IIA subdomain[98] and the geometry of the pocket of IIA is found to be quite different to that of IIIA. Bombieri *et al*[91] reported that human serum albumin consists of 14 cavities. Cavity 14 was found to be a large, hydrophobic pocket situated between the IA and IIA subdomains. Four highly polar amino acid residues surround the cavity and may allow the entrance of a ligand into the region.[91] The binding interaction between the Gd (III) chelate BOPTA and HSA was investigated. $[Gd(BOPTA)]^{2-}$ was found to dock into cavity 14 (Figure 1.26). The results indicate that the approach of the metal complex is dictated more by the electronic properties of the complex than its geometry.[91]

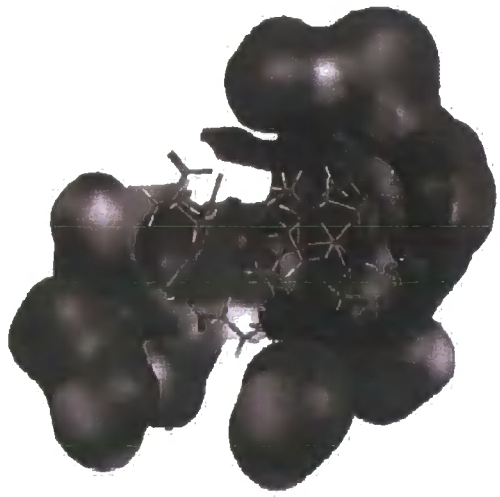

Figure 1.26: MEP representation of the cavity 14 docked with $[Gd(BOPTA)]^{2-}$

Data generated from the binding interactions of a variety of substrates with serum proteins provide useful information relating to contrast agent design. The non-covalent interaction of Gd (III) complexes with HSA can be conveniently studied by relaxometric methods using a low-resolution spectrometer operating at a fixed frequency. Those typical for MRI applications operate in the range of 20 - 60 MHz nowadays. Titration of a dilute solution containing the Gd (III) chelate and the protein causes an increase in the relaxation rate when a binding interaction between the complex and protein occurs, as a result of the increased reorientational correlation time of the macromolecular adduct.[99]

1.9.2 Binding requirements

The effect of hydrophobicity of the Gd (III) chelates and the affinity for serum albumin was investigated by Aime and co-workers for a series of macrocyclic Gd (III) complexes based upon $[Gd(DOTA)(H_2O)]^-$, bearing an increased number of lipophilic residues (BOM = benzyloxymethyl) (Figure 1.27).[3,4]

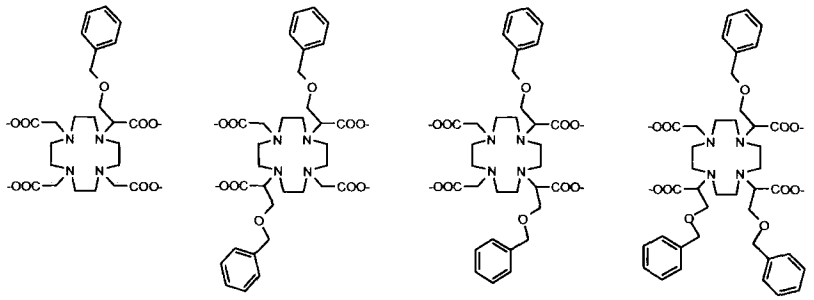

Figure 1.27: Chemical structures of a series of ligands bearing increasing lipophilic residues

Upon interaction with serum albumin an increase in relaxivity was observed for each of the complexes resulting in a lengthening of the rotational correlation time, τ_R.[3] The data obtained showed the binding affinity of $K_A = 1.7 \times 10^3\ M^{-1}$ was greatest for the tri-substituted product $[Gd(DOTA)\text{-}(BOM)_3]^-$, this was of the same order of magnitude as that reported for endogenous substrates like testosterone and aldosterone.[100] Competition studies of $[Gd(DOTA)\text{-}(BOM)_3]^-$, showed that the complex was displaced from the protein when equimolar amounts of Warfarin and Ibuprofen were added, suggesting $[Gd(DOTA)\text{-}(BOM)_3]^-$ interacts with both subdomains IIA and IIIA.[100]

The binding affinity for the two isomers (cis and trans) of $[Gd(DOTA)\text{-}(BOM)_2]^-$ were of similar order $K_A = 3.2 \times 10^2\ M^{-1}$ and $K_A = 3.6 \times 10^2\ M^{-1}$ respectively. For the chelate containing only one (BOM) group $[Gd(DOTA)\text{-}(BOM)]^-$ only a weak interaction was formed with serum albumin $K_A = < 1 \times 10^2\ M^{-1}$.[3] Comparison of the relaxivity values of the Gd (III) derivatives in water is shown in the associated NMRD profiles (Figure 1.28).

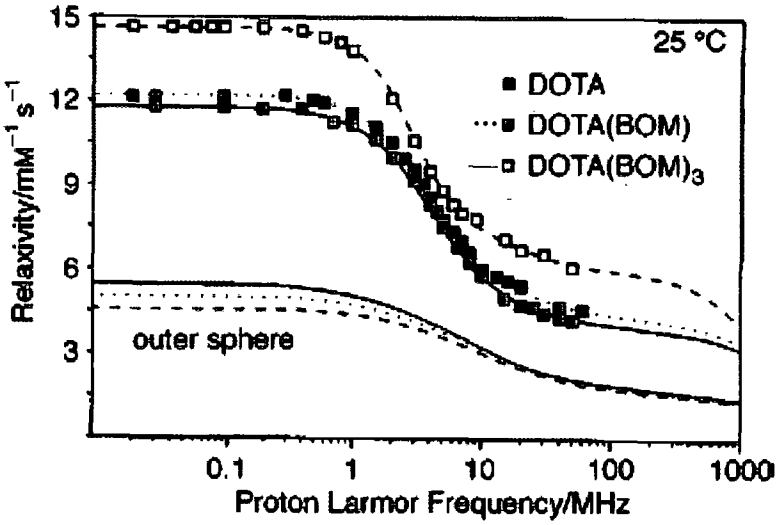

Figure 1.28: $1/T_1$ NMRD profiles for $[Gd(DOTA)]^-$, $[Gd(DOTA)\text{-}(BOM)]^-$ and $[Gd(DOTA)\text{-}(BOM)_3)]^-$ complexes at 298 K. The lower curves represent the outer sphere contribution to the profiles[4]

It was apparent that the binding association constants are directly related to the number of hydrophobic residues present on the surface of the chelate, and these findings are addressed in the design of contrast agents suitable for imaging the blood pool.[4]

1.9.3 Receptor Induced Magnetisation Enhancement (RIME)

In order to image blood vessels efficiently, Gd (III) chelates need to remain in circulation and not redistribute into the interstitial spaces for a long enough time to allow detailed imaging.[8] High molecular weight species are desirable as they have enhanced relaxivities due to an increased rotational correlation time. In addition, they cannot be excreted by the usual method of glomerular excretion and are not able to permeate into the interstitial spaces.[8] The receptor induced magnetisation enhancement (RIME) strategy involves a low molecular weight Gd (III) complex which is chemically designed to bind non-covalently to substrates like serum proteins.[8] Binding to a macromolecule causes an increased concentration of the Gd (III) complex in the area of the receptor molecule, giving selective enhancement of the target relative to the background, increasing the relaxation enhancement upon binding.[101] The bound form of the agent is in equilibrium with a small amount of the free agent, which acts like an extracellular agent and is excreted renally over

time, avoiding the problems associated with slow excretion sometimes exhibited by covalently bound macromolecular systems.[8] Binding allows selective enhancement of arteries and veins, relaxation enhancement due to increased molecular tumbling time and increased half-life of the drug *in vivo*, allowing the radiologist time to image multiple body regions and to employ pulse sequences which give high resolution images.[102] Relatively rigid paramagnetic macromolecular complexes have been generated *in vivo*, in the blood pool, through reversible non-covalent hydrophobic interactions of small lipophilic Gd (III) chelates with serum. These include MS-325 (AngioMARK™, EPIX), MP-2269 (Mallinckrodt), $[Gd(BOPTA)(H_2O)]^{2-}$ (Multihance™, Bracco) and $[Gd(EOB\text{-}DTPA)(H_2O)]^{2-}$ (Eovist™, Schering).

1.9.4 MS-325

MS-325 was the first representative of an RIME contrast agent and is currently in phase III clinical trials. (Figure 1.29).[101] The complex is monomeric and is based upon the parent compound $[Gd(DTPA)]^{2-}$.

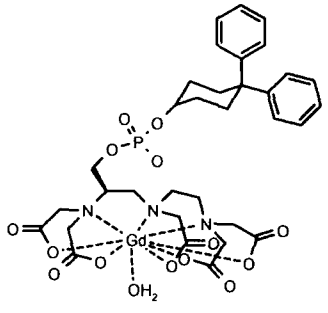

Figure 1.29: Chemical structure of MS-325

A pendant biphenylcyclohexyl moiety attached via a phosphodiester link is inserted into the DTPA backbone, which increases the binding affinity towards HSA, at the same time representing a steric impediment to prevent dissociation of the complex.[102] MS-325 is reported to be more thermodynamically and kinetically inert to metal ion substitution that the parent compound, $[Gd(DTPA)]^{2-}$. Studies in rabbits (12-16) revealed an average blood half-life for MS-325 of ~ 2.5 hours, compared with ~ 10 minutes for non-bound agents.[103] The blood persistence of the

bound agent serves as an aid in delineating abnormal vascular beds and increased vascularity associated with fast growing tumours.[103] The binding properties of MS-325 with HSA, have been extensively investigated and results suggest MS-325 binds to a single site on the serum protein (site II region)[101], with an affinity constant of K_A = $3x10^4$ M^{-1} (298 K). The interaction with serum albumin for the complex is moderate, at typical circulating concentrations of 0.1 mM, 88% of the complex is non-covalently bound.[101] Binding to HSA does cause an increase in relaxivity from 7.7 $mM^{-1}s^{-1}$ as the free chelate to 48.9 $mM^{-1}s^{-1}$ in the hypothetical fully bound complex (20 MHz, 298 K).[3] This increased relaxivity is the result of the rotational diffusion rate of the molecule being decreased by almost a factor of 100. Also, the outer sphere relaxivity increases by a factor of 2-4, due to the presence of long lived (> 1 ns) water molecules in the second coordination sphere.[101] The electronic relaxation rate, $1/T_{1e}$ also slows upon binding. However, the water exchange rate is slowed by a factor of 2-3, which quenches the amount of relaxation enhancement observed (see Figure 1.30).

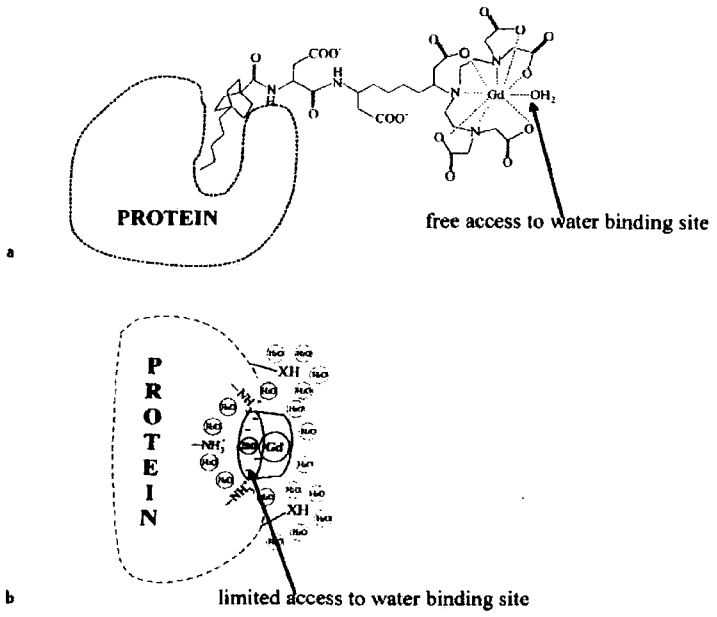

Figure 1.30: Effect of protein binding on the water binding site. (a) The hydrophobic side chain of the ligand, bound to the protein is far from the Gd (III) chelate, thus protein binding does not influence water exchange. (b) The Gd (III) chelate is bound to the protein via electrostatic forces. The water binding site of the complex is partially blocked by the protein, thus the water exchange rate is diminished.[8]

1.9.5 MP-2269

MP-2269 (Figure 1.31) is a monomeric non aromatic Gd (III) complex. Similarly to MS-325, it is based upon $[Gd(DTPA)]^{2-}$. The hydrophobic pentylbicyclo-[2.2.2] octane side chains interact with serum albumin allowing the compound to remain in the intravascular space sufficiently long for imaging to be carried out following intravenous injection.[103]

The negative charges from both the aspartyl linkers and the terminal $[Gd(DTPA)]^{2-}$ group impart water solubility.[104]

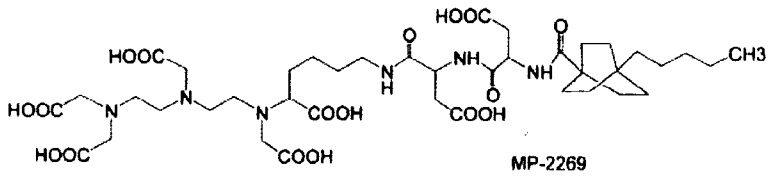

Figure 1.31: Chemical Structure of MP-2269

If the distance between the metal and protein binding site of the ligand is relatively large then water exchange is not affected by the protein interaction, as was seen for the Gd (III) chelate MP-2269 (Figure 1.30).[8] However, the τ_R value of MP-2269 bound to bovine serum albumin was determined independently using deuterium NMR. Adzamli *et al*[105] reported that the τ_R value of the bound contrast agent is 8 ns, significantly shorter than the τ_R value expected for a fully immobilised ligand of 20-22 ns. This indicates there is some segmental mobility of the contrast agent with respect to the protein one. The remarkable internal flexibility has been attributed to the relatively long distance between the Gd-binding and the protein binding sites of the molecule.[8] Upon interaction with BSA the relaxivity was found to increase from 5.64 $mM^{-1}s^{-1}$ to 24.5 $mM^{-1}s^{-1}$ (20 MHz, 310 K).[8]

The problems associated with increased residence times, τ_m, upon formation of a HSA adduct, as discussed earlier, limit the efficacy of some newer, second generation contrast agents. The complex $[Gd(DTPA)(BOM)_3]$ (Figure 1.32) was studied in parallel to MS-325, where it was reported that the water exchange rates

were slowed by almost 50% upon adduct formation with HSA, compared to the free chelate.

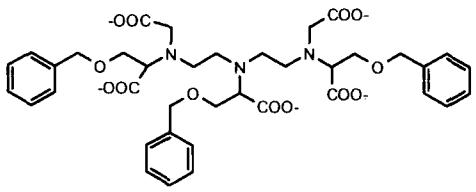

Figure 1.32: Chemical structure of the ligand DTPA-BOM$_3$

However, Aime and co-workers[106] reported that the relaxivity observed for the latter complex of 8.8 $mM^{-1}s^{-1}$ (20 MHz, 298 K) was significantly higher than that of MS-325 as the free chelate and the macromolecular compound (see Figure 1.33). Due to similar values of water exchange rate, τ_m and rotational correlation time, τ_R for both complexes, the gain in relaxivity for the $[Gd(DTPA)(BOM)_3]^-$ complex, can be attributed to the longer value of T_{1e}.[106]

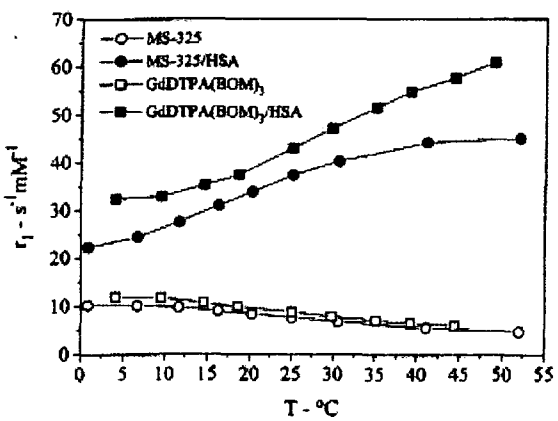

Figure 1.33: Relaxivities of free (□, ○) and HSA-bound (■, ●) Gd (III) complexes as a function of the temperature (pH 7.5, 50 mM HEPES buffer, 20 MHz). The profiles of the bound chelates were calculated from solutions containing 0.1 mM of the complexes and a large excess (1.7 mM) of HSA[106]

As HSA is known to transport fatty acids, Caravan *et al* reported the studies of two Gd (III) chelates with fatty acid substituents, [Gd(C_8-DOTP)] and [Gd(C_{11}-DOTP)], based upon the parent compound $[Gd(DOTP)]^{5-}$ (see Figure 1.34). Similarly to the parent complexes, they contained no inner sphere water molecules (q=0) and were found to relax well due to a large second sphere contribution, resulting from the highly charged tetraphosphonate surface. At the concentrations used in the study

(less than 20 mM of complex), the fatty acid derivatives [Gd-(C_8DOTP)] and [Gd-(C_{11}DOTP)] were not found to form micelles, which may have increased the rotational correlation time.[107]

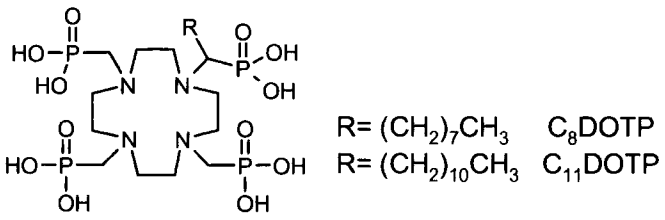

Figure 1.34: Chemical structure of the fatty acid derivatives of $[Gd(DOTP)]^{5-}$

Upon interaction with serum albumin, (both bovine and human were studied), dramatic increases in the observed relaxivity were observed due to an added τ_R effect. The percentage of the complex bound to protein in each complex was found to be greater with non-defatted human serum albumin than bovine. The binding interaction with HSA was greatest for the fatty acid of increased chain length, [Gd(C_{11}-DOTP)] with a modest affinity of $K_A = 249 \times 10^{-3}$ M^{-1}. [Gd(C_{11}-DOTP)] was found to bind to multiple fatty acid sites on the serum molecule. The relaxivity of $[Gd(C_{11}\text{-DOTP})]^{5-}$ bound to albumin is remarkably high for a q = 0 compound, with the relaxivity at 310 K being greater than a number of macromolecular q = 1 conjugates that have been examined as potential blood pool agents.[107] The results show how second sphere relaxivity can provide an enhancement to the observed relaxivity if long lived water molecules can get close enough to the Gd (III) ion, or if the complex can bind several water molecules at once for a lifetime in the order of nanoseconds.[107]

1.9.6 $[Gd(BOTPA)]^{2-}$ and $[Gd(EOB\text{-}DTPA)]^{2-}$ with HSA

Relaxivity studies on the Gd (III) complexes of BOPTA and EOB-DTPA indicated the relaxivity was higher than expected on the basis of correlation times. Crystallography studies showed there is a reduced distance between the gadolinium central ion and the inner sphere water molecules with respect to the parent complex, $[Gd(DTPA)]^{2-}$.[3] The addition of the hydrophobic, aromatic substituents in these structures has been shown to promote protein binding. As a

result of the modest non-covalent interactions with serum albumin, both complexes act as blood pool contrast agents and can provide useful contrasts to the compound MS-325. Relatively modest changes in the structure of a Gd (III) chelate can have major effects upon protein binding; the results of this allow fine tuning in the design of complexes to produce the required response. For example, MS-325 is reported as being 94.3% bound in a 4.5% solution of HSA. In contrast, $[Gd(EOB\text{-}DTPA)]^{2-}$ is reported as only 10% bound in a 5% solution of HSA with a concentration of 1.5 mmol L^{-1}. MS-325 and EOB-DTPA have been found to interact with several sites on the protein molecule. At increased concentrations of complex as many as 20 to 25 molecules can bind to a single protein molecule.[8] Upon binding to serum albumin, there is an increased τ_R effect for $[Gd(EOB\text{-}DTPA)]^{2-}$ that Chen *et al*[8] reported as 9.8 ns, which is much less than the increased effect seen for MS-325 of 20-30 ns, measured under the same experimental conditions. An increase in tumbling can be observed for $[Gd(EOB\text{-}DTPA)]^{2-}$ in the frequency range of 40-60 MHz, the fields used in medical MRI (see Figure 1.35).

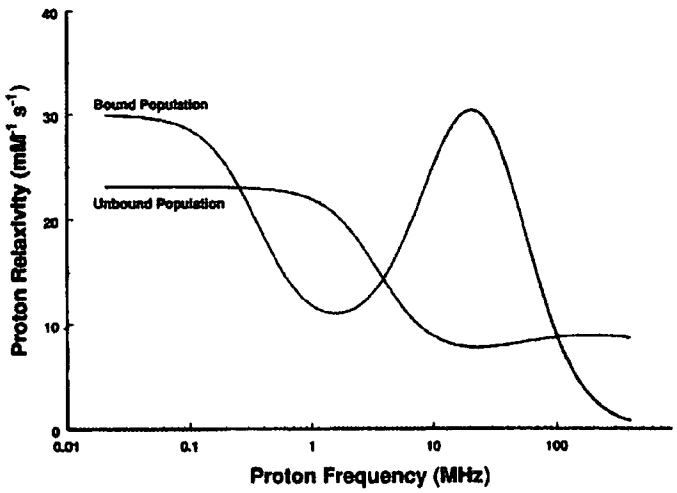

Figure 1.35: NMRD profile of bound and unbound populations of $[Gd(EOB\text{-}DTPA)]^{2-}$ in 4% HSA solution

Chapter 2

Di-aqua Gadolinium Complexes and Protein Interaction

2 Di-Aqua Gadolinium Complexes and Protein Interaction

2.1 Introduction

Heptadentate ligands form lanthanide complexes, which allow an increase in hydration around the metal centre, which should improve the relaxivity of the contrast agent administered. Attempts to synthesise heptadentate ligands incorporating conventional carboxylate groups have failed for many reasons, such as a reduction in the kinetic and thermodynamic stability of the complex with respect to cation mediated or acid dissociation, meaning the species are unsuitable for use *in-vivo*.[37] In addition, heptacoordinate species are more likely to interact with endogenous anions or protein carboxylate groups present in human serum. These molecules often bind directly to the lanthanide centre, reducing the hydration number and thereby causing a reduction in the observed relaxivity.

2.2 aDO3A

As discussed in Chapter 1, Messeri *et al*[37,38] recently synthesised a heptadentate ligand, aDO3A **(2)** (Figure 2.1), which when complexed to gadolinium gave a relaxivity value of 12.3 $mM^{-1}s^{-1}$ (20 MHz, 298 K). This high relaxivity value is maintained in the presence of serum, with anion binding believed to be suppressed by electrostatic repulsion by the pendant carboxylate arms.

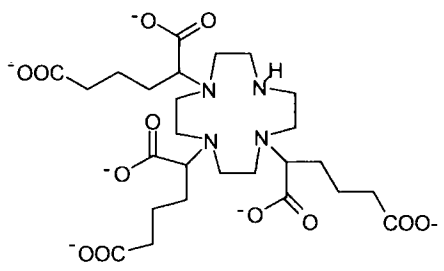

Figure 2.1: Chemical structure of aDO3A (2)

The importance the rotational correlation rate, τ_R, plays upon relaxation of paramagnetic complexes at the field strengths used in MRI (20-60 MHz 0.5-1.5 T), was earlier discussed (Chapter 1). There have been numerous attempts to slow

down the rate of rotation, including covalent or non-covalent attachment of the complex to dendrimers, macromolecules and polysaccharides.

The near ideal characteristics of the heptadentate complex, $[Gd(aDO3A)]^{3-}$, such as an optimised water exchange rate, τ_m, and electronic relaxation factor, τ_s, meant it was an excellent candidate for incorporation into high molecular weight conjugates, leading to an increased τ_R effect. The short water exchange lifetime, τ_m, results in high relaxivities being achievable, as the τ_R of the complex will be increased upon formation of the macromolecular adduct. Earlier work by Messeri *et al*[38] involved coupling of the gadolinium complex $[Gd(aDO3A)]^{3-}$, with a high molecular weight hydrophilic amide, generating the derivative, [Gd(aDO3A-AG)] with a molecular weight of 4094.

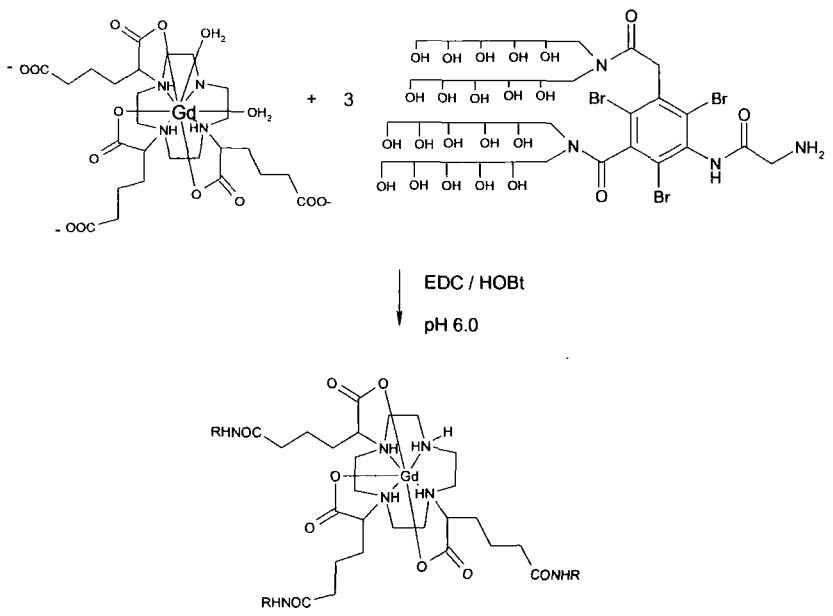

Scheme 2.1: Synthetic route for [Gd(aDO3A-AG)]

The relaxivity of the free complex [Gd(aDO3A-AG)] in water was measured as 27.7 $mM^{-1}s^{-1}$ (65 MHz, 293 K, pH 7.2); this was significantly higher than the value obtained for the parent complex. However, the high relaxivity value was not sustained in the presence of human serum, where the relaxivity fell to 15.5 $mM^{-1}s^{-1}$

(65 MHz, 293 K, pH 7.2). This is explained by the neutralisation of the overall charge of the high molecular weight conjugate. Upon formation of three amide bonds, the peripheral negative charge is neutralised, hence the complex becomes more susceptible to binding endogenous anions such as carbonate, lactate or phosphate.

2.3 Protein Binding

The most significant results to date to slow down the rate of rotation, τ_R, for a Gd (III) complex involve the non-covalent binding of a Gd (III) complex to the slowly tumbling macromolecule human serum albumin, through incorporation of hydrophobic substituents. It is well established that the presence of hydrophobic moieties are the basic requirements for binding a substrate to serum as well as the effect of negative charges on the complex.[3]

$[Gd(aDO3A)]^{3-}$ has a peripheral negative charge, hence the introduction of a hydrophobic moiety should enhance the binding affinity for the serum protein, resulting in an increase in the rotational correlation time, which should represent an ideal heptadentate contrast agent. Inserting an aromatic functionalised group would increase the hydrophobicity of the complex as well as facilitating studies into the luminescence behaviour of the related Eu (III) or Tb (III) complexes by using the aryl moiety as a sensitiser for lanthanide emission.

As a result of extensive research involving the study of human serum albumin, including competitive assays and detailed investigations regarding the binding interaction of several drugs and metabolites, detailed information regarding the binding domains of the protein has been obtained.[3] This provides definition of the structural properties that may enhance binding.

2.4 Emissive Lanthanide Complexes

2.4.1 Lanthanide Luminescence

The lanthanides usually exist as trivalent cations, in which case their electronic configuration is $[Xe]f^n$ where $(0 \leq n \leq 14)$. The transitions of the *f* electrons are responsible for the interesting photophysical properties of the lanthanide (III) ions such as large Stokes shifts, long lived luminescence and sharp absorption and emission lines.[108,109] The valence 4*f* electrons of the lanthanide (III) ions are well shielded from the environment by $5s^2$ and $5p^6$ shells, resulting in minimal involvement in binding. The strong shielding effect results in small values for ligand field splitting which are rarely more than a few hundred cm^{-1}. Minimal interactions with the ligand field and 4*f* electrons allow limited mixing of electronic and vibrational wavefunctions, which are Laporte forbidden. The forbidden nature of the *f-f* transitions makes photoexcitation of the lanthanide (III) ions difficult as they have very weak, extinction coefficients, typically in the range of 0.5-3 dm^3 mol^{-1} cm^{-1}.[109]

2.4.2 Excitation Methods

Direct excitation can be achieved using a laser but a more practical method involves exciting the lanthanide (III) ion indirectly following incorporation of a sensitising chromophore. Ordinarily, the presence of a chromophore, absorbing incident radiation would further decrease the fluorescent yield of the metal ion. However, by exciting the aromatic chromophore in this ligand, it is possible to excite the lanthanide (III) ion, which is referred to as sensitised emission (Figure 2.2). The incorporated chromophore, usually an organic compound should possess a high extinction coefficient, which transfers energy to the proximate lanthanide (III) ion, resulting in excitation.[108,109]

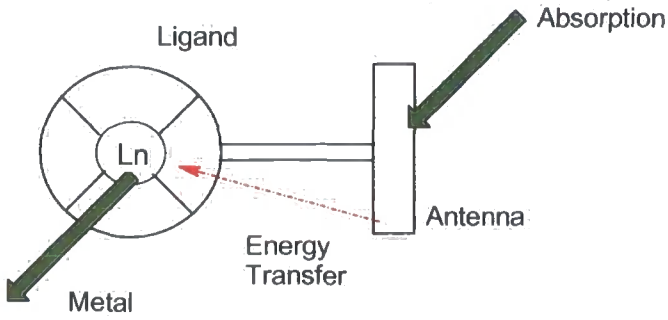

Figure 2.2: The principle of sensitised emission. Energy transfer is favoured by a short distance between the aryl sensitizer and the metal ion[108]

The acting chromophore also known as the antenna group excites the lanthanide (III) ion via an intermolecular energy transfer mechanism. Following excitation of the lanthanide (III) ion, there are three excited states that may be perturbed leading to emission, including the singlet state of the chromophore, its intermediate triplet excited state and the excited state of the lanthanide ion. These photophysical processes are depicted in Figure 2.3.[110]

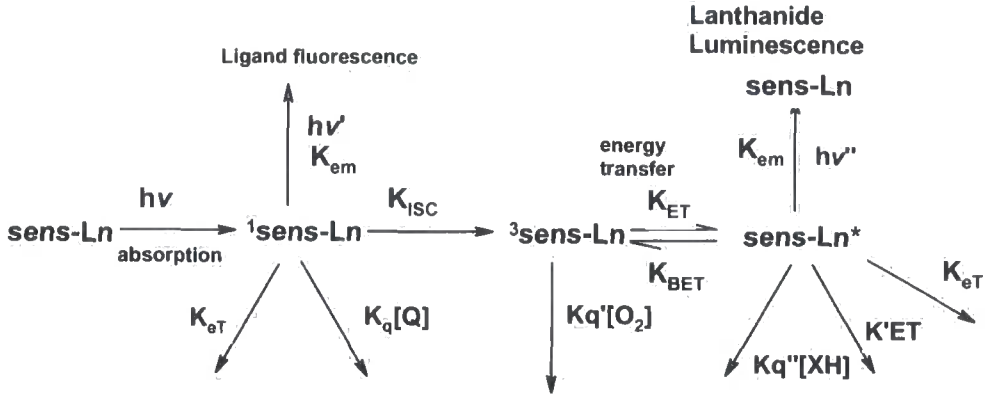

Figure 2.3: Scheme showing the three main photophysical processes occurring during sensitised lanthanide luminescence[110]

The emissive states of the lanthanide can be quenched by vibrational energy transfer to higher harmonics of solvent and ligand oscillators, i.e. OH and amine NH groups. Therefore, to make lanthanide luminescence as effective as possible, the ligand ideally should effectively shield the lanthanide ion from the quenching effect of OH oscillators in water.[109,111]

The gadolinium (III) ion has a very long electronic relaxation time, making it suitable for use in MRI, but its extreme line broadening makes NMR analysis impossible. The Gd (III) ion is also unhelpful in fluorescence studies, as a

consequence of the large difference between the ground state ($^8S_{7/2}$) and its first excited state ($^6P_{7/2}$). The neighbouring ion Eu (III) ion emits fairly strongly in the visible region of the spectrum when directly excited at 397 nm and does not possess the limitations observed for Gd (III). Therefore, as a result of similarities in their ionic radii, Eu (III) analogues can be used as valid models to provide information regarding the properties of gadolinium (III) complexes in solution.

2.5 Synthesis

Initial work was directed towards the synthesis of the macrocyclic ligand 1,4,7,-tris-[4'-methoxycarbonyl-1'-methoxycarbonylbutyl]-1,4,7,10-tetraazacyclododecane also known as aDO3A **(2)**, using the synthetic route established by Messeri *et al*[37,38]. This is shown in Scheme 2.2.

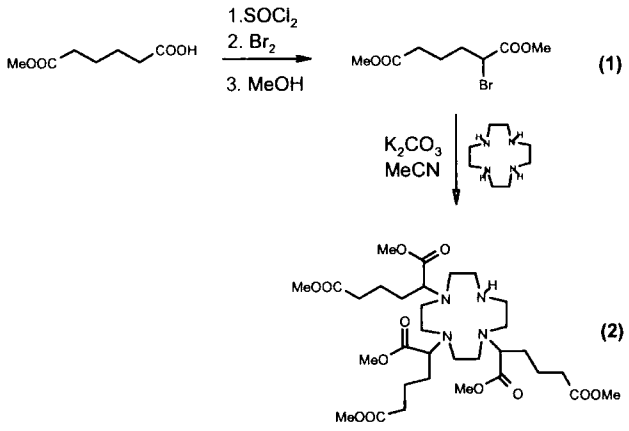

Scheme 2.2: Synthetic route for the preparation of aDO3A (2)

1,4,7,10-Tetraazacyclododecane was alkylated using 2.9 equivalents of dimethyl 2-bromo-adipate **(1)** in the presence of potassium carbonate as the selected base and hot acetonitrile. Attempts had been made to synthesise the product using the weaker base, sodium hydrogen carbonate, which was believed to increase the selectivity of the reaction, producing an improved yield of the required tri-substituted product, rather than the over alkylated tetra substituted specie. However, the weaker base resulted in an increased amount of the undesired carbamate by-product being produced. This results from hydrogen carbonate attack on one or more of the cyclen ring N-H groups. Although, carbamate by products were still present from alkylation methods using potassium carbonate, the yield

was found to be far less. The reaction mixture was heated at 60°C for 36 hours; increased reaction periods were found to increase the yield of tetrasubstituted derivatives. The tri-alkylated product **(2)** was isolated from its impurities following chromatographic purification and was obtained in a moderate yield of 33%.

The tri-alkylated product was then reacted further following alkylation of the remaining secondary NH position. Initially, three analogues of the parent $[Gd(aDO3A)]^{3-}$ complex were synthesised, incorporating a hydrophobic aromatic group. Earlier work in this study was carried out in collaboration with S. Burns an undergraduate project student. Substitution of the free NH on the cyclen ring was carried out in a similar fashion for each of the aDO3A analogues. The synthesis of a tert-butyl benzyl analogue of **(3)** is shown in Scheme 2.3.

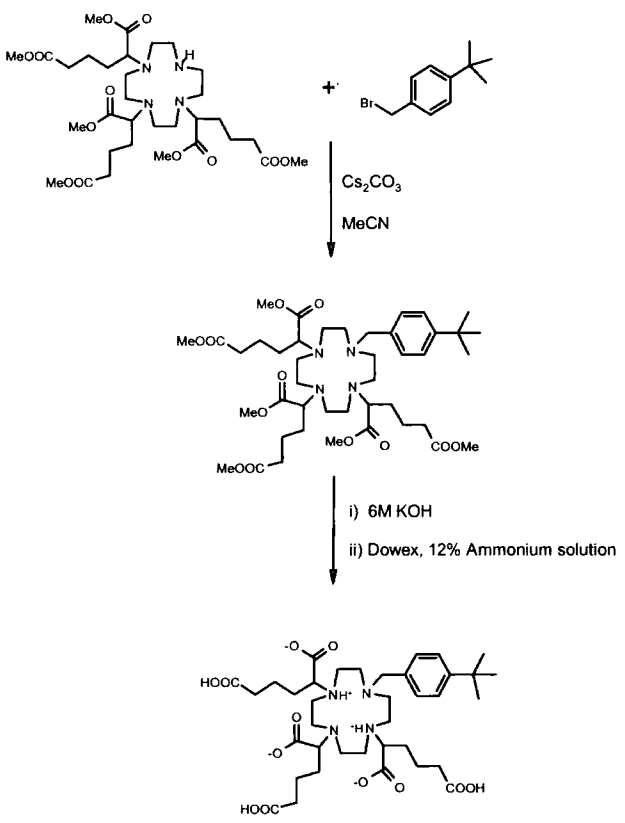

Scheme 2.3: Synthetic route to the tert-butyl benzyl derivative (3)

The synthesis of **(3)** involved alkylation of the free NH group of 1,4,7,-tris-[(4'-methoxycarbonyl)-1'methoxycarbonylbutyl]-1,4,7,10,-tetraazacyclododecane **(2)**, by heating at 60°C, in the presence of 4-tertbutyl-benzyl bromide and caesium carbonate in hot acetonitrile. Potassium hydroxide solution (6 M) was used to remove the methyl ester protecting groups by heating overnight at 90°C. Complete hydrolysis was confirmed using ^{1}H NMR, where the characteristic methyl resonances in the region of 3.50 to 3.75 ppm were lost, giving rise to the ligand $\mathbf{L^1}$. Europium (III) and gadolinium (III) lanthanide complexes of $\mathbf{L^1}$ were synthesised, allowing both relaxometric and luminescence studies. The complexes were made following reaction of ligand $\mathbf{L^1}$ with the hydrated lanthanide chloride salt at pH 5.5 (90°C, 18 hours see Scheme 2.4).

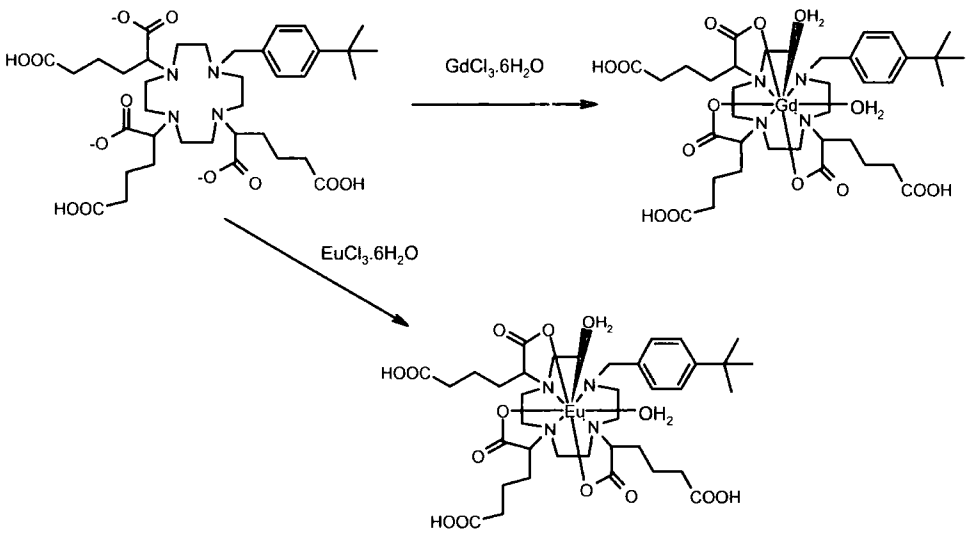

Scheme 2.4: Synthetic route for the complexation of $\mathbf{L^1}$

The remaining two ligands involved in earlier work involved the insertion of a longer length pendant arm varying slightly in lipophilicity. The synthesis of the pendant arms toluene-4-sulfonic acid 2-(-4-methoxy-benzyloxy)-ethyl-ester **(6)** and -4-sulfonic acid 2-(-4-tert-butyl-benzloxy)-ethyl-ester **(7)** was undertaken by the general method shown in Scheme 2.5.

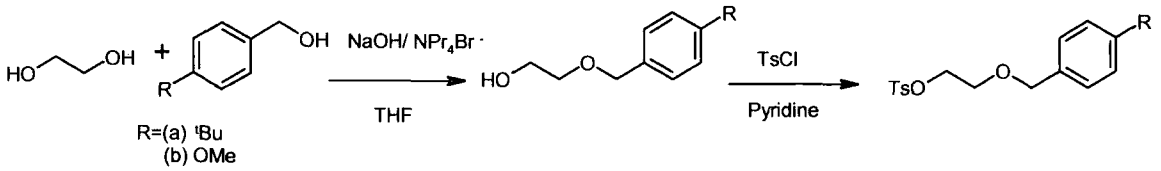

Scheme 2.5: Synthetic route for the synthesis of the pendant arm (6) & (7)

The alcohol was synthesised from ethylene glycol and 4-tert-butyl benzyl bromide; attempts to form the bromide or triflate from the alcohol failed, therefore the alternate tosylate was synthesised in 73% yield. The final arm was added to the ligand **(2)** using the same method as shown in Scheme 2.4. The lability of the tosylate leaving group resulted in completion of the reaction in approximately four hours. The gadolinium complexes were synthesised by the same method as for $[GdL^1]^{3-}$, (Scheme 2.4) and the three gadolinium (III) complexes are shown in Scheme 2.6. The europium (III) analogue was also synthesised for L^2.

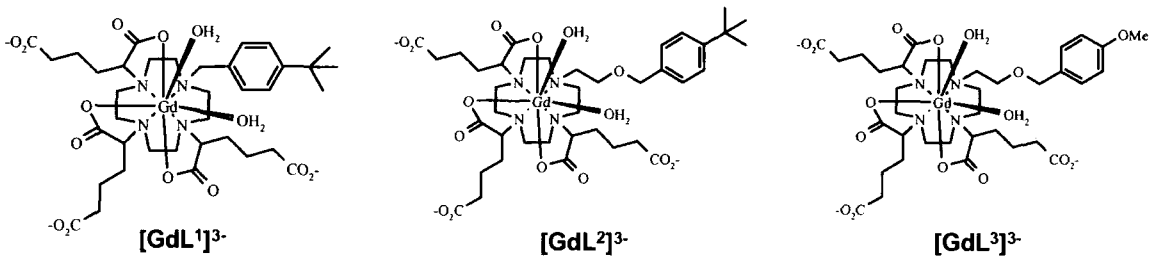

Scheme 2.6: Chemical structures of the gadolinium complexes $[GdL^1]^{3-}$, $[GdL^2]^{3-}$ and $[GdL^3]^{3-}$.

2.6 Luminescence Emission Spectra

The metal emission spectrum for each of the europium complexes $[EuL^1]^{3-}$, $[EuL^2]^{3-}$ and $[EuL^3]^{3-}$ was recorded in water. Each of the europium (III) complexes produced spectra of similar form. Figure 2.4 shows that obtained from the complex $[EuL^2]^{3-}$.

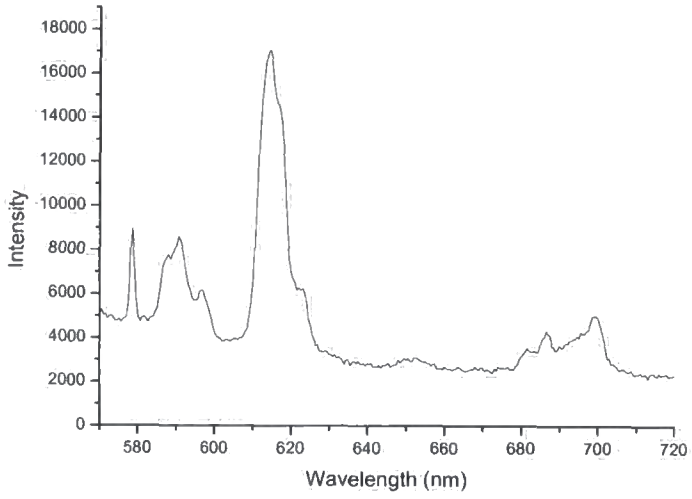

Figure 2.4: Europium emission spectrum obtained for $[EuL^2]^{3-}$ in water, λ_{exc} = 309 nm, 420 nm filter.

The spectrum was found to consist of five distinct bands. From left to right these bands represented the $\Delta J = 0, 1, 2, 3, 4$ transitions, originating from the emissive $^5D_0$ level of Eu (III) and terminating in the ground state $^7F_0$, $^7F_1$, $^7F_2$, $^7F_3$, $^7F_4$ levels respectively. Figure 2.5 shows the energy level diagram of the 4*f* levels involved in Eu (III) luminescence.[109,110,111]

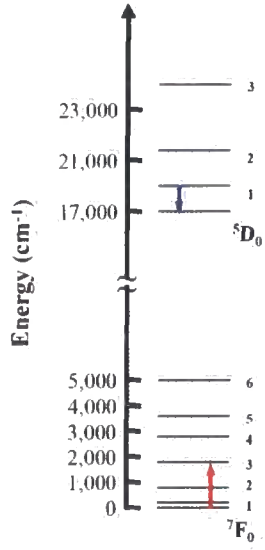

Figure 2.5: Partial energy level diagram representing the 4*f* energy levels involved in Eu (III) luminescence

The bands of the spectrum are fairly sharp resulting from the contracted nature of the europium *f* orbitals interacting weakly with the ligand. The $\Delta J = 2$ and $\Delta J = 4$ bands are termed hypersensitive bands, and are particularly sensitive to the co-ordination environment of the Eu (III) ion. The excited Eu (III) ions can be quenched following vibrational energy transfer. If a species can reversibly bind directly to the Eu (III) centre causing displacement of water molecules then the emission intensity and lifetime can be dramatically altered. This has been demonstrated by Parker and co-workers who studied a variety of anions, such as phosphate, acetate, lactate, carbonate and citrate for a series of europium complexes and reported their differing influences upon the emission spectra obtained.[15,16,37,112]

To assess anion binding, emission spectra for the europium (III) complex, **$[EuL^2]^{3-}$** were recorded in water, in a mixed anion solution consisting of 30 mM $NaHCO_3$, 100 mM NaCl, 0.9 mM Na_2HPO_4, 0.13 M sodium citrate, 2.3 mM sodium lactate and also in HCO_3^- solution, following direct excitation of europium (III) at 397 nm, (Figure 2.6).

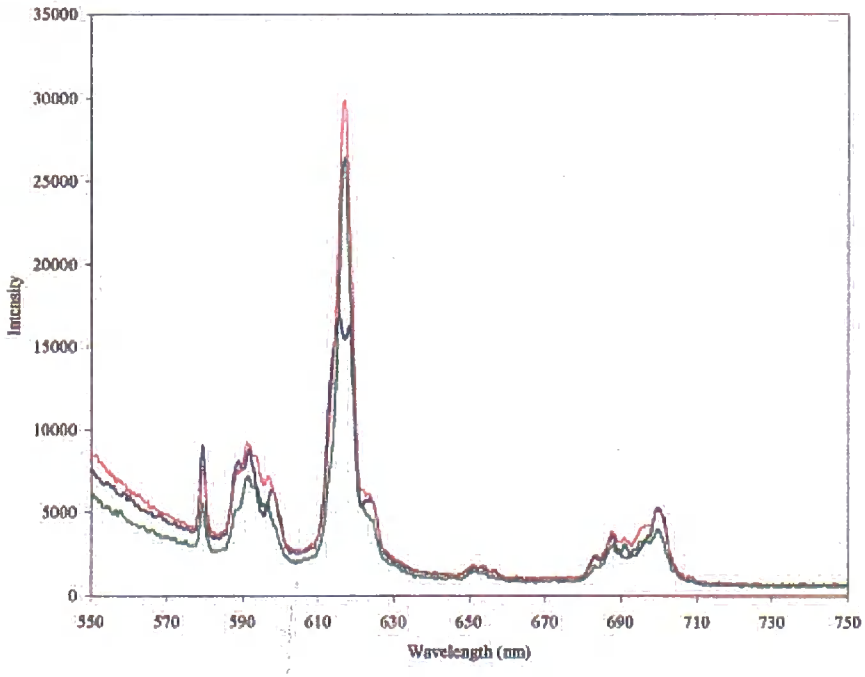

Figure 2.6: Europium emission spectra of $[EuL^2]^{3-}$ measured in the presence of water (blue), mixed anion solution (pink) and HCO_3^- solution (green)

Figure 2.6 shows there are obvious differences between the spectrum obtained in water compared to that measured in anion solution. The form and intensity of both the $\Delta J=2$ and $\Delta J=4$ emission band change and there is a two fold increase in intensity of the $\Delta J=2$ manifold, corresponding to displacement of bound water molecules by the competing anions in solution ($q=2 \rightarrow q=0$). As the spectrum of the complex in HCO_3^- is almost identical to that in mixed anion solution it can be seen that carbonate binds preferentially. The hypothesised formation of ternary complexes by anions can be seen in Figure 2.7.

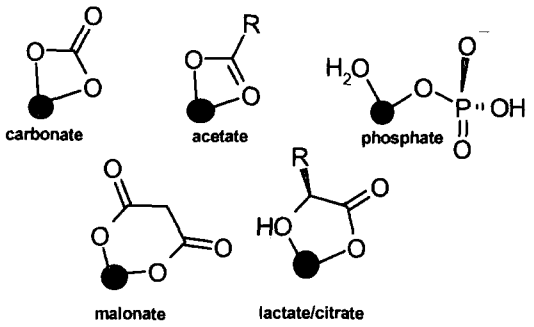

Figure 2.7: Representation of the hypothesised formation of ternary anion complexes

The affinity of CO_3^{2-}/HCO_3^- for the negatively charged $[EuL^2]^{3-}$ ligand is expected to be lower than for neutral complexes, due to the increased electrostatic repulsion between the complex and the anions.[15,16,37]

2.7 Lanthanide Hydration States

The hydration number (q) can be determined for Eu (III) complexes by measuring the rate constants for radiative decay of the Eu $^5D_0$ excited state in both H_2O and D_2O The technique is usually associated with an error of 20%.[113] Application of a correction factor in Equation (2.1) allows calculation of q values, where A is a constant of 1.2 for europium complexes, Δk is the difference between the rate constant measured in H_2O and D_2O and the correction factor (associated with the quenching effect of unbound waters) to be applied for Eu (III) is -0.25.[111] The degree of hydration of $[EuL^1]^{3-}$ and $[EuL^2]^{3-}$ in the presence of excess carbonate was also measured.

$$q = A[(k_{H_2O} - k_{D_2O}) - \Delta k_{corr}] \quad \textbf{(2.1)}$$

Complex	$k(H_2O)$ ms^{-1}	$k(D_2O)$ ms^{-1}	q
$[EuL^1]^{3-}$	3.33	1.18	2.28
$[EuL^1]^{3-}$/ bicarbonate	2.27	0.99	1.24
$[EuL^2]^{3-}$	2.86	0.92	2.03
$[EuL^2]^{3-}$/ bicarbonate	1.82	0.88	0.83

Table 2.1: Rate constants for the depopulation of the excited state of $[EuL^2]^{3-}$ (approximately 0.1 mM complex, added bicarbonate concentration 30 mM).

The q values obtained (Table 2.1) show there are two water molecules bound to the europium (III) centre for each complex, similar to the parent compound, $[Eu(aDO3A)]^{3-}$. The lifetimes of the Eu (III) complexes were also measured in the presence of sodium hydrogen carbonate. The reduction in hydration number suggests the complex is only weakly binding to bicarbonate and the waters are not completely displaced by the added anion. In the presence of bovine serum albumin, BSA, (0.1 mM **$[EuL^2]^{3-}$**, 0.7 mM BSA), there was very little change in the form of the emission spectrum. This suggests there is no significant change in the coordination environment of the Eu (III) ion, also proving there is little interaction between the metal centre and the protein.

2.8 Relaxometric studies

2.8.1 Relaxivity

Proton relaxivity refers to the efficiency of a paramagnetic substance to enhance the relaxation rate of the water protons and thus its efficiency to act as a contrast agent for use in MRI.[3] Relaxivity is usually expressed in units of $mM^{-1}s^{-1}$. The magnitude gives an indication of the number of water molecules directly attached to the Gd (III) centre. For example, $[Gd(DOTA)]^-$ analogues typically have values in the range of 4-5 $mM^{-1}s^{-1}$ (298 K, 20 MHz, pH 7.4).[1]

2.8.2 Relaxivity Measurements

Longitudinal proton relaxation rates were measured by the common (180° -τ- 90°) inversion recovery pulse sequence, using a custom built 65 MHz NMR

spectrometer, operating at ambient temperature 295 K or a Bruker Minispec Mq60 instrument operating at 20 MHz and 310 K. Relaxivity values can be calculated according to the Equations 2.2 and 2.3, where (d) is the diamagnetic contribution and (p) is the paramagnetic contribution to the observed relaxation rate.[1,3]

$$\frac{1}{T_1^{obs}} = R_1^{obs} = R_{1p} + R_{1d} \quad \textbf{(2.2)}$$

$$R_{1p} = \frac{1}{T_1^{obs}} - \frac{1}{T_1^{d}} \quad \textbf{(2.3)}$$

The diamagnetic contributions of water, nitric acid and aqueous solutions of human serum albumin were determined from the relaxivity measurements for a series of gadolinium standards in water, in collaboration with A. Congreve. The diamagnetic contributions determined for the Bruker Minispec instrument (310 K) were 0.25 s^{-1} (water), 0.26 s^{-1} (2.5 M nitric acid solution) and 0.38 s^{-1} (0.7 mM human serum albumin solution). The diamagnetic correction values for water and nitric acid determined for the 65 MHz spectrometer by M. Lowe were 0.38 s^{-1} and 0.26 s^{-1} respectively.

The concentration of gadolinium in the aqueous relaxivity samples was determined following digestion using an equal volume of 5 M nitric acid. The relaxivity of free gadolinium (III) in 2.5 M nitric acid at 20 MHz, 310 K was measured as 8.74 $mmol^{-1}s^{-1}$, compared to the value of 11.66 $mmol^{-1}s^{-1}$ at 65 MHz, 295 K. The relaxivity of the samples was determined using Equation 2.4.

$$r_{1p} = \frac{R_{1p}}{[Gd]} \quad \textbf{(2.4)}$$

2.8.3 Relaxivity measurements of $[GdL^1]^{3-}$, $[GdL^2]^{3-}$ and $[GdL^3]^{3-}$

The relaxivities of the three gadolinium complexes were also measured in the presence of bovine serum albumin to assess the enhancement upon binding Table

2.2).

Complex	Free complex ($mM^{-1}s^{-1}$)	Bound BSA complex ($mM^{-1}s^{-1}$)
$[GdL^1]^{3-}$	8.7	17.1
$[GdL^2]^{3-}$	10.2	12.2
$[GdL^3]^{3-}$	9.0	12.0

Table 2.2: Relaxivity values of each complex as the free unbound specie and in the presence of BSA (0.7 mM), 65.6 MHz, 295 K.

The relaxivity values obtained were of similar magnitude to that for the parent complex, $[Gd(aDO3A)]^{3-}$ of 13.9 $mM^{-1}s^{-1}$ (65.6 MHz, 295 K, pH 7.20).[38] Upon addition of BSA (0.7 mM *in vivo* concentration), the relaxivity was enhanced. This suggests the complex remains as a di-aqua species but the binding interaction with the protein was relatively weak, compared to some of the complexes discussed earlier in Chapter 1. The gadolinium complex, [Gd-(PCTP)-[13] has a relaxivity of 7.7 $mM^{-1}s^{-1}$ (20 MHz, 298 K), which increases significantly for the protein bound adduct of [Gd-(PCTP)-[13]-HSA] to a limiting value of 45 $mM^{-1}s^{-1}$ (20 MHz, 298 K).[3]

For each complex, the concentration of BSA was gradually increased beyond 0.7 mM, and the relaxivity values were measured. The form of the binding isotherm is determined by the strength of the binding interaction and for weakly bound complexes a limiting value may not be reached. The gadolinium (III) complexes, $\mathbf{[GdL^2]^{3-}}$ and $\mathbf{[GdL^3]^{3-}}$ were found to exhibit no significant enhancement of relaxivity upon increasing BSA addition. In comparison for $\mathbf{[GdL^1]^{3-}}$ moderate increases in relaxivity resulted upon addition of excess amounts of protein (Figure 2.8).

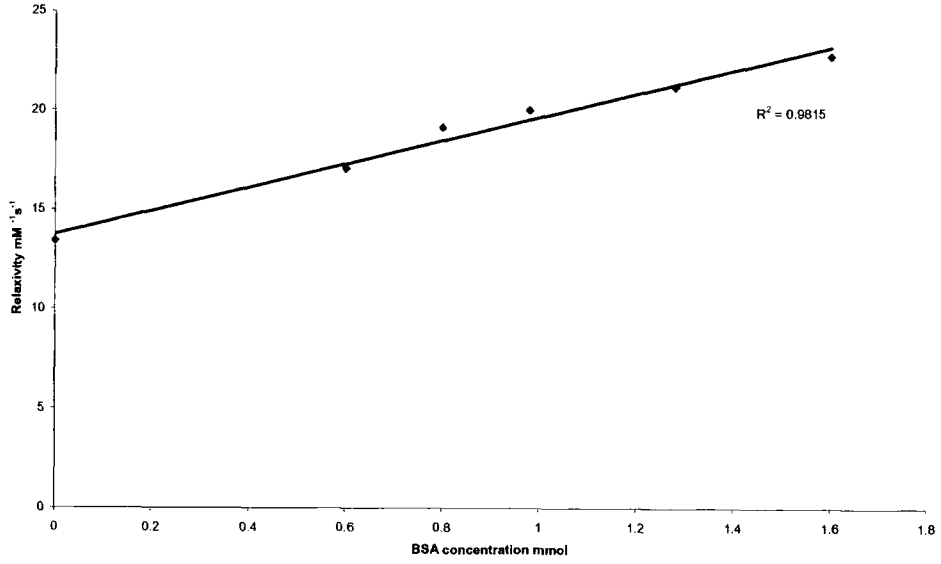

Figure 2.8: Relaxivity dependence of $[GdL^1]^{3-}$ upon addition of increasing BSA concentrations (0.34 mM, 65.6 MHz, 298 K)

The relaxivity dependence is expected to be a saturation curve. However, due to the limited solubility of the protein, it was not possible to obtain sufficient data points to allow the binding constant, K_A to be estimated accurately.

2.8.4 Nuclear Magnetic Resonance Dispersion (NMRD) Profiles

As a result of the strong temperature and field dependence of proton relaxation rate, relaxivity measurements made at a single field and temperature yield little information regarding the behaviour of a paramagnetic complex. Therefore, it is now common practice to study the relaxation rate at variable field over four orders of magnitude. The NMRD profile was obtained for the gadolinium complex, $[GdL^3]^{3-}$ by measuring the proton relaxation rate between 0.01 and 65 MHz. The NMRD profile obtained is shown in Figure 2.9.

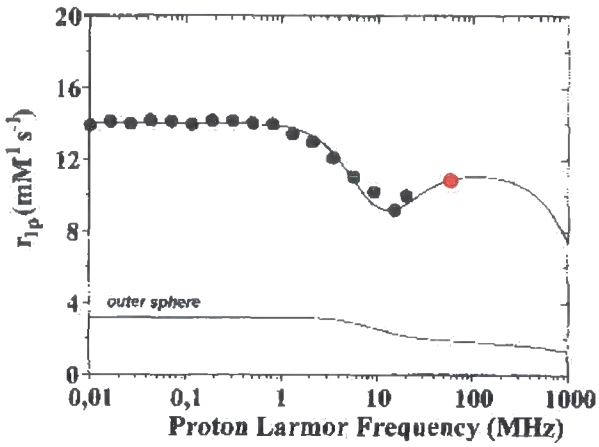

Figure 2.9: $1/T_1$ NMRD profile for $[GdL^1]^{3-}$ at 298 K. The lower curve represents the calculated outer sphere contributions to the profile. The red data point corresponds to the 65 MHz relaxivity value measured independently. The line shows the fit to the experimental data set. The lower curve represents the calculated outer sphere relaxivity.

The peak of relaxivity around 100 MHz reproduces the characteristic relaxivity peak of slowly tumbling systems and here suggests both a short electronic relaxation time and the dependence of relaxivity upon the rotational dynamics of the complex. By adopting some standard values, e.g. q = 2, the fitting of the NMRD profile using established methods allows a determination of the parameters which determine the overall relaxivity (Table 2.3). In addition, parameters such as water exchange rate ($K_{ev} = 1 / \tau_m$) and rotational correlation time, τ_R, of Ln (III) complexes can be obtained using ^{17}O NMR spectroscopy studies. Over recent years, confidence has grown in this technique as more data is acquired for the fitting of these profiles.

Parameter	^{17}O NMR[a]	NMRD[b]
$^{c}\Delta^2$ (s^{-2})	8.8×10^{19}	8.8×10^{19}
τ_v (ps)	15	15
τ_R (ns)	0.12	0.12
τ_m (ns)	38	40
r (Å)	2.98	2.98
q	2	2

a (Å)	-	3.9
D (cm^2 s^{-1})	-	2.24×10^{-5}

Table 2.3: Parameters obtained from the fitting of ^{17}O NMR and spectroscopic NMRD data for $[GdL^3]^{3-}$ measured independently in Turin, Italy. [a] Measured at 2.1 T, 4.4 mM solution; [b] Measured at 298 K; [c]Δ^2 is the mean squared zero field splitting (ZFS) energy.

In the case of small Gd (III) chelates the water exchange lifetime, τ_m, may be long enough to become a limiting factor in the relaxation enhancement exhibited by Gd (III) complexes. The ^{17}O NMR spectra obtained show the transverse relaxation rate of the ^{17}O NMR resonance increases as the temperature decreases for **$[GdL^3]^{3-}$**, consistent with fast exchange conditions (Figure 2.10).

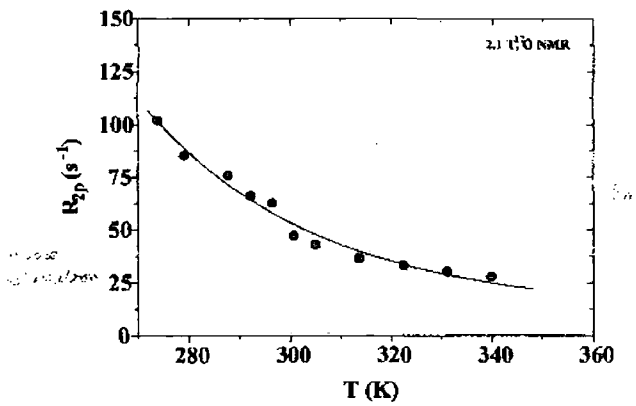

Figure 2.10: Temperature dependence of the paramagnetic contribution to the transverse ^{17}O NMR water relaxation rates of a 4.4 mM solution of $[GdL^3]^{3-}$ (2.1 T).

When the Gd (III) complex is bound to a slowly tumbling substrate, such as serum albumin the optimum value for the water exchange time, τ_m, is in the range of a few nanoseconds. The complex, **$[GdL^3]^{3-}$**, was found to have a τ_m value of approximately 39 ns, which is comparable to other di-aqua species, such as the parent complex $[Gd(aDO3A)]^{3-}$ whose water exchange time is approximately 30 ns.

As discussed earlier, for low molecular weight Gd (III) chelates the rotational correlation time, τ_R, is also a major limiting factor of relaxivity. A τ_R value of 120 ps was obtained for the complex **$[GdL^3]^{3-}$**, which is significantly higher than the rotational correlation time, τ_R, for the monoaqua complex, $[Gd(DTPA)]^{2-}$ (RMM

388.26) of 58 ps.[1]

Figure 2.11 is a simulation of the possible relaxivity values achievable had the τ_R, value of **[GdL^3]$^{3-}$** been 100 times greater. The peak at 91 mM^{-1}s^{-1} of approximately 60 MHz is unlikely to be obtained unless the binding constant for the non-covalent interaction between the protein and the complex is enhanced.

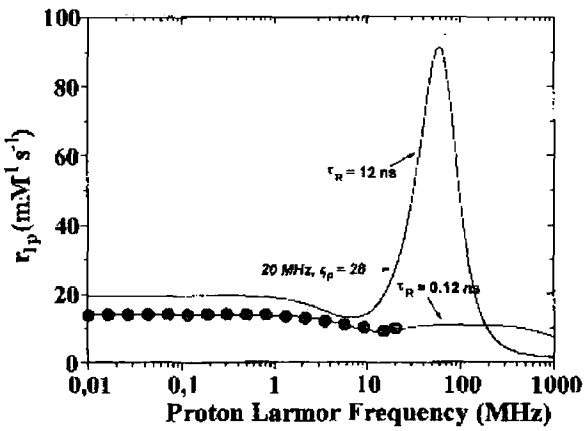

Figure 2.11: Simulation of the relaxivity theoretically achievable should the value of rotational correlation time, τ_R, be increased by a factor of 100 for [GdL^3]$^{3-}$

The relationship between the water proton relaxation rate and human serum albumin concentration is shown in Figure 2.12. From the plot an estimation of the binding strength, K_A for the complex **[GdL^3]$^{3-}$** to human serum albumin could be made, provided the assumption was made that there was only one binding site per protein molecule.

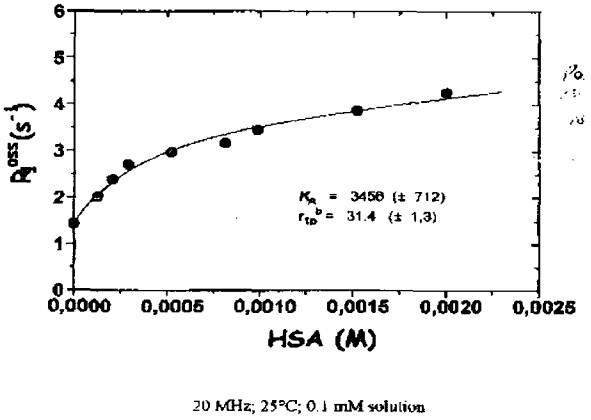

Figure 2.12: Plot of the water proton relaxation rate of a 0.1 mM solution of $[GdL^3]^{3-}$ as a function of the concentration of added human serum albumin

Direct assessments of the relaxivity of the macromolecular adduct (r_1^b) were also determined. A K_A value of 3,500 ± 7 M^{-1} was obtained which corresponds to a K_d value of 0.3 mM. Therefore, for the complex $[GdL^3]^{3-}$ in the presence of serum albumin (0.7 mM), more than 50% of the complex is bound to protein. The limiting value r_1^b value obtained at 20 MHz was 31.4 $mM^{-1}s^{-1}$, which is lower than theoretically possible, and may be related to the relatively weak interaction between the complex and the protein, or to poor coupling of the motion of the macromolecule to the lanthanide bound water molecules. Nevertheless, the relaxivity value obtained in the presence of typical serum protein concentrations is similar to that of Epix's complex MS-325.[3]

The results obtained are consistent with the hypothesis that the three complexes synthesised were di-aqua species and the usual problems associated with displacement of inner sphere water molecules in the presence of serum albumin were overcome. Although the complex, $[GdL^1]^{3-}$ was found to show some relaxivity enhancement in the presence of serum albumin the desired high relaxivity values were not achieved. This is related to the relative weakness of the binding interaction of the complex with the protein or to poor motional coupling between the macromolecule and the metal bound water molecules. Effective motional coupling is decreased for complexes in which there is rapid internal flexibility of the pendant arms. This may have been the case for the complexes $[GdL^2]^{3-}$ and

$[GdL^3]^{3-}$ with respect to $[GdL^1]^{3-}$.

2.9 Comparative Study of Structurally Related Gadolinium complexes

These results led to the design of a series of structurally related gadolinium complexes with increased hydrophobicity and rigidity of the pendant arms, in an attempt to reduce the effects of internal flexibility, preventing the complex from tumbling independently of the macromolecule. The complexes were still required to overcome displacement of water molecules in the presence of protein and needed to retain good thermodynamic and kinetic stability. The rationally designed complex, MS-325 (Figure 2.13) is reported to have a binding constant, K_A with serum albumin of 3×10^4 M^{-1}, resulting from a strong single binding site associated with the hydrophobic interaction of the bulky hydrophobic di-phenyl cyclohexyl group. Similar hydrophobic groups were incorporated into the parent complex, $[Gd(aDO3A)]^{3-}$.

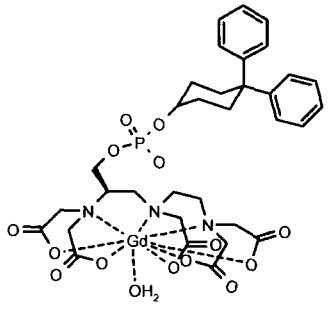

Figure 2.13: Chemical structure of the gadolinium blood pool agent MS-325

The pendant arm of L^4 was synthesised from the reaction of the starting material 3,5-di-tertbutyl-phenol with bromoethanol and potassium carbonate as a base, which was subsequently reacted with para-toluenesulphonyl chloride to generate a more labile leaving group (Scheme 2.7).

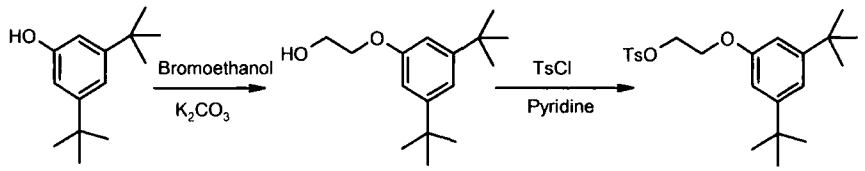

Scheme 2.7: Synthesis of the pendant arm (2-(3,5-dimethyl-phenoxy)-ethyl-p-toluene sulphonate)

The gadolinium complex **[GdL^4]$^{3-}$** (Figure 2.14) was synthesised by the same method as in Scheme 2.3.

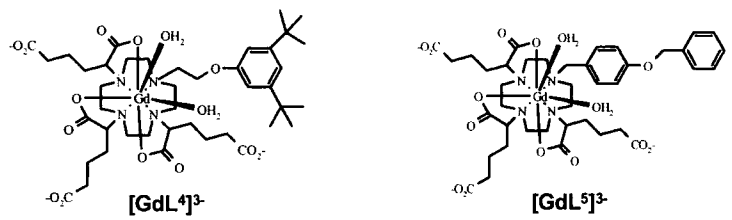

Figure 2.14: Chemical structure of [GdL^4]$^{3-}$ and [GdL^5]$^{3-}$ respectively

Complex **[GdL^5]$^{3-}$** was synthesised according to Scheme 2.3 from the direct alkylation of **(2)** and 4-benzyloxybenzyl chloride, followed by subsequent hydrolysis and reaction with hydrated gadolinium chloride (Figure 2.14).

The longitudinal proton relaxation rates were measured for **[GdL^4]$^{3-}$** and **[GdL^5]$^{3-}$** by inversion recovery methods at 65 MHz, operating at 295 K. The interaction of the complex with protein was also observed by adding bovine serum albumin (BSA) at a concentration of 0.7 mM to each sample.

Complex	Relaxivity Free complex $mM^{-1}s^1$	Relaxivity of Bound complex $mM^{-1}s^{-1}$
[GdL^4]$^{3-}$	6.9	10.0
[GdL^5]$^{3-}$	9.6	13.1

Table 2.4: Relaxivity values for complex [GdL^4]$^{3-}$ and [GdL^5] $^{3-}$65 MHz, 295 K as the free complex, and as BSA bound complex (0.7 mM added protein).

The results showed there was no significant enhancement with the interaction of BSA, suggesting there was little binding of the complex to the macromolecule.

In parallel with this study, three complexes ($[ASGdL^1]^{3-}$, $[ASGdL^2]^{3-}$ and $[ASGdL^3]^{3-}$) were synthesised and characterised by A. Subbiani, an Italian Erasmus student (see Figure 2.15).

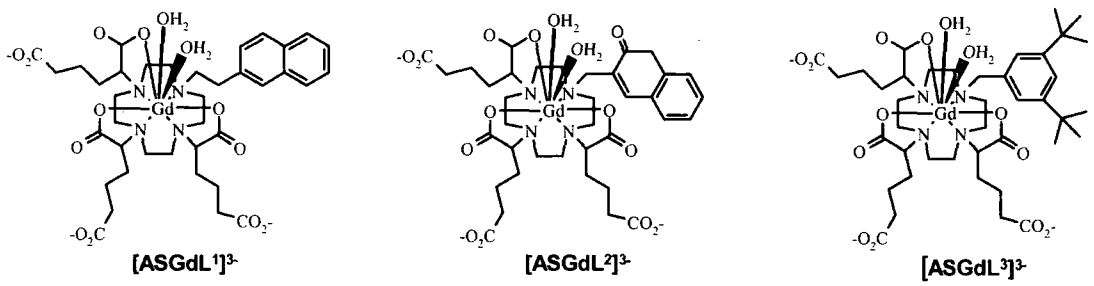

Figure 2.15: Chemical structures of the three additional gadolinium complexes

The longitudinal proton relaxation rates were measured for these complexes at 65 MHz, 295 K. The samples were analysed independently in water followed by the addition of a large excess of poly-β-cyclodextrin (20 equivalents). Cyclodextrins are truncated cone shaped molecules with hollow tapered cavities. They possess a hydrophobic central cavity suitable for the inclusion of various organic molecules and were one of the first receptor compounds recognised for the effective binding of organic substrates.[114] Poly-β-cyclodextrins are systems containing several cyclodextrin units linked through the formation of an ethereal bond at C_6 of a glycosidic residue (Figure 2.16).[115]

Figure 2.16: Structural sketch of poly-β-cyclodextrin derivative obtained by the cross linking of β-cyclodextrin monomers with 1-chloro-2,3-epoxy-propane

Poly-β-cyclodextrins are believed to contain aromatic binding sites allowing strong interaction with a functionalised complex, as was reported for hydrophobic p-bromobenzyloxysubstituents by Aime and co-workers.[115] Here the relaxivity enhancement of the macromolecular compound was reported as being 4.1 times higher than that of the free complex.

Complex	Relaxivity free complex $mM^{-1}s^{-1}$	Relaxivity Bound complex $mM^{-1}s^{-1}$
$[ASGdL^1]^{3-}$	9.7	12.01
$[ASGdL^2]^{3-}$	10.12	13.90
$[ASGdL^3]^{3-}$	11.25	14.11

Table 2.5: Relaxivity values of the complexes $[ASGdL^1]^{3-}$, $[ASGdL^2]^{3-}$ and $[ASGdL^3]^{3-}$ in water and poly-β-cyclodextrin at 65 MHz, 295 K

The magnitudes of the relaxivity values suggest each of the complexes are di-aqua species. The larger size of the poly-β-cyclodextrin causes an elongation of the molecular reorientational time of the paramagnetic macromolecular adduct, resulting in a slight increase in the relaxation enhancement. The increased values were not particularly impressive suggesting there was only a relatively weak interaction of the complex with the macromolecule.

2.9.1 Complexes with increased rigidity

It was confirmed earlier, that the weaker interaction of protein with the complexes, $[GdL^2]^{3-}$ and $[GdL^3]^{3-}$ compared to $[GdL^1]^{3-}$ may be the result of a greater degree of motional coupling between the complex and the protein, as a result of the longer pendant arm. The interaction of the bulky, hydrophobic fluorene group with serum albumin was expected to be stronger than that seen for smaller aromatic species.

Two macrocyclic ligands were synthesised incorporating the fluorene group, L^6 and L^7. The ligands differed only by the rigidity of the carbon linker used to attach the pendant arm to **(2)**. The carbon chain differed in length from C_2 $[L^6]$ to C_1 $[L^7]$ in order to assess the influences of internal flexibility of the pendant arm upon interaction with protein. The pendant arm for $[L^7]$ was purchased as 9-fluorenemethanol and converted to the tosylate **(14)** using para-toluenesulphonyl chloride in the presence of pyridine. The C_2 pendant arm derivative of $[L^6]$ involved the reduction of 9-fluorene-acetic acid using borane-THF solution to produce the alcohol **(15)**, which was then converted to the tosylate by the same procedure as that for **(14)**. The gadolinium complexes $[GdL^6]^{3-}$ and $[GdL^7]^{3-}$ (Figure 2.17) were

then generated using the same methods as those in Schemes 2.3 and 2.4.

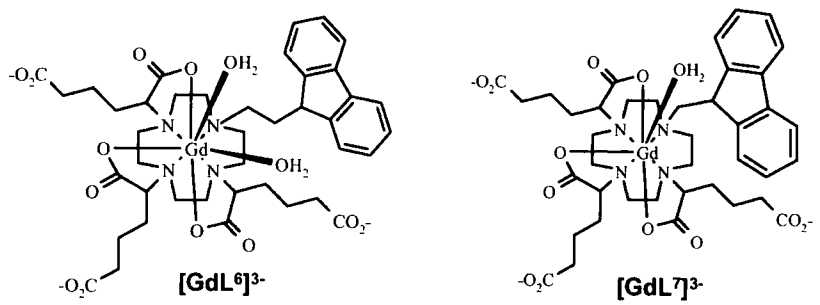

Figure 2.17: Chemical structures of $[GdL^6]^{3-}$ and $[GdL^7]^{3-}$

The relaxivity values of the gadolinium complexes $[GdL^6]^{3-}$ and $[GdL^7]^{3-}$ were measured using the Bruker Minispec spectrometer operating at 60 MHz and 310 K. The value obtained for $[GdL^6]^{3-}$ was 7.9 $mM^{-1}s^{-1}$ whilst that for the complex $[GdL^7]^{3-}$ was 3.86 $mM^{-1}s^{-1}$ suggesting that the complex was only a mono-aqua species. The relaxivity values were measured in the presence of human serum albumin, for the complexes $[GdL^6]^{3-}$ and $[GdL^7]^{3-}$. Minimal changes in relaxivity values were observed for $[GdL^6]^{3-}$ suggesting there was little interaction with protein, whereas $[GdL^7]^{3-}$ was found to be only partially soluble in the presence of serum albumin.

Relaxivity values obtained at 37°C are consistently lower than those obtained at 22°C because under conditions of fast water exchange, relaxivity is inversely proportional to temperature, as it depends primarily on the rotational correlation time, τ_R, of the whole complex.

2.9.2 A Gadolinium Acridone complex

There has been considerable interest within the Parker group towards the design of new emissive sensory systems, based upon luminescent lanthanide (III) complexes. The lanthanide (III) ions have long radiative lifetimes; an attractive feature for luminescent probes.[116] The highly fluorescent behaviour and stability of the acridone molecule (Figure 2.18) explains why it has readily been exploited as a suitable chromophore for sensitised emission within lanthanide (III) complexes.

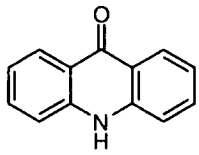

Figure 2.18: Chemical structure of acridone

Monosubstituted N-acridoneethyl 1,4,7,10-tetraazacyclododecane (Figure 2.19) was donated by Y. Bretonnéire, a post doctoral researcher within the Parker group.

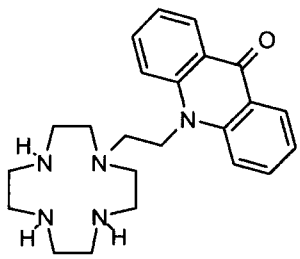

Figure 2.19: Chemical structure of monosubstituted N-acridoneethyl 1,4,7,10-tetraazacyclododecane

The remaining free NH groups of monosubstituted N-acridoneethyl 1,4,7,10-tetraazacyclododecane were alkylated using excess dimethyl 2-bromo-adipate **(1)** in the presence of hot acetonitrile and caesium carbonate as base, to produce **(18)** (Figure 2.20), which was purified by column chromatography. Following, hydrolysis of **(18)** in the presence of lithium hydroxide (1 M) the ligand **[L^8]** (Figure 2.20) was complexed using the hydrated lanthanide chloride salts of both europium (III) and gadolinium (III), to give **[GdL^8]$^{3-}$** and **[EuL^8]$^{3-}$**.

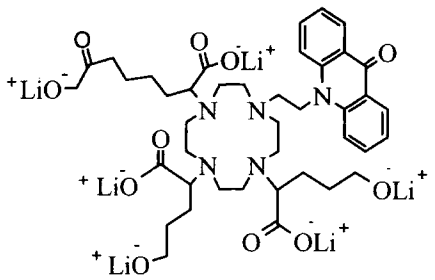

Figure 2.20: Chemical structure of the ligand [L^8]

The relaxivity of the gadolinium complex, **[GdL^8]$^{3-}$** was measured using a Bruker Minispec Mq60 spectrometer at the magnetic field strength of 60 MHz and 310 K. The relaxivity of the free complex **[GdL^8]$^{3-}$** was measured as 7.1 $mM^{-1}s^{-1}$. To a solution containing **[GdL^8]$^{3-}$** was added a small amount of human serum albumin (1 mg), which resulted in a large increase in the observed relaxivity to 28.8 $mM^{-1}s^{-1}$. This suggested the complex binds well to the protein, reducing its tumbling rate in solution. However, further additions of human serum albumin resulted in no further increase in the longitudinal relaxation rate, possibly as a result of saturation of the protein.

Europium (III) complexes with acridone ligands have been studied extensively as luminescent probes for the determination of cellular bicarbonate concentrations. The bicarbonate ion is an essential component of biological systems but little information is known about how HCO_3^- is localised within the cellular component. This is of biological importance as the concentration of HCO_3^- is responsible for controlling many physiological processes such as cyclic AMP regulation. A series of cationic, neutral and anionic europium complexes incorporating the acridone groups have been reported and their interaction with bicarbonate monitored.[117,118] Some complexes were monitored using a cellular lystate media (NIH 3T3 cells), which contains various proteins and significant concentrations of lactate and various phosphorylated species. Confocal fluorescence microscopy images of some of these complexes have been produced showing the localisation of the complex inside the mouse fibroblast NIH 3T3 cells. These are depicted in Figure 2.21.

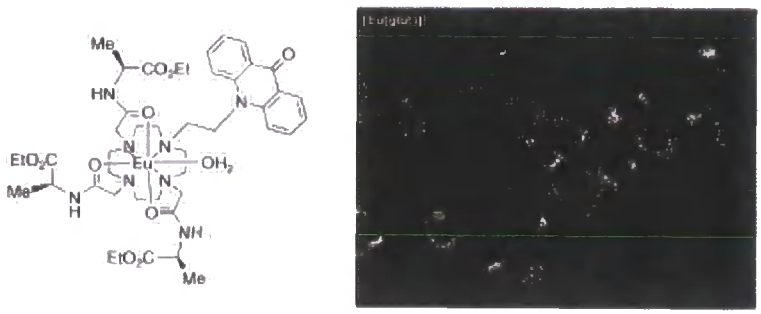

Figure 2.21: Confocal fluorescence microscopy images for the corresponding europium complex which shows the localisation of the complex inside the mouse fibroblast NIH 3T3 cells – the oval shaped dark centre being the nucleus.

The europium (III) complex $[EuL^8]^{3-}$ has very different pendant arms to the complex depicted in Figure 2.21. The pendant anionic groups are believed to play a role in the inhibition of anion binding. The complex $[EuL^8]^{3-}$ shares the same aromatic chromophore, so that the interaction with cells is of interest.

The fibroblast NIH 3T3 mouse cells were cultured to 70% confluence, and loaded with the europium complex, $[EuL^8]^{3-}$ as a DMEM solution; the loading time for the cells was 24 hours at a concentration of 0.5 mM of $[EuL^8]^{3-}$. The cells were washed with phosphate buffered saline and mounted onto slides for confocal microscopy (Zeiss LSM 510 Meta). Confocal microscopy is a type of fluorescence microscopy where a laser is used to provide the excitation light, which reflects off a dichroic mirror. The Eu (III) complex fluoresces by sensitised emission of the acridone group, and the emitted light is descanned by the same mirrors used to scan the excitation light from the laser. The light intensity is measured by a detector such as a photomultiplier tube. For the image of the Eu (III) complex the excitation wavelength was 405 nm. An emission filter (LP) of 420 nm was also used. The image taken of $[EuL^8]^{3-}$ is depicted in Figure 2.22.

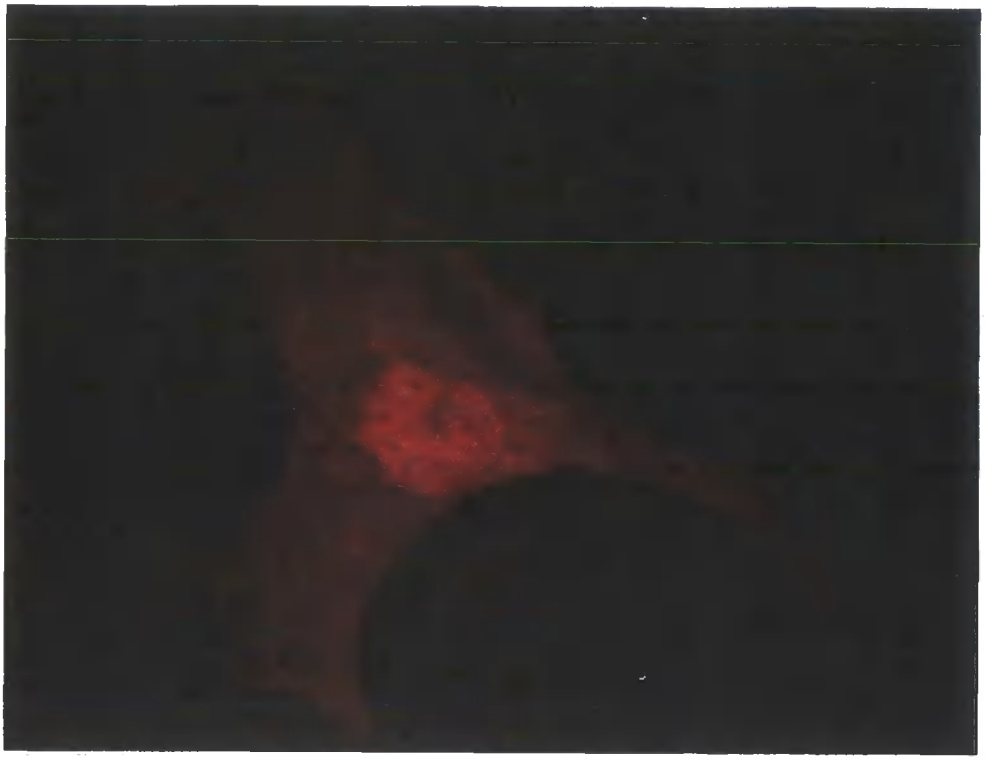

Figure 2.22: Confocal microscope image of $[EuL^8]^{3-}$ inside mouse fibroblast NIH 3T3 cells.

It can be clearly seen from the image that the complex $[EuL^8]^{3-}$ is distributed throughout the cell cytosol and appears to be particularly concentrated in the cell nucleus. Diffusion into cells is reported as particularly difficult for such anionic complexes and usually a longer loading time is required. However, the images obtained prove that $[EuL^8]^{3-}$ does diffuse into the mouse cell. The images were of relatively low intensity and it was observed that many of the cells were found to die over a period following addition of the complex. This behaviour is in contrast to the behaviour of $[EuL^6]^{3+}$ which exhibited relatively low toxicity (up to 1 mM loadings).

2.10 Effect of pH upon Relaxivity

The relaxation rates of the complexes $[GdL^1]^{3-}$ to $[GdL^8]^{3-}$ were determined at pH 5.5 as the free complex or pH 7.4 in serum solutions. However, the effect of pH towards the longitudinal relaxation rate was also determined; Figure 2.23 shows the pH dependence of $[GdL^1]^{3-}$ upon relaxivity.

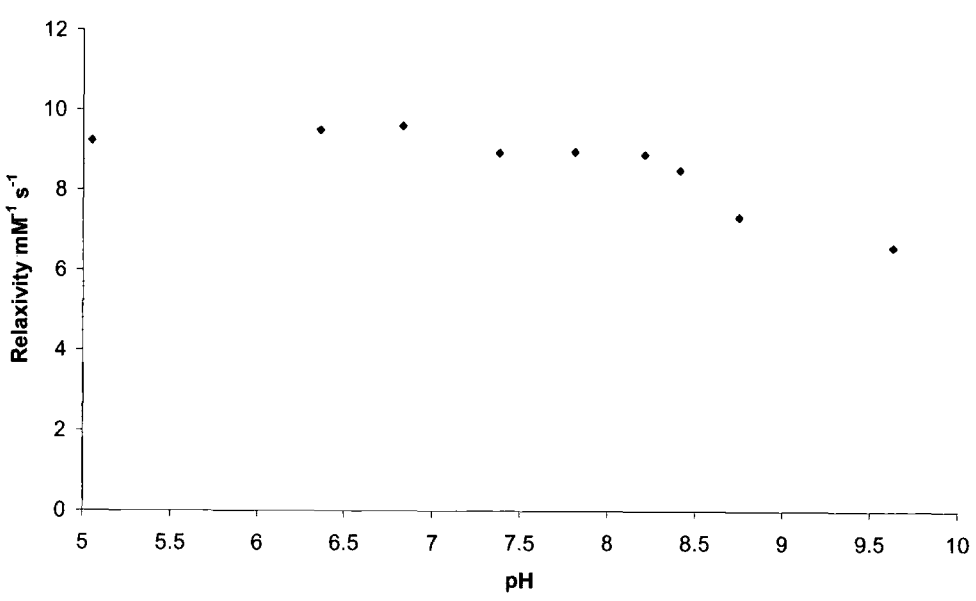

Figure 2.23: Effect of pH upon relaxivity for $[GdL^1]^{3-}$ (310 K, 20 MHz)

The observed relaxivity typically does not change below pH 6.8, however, increasing the pH above this value reveals a small reduction in the relaxivity value. This suggests that competitive anion binding may be occurring to the metal ion centre, in the form of carbonate from atmospheric carbon dioxide. The bidentate carbonate anion binds to the gadolinium centre creating a ternary complex. The pH dependence of the parent complex $[Gd(aDO3A)]^{3-}$ was determined by Messeri.[37,38] Here a decrement was seen in the observed relaxivity beyond pH 8.5 due to carbonate binding to the gadolinium (III) centre. This was confirmed from the luminescence of the europium (III) complex. At physiological pH, the parent complex, $[Gd(aDO3A)]^{3-}$ was found to possess two inner sphere water molecules. For complexes $\mathbf{[GdL^1]^{3-}}$ to $\mathbf{[GdL^8]^{3-}}$, where the free NH group on the cyclen ring is substituted, the binding of anions at physiological pH is significant. This may be explained by a loss of the hydrogen bonding network allowing easier displacement of bound water molecules by bidentate ligands.

2.11 aDO2A based systems

The network of hydrogen bonding promoted by the free NH group seen in $[Gd(aDO3A)]^{3-}$ may explain why the complex is less resistant to the binding of bidentate anions at physiological pH, compared to the tetrasubstituted complexes

$[GdL^1]^{3-}$ to **$[GdL^8]^{3-}$**.

This led to the theory that substitution of only one free NH group of the ligand 1,7-bis[(4'methoxycarbonyl)-1'-methoxycarbonylbutyl-1,4,7,10-tetraazacyclododecane (aDO2A) (Figure 2.24), incorporating a hydrophobic substituent capable of protein binding, would produce increased relaxivity values but may inhibit anion binding at physiological pH.

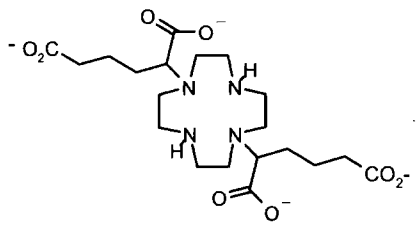

Figure 2.24: Chemical structure of the ligand aDO2A

The complex $[Gd(BOPTA)]^{2-}$ (Gadobenate) is a derivative of $[Gd(DTPA)]^{2-}$ incorporating a benzyloxy substituent, and is a promising candidate for imaging of the liver and myocardium of animals.[119] The potassium salt of 3-benzyloxy-2-chloro-propionic acid was donated by Bracco SPA (Italy). The compound was readily converted to the methyl ester following addition of methanol and acetyl chloride under anhydrous conditions to produce **(19)** (Figure 2.25).

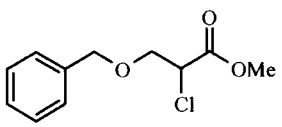

Figure 2.25 Chemical structure methyl-3-benzyloxy-2-chloro-propionate (19)

Attempts were made to directly alkylate methyl-3-benzyloxy-2-chloro-propionate **(19)** to the ligand aDO2A in the presence of hot acetonitrile and caesium carbonate. The reactions proved extremely slow even in the presence of excess amounts of **(19)**. Initial attempts to purify the crude reaction mixture by flash column chromatography failed due to the overwhelming presence of closely eluting impurities. The increased impurities observed by this reaction may have resulted from the intramolecular rearrangement of the labile methyl ester group, therefore the tertiary butyl ester was formed which was expected to have increased

stability. Similarly, the reaction of tert-butyl-3-benzyloxy-2-chloro-propionate with aDO2A proved unsuccessful. The yield of required product may be enhanced by increasing the chemical reactivity of the leaving group of the tert-butyl ester. Tert-butyl-3-benzyloxy-2-iodo-propionate was produced following a Finkelstein[120] reaction, carried out in the presence of acetone and sodium iodide. Frustratingly, still no reaction occurred with the addition of aDO2A. The initial reaction route was repeated using an increased scale in attempt to directly alkylate aDO2A using excess amounts of **(19)**. Careful purification by flash column chromatography resulted in very small yield of the required product (less than 5%). However, subsequent hydrolysis and purification using strong cation exchange resin resulted in the yield of product being negligible.

2.12 Suggestions for Further Work

The aDO2A based system still remains of interest as the binding of anions may be significantly decreased due to the increased hydrogen bonding network. Attempts to synthesise a similar based system following substitution of the benzyloxy pendant arm for a more hydrophobic tri-phenyl substituent may prove more successful.

2.13 Summary

The relaxivity enhancement obtained for $[GdL^1]^{3-}$ and $[GdL^3]^{3-}$ in the presence of serum protein concentrations was significant but much less than the theoretical maximum for di-aqua gadolinium complexes. A comparative analysis of several structurally related complexes gave no significant benefit, although an N-ethyl-acridone complex shows some promise.

The protein binding interaction of commercially important contrast agents is discussed later in Chapter 6, where only modest enhancements in relaxivity were displayed. This stresses the significance of some of the complexes that have been discussed here as potential contrast agents for MRI.

Chapter 3

Phosphonate based macrocyclic compounds

3 Phosphonate based macrocyclic complexes

3.1 Introduction and Synthesis

The phosphonate analogue (Figure 3.1) of the aDO3A ligand **(2)** was identified in Chapter 2 as a key ligand, which in its lanthanide complexes would possess a higher peripheral negative charge. In addition the dual basicity of the P(V) acid system allows for introduction of 3 ester groups whilst retaining a (-3) peripheral charge.

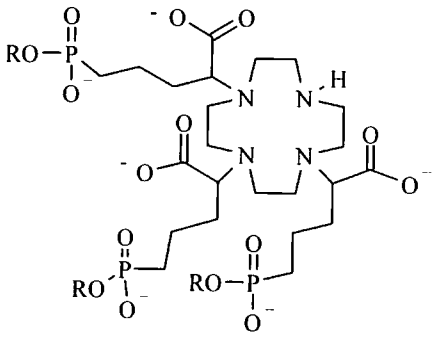

Figure 3.1: The Phosphonate target molecule based upon the ligand aDO3A (2)

The synthetic pathway began by protection of 5-bromopentanoic acid, involving conversion to the tert-butyl ester, following the method of Schmidt *et al.*[121] The alcohol was stirred in oxalyl chloride to generate the acid chloride, which was, in turn reacted with tert butanol in the presence of pyridine. The pyridine acts as a nucleophilic catalyst and a base preventing a high acid concentration from being generated. The white pyridinium salts produced from the reaction were filtered off using a short column of silica gel.

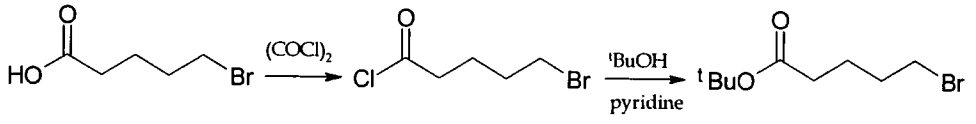

Scheme 3.1: Synthesis of tert-butyl-5-(diethoxy-phosphonyl)-pentanoate (21)

The bromo functionality of the ester **(21)** was converted into a phosphonate ester by heating under reflux in the presence of excess trimethylphosphite, via a Michaelis-Arbusov[122] reaction, to yield t-butyl-5-(dimethylphosphonyl)-pentanoate as the desired product, in moderate yield (Scheme 3.2).

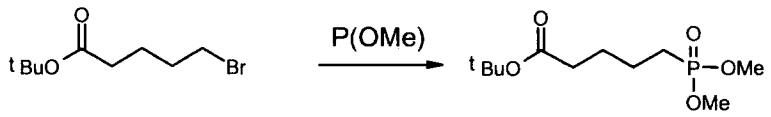

Scheme 3.2: 5-(dimethylphosphonate)-pentanoic acid-(tert-butyl) ester

Analysis of the reaction mixture by phosphorus NMR and electrospray mass spectrometry revealed the presence of dimethylated products. Such behaviour is consistent with reactive methyl groups in the phosphite reagent being susceptible to de-alkylation, following attack of Br^- by an S_N2 type mechanism. The MeBr product then again reacts with excess phosphite reagent, resulting in the generation of the two impurities shown in Scheme 3.3. Formation of such impurities from Arbusov reactions has previously been reported[123]. However, these have been found to be less prevalent with triethylphosphite as a reagent.

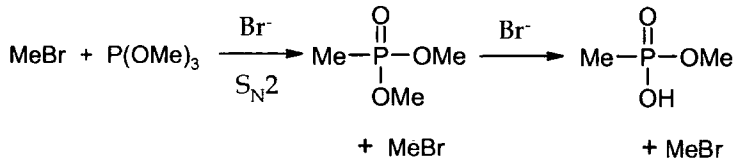

Scheme 3.3: Generation of Arbusov reaction impurities

Accordingly, tert-butyl protected 5-bromopentanoic acid **(21)** was reacted with excess triethylphosphite, no dealkylation products were produced and tert-butyl-5-(diethoxy-phosphonyl)-pentanoate **(22)** was isolated with a large increase in yield.

Deprotection of the tert-butyl ester **(22)** group using trifluoroacetic acid proceeded quantitatively to yield **(23)**. Bromination alpha to the carboxylic acid group was undertaken by using a Hell-Volhard-Zelinski[124] reaction using thionyl chloride and molecular bromine. The reaction was quenched by pouring onto cooled ethanol, resulting in the formation of the ethyl ester, **(24)**.

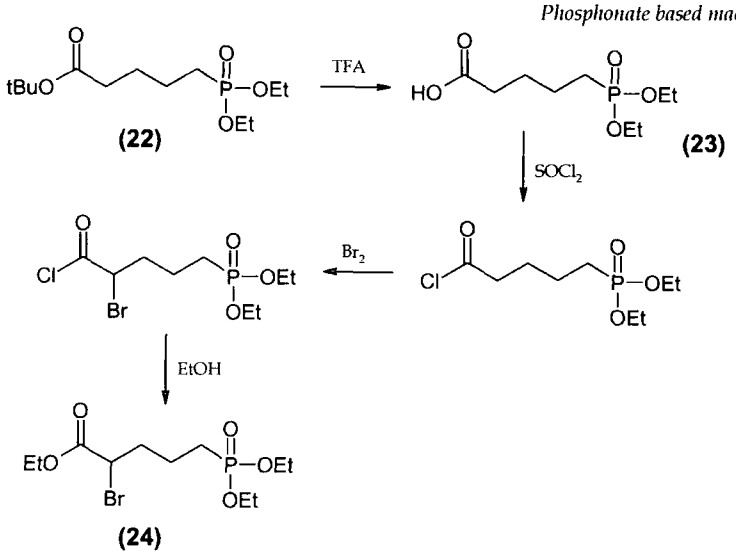

Scheme 3.4: Synthetic route for the synthesis of racemic (24)

Methanol had also been evaluated as a quenching agent but this led to generation of two major impurities as well as the required product. ^{31}P, ^{1}H NMR and ESMS analysis confirmed these impurities were associated with the exchange of ethyl groups with methyl substituents. For this reason ethanol was the preferred solvent of choice for quenching the acid bromide.

Attempts were made to alkylate directly 1,4,7,10-tetraazacyclododecane with three equivalents of **(24)**, in the presence of base and hot acetonitrile, to produce a tri-alkylated phosphonate product. This reaction was very slow and resulted in a variety of substituted products after 7 days. The desired product was isolated in extremely low yield, approximately 3%, following purification by column chromatography. Characterisation of the product revealed the presence of both tri and di-alkylated species. Unfortunately, due to their common retention values these two species could not be separated, even by reverse phase HPLC.

With this disappointing result, a new approach was attempted involving the use of the octahedral chromium tricarbonyl complex of tetraazacyclododecane, as a protecting group for three of the ring nitrogens in 1,4,7,10-tetraazacyclododecane[ref4]. The related molybdenum complex was used in a parallel manner, which was then suspended into DMF and benzyl bromide was added. Decomplexation of the molybdenum moiety in aqueous acid resulted in the

isolation of the monoalkylated amine. Alkylation of the remaining three nitrogens of the cyclen ring was attempted by adding excess **(24)** in the presence of dry acetonitrile and base, and heating under reflux. Again, attempts were made to purify the crude reaction mixture, to isolate the desired tetra-substituted product, from which the protecting group could be removed following hydrogenation. Unfortunately, the desired product was never isolated from its major impurities.

The next plan of attack involved slightly modifying the method of Yang *et al*[125], which involved the reaction of three equivalents of ethyl trifluoroacetate in the presence of methanol and triethylamine to produce a protected, trisubstitued cyclen. 1,4,7,10 tris-trifluoromethyl carbonyl-12-N-4 **(25)** was isolated in respectable yield of 80%. The required product was isolated by passing through a short silica gel column. The tri-substituted product has a much higher R_f value than any of the other related species. Subsequent alkylation of the free NH group of the macrocycle, using BOC anhydride was achieved in methanol **(26)**. Again, a high yield of material was obtained following purification by column chromatography. Straightforward deprotection of the ethyl trifluoroacetate arms was carried out in the presence of potassium hydroxide, to yield the monocarbamate **(27)**. Excess amounts of **(24)** were added to **(27)** in the presence of caesium carbonate as base and hot acetonitrile. The required product **(28)** was isolated following careful purification by flash column chromatography with a low reaction yield of 22%. The BOC protecting group was removed using trifluoroacetic acid in the presence of dichloromethane to yield **(29)** quantitatively (Scheme 3.5).

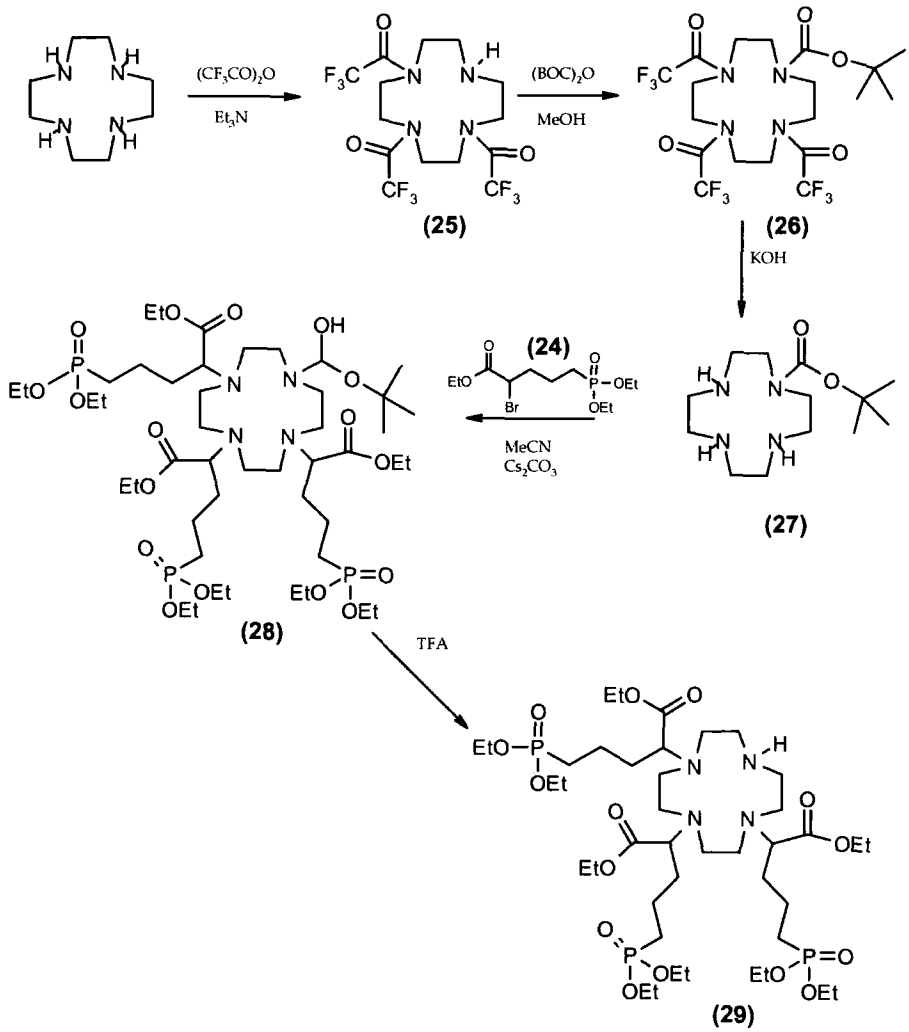

Scheme 3.5: Synthesis of tri-substituted phosphonate derivative of the aDO3A derivative (29), as a mixture of stereoisomers.

Attempts were made to hydrolyse the ethyl ester groups of **(29)** by base hydrolysis using lithium hydroxide (1 M) and heating for 18 hours. Following D_2O exchange and subsequent ^1H NMR analysis it was apparent that not all of the ester groups had hydrolysed. The concentration of lithium hydroxide was increased (3 M) and the resulting solution heated at 120°C for a further 18 hours. Removal of the carboxylate ethyl esters was evident in ^1H NMR and ESMS analysis. The hydrolysis of one of the phosphonate ester groups (EtO) was also apparent. However, the other phosphonate ethyl ester remained intact. The ligand was therefore heated using more strongly acidic conditions (hydrochloric acid, 6 M). Dramatic changes were seen in the ^1H NMR spectra of the reaction products suggesting the ligand was fully hydrolysed although the existence of some very sharp peaks posed questions. Attempts were made to purify the ligand using a strong cation exchange

resin (Dowex 50 W). The product was not retained on the column, eluting quickly in water. This product was analysed by ^{1}H and ^{13}C NMR where it was obvious from a reduction in the number of carbon signals and no resonance to represent the (NCH_2) groups of the cyclen ring that the complex had degraded. At this early point it was unclear whether the problems had occurred during acid hydrolysis or base hydrolysis so the reactions were repeated. The reaction of **(29)** with lithium hydroxide (0.5 M) followed by gentle heating (60°C, 18 hours) confirmed degradation of the product was occurring at this stage. In the presence of increased concentration of base and increased temperatures the yield of this undesirable product would have been more significant. Attempts were made to directly hydrolyse all ethyl ester groups of **(29)** using hydrochloric acid (6 M) upon heating under reflux for 18 hours. ^{1}H NMR confirmed some ethyl signals remained of which no change was observed following further heating for another 18 hours. Earlier work within the Parker group[126] and the work of Sherry *et al*[43] for phosphinate hydrolysis employed the stronger acid, hydrogen bromide in acetic acid. The reaction conditions were tested for the hydrolysis of all ethyl ester groups of **(24)**. The ligand **(24)** was heated at 100°C for 18 hours in the presence of excess hydrogen bromide acetic acid solution. The mixture was allowed to cool to room temperature and added dropwise into a cooled solution of diethyl ether; some precipitate formed. The diethyl ether was removed under reduced pressure. The acetic acid was removed from the solution as its toluene azeotrope. ^{1}H NMR analysis confirmed full hydrolysis of the ligand had occurred. The cyclen derivative with phosphonate peripheral arms **(29)** was fully hydrolysed upon heating for 48 hours in the presence of hydrogen bromide solution in acetic acid. The pH of the acidic solution was increased to pH 5.5 and complexation of the europium (III) and gadolinium (III) complexes was carried out, as in Scheme 3.6

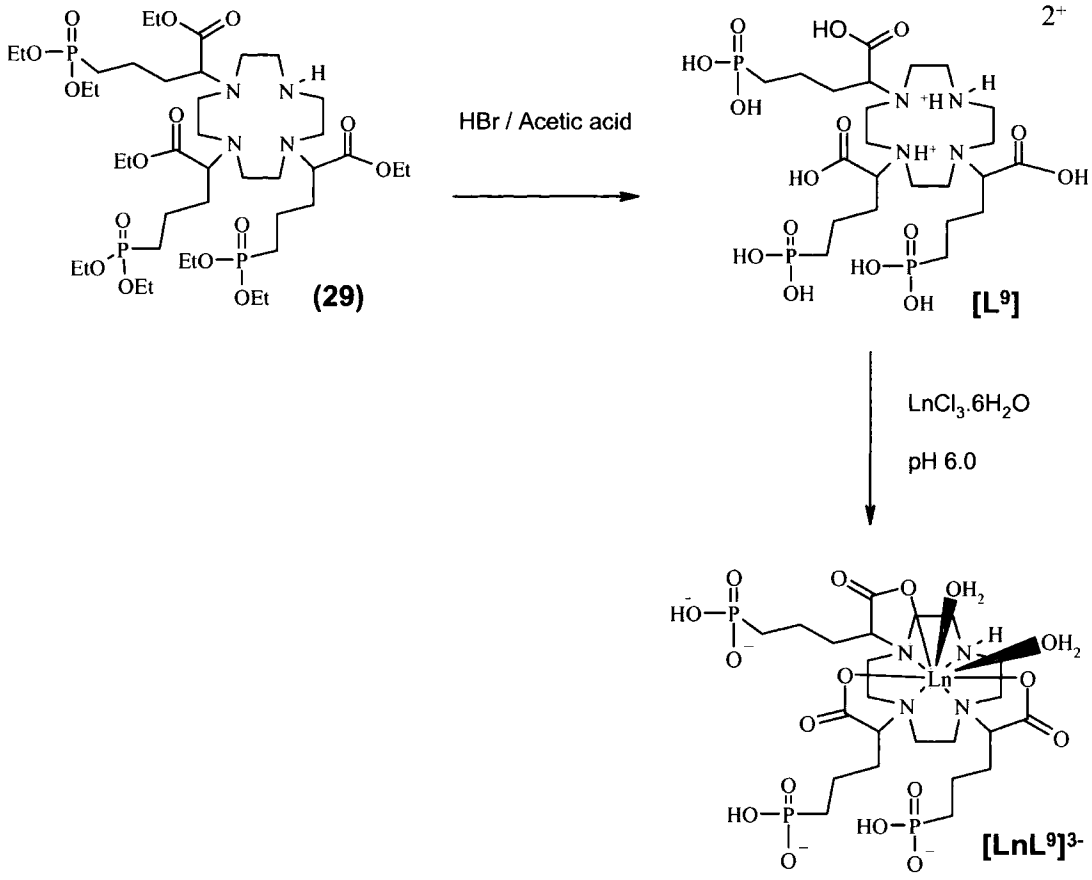

Scheme 3.6: Synthetic route for the complexation of [L^9]

3.2 Relaxivity Measurements

The relaxivity of the gadolinium complex **[GdL^9]$^{3-}$** was measured at 60 MHz and 310 K. The pH of the complex in solution was 6.8 and the relaxivity value obtained was 7.3 $mM^{-1}s^{-1}$. This is similar in magnitude to previously studied lanthanide complexes possessing two inner sphere water molecules at the lanthanide (III) centre, suggesting that **[GdL^9]$^{3-}$** is a di-aqua species.

The NMRD profile for the complex **[GdL^9]$^{3-}$** was measured in water at pH 6.8, between the magnetic fields 0.01 to 20 MHz in Durham at three different temperatures 288 K, 298 K and 310 K (Figure 3.2). The profile was found to be typical of a di-aqua gadolinium[1,37] complex and resembled that obtained for $[Gd(aDO3A)(H_2O)_2]^{3-}$.[37,38]

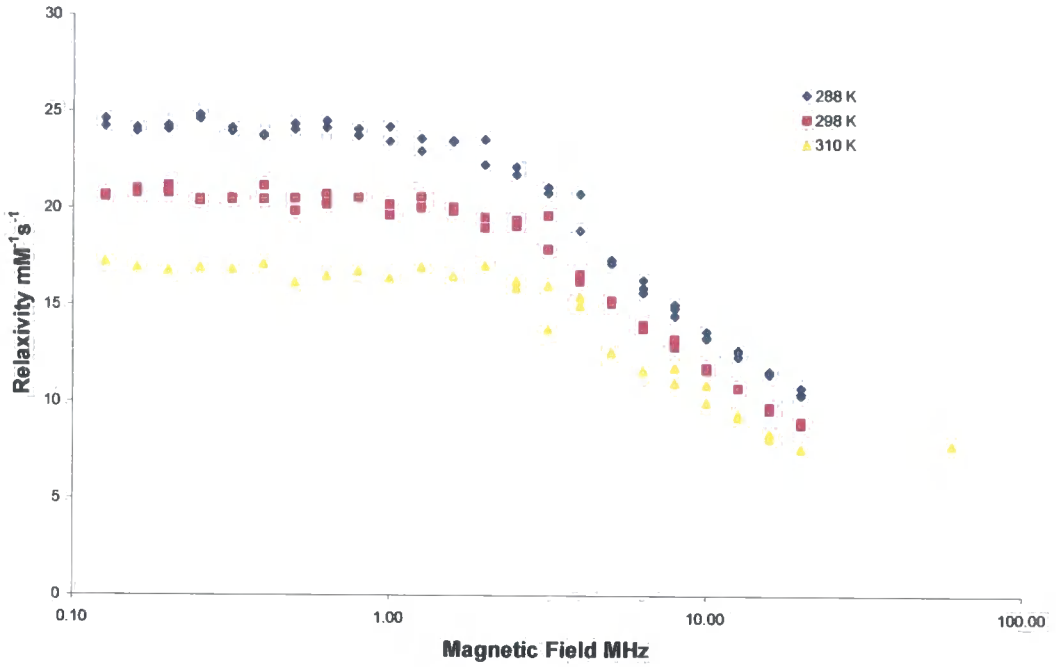

Figure 3.2 NMRD profile for $[GdL^9]^{3-}$ at 288 K, 298 K and 310 K operating at the magnetic fields 0.01 to 20 MHz. An additional point for the relaxivity of $[GdL^9]^{3-}$ at 60 MHz, 310 K is added.

To assess the characteristics of complex behaviour in solution, the relaxivity of **$[GdL^9]$** was measured as a function of pH at 60 MHz, 310 K (Figure 3.3.). The relaxivity values were found to be constant across the pH range 3.5 to 6.

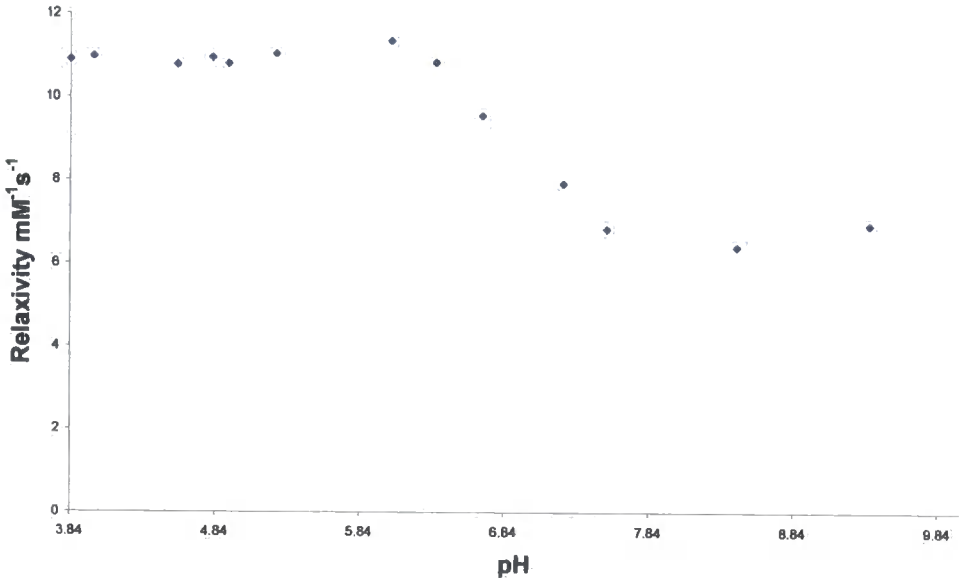

Figure 3.3: Relaxivity as a function of pH for $[GdL^9]^{3-}$

As the pH was increased beyond pH 6 there was an obvious decrease in the observed relaxivity. This may result from the di-aqua complex being susceptible to the binding of dissolved carbonate in solution deriving from atmospheric carbon dioxide at increased pH. Alternatively, the reduction may be associated with deprotonation of the three phosphonate OH groups in the side-arms, although the apparent protonation constant observed (at 6.8) is slightly lower than expected for such systems. The marked change in relaxivity may also be related to a large variation in the second sphere contribution to the observed relaxivity and/or the onset of 'intermolecular' phosphonate ligation. This latter effect would be expected to be concentration, pH and time dependent.

The reversibility of this pH dependence was examined, but a time-dependent phenomenon was observed. Using a sample that had aged in solution for 2 days, the pH was increased; particulate matter was found to precipitate out of solution. The amount of precipitate formed was observed to be time-dependent, suggesting some form of oligomerisation reaction was occurring. Oligomer formation is concentration dependent so the relaxation rate of the complex was measured as a function of complex concentration (Figure 3.4) for a freshly prepared sample of the complex. The linearity of the paramagnetic relaxation rate versus concentration plot (Figure 3.4) is not in accord with oligomerisation at pH 6.8, on the experimental timescale used (< 2 hours).

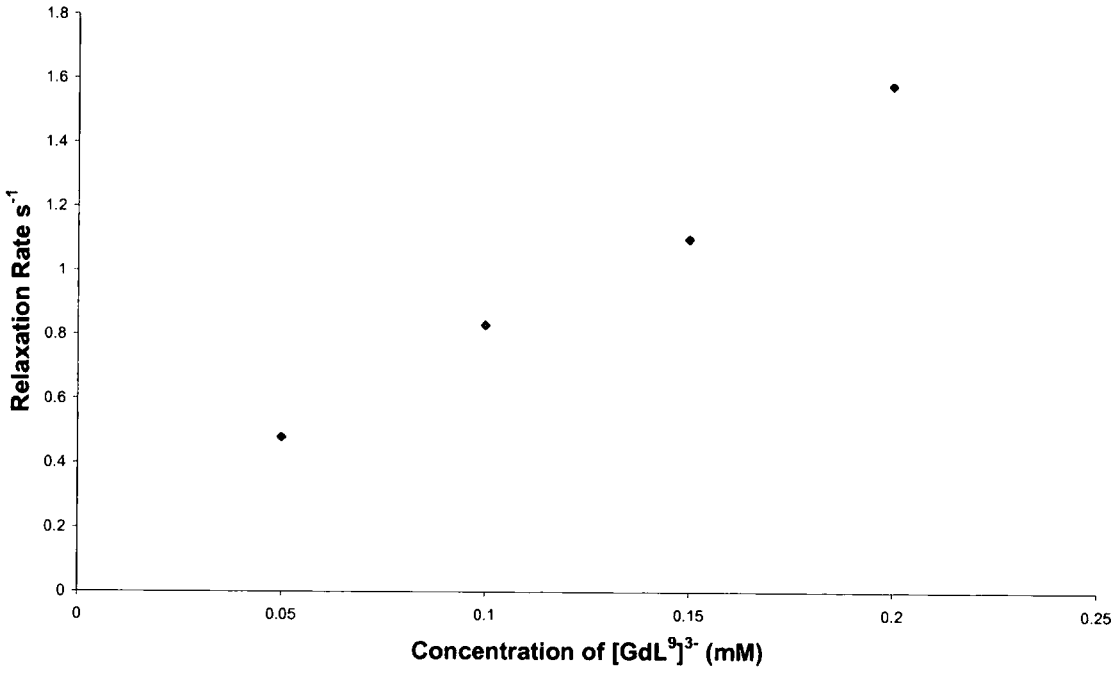

Figure 3.4: Concentration dependency of relaxivity for $[GdL^9]^{3-}$ (pH 6.8, freshly prepared solution

3.3 Semi quantitative assessment of anion effect on relaxivity

As it was believed that anions were binding to the gadolinium centre causing a reduction in the observed relaxivity, the relaxivity of $[GdL^9]^{3-}$ was recorded as a function of the concentration of biological anion background. The simulated anion background solution contained carbonate (30 mM), phosphate (0.9 mM), citrate (0.13 mM) and lactate (2.3 mM), and the pH of the added anion solution was 7.3. The complex $[GdL^9]^{3-}$ was taken as a solid and dissolved into the anion background solution. The longitudinal relaxation time, T_1 of the solution was measured but the value was extremely long similar to that of pure water solutions containing no paramagnetic material. Aliquots (20 µl) of the anion solution were also added to a solution of $[GdL^9]^{3-}$ and the relaxivity was measured at 60 MHz, 310 K. Instantly, upon addition of anions the relaxivity was found to decrease significantly suggesting complete displacement of bound water molecules by competing anions.

Previous research within the Parker group has shown the most common anions that are found to displace inner sphere water molecules from lanthanide (III) complexes are phosphate, lactate and carbonate.[15,16,112,127] To assess which anion was most

prominent in the displacement of inner sphere water molecules, carbonate (sodium hydrogen carbonate, to a limiting pH of 8.7), lactate (D-Lactic acid sodium salt solution, pH 7.7), and phosphate (di-sodium hydrogen phosphate to a limiting pH of 8.6), were added individually in large excess, as solids to solutions containing the same concentration of **[GdL^9]$^{3-}$**. The relaxivity was then measured at 60 MHz, 310 K (Table 3.1).

Anion	Relaxivity $mM^{-1}s^{-1}$ (60 MHz, 310 K)
no anions	7.9
hydrogencarbonate	4.9
lactate	8.2
hydrogenphosphate	3.0

Table 3.1: Relaxivity values obtained depending on anion used

The results show that carbonate and phosphate both lead to relaxivity reductions consistent with the displacement of water molecules from the gadolnium (III) centre. However, it was noted that in the presence of hydrogenphosphate the relaxivity value reduces to a value consistent with that of purely outer sphere effects. Lactate is not found to compete with inner sphere water molecules even when the concentration of lactate present in solution is significantly increased. The relaxivity value measured for **[GdL^9]$^{3-}$** is actually slightly higher in the presence of lactate than it is as the free complex.

3.4 Protein Binding Studies

The relaxivity of the carboxylate analogue [Gd(aDO3A)]$^{3-}$ of the complex **[GdL^9]$^{3-}$** was not found to be significantly enhanced in the presence of serum albumin. However, the phosphonate analogue may exhibit differing behaviour as the solution speciation of the complex may not be the same. In the presence of human serum albumin at a concentration of (0.6 mM), similar to in-vivo concentration, the relaxivity is dramatically enhanced from 7.9 $mM^{-1}s^{-1}$ to 43.5 $mM^{-1}s^{-1}$. The protein binding study was repeated for a solution containing a lower concentration of complex [GdL^9]$^{3-}$. The results revealed a relaxivity enhancement from 8.5 to 30.2

$mM^{-1}s^{-1}$. The concentration of protein bound complex under these conditions may not be as high.

An NMRD profile (0.01 to 80 MHz) was measured at 298 K for an 0.2 mM solution of **$[GdL^9]^{3-}$** at pH 7.2 in the presence and absence of human serum albumin. In the presence of 1 mM human serum albumin, the curve was typical of a protein bound complex with a 400% enhancement in the relaxivity at 40 MHz (Figure 3.5). Such behaviour is reminiscent of the relaxivity gains obtained when $[Gd(DOTP)]^{5-}$, a q=0 complex with a pH independent relaxivity profile, interacts with protein. This suggests that in the bound complex, at least one coordinated water molecule has been displaced.

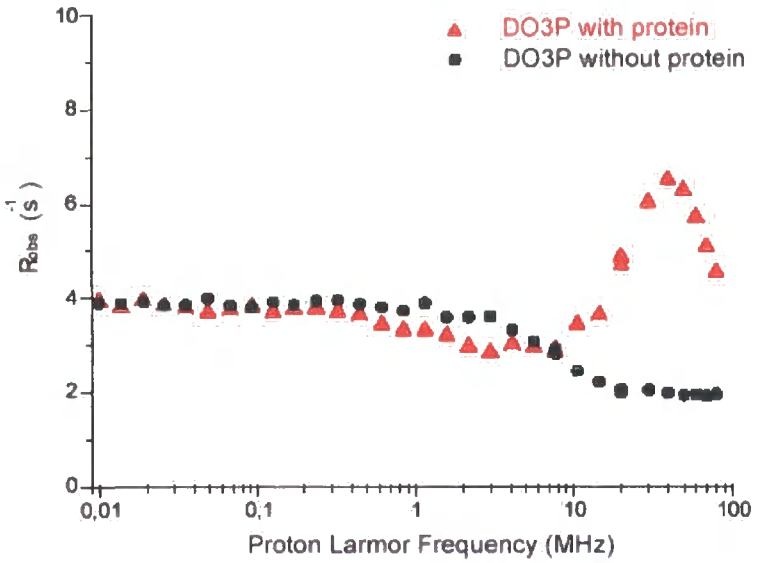

Figure 3.5 NMRD profile for $[GdL^9]^{3-}$ (0.2 mM) in the absence (circles) and presence of 1 mM human serum albumin (triangles), showing the marked relaxivity enhancement around 20-60 MHz of the protein bound complex.

It had previously been shown that inorganic phosphate was able to displace the inner bound water molecules from the gadolinium centre resulting in a reduction in the observed relaxivity. Phosphate anions were added to the protein solution to understand if the complex when strongly bound to serum albumin was able to withstand competition from competing anions. The results showed, for the complex **$[GdL^9]^{3-}$** in the presence of protein, phosphate anions were still able to displace the

inner sphere water molecules resulting in a large reduction in the observed relaxivity.

3.5 Conclusions

[GdL^9]$^{3-}$ was synthesised and characterised successfully as a di-aqua complex. Unlike [Gd(aDO3A)]$^{3-}$ it does show a marked PRE effect in binding serum albumin, similarly to [Gd(DOTP)]$^{5-}$. However, it is sensitive to substitution of the coordinated waters by common added anions, hence reducing the observed relaxivity.

Chapter 4

Sulphonamide Based Systems

4 Sulphonamide Based Systems

4.1 Introduction

Human serum albumin (HSA) is a 67 kDa protein and is the most abundant protein in blood plasma, typically present at a concentration of 0.7 mM. It consists of three structurally homologous, largely helical (67%) domains I, II, and III. Each domain is further divided into two sub-domains denoted A and B.[95] The main physiological role of HSA deals with the transport of a huge number of substrates. Most information regarding the binding properties of drugs and substrates has been identified on the basis of extensive competitive assays.[3,97] It was apparent from previous research that serum albumin contains many metal binding sites which have different binding specificities, the most common belonging to Ni^{2+}, Cu^{2+} and Zn^{2+}. It was well established that HSA contained binding sites that have a high affinity for zinc yet until recently very little was known about the whereabouts of this binding pocket. Stewart *et al*[128] proposed, following detailed X-ray crystallography studies, that the zinc site lies at the interface of the domains I and II, and is essential in the transport of the metal ion and its delivery to cells and tissues.

4.2 Zinc

Zinc is essential for many physiological processes, such as the development and function of all cells, maintaining the immune system and transmission of genetic information. The concentration of Zn^{2+} in blood plasma is approximately 19 μM, most of which is bound to serum albumin with an affinity constant of log K_d = -7.53.[129]

4.3 Sulphonamides

Previously the simple pyridyl based trifluoromethanesulphonamides systems (1) and (2) (Figure 4.1) were identified as suitable zinc (II) binding ligands, capable of forming ML_2 complexes at ambient pH when the free concentration of zinc is in the micro to nanomolar range.[130]

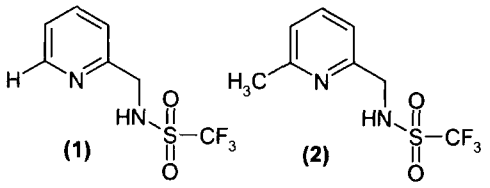

Figure 4.1: Chemical structure of simple pyridyl based trifluoromethanesulphonamides ligands[130]

The ligands were incorporated into various macrocyclic ligands with the intention of increasing the affinity of zinc for such a system, which may produce a suitable derivative that can be integrated into practical luminescent or pZn sensitive MRI probes.

The pyridyl trifluoromethanesulphonamide moiety was incorporated into the macrocyclic system using an ethyl or a propylamide group linkage. The pendant arms of the macrocyclic system also differed, which affected the peripheral charge (Figure 4.2).

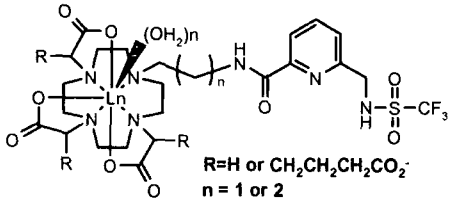

Figure 4.2: Pyridyl trifluoromethanesulphonamide lanthanide complex

The lanthanide (III) complexes **[1]** to **[4]** (Figure 4.3) were synthesised and characterised by Aileen Congreve[130] with proposed binding affinities for zinc. Due to the high concentration of zinc found in human serum albumin it was anticipated that these complexes may bind to the serum protein with a relatively high affinity.

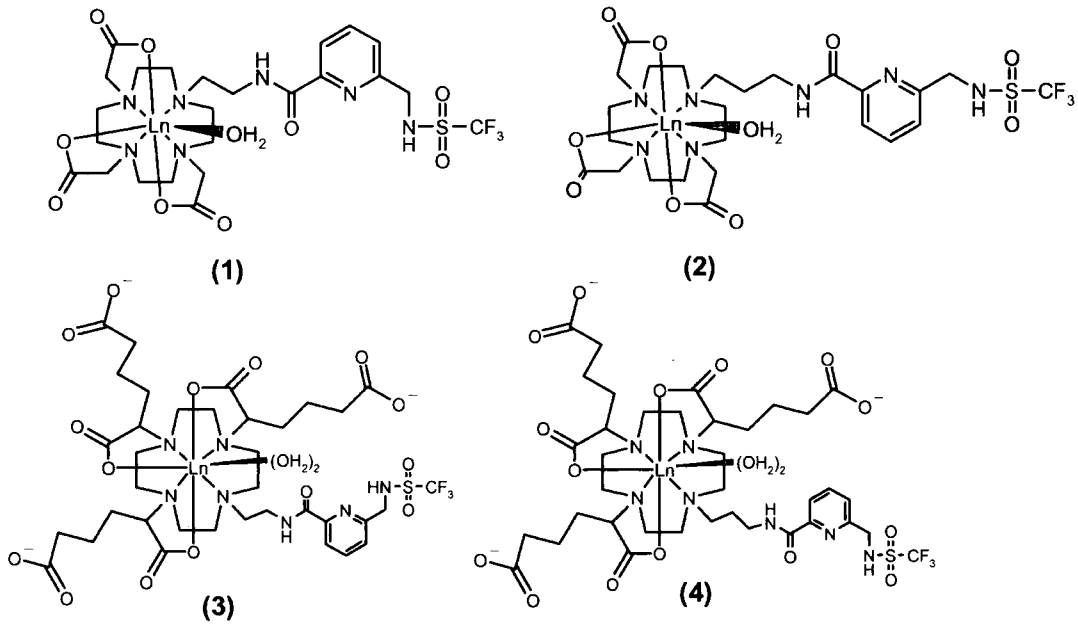

Figure 4.3: Chemical structures of the lanthanide complexes [1] to [4]

4.4 Protein Binding Studies

Complexes **[1]** to **[4]** were first synthesised and characterised by A. Congreve in Durham. The relaxivities of the free gadolinium complexes **[1]** to **[4]** were determined at 60 MHz, 310 K (Table 4.1). The observed longitudinal relaxivity values for complexes **[1]** and **[2]** were much lower than those for complexes **[3]** and **[4]**. This was a consequence of the hydration state of the complex. The DO3A based systems **[1]** and **[2]** contain only one inner sphere water molecule, which is consistent with their lower relaxivity values and was confirmed by luminescence studies of the europium analogue. The relaxivity values obtained for complexes **[3]** and **[4]** based upon aDO3A **(2)** were significantly higher than for **[1]** and **[2]**, indicating that they are di-aqua based systems, similar to the parent complex $[Gd(aDO3A)]^{3-}$.

Complex	Relaxivity Free Complex $mM^{-1}s^{-1}$ (60 MHz, 310 K)
[1]	4.34
[2]	4.35
[3]	8.71
[4]	13.6

Table 4.1: Relaxivity values determined for gadolinium (III) complexes [1] to [4] at pH 6

The interaction with human serum albumin (HSA) was determined for each of the gadolinium complexes **[1]** to **[4]** at 60 MHz and 310 K. Affinity constants towards HSA were measured for each of the complexes using the proton relaxation enhancement (PRE) method. This method allows binding parameters to be determined by exploiting the differences in the NMR water solvent relaxation rates between bound and unbound substrates.[3] The scenario of multiple binding sites on the protein is the main limitation of this method, so it is common practice to assume only one binding site exists per protein molecule. In addition to providing estimations of binding strength, the technique also allows the relaxivity of the paramagnetic macromolecular adduct to be measured.[3]

The protein binding curves obtained for each of the complexes are depicted in Figures 4.4 to 4.7.

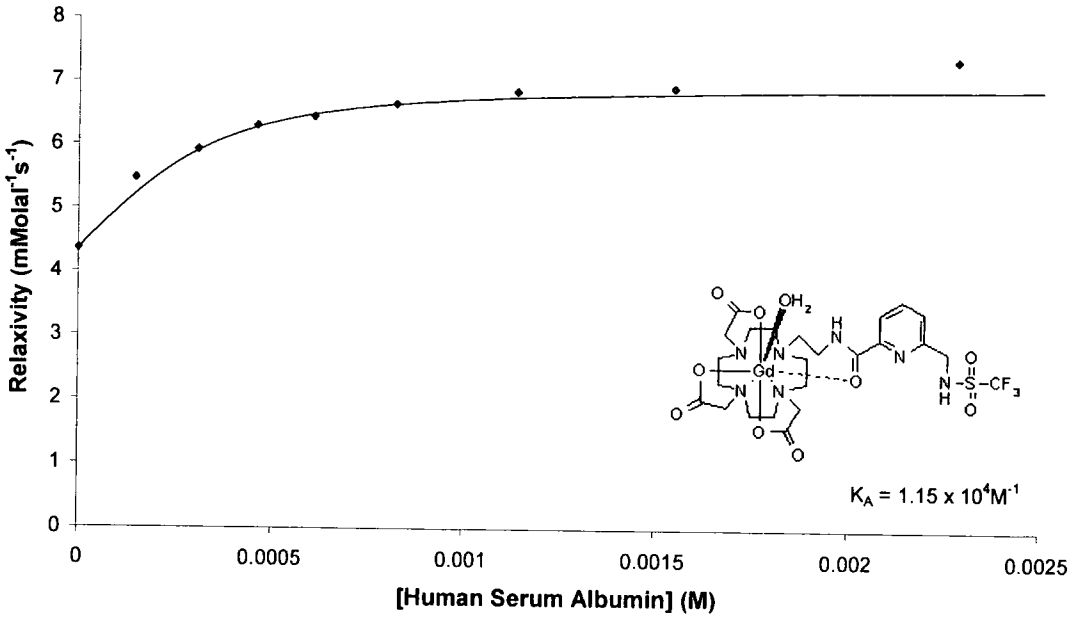

Figure 4.4: Increase in the observed relaxivity of [1] (0.32 mM) with increasing HSA concentration (60 MHz, 310 K)

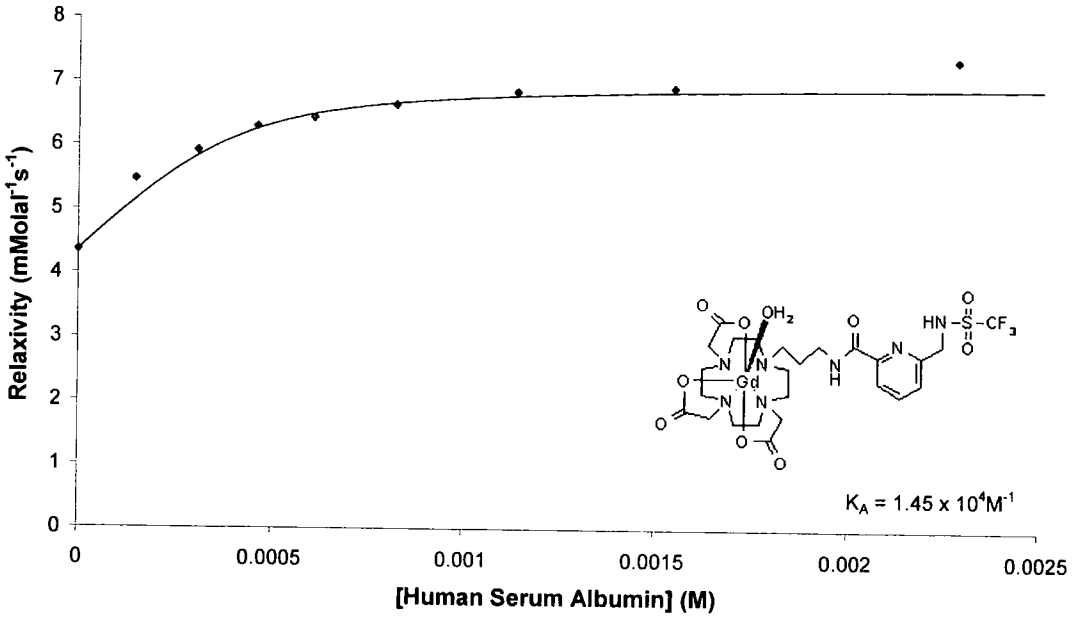

Figure 4.5: Increase in the observed relaxivity of [2] (0.40 mM) with increasing HSA concentration (60 MHz, 310 K)

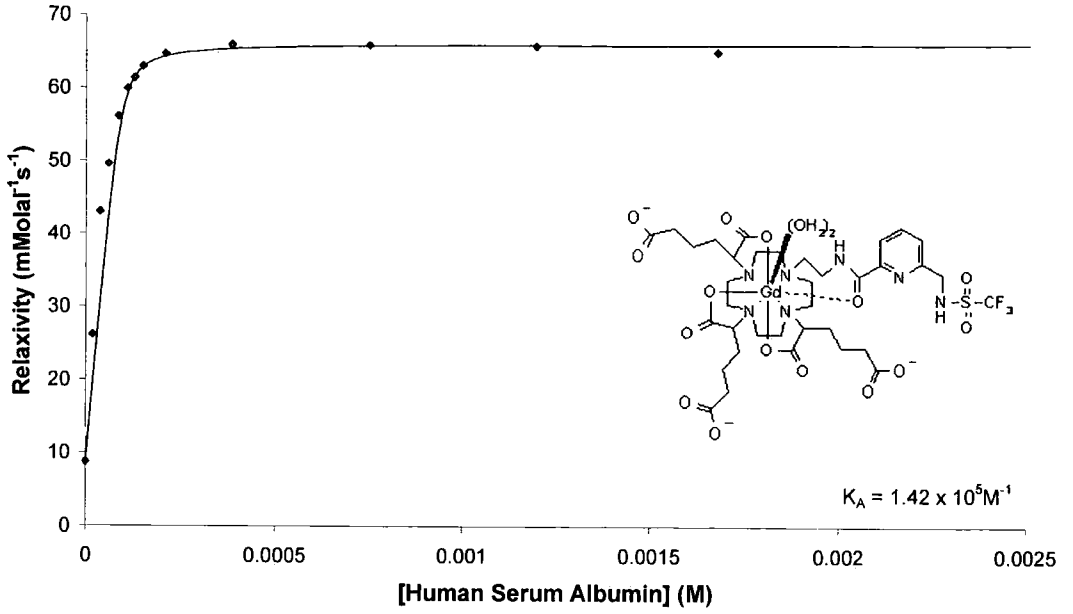

Figure 4.6: Increase in the observed relaxivity of [3] (0.25 mM) with increasing HSA concentration (60 MHz, 310 K)

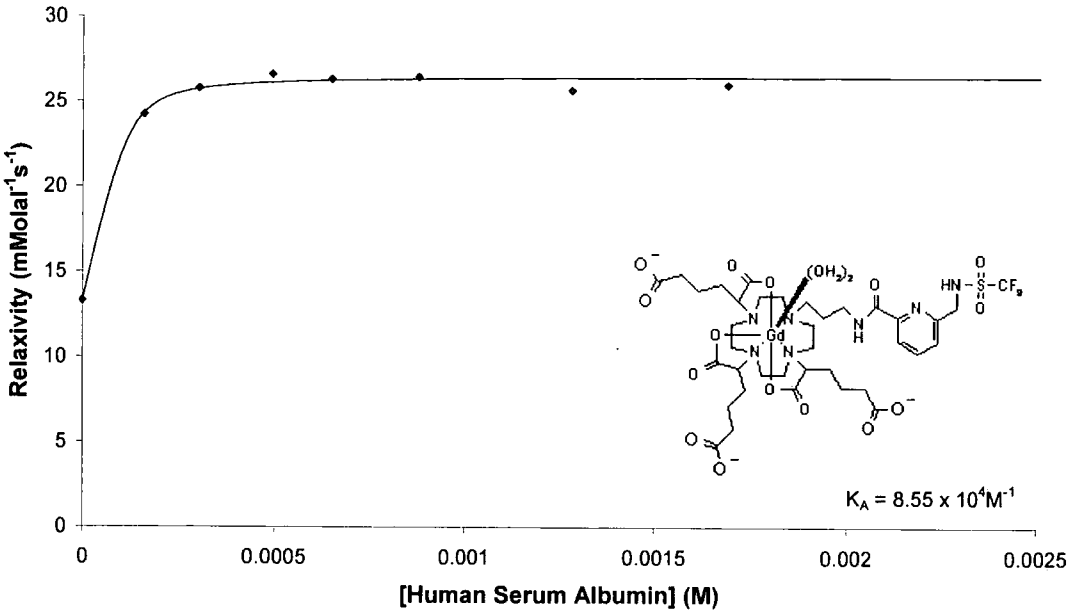

Figure 4.7: Increase in the observed relaxivity of [4] (0.12 mM) with increasing HSA concentration (60 MHz, 310 K)

The binding studies show an increase in the observed relaxivity for each of the complexes upon addition of HSA (Table 4.2). The results were significantly higher for the negatively charged complexes based on the parent compound, $[Gd(aDO3A)]^{3-}$, compared to the neutrally charged DO3A based systems. As it is well established that protein binding requires hydrophobic substituents and negatively charged groups[3] this may explain the much larger enhancement towards

the observed relaxivity for the [Gd(aDO3A)-HSA] based systems.

Complex	Binding Affinity K_A (M^{-1})
[1]	1.15×10^4
[2]	1.45×10^4
[3]	1.42×10^5
[4]	8.55×10^4

Table 4.2: Binding Affinity constants determined for the Gadolinium (III)-HSA complexes

The results obtained for the gadolinium (III) complex **[3]** are extraordinary. The relaxivity values obtained are in the same range as the theoretical maximum for such a di-aqua system, with which until now, such significant results have not been achieved. At blood plasma concentrations of HSA of approximately 0.7 mM, the HSA-adduct **[3]** ideally was found to reach its maximum saturated relaxivity value (Figure 4.6). Increasing the concentration of HSA above this value had little effect upon the observed relaxivity.

Due to such unprecedented results for **[3]** upon addition of human serum albumin, the synthesis of the complex was repeated to ensure the results obtained were reproducible. At this point, it should be clarified that upon review of the analytical data for the characterisation of complex **[3]**, it was suggested that the complex might not be entirely homogenous. This point is discussed further towards the end of this chapter.

4.5 Internal Flexibility

The proton relaxivity of small molecular weight Gd (III) complexes for MRI is mainly limited by fast rotation. The formation of macromolecular agents can be used to slow down rotation and thus increase relaxivity. However, the increase is often much less than expected on the basis of molecular weight due to the internal flexibility of the macromolecule.[8] If the linker group between the Gd (III) chelate and the macromolecule is too long, the complex rotates independently of the

protein and hence the increased τ_R effect is not transmitted to the complex. This limits the relaxivity enhancement. This is seen in the lower relaxivities determined for complexes **[1]** and **[4]**, whereas complex **[3]** is found to have significantly higher relaxivity values as a consequence of the less flexible C_2 linker group.

It was suggested that the complexes **[1]** and **[4]** adopt different conformations in solution which may differ in the binding to HSA. The change in conformation may result from hydrogen bonding between the pyridyl nitrogen and the amide hydrogen; a similar observation was made by Hunter and Purvis[131] for a 2,6-diamide substituted pyridine based system (Figure 4.8).

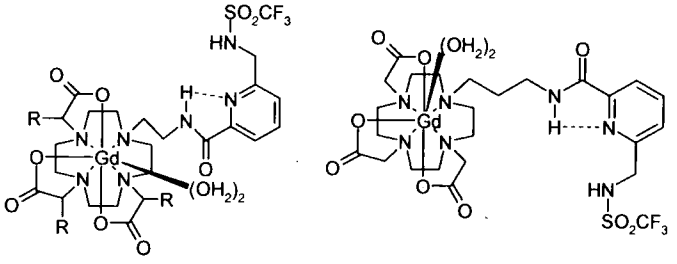

Figure 4.8: Proposed conformation for complexes [3] and [4][131]

The NMRD profiles (Figures 4.9 to 4.12) for each of the four gadolinium complexes were recorded in Durham both as the free complex and the bound adduct with HSA, using a field cycling spectrometer operating between the magnetic fields of 0.01 and 20 MHz at 298 K.

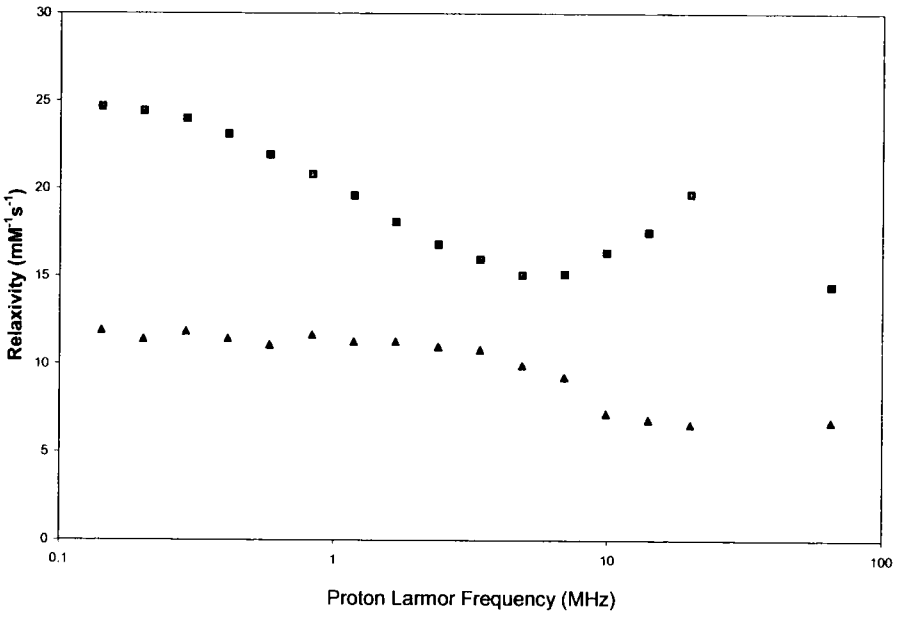

Figure 4.9: NMRD profile of [1] in the presence ■ and absence▲ of HSA at 298 K

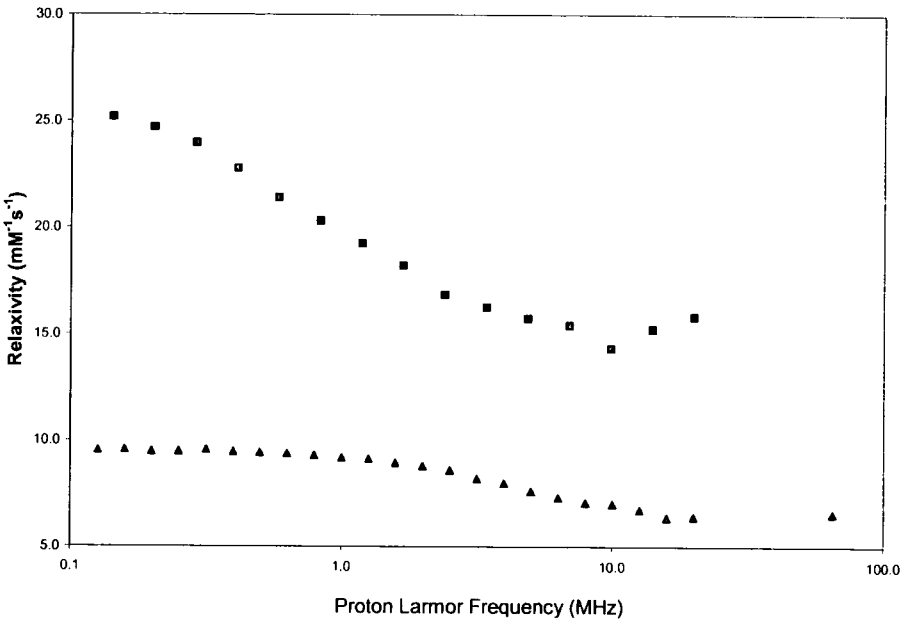

Figure 4.10: NMRD profile of [2] in the presence ■ and absence▲ of HSA at 298 K

The relaxivity of the DO3A based systems **[1]** and **[2]** was doubled on formation of an adduct with HSA (Figures 4.9 and 4.10). As the NMRD profile was only measured to 20 MHz, the additional point obtained at 60 MHz was added. This gave rise to the typical high field relaxivity peak in the region of 20-60 MHz, resulting from an increased τ_R effect.[1,3,4] The NMRD profiles show the τ_R effect is greater for the more rigid spacer (C_2) for the Gd (III) complex **[1]** due to more

efficient coupling of the complex with respect to the macromolecule. This behaviour was also mirrored in the aDO3A based systems, suggesting the C_3 linker allows too much rotational freedom, limiting the observed relaxivity.

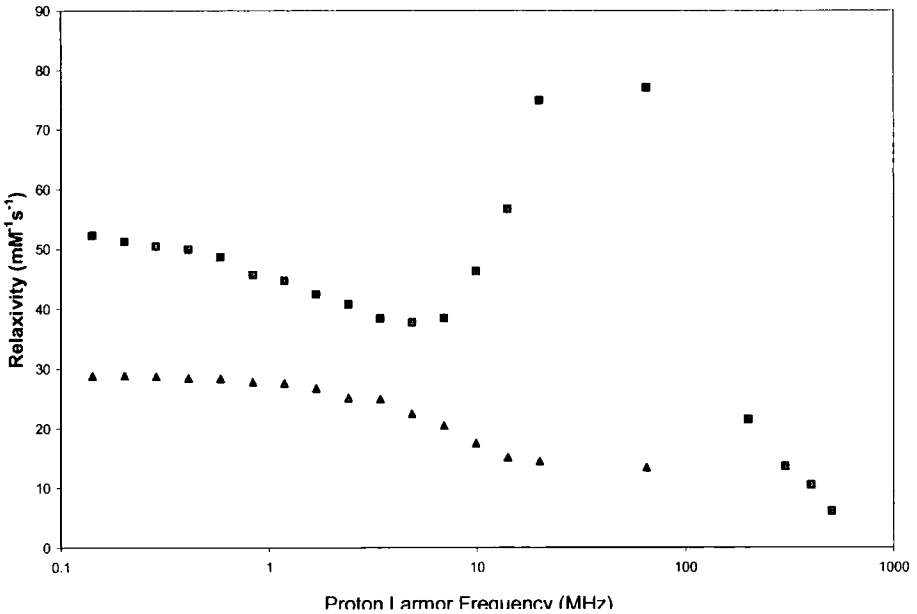

Figure 4.11: NMRD profile of [3] in the presence ■ and absence▲ of HSA at 298 K

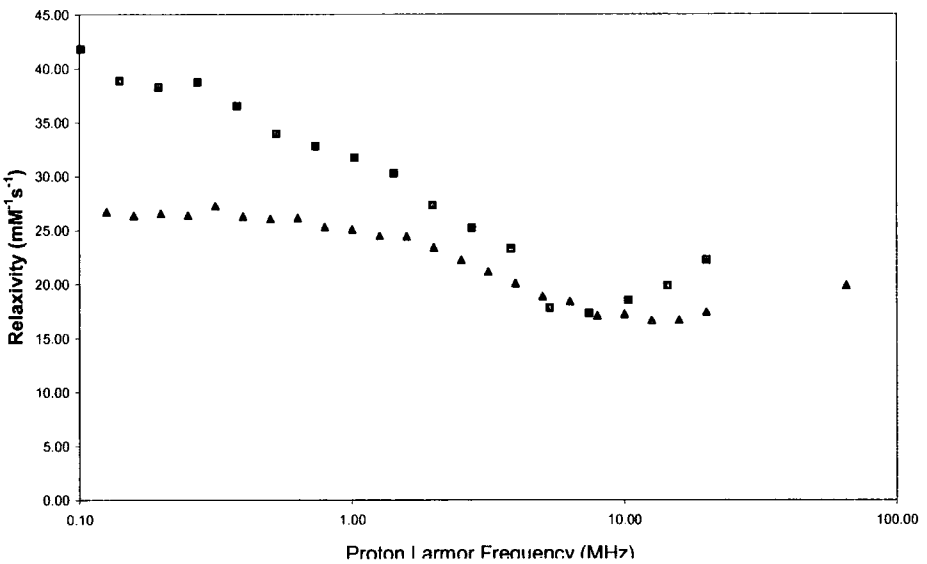

Figure 4.12: NMRD profile of [4] in the presence ■ and absence▲ of HSA at 298 K

The Solomon-Bloembergen-Morgan theory predicts that gadolinium (III) complexes possessing two inner sphere water molecules and optimised values of rotation, electron paramagnetic relaxation and water exchange times, can have maximum

proton relaxivities in the range of 100 $mM^{-1}s^{-1}$.[1,10] However, this theoretical maximum has never been achieved as di-aqua complexes are prone to the displacement of inner sphere water molecules by competing anions or protein amino acid side chains, or slow limiting water exchange rates. The enhancement in relaxivity for **[3]** is remarkable suggesting the complex remains as a di-aqua species in the presence of protein, in addition to optimised water exchange times, similar to the parent complex $[Gd(aDO3A)]^{3-}$. The Gd (III) complex **[3]** is found to tumble coherently with the macromolecule maximising the τ_R effect, resulting in such high relaxivity values.

The complex **[3]** was independently analysed by collaborators in Turin, including a separate NMRD analysis between the magnetic fields of 0.01 to 40 MHz (Figure 4.13). This was valuable as it gave more information regarding the high field region.

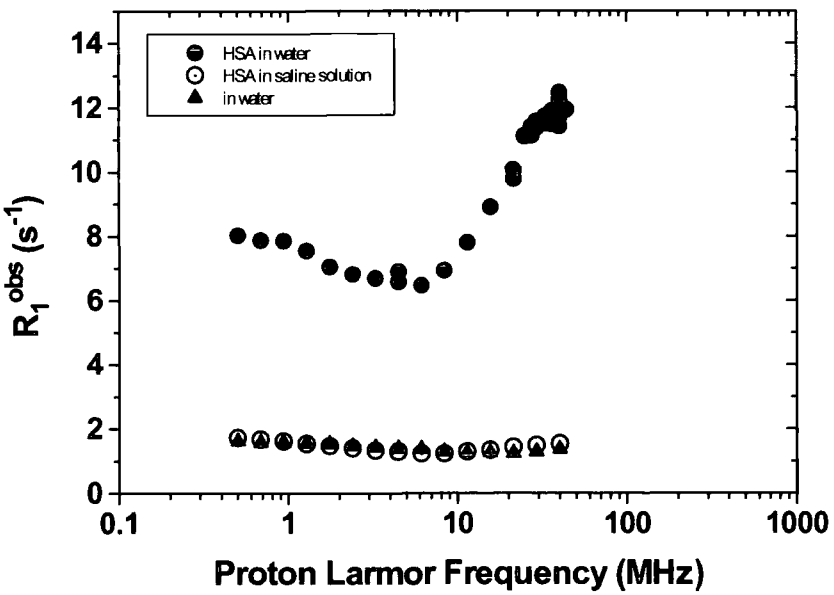

Figure 4.13: NMRD profile for complex [3] (0.25 mM) in the presence of HSA measured by collaborators in Turin

The independent results measured in Turin (Figure 4.13) concurred with the data produced in Durham. As it can be seen from Figure 4.13, the results suggest that maximum relaxivity is seen at 40 MHz, almost 20% higher than the relaxivity obtained at 20 MHz. The concentration of the complex in addition to the

longitudinal relaxation rates measured predict relaxivity values for the complex **[3]** are in the range of 85 $mM^{-1}s^{-1}$ at 40 MHz, 298 K.

4.6 Effects of Anions on Relaxivity

In the presence of human serum albumin, the gadolinium (III) complex **[3]** displays a massive enhancement in the relaxivity. Human serum solution contains not only serum albumin but also other competing proteins such as glycoproteins and extracellular anions. They were added to the complex to observe the effect upon relaxivity. The values were significantly lower in human serum solution than in the presence of serum albumin (see Table 4.3), resulting from the displacement of bound water molecules by anions in solution, and hence low relaxivity values.

	Relaxivity ($mM^{-1}s^{-1}$) (60 MHz, 37°C)
[3]	8.7
[3] in 0.7 mM HSA	67.5
[3] in human serum	14.1

Table 4.3: Relaxivity values determined for [3] as the free complex, in HSA and in human serum.

The displacement of inner sphere water molecules by competing anions was confirmed from anion binding studies, where the relaxivity was measured as a function of the concentration of biological anion background. The simulated anion background contained carbonate (30 mM), phosphate (0.9 mM), citrate (0.13 mM) and lactate (2.3 mM). The resulting solution was added in aliquots (50 µl), to a solution containing complex [3]. The resulting change in relaxivity was monitored at 60 MHz, 310 K and is depicted in Figure 4.14.

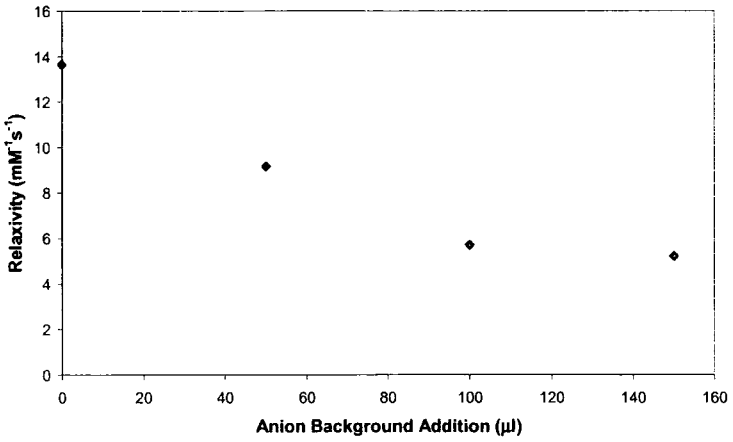

Figure 4.14: Relaxivity changes of [3] as a function of the concentration of the solution containing added salts.

The 'anion binding' experiment showed significant decreases in the observed relaxivity as the concentration of biological anions was increased, confirming extracellular anions were binding to the metal centre displacing bound water molecules. Sensitised emission studies for the europium (III) analogue performed by Aileen Congreve[130] revealed at pH > 7.5, carbonate anions bind to the gadolinium (III) metal ion, whereas at pH < 7.5 phosphate anions are responsible for the displacement of water molecules. The relaxometric results displayed by complex **[3]** were unprecedented, the formation of the HSA adduct resulting in an enhancement of approximately 700%. However, the relaxometric results in the presence of human serum were disappointing as extracellular anions in solution were competing with the water molecules bound to the metal centre.

4.7 Effect of pH on Relaxivity

The relaxivity of **[3]** was monitored as a function of pH. As the pH was increased above 6.5, a small amount of precipitate was found to form out of solution. It was believed that the gadolinium complex **[3]** was forming oligomers, which precipitated with an increase in pH, this process being only slowly reversible. This process may be tentatively associated with sulphonamide deprotonation (pK_a of the NH deprotonation is approximately 7.3).[132]

Therefore, the best conditions to study the behaviour of the free complex were in the pH range of 5.0 to 5.5. Oligomerisation problems were not found to occur in

protein solutions as the complex is solubilised; no significant pH variation was seen in the range 5.5 to 7.5.

The tendency to form oligomers is also inhibited in the presence of competing anions but the observed relaxivity is lowered as a consequence. No problems associated with oligomer formation was seen for systems with C_3 linker groups, **[2]** and **[4]** and the C_2 complex with acetate arms **[1]** rather than carboxylate arms.

4.8 Derivatives of Complex [3]

Three ligands were synthesised with respect to the chemical structure of **[3]** with the intention of assessing which part of the molecule was responsible for the significant binding affinity for HSA.

The trifluorosulphonamide functional group was also substituted for a less hydrophobic trimethanesulphonamide, which also has a much higher pKa value, so that problems associated with oligomerisation may be suppressed.

4.9 Synthesis of derivatives

The synthesis of $\mathbf{L^{10}}$ was carried out using the established synthetic methods reported by Congreve[130,132] (Scheme 4.1).

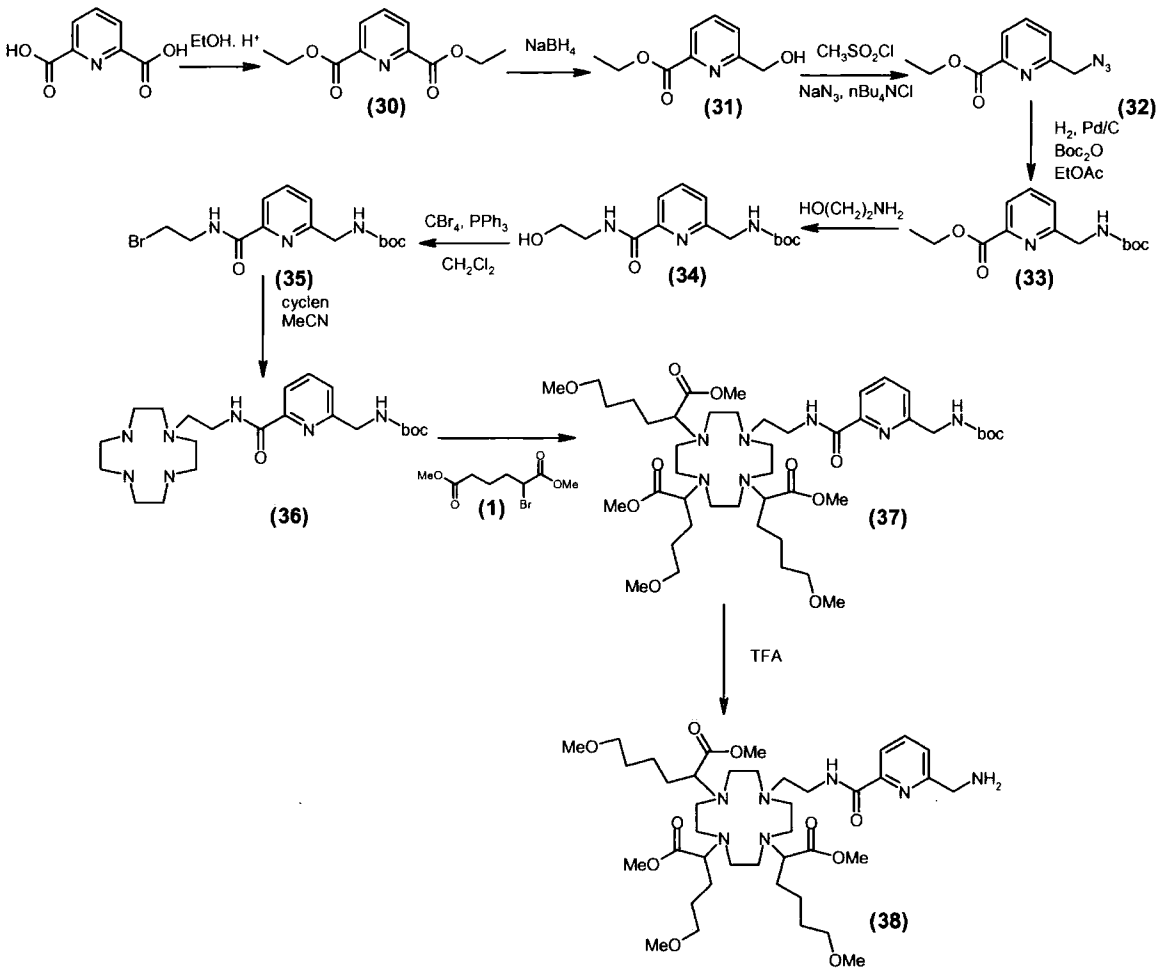

Scheme 4.1:Synthetic Route for the production of compound 38

Pyridine-2,6-dicarboxylic acid was converted into diethyl-pyridine-2,6-dicarboxylate **(30)** following esterification with anhydrous ethanol. The product was reduced to yield the alcohol **(31)** following reaction with sodium borohydride, which was subsequently converted to the azide **(32)**. The azide was hydrogenated using palladium on carbon catalyst, using 40 psi hydrogen gas using a Parr hydrogenator apparatus. The resulting amide was protected using BOC anhydride in the same reaction pot to produce **(33)** in moderate yield. EDC coupling of **(33)** with ethanolamine resulted in formation of the hydroxy amide **(34)**. This was converted into the corresponding bromide **(35)**, following reaction with carbon tetrabromide and triphenylphosphine in dichloromethane. Monoalkylation of cyclen was achieved by reaction of **(35)** with cyclen in large excess, in chloroform. The product was extracted from dichloromethane to yield **(36)**. Alkylation of the three remaining ring nitrogen atoms was achieved by stirring **(36)** in the presence of

excess dimethyl-2-bromo-adipate **(1)** and anhydrous acetonitrile to produce **(37)**. The BOC protecting group was removed by stirring **(37)** in the presence of trifluoroacetic acid and dichloromethane to yield the amine **(38)**. The ligand L^{10} was formed following hydrolysis of **(38)** using lithium hydroxide (1 M). The resulting ligand, L^{10} was then complexed with gadolinium (III) using the hydrated chloride salt (Scheme 4.2).

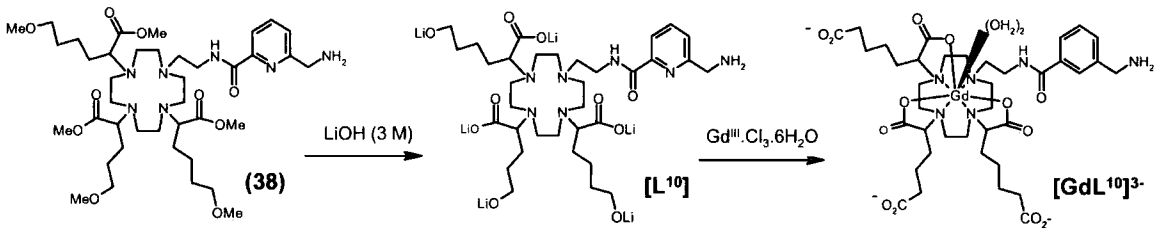

Scheme 4.2: Synthetic procedure for the complexation of $[GdL^{10}]^{3-}$

Ligand, L^{11} was synthesised in a similar manner as Scheme 4.1, where the amine **(38)** was sulphonylated using methanesulphonylchloride in the presence of triethylamine in dichloromethane to yield the product **(39)**, which was purified by flash column chromatography. Subsequent hydrolysis of the methyl esters using lithium hydroxide (1 M) gave the desired product L^{11}, confirmed by the disappearance of the methyl ester resonance in the ^1H NMR spectrum. The ligand L^{11} was complexed to gadolinium (III) by heating at 90°C in the presence of the gadolinium chloride salt (Scheme 4.3).

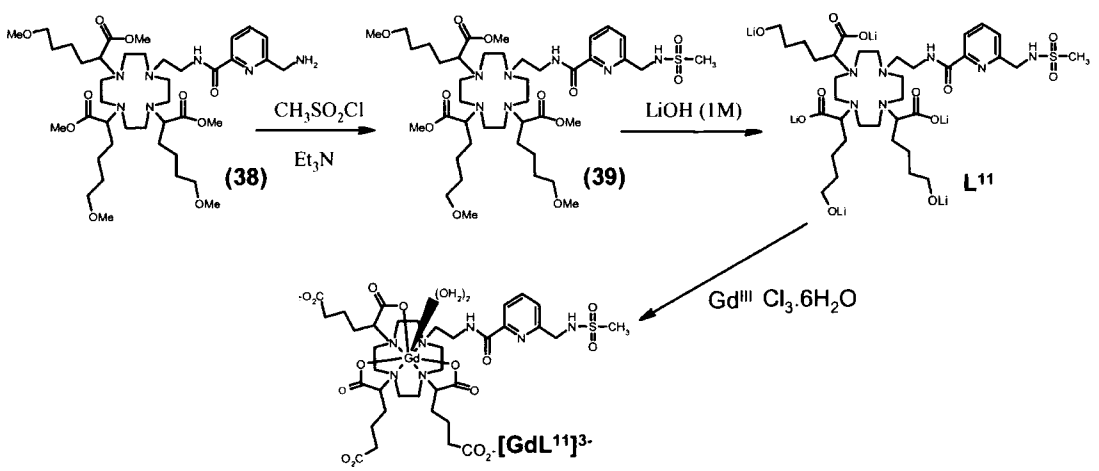

Scheme 4.3: Synthetic procedure for the synthesis of $[GdL^{11}]^{3-}$

The synthesis of the ligand L^{12} is depicted in Scheme 4.4.

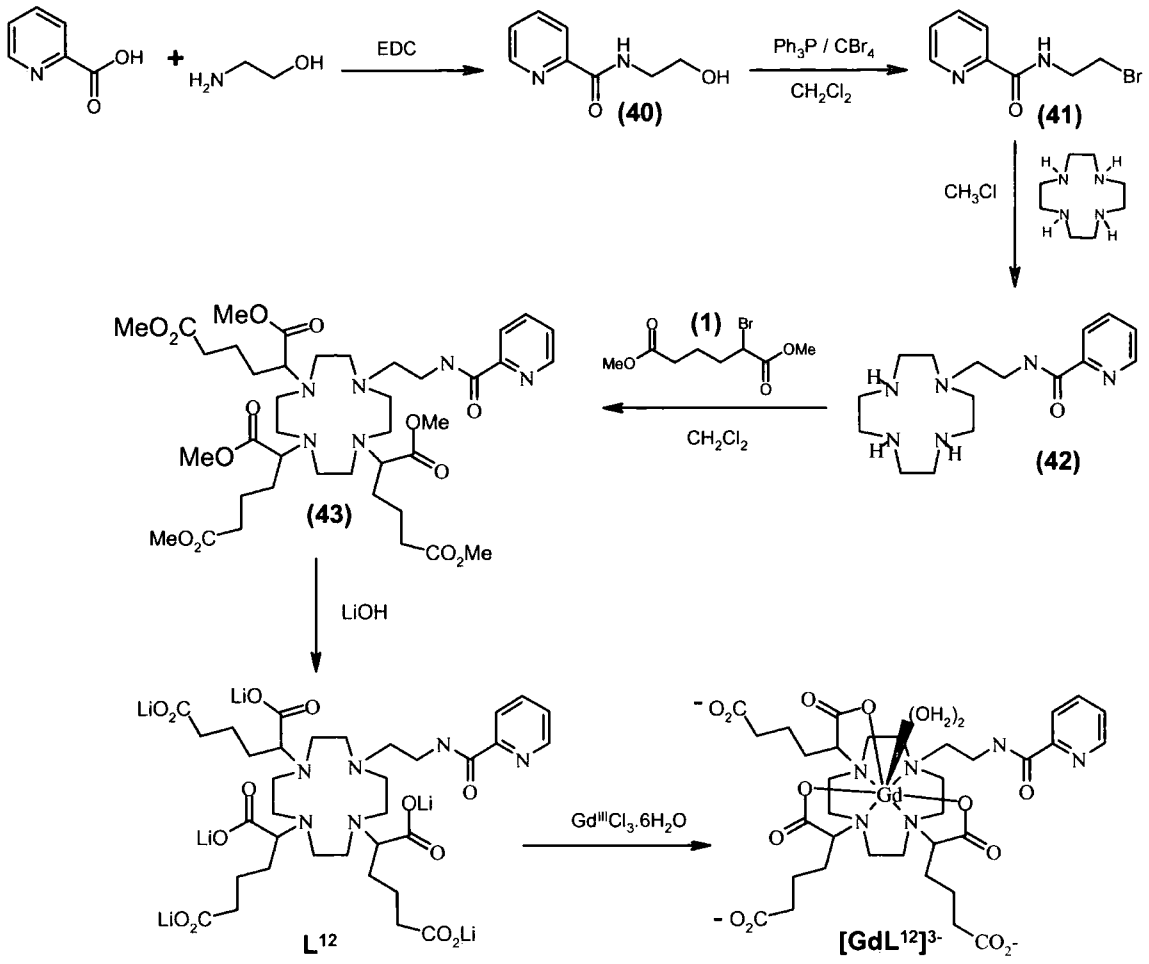

Scheme 4.4: Chemical synthesis of the gadolinium complex $[GdL^{12}]^{3-}$

Picolinic acid was converted to the corresponding ester by stirring the acid in the presence of ethanol with acetyl chloride used as a catalyst. EDC coupling of picolinic ethyl ester with ethanolamine afforded the amide **(40)**. Triphenylphosphine and carbon tetrabromide were used to convert **(40)** into the corresponding bromide **(41)**. In the presence of a large excess of cyclen, which also acted as a base, compound **(41)** was added to yield **(42)**. Attempts to directly alkylate the free NH position of 1,4,7-tris-[(4'-methoxycarbonyl)-1'-methoxy-carbonylbutyl]-1,4,7,10-tetraazacyclododecane **(2)** were unsuccessful as a number of impurities were produced, and the desired product could only be isolated in very low yield. The remaining three NH groups of the cyclen ring were alkylated in the presence of excess dimethyl-2-bromo-adipate **(1)**, caesium carbonate and acetonitrile to produce **(43)**. The hydrolysis of **(43)** was achieved by stirring the

reaction in the presence of lithium hydroxide (1 M) at 90°C to produce L^{12}. Complexation of the ligand to gadolinium (III), was carried out in the presence of the lanthanide chloride salt in aqueous solution.

4.10 Relaxometric Studies of $[GdL^{10}]^{3-}$, $[GdL^{11}]^{3-}$ and $[GdL^{12}]^{3-}$

The relaxivity of each of the three gadolinium complexes was carried out using the Bruker Minispec mq 60 instrument operating at 60 MHz and 310 K. Results are tabulated in Table 4.4.

Complex	Relaxivity Free Complex $mM^{-1}s^{-1}$ (60 MHz, 310 K)	Relaxivity Bound Complex $mM^{-1}s^{-1}$ (60 MHz, 310 K)
$[GdL^{10}]^{3-}$	9.87	16.85
$[GdL^{11}]^{3-}$	7.90	9.68
$[GdL^{12}]^{3-}$	7.80	11.49

Table 4.4 Relaxivity values determined for $[GdL^{10}]^{3-}$, $[GdL^{11}]^{3-}$ and $[GdL^{12}]^{3-}$

The relaxivity results obtained for each of the complexes were disappointing compared to the unprecedented values obtained for complex **[3]**. In the presence of HSA there was only a small enhancement in the observed relaxivity for each complex. However, upon further addition of protein no increase was observed.

4.11 Synthesis of L^{13}

As mentioned earlier in this chapter the synthesis of the gadolinium complex **[3]**, synthesised by A. Congreve, was repeated in order to assess the reproducibility of the protein binding results.

The complex was synthesised in a similar manner to **[GdL^{11}]$^{3-}$** and is shown in Scheme 4.5. The amine **(38)** was sulphonylated using trifluoromethanesulphonyl chloride in the presence of triethylamine rather than Hunig's base used in the reported synthesis. Hunig's base was found to cause problems during purification, as it eluted with the same retention factor as the required product.

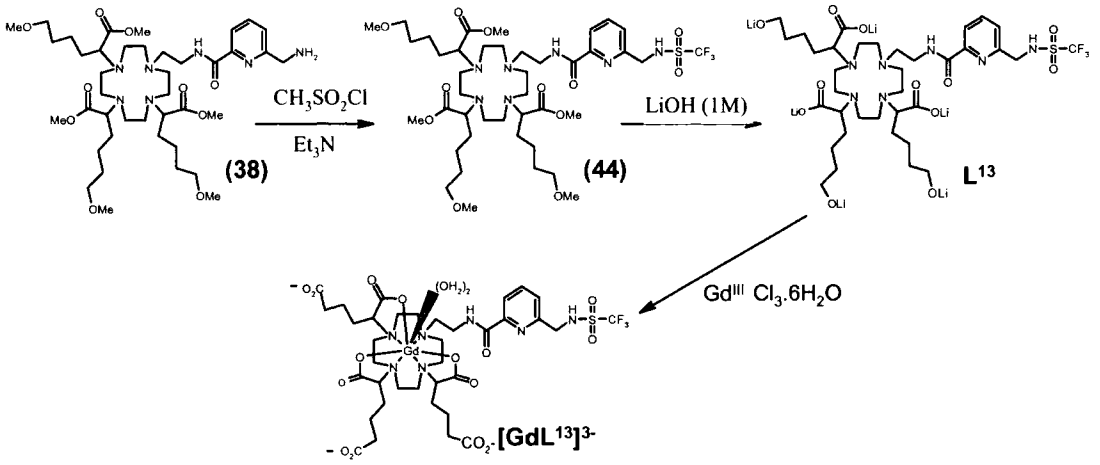

Scheme 4.5: Synthetic procedure for the synthesis of [GdL^{13}]$^{3-}$

The relaxivity of the complex **[GdL^{13}]$^{3-}$** was measured as the free complex and in the presence of human serum albumin (HSA); the results obtained were unexpected as they were very different to those originally reported for the same complex **[3]**.

	Relaxivity Free Complex mM^{-1}s^{-1}	**Relaxivity Bound Adduct mM^{-1}s^{-1}**
[GdL^{13}]$^{3-}$	8.31	21.80

Table 4.5: Relaxivity values determined for [GdL^{12}]$^{3-}$ (310 k, 60 MHz)

On closer inspection of the analytical data for the characterisation of gadolinium complex **[3]** that had given such unprecedented results on the addition of human serum albumin, it was suggested that the complex was not homogenous. MALDI-TOF mass spectrometry analysis of the complex confirmed the presence of the desired product with a mass 1067, in addition to several major impurities, including uncomplexed ligand. Electrospray mass spectrometry data for the ligand prior to hydrolysis also confirmed the presence of a major impurity (mass 962) and the required product (mass 998). The ^{1}H NMR spectrum was very broad but the aromatic region of the spectrum did suggest the presence of two species, in ratio

`5:1. Two resonances were found in the ^{19}F NMR spectrum at -75.9 and -78.8 ppm, representing the impurity and the required product. The impurity was estimated to be present at 30% of the main product.

The structure of the major impurity was suggested to be that shown in Figure 4.15 which seemed to be consistent with the mass spectral and ^{1}H NMR data obtained.

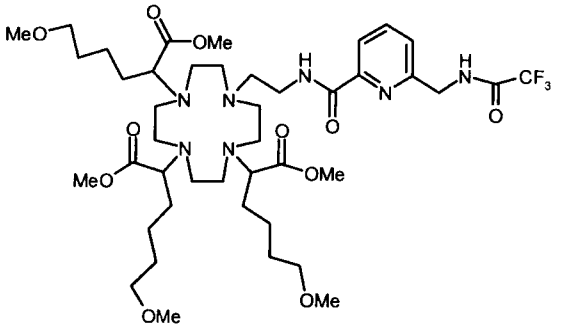

Figure 4.15: Chemical structure of the likely impurity present in [3]

Attempts to synthesise the suggested impurity independently (depicted in Figure 4.15) were unsuccessful. The amine **(38)** was reacted with trifluoroacetic anhydride in the presence of triethylamine and dichloromethane. Attempts to purify the required product by flash column chromatography produced a mixture of compounds whose identity, assessed by ^{1}H NMR was not that of the required product, but was consistent with non-selective acylation at one or more of the amide NH sites, and even at the aryl ring.

4.12 Summary

The relaxivity results obtained for each of the derivative complexes were disappointing compared to the unprecedented values obtained for complex **[3]**. The most significant enhancement reported in the study was associated with the protein bound adduct for the free amide complex, $[GdL^{10}]^{3-}$. However, the enhancement observed in saturated protein solutions was minimal. None of the complexes including that of $[GdL^{13}]^{3-}$, which initially was believed to be the same as complex **[3]**, gave the unprecedented relaxivity enhancements that were observed for **[3]**.

The less hydrophobic methylsulphonamide complex, $[GdL^{11}]^{3-}$ was found to have minimal interaction towards human serum albumin with respect to the trifluorosulphonamide complex **[3]**. This may suggest that as the sulphonamide pK_a of $[GdL^{11}]$ is higher than that of complex **[3]**, (ca. 12 compared to 7.5), and consequently protonated at ambient pH, it may be that deprotonation of the sulphonamide NH is required for a strong interaction with protein.

The insolubility problems associated with complex **[3]** at neutral pH, a phenomenon which was found to be time dependent, result in reproducibility issues, limiting the use of such system as a potential contrast agent. Further work may include the attachment of more water-soluble functionalised groups to complex **[3]**, in an attempt to reduce any oligomerisation, and the associated pH and time dependent effects.

Chapter 5

NMR and chiroptical examination of the diastereoisomers of (S) – [Eu-(EOBDTPA)]$^{2-}$

5 NMR and chiroptical examination of the diastereoisomers of (S)- [Eu-(EOBDTPA)]$^{2-}$

5.1 Introduction

[Gd(DTPA)]$^{2-}$ or Gadopentetate Dimeglumine, marketed as Magnevist ™ by Schering AG, was the first Gd (III) containing compound ever to be approved by the FDA in 1988; it has since been used in more than 25 million people.[88]

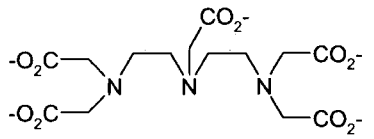

Figure 5.1: [DTPA]$^{5-}$

It is an example of an extracellular, hydrophilic, low molecular weight gadolinium chelate. These types of contrast agent are non-specific compounds, that following intravenous injection are rapidly excreted from the vascular compartments into interstitial spaces and do not pass plasma membranes, excretion occurring via the urinary system.[133] Current research in this area seeks to devise methods of targeting the paramagnetic complex to selected tissues, and a first step in this direction was the discovery that gadolinium complexes of certain analogues of DTPA, such as BOPTA and EOB-DTPA, clear the body via the biliary system rather than the renal system.[134]

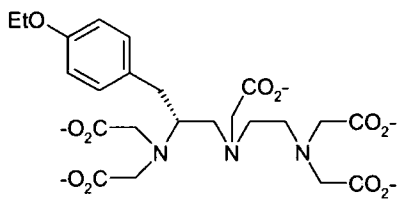

Figure 5.2: [EOB-DTPA]$^{5-}$

[Gd-(EOB-DTPA)]$^{2-}$ (international non proprietary name: gadoxetic acid, disodium salt), which is currently undergoing phase III clinical trials, exhibits very different pharmacodynamic behaviour and hence a distinctive biodistribution profile in human patients. It shows the specific uptake by hepatocytes not by cancerous tissue, allowing the detection and differentiation of hepatic tumours. In addition to

its use as an MRI contrast agent, $[Gd\text{-}(EOB\text{-}DTPA)]^{2-}$ has also been successfully tested in patients as a potential contrast agent for computed tomography (CT).[135,136]

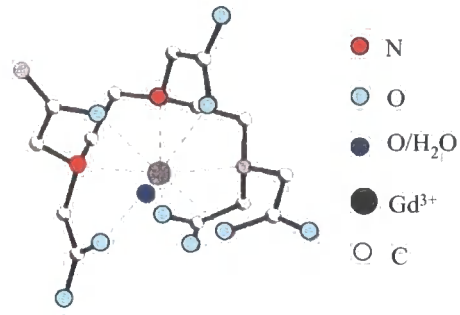

Figure 5.3: X-ray structure of $[Gd\text{-}DTPA]^{2-}$, hydrogen atoms are omitted for clarity[137]

Currently, all gadolinium (III) based chelates approved for use in MRI are nine coordinate complexes in which the ligand occupies eight binding sites at the metal centre and a ninth coordination site is occupied by a single water solvent molecule. The nine coordinate lanthanide complexes of DTPA, involve binding of the lanthanide metal to three nitrogens and five monodentate carboxylate oxygen atoms of the DTPA ligand, both in solid and in solution states. An inspection of the crystal structures shows that diethylenetriamine moieties in these complexes always occur either in the λλ or δδ conformations.[1,2]

In solution the complex exists as a mixture of interconverting conformers, as was originally suggested on the basis of variable temperature ^1H NMR studies for the diamagnetic La (III) and Lu (III) complexes of DTPA derivatives recorded by Rizkalla *et al.*[138] The crystal structures of complexes of DTPA show in some cases, that the coordination around the central lanthanide ion is completed by a neighbouring carboxylate group, rather that one solvent water molecule. Detailed X-ray absorption studies of $[Gd(DTPA)]^{2-}$, have also shown that the local structure around the Gd (III) ion in aqueous solution is similar to that observed in the crystals.[8] When viewing the $[Ln(DTPA)(OH_2)]^{2-}$ chelate up the N_3O basal plane, it becomes apparent that there are two enantiomeric conformations, defined by the three NC-CO torsion angles (Λ: negative). This gives rise to differing right or left

handed orientations of three of the acetate arms, associated with different Δ or Λ helicites about the metal centre (Figures 5.4 and 5.5).[137]

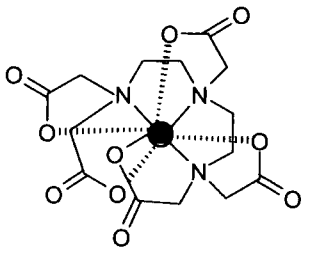

Figure 5.4: In the Λ complex, the NCCO torsion angle is negative

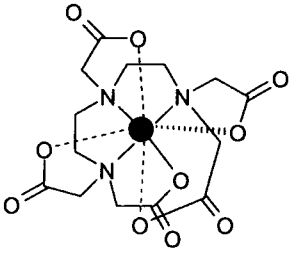

Figure 5.5: View up the Ln-water vector, or down the N_3O basal plane, for the Δ complex

As a result, the two conformers λλ and δδ, distinguished by the helicity of the C-C ethylene bond relative to the Ln (III) N-N plane, may interconvert through a shuffling of the acetate groups accompanied by a flip in the diethylenetriamine backbone. The nitrogen atom N-6, in this case, is rendered chiral upon complexation.[127]

The introduction of the lipophilic ethoxybenzyl moiety, creates a stereogenic centre at C-4 (Figure 5.2), as in the case of (S)-EOB-DTPA and renders each of the conformations diastereoisomeric. Thus, there are 4 diastereoisomeric complexes for (S)-[Ln-(EOB-DTPA)(H_2O)]$^{2-}$ (see Figure 5.6), distinguished by an S or R configuration at N and by a Δ/Λ helicity about the metal centre. The analysis does not include consideration of the preferred δ or λ confirmation of each of the NCCN chelate rings.

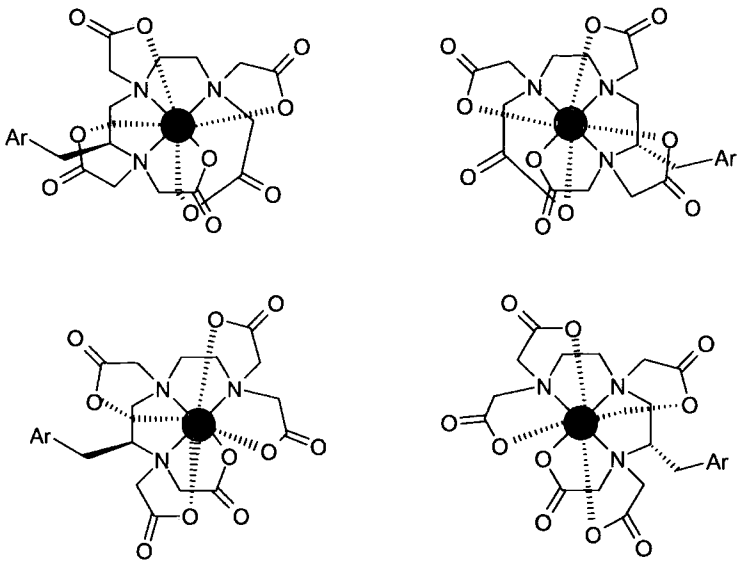

Figure 5.6: Four possible diastereoisomeric complexes for (S)-[Eu-EOB-DTPA(H_2O)]$^{2-}$

The ligand EOB-DTPA used throughout the investigation was of (S) absolute configuration; the compound was synthesised and donated by Schering Research laboratories AG, Berlin Germany. None of the (R) enantiomer was provided for study.

Protein binding studies of [Gd-(S)-(EOB-DTPA)(H_2O)]$^{2-}$ versus [Gd-(R)-(EOB-DTPA)(H_2O)]$^{2-}$, in the presence of human serum albumin, and the non-covalent binding of the paramagnetic complexes to the macromolecule had earlier been studied. Each isomer was found to bind in a non-covalent manner to human serum albumin. However, the affinity of the (S) isomer for the protein was much greater than that for the (R) isomer.[139] This may have been a reason for the preference of the (S) enantiomer being studied rather than the (R) configuration.

Previous work on (S)-EOB-DTPA carried out by Schmitt-Willich *et al*[140] involved complexation of the ligand with the lanthanide metal gadolinium, generating two chiral centres, hence two diastereoisomers of (S)-[Gd-(EOB-DTPA)(H_2O)]$^{2-}$. It was shown that the two diastereoisomers could be separated by reversed phase HPLC, resulting in a ratio of the two components of 65:35 (Figure 5.7).

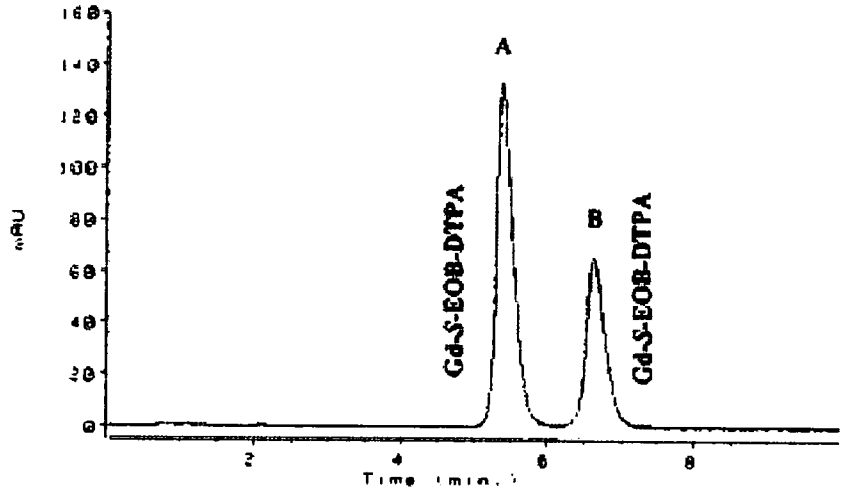

Figure 5.7: Separation of the diastereoisomers A and B of [Gd-EOB-DTPA]

The two diastereoisomers were postulated to differ in the configuration at the central nitrogen atom N-6. Information regarding the local helicity of the metal complex at this point had not yet been obtained.

5.2 Project Aims

The aims of the project were to synthesise the europium analogue of (S)-EOB-DTPA and examine the ^{1}H-NMR behaviour and chiroptical spectroscopic properties. The large dipolar contribution to the paramagnetic shift of the Eu (III) complexes aids NMR spectral analysis. Also, europium (III) is luminescent in aqueous solution and retains this luminescence when bound as a complex. Europium exhibits multiple emissions (due to several electronic transitions), whose relative intensities and line splitting patterns (band structuring) are sensitive to the detailed nature of the ligand environment about the metal centre.[108] As the complexes synthesised are chiral they can be studied by chiroptical spectroscopy. This includes circular dichroism, CD (the differential absorption of left and right circularly polarised light) and more particularly circular polarised luminescence, or CPL, (the differential spontaneous emission of left and right circularly polarised light).[141]

Chiroptical spectroscopy can provide unique information regarding coordination geometry, stereochemistry, electronic state structure, and the interactions between a complex and its environment. Whereas CD reflects the ground state structure, CPL

probes the structure of the excited state, which can provide us with information about the helicity of the metal complex around the europium centre.[127] From the extensive knowledge previously obtained within the Parker research group, concerning structurally related chiral complexes based upon the cyclen skeleton, and the effects of complex geometry and isomerism, comparative analysis with this DTPA based system could be made.[127, 142]

5.3 Solution NMR analysis

The europium (III) complex **[EuL^{14}]** of (S)-EOB-DTPA was prepared by a slightly modified method to that already established for the synthesis of the gadolinium (III) analogue reported by Schmitt-Willich *et al.*[140] Following heating of the ligand in the presence of equimolar quantities of europium (III) chloride, suspended in equivalent volumes of water and methanol mixture, the solution pH was adjusted to pH 5.5., using 0.1 M sodium hydroxide. The mixture was then concentrated by reduced pressure and the resulting concentrate added dropwise to a warmed solution of ethanol. Upon heating, a turbid solution resulted, which was centrifuged, the white solid collected, washed with ethanol and dried. This solidified product was dissolved into water and the pH adjusted to remove any free lanthanide material present as the free lanthanide hydroxide, which if un-removed may have affected the quality of the analytical spectra obtained.

Similarly to earlier work, the complex (S)-[Eu-(EOB-DTPA)(H_2O)]$^{2-}$, **[EuL^{14}]** was analysed again by reversed phase HPLC, which revealed the presence of two species (diastereoisomers), which were individually collected by preparative HPLC. The isometric ratios of 57:43 were very similar to those found for the related Gd (65:35) and La (60:40) analogues.[140] The separated complexes when stored in solution were held at 4°C, to minimise the rate of isomer interconversion. ^{1}H NMR stability studies for the separated diastereoisomers of **[EuL^{14}]**, were evaluated over a three month time period at this temperature, and evidence for <5% interconversion was found. However, at ambient temperature, interconversion was found to occur, reaching equilibrium within approximately 72 hours. This value was in conflict with the behaviour of the separated (S)-[Gd-(EOB-DTPA)]$^{2-}$

diastereoisomers earlier studied by Schmitt *et al*,[140,8] where interconversion was found to be very slow, the half-life time of one of the Gd (III) isomers being 13100 hours at pH 9 and 25°C. At thermodynamic equilibrium, the ratio of the isomers was found to be 65:35. The first order rate constant for the interconversion between the isomers is pH dependent, suggesting that the isomerisation is an acid catalysed process similar to the dissociation of the complex.[8,140] NMR studies of the two (S)-[La-(EOB-DTPA)]$^{2-}$ complexes, had earlier given no evidence for the presence of enantiomers that differ in the orientation of the acetate groups. Although four are theoretically possible for the system, two are mirror images of one another and therefore discrimination by NMR is impossible. Proton NMR analysis of the europium mixture of the complex (S)-[Eu-(EOB-DTPA)]$^{2-}$, **[EuL^{14}]** revealed the presence of two species (D_2O, 200 MHz), Figure 5.8. Although it was obvious that there was one major isomer, the shifted resonances of the minor isomer were significantly broader than those associated with the major species.

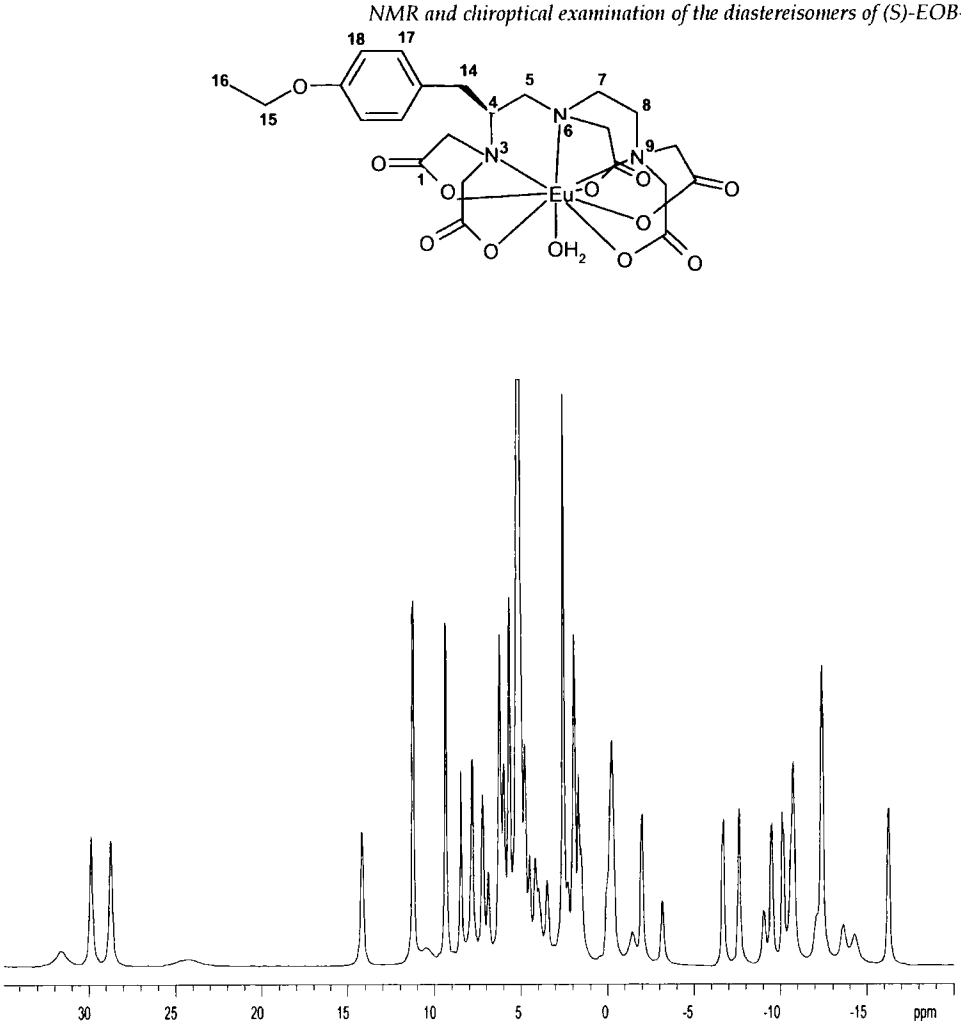

Figure 5.8: ^{1}H NMR spectrum (200 MHz, D_2O, 296 K) of the mixture of diastereoisomers of (S)-[Eu-(EOB-DTPA)]$^{2-}$ [EuL^{14}].

A detailed variable temperature NMR study of the mixture was undertaken over the range of 4°C to 92°C. The broadened, shifted resonances of the minor isomer were found to be much sharper upon heating. Upon closer inspection of the completed variable temperature study, the spectral data revealed there were only two species in solution, each with an equal number of isochronous resonances.[137] There was no firm evidence to suggest that an exchange process between the two observed isomers was occurring, as line broadening variations involving the minor isomer were not echoed by spectral changes in resonances of the major species (Figures 5.9 and 5.10). The temperature dependence of the chemical shift variations for every resonance in each isomer was the same and within experimental error followed the expected T dependence of the paramagnetic shift.[108] Such behaviour

precludes the presence of an intramolecular exchange process between the observed species, on the NMR timescale.

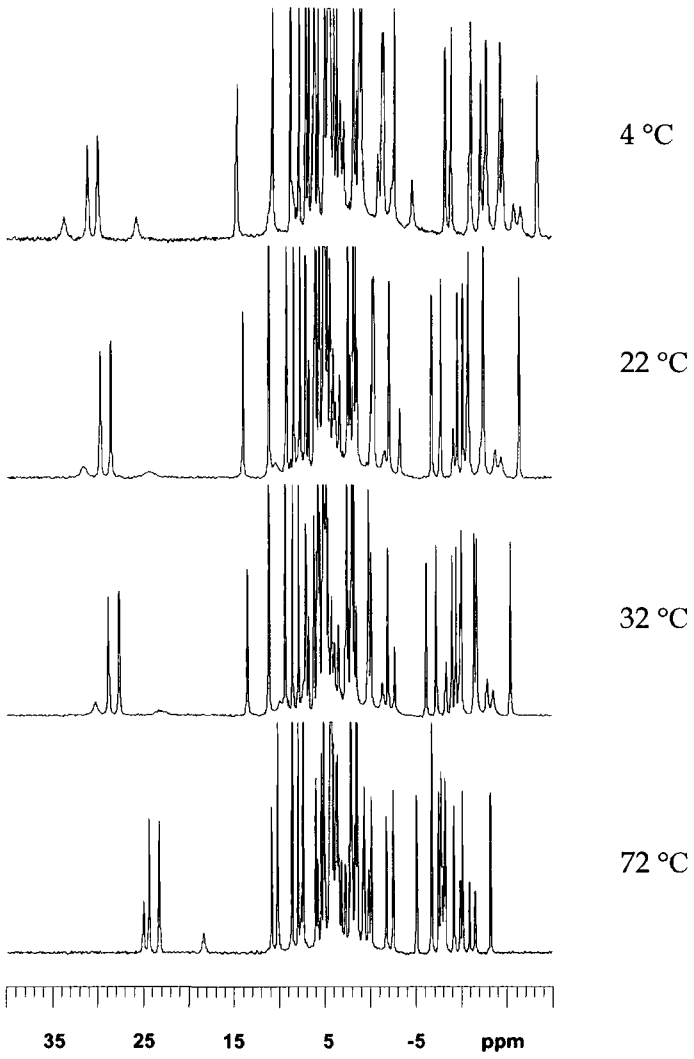

Figure 5.9: Variable temperature proton NMR spectra (300 MHz, D_2O) of the stereoisomeric mixture of (S)-[Eu-(EOB-DTPA)]$^{2-}$, [EuL^{14}] between 4°C and 72°C.

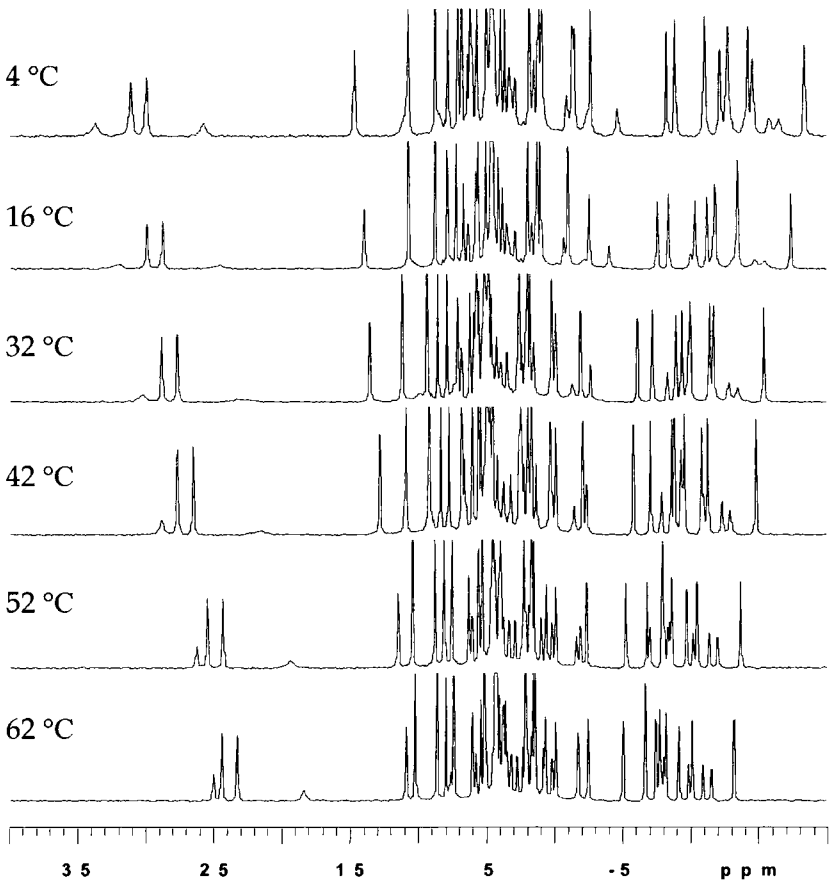

Figure 5.10: Variable temperature proton NMR spectra (300 MHz, D_2O) of the stereoisomeric mixture (S)-[Eu-(EOB-DTPA)]$^{2-}$, [EuL^{14}] between 4°C to 62°C.

The proton spectrum of the major isomer was fully assigned using COSY (proton - proton correlation) experimental methods (Figure 5.11), the interpretation of spectra being aided by comparison to earlier studies on structurally related derivatives of cyclen following the work of other members of the research group.[143,144,145] The resonances of each proton in the complex were anisochronous, except for the ortho/meta aryl protons at +28.9 and +10.9 ppm. The three protons at C_4 and C_5 form a mutually coupled sub-set, with the axial proton, H_5^{ax}, resonating to highest frequency at 28.0 ppm. Similarly, the four protons at C_7 and C_8 in the unsubstituted 5-ring chelate, formed a distinctive mutually coupled sub-set of resonances, with H_8^{ax} resonating at 29.0 ppm. Each proton in the five CH_2CO groups is chemical shift non-equivalent, and five mutually coupled sets were

identified. In Figure 5.11 these are arbitrarily labelled $H_{ac\text{-}x}/H'_{ac=x}$ (x= 1to 5), but could not be assigned to a given carbon. The relative shift and form of the resonances, for the minor isomer were similar to that of the major species (aside from the greater degree of line-broadening and the slightly smaller overall paramagnetic shift), suggesting that each complex adopts a very similar coordination environment and geometry.[137]

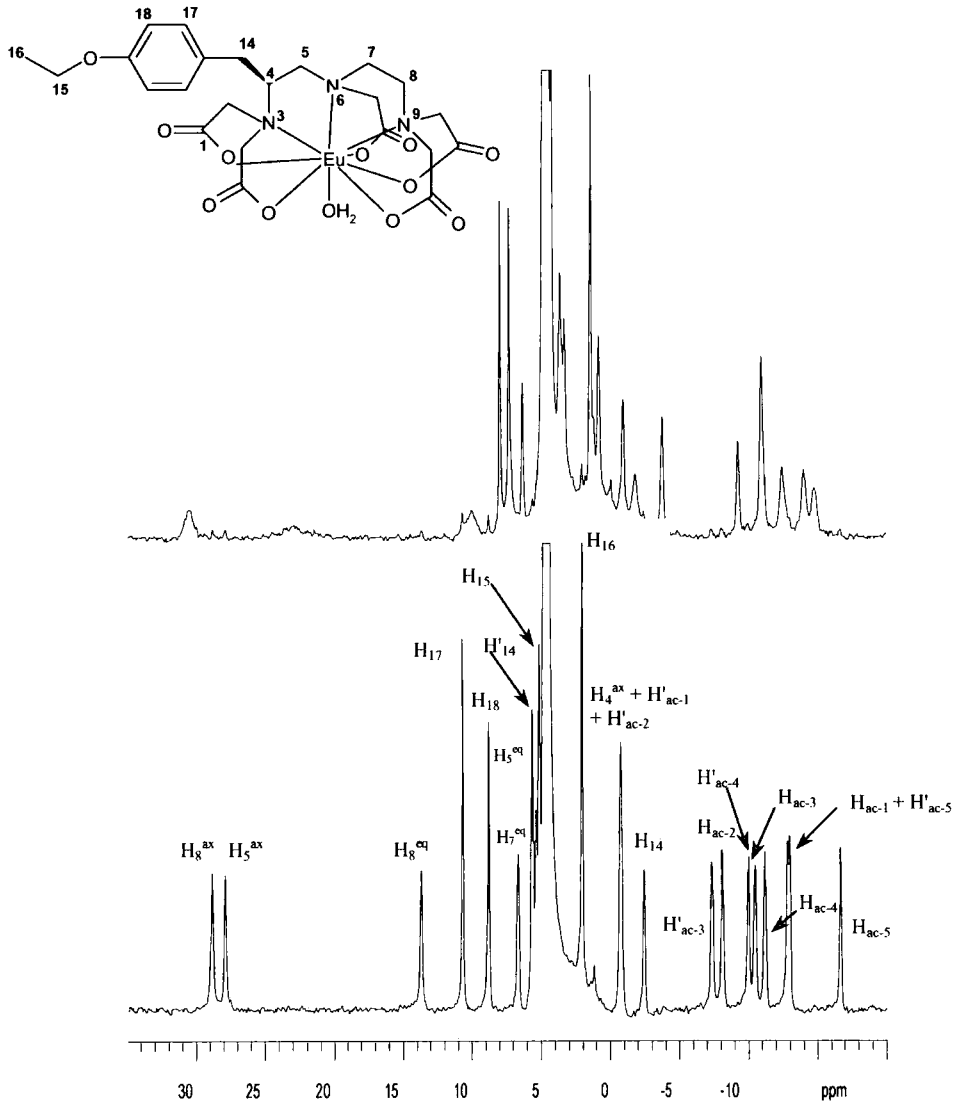

Figure 5.11: ^{1}H NMR spectra (500 MHz, D_2O, 296 K, 2 mM complex) of the separated isomers; upper: minor isomer; lower: major isomer showing the assignment obtained by COSY analysis.

Inner sphere proton relaxivity is linearly proportional to the number of water molecules directly coordinated to the central Ln (III) metal ion as shown by Equation 5.1, where *c* is the molal concentration, q is the number of bound water molecules per Ln ion (hydration number), P_m is the mole fraction of the bound water molecules, τ_m is the lifetime of the water molecule residing on the Ln (III) centre (equal to the reciprocal water exchange rate $1/k_{ex}$), and $1/T_{1m}$ is the longitudinal proton relaxation rate.[3]

$$\left(\frac{1}{T_1}\right) = \frac{cq}{55.5}\left(\frac{1}{T_{1m}+\tau_m}\right) = P_m \frac{1}{T_{1m}+\tau_m} \qquad \textbf{(5.1)}$$

The above equation shows clearly that proton relaxivities cannot be determined without knowing the hydration number. Determination of hydration number can be calculated from solid state structures, however there are examples of a change in hydration number observed from the solid state to the solution state. Therefore, the determination of hydration number in aqueous solution is important and there are several experimental techniques available, although none can be directly applied to Gd (III) chelates.[111]

The hydration states for the Eu (III) complex **[EuL^{14}]** were determined by laser-induced luminescence, where the difference in luminescence lifetimes measured in H_2O and D_2O solutions, is related to the hydration number, q of the complex based upon the following equation, where τ is the luminescence lifetime and A_{Ln} is a proportionality constant specific to a given lanthanide. For Eu (III) complexes, A = 1.05 ms^{-1}.[3]

$$q = A_{Ln}(\tau^{-1}_{H_2O} - \tau^{-1}_{D_2O}) \qquad \textbf{(5.2)}$$

The values obtained for the major isomer were ($k^{major}_{H_2O}$ = 1.65 ms^{-1}; $k^{major}_{D_2O}$ =0.50 ms^{-1};q=1.1) and for the minor isomer ($k^{minor}_{H_2O}$ =1.63 ms^{-1}; $k^{minor}_{D_2O}$ = 0.51 ms^{-1}; q = 1.0); the values are consistent with the presence of a single quenching water molecule.

The results are in agreement with the measured hydration value for the complex [Dy-(EOB-DTPA)]$^{2-}$, determined by the induced water ^{17}O shifts for the Dy (III) metal ion, where a hydration value of 1.2 was measured.[8]

5.4 Chiroptical Spectroscopy

The chirality of the complex (S)-[Eu(EOB-DTPA)(H_2O)]$^{2-}$, **[EuL^{14}]** allows chiroptical techniques such as circular dichroism (CD) and circular polarised luminescence (CPL) to be used. Chiroptical properties of lanthanides are particularly sensitive to ligand coordination geometry and stereochemistry, electronic state structure, and the interactions between a complex and its environment. In chiroptical spectroscopy, different mechanisms are used to determine band intensities and compared to conventional spectroscopy; further structural information may be available.[127]

5.5 Circular Dichroism

If light is composed of two plane waves of equal amplitude but differing in phase by 90°, then the light is said to be circularly polarised. Circular dichroism (CD) is observed when optically active matter absorbs left and right handed circular polarised light slightly differently.[146] When circular polarised light passes through the optically active sample with a different absorbance, A, for the two components, the amplitude of the stronger absorbed component will be smaller than that of the less absorbed component. The consequence is that a projection of the resulting amplitude will now yield an ellipse instead of the usual line. This occurrence of ellipicity is called circular dichroism.[146] The technique requires a source of monochromatic left and right circularly polarised light produced by a photoelastic modulator, (in older instruments a Pockels cell), which produces alternatively right and left circularly polarised light with a switching frequency of about 50 kHz, which is detected by a photomultipler tube. The current output of the tube is converted to a voltage signal, the mean intensity of which is proportional to the total CD. The other signal is fed into a lock-in amplifier, where the alternating current (AC) ripple present in the large direct current (DC) background is amplified

by means of a phase sensitive detector, and is proportional to the CD intensity.[147]

The CD experiment thus produces two signals. One signal results from the differential absorption of one component over the other and is proportional to the circular dichroism. The remaining signal is averaged and related to the mean light absorption. The ratio of these signals is the absorption dissymmetry factor, g_{abs} defined by the following equation, where ε_L and ε_R correspond to extinction coefficients for left and right circularly polarised components of the emitted radiation.[146]

$$g_{abs}(\lambda) = \frac{2(\varepsilon_L - \varepsilon_R)}{(\varepsilon_L + \varepsilon_R)} \qquad (5.3)$$

A CD spectrum is a plot of $\Delta\varepsilon$ versus wavelength and since different electronic transitions involve the redistribution of electrons of different handedness, any one molecule may give rise to both positive and negative CD signals.

5.6 CD measurements of (S)-[Eu-(EOB-DTPA)(H_2O)]$^{2-}$

The CD spectrum of (S)-EOB-DTPA ligand in water was recorded in the ultra-violet region, (pH 7.5, 295K) and compared to the spectra obtained for the Eu (III) complex **[EuL^{14}]**. Two bands were seen for the enantiomerically pure free ligand; a positive band at 245 nm (g_{245} = +3 x 10^{-4}) and a negative band at 276 nm (g_{abs} = -6 x 10^{-4}) were distinguished. The CD spectra obtained for each of the diastereoisomers of **[EuL^{14}]** were found to be very similar to those of the free ligand, with a slight reduction in the measured dichroism (approximately 40% lower in terms of the measured g values). Generally, circular dichroism measurements require a higher concentration of the lanthanide complex as most 4 *f-f* transitions are parity forbidden and have very low molar absorptivities, (values for ε for Eu (III) transitions are typically < 1 dm^3 mol^{-1} cm^{-1}).[127] For this reason, it was decided to measure the high resolution CPL spectra instead, as this technique combines instrument sensitivity with structure selectivity and can be carried out on dilute solutions of lanthanide complex, e.g. 0.5 to 10.0 mM solutions. CPL also has the

advantage that in some cases, an enantiomerically enriched excited state can be generated from a racemic ground state.[148]

5.7 Circularly polarised luminescence

Circularly polarised luminescence (CPL) is the emission analogue of circular dichroism. While CD probes the geometry of molecules in the ground state, CPL probes the chirality of the emitting excited states.[147] CPL is particularly valuable to investigate transitions that cannot be easily studied by absorption techniques, such as the intraconfigurational *f-f* electronic transitions of the lanthanide (III) ions that obey magnetic dipole selection rules (e.g. $\Delta J = 0, \pm 1$ except $0 \leftrightarrow 0$). These are often associated with large optical activity and therefore intense CPL interactions. CPL spectroscopy has been shown to be a very useful tool for studying the solution structure and dynamics, of a wide variety of chiral luminescent species.[149]

CPL instrumentation is not readily available, however suitable instruments had been assembled by several research groups. The instrumental developments have paralleled those in the field of CD.[150] The experiment procedure involves the sample being excited at 90° from the direction of the emission detection source. The emitted light passes through a circular analyser incorporating a photoelastic modulator (PEM), operating at a frequency of 50 kHz, which acts as an oscillating quarter wave plane. This results in right and left circularly polarised light being converted into the appropriate linear polarisation, selected by the linear polarizer, and subsequently wavelength resolved by the emission monochromator and detected by the photomultiplier. Different enantiomers (Δ and Λ) will preferentially absorb CPL light leading to an enantiomeric excess in the excited state.

In CPL spectroscopy, the degree of emitted circular polarised light is commonly reported in terms of the emission dissymmetry ratio, g_{em}, which is defined in Equation 5.4, where I_L and I_R, are the emission intensities for left and right handed circularly polarised light.

$$g_{em}(\lambda) = \frac{2(I_L(\lambda) - I_R(\lambda))}{(I_L(\lambda) + I_R(\lambda))} \qquad \textbf{(5.4)}$$

The large number of possible transitions between different J states renders chiroptical spectra very complicated for most lanthanide systems, with the exception of europium (III) complexes.[127] This is due to the absence of degeneracy of the emissive $^5D_0$ excited state.[142] Europium (III) emission spectra can predict the oscillator strength of the $^7F_2 \leftarrow ^5D_0$ transition, which is exquisitely sensitive to the coordination environment around the metal ion centre. Most CPL spectra recorded in the literature for Eu (III) complexes have been for the emissions associated with the $^5D_0 \rightarrow {}^7F_J$ (J = 0-6) transition manifolds. The strongest emissions are invariably observed in the $^5D_0 \rightarrow {}^7F_{1,2,4}$ transition regions, with the 0 → 2 emission intensity exhibiting a hypersensitivity to the ligand environment (as characterised by donor atom types, coordination number, and coordination geometry). In Eu (III) CPL studies, the best probe transitions are those occurring within the $^5D_0 \rightarrow {}^7F_1$ emission region (~ 16,700 - 17,100 cm^{-1}).[127]

In order to use CD and CPL to probe the chirality of lanthanide complexes, absorption and emission transitions should be selected that obey selection rules for lanthanide optical activity.[151,152] The sign and magnitude of the optical activity associated with a given transition between two states a and b is assessed by the rotary strength (Equation 5.5), where τ_{ab} is the angle between electric vector, μ, and magnetic vector, m.

$$R_{ab} = |\mu| |m| \cos \tau_{ab} \quad (5.5)$$

The intensity of the CD and CPL bands are therefore dependent upon the magnetic and electric dipole strengths of the transition. The dissymmetry value is a measurement of the degree of chirality sensed by the electronic absorption or emission transitions. The greatest dissymmetry factors should be exhibited by transitions, which are magnetic-dipole allowed, and electric dipole forbidden, whereas the most intense CPL transitions will tend to be both magnetic and electric dipole allowed.

5.8 CPL measurements of (S)-[Eu-(EOB-DTPA)(H_2O)]$^{2-}$

The metal based CPL emission spectrum in the transition $^7F_0 \rightarrow {}^5D_0$ was measured for each of the separated isomers of the complex (S)-[Eu-(EOB-DTPA)(H_2O)]$^{2-}$, **[EuL^{14}]** complex in an aqueous media, at pH 7.5, 282 K. The lower temperature was chosen to minimise the risk of any isomer interconversion on the experimental time scale, and revealed the presence of only one peak centred at 579.7 nm (Figure 5.12).

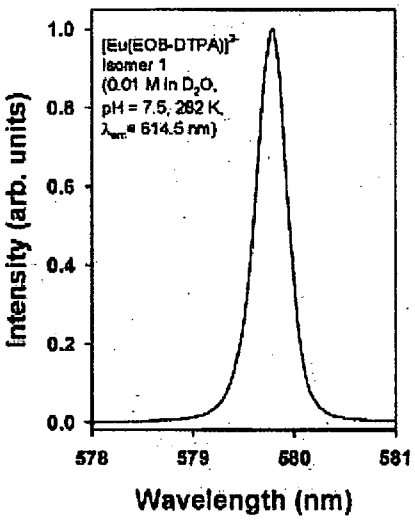

Figure 5.12: The $^7F_0 \rightarrow {}^5D_0$ CPL emission spectra for (S)-[Eu-(EOB-DTPA)(H_2O)]$^{2-}$, [EuL^{14}] showing each isomer was the same.

CPL spectra were measured for the $^5D_0 \rightarrow {}^7F_1$ transition, following excitation at the maximum of the $^5D_0 \rightarrow {}^7F_0$ excitation transition at 579.7 nm. The magnitudes of the g_{em} values were slightly different between the two isomers (see Figure 5.13). The CPL spectra were also measured for the $^5D_0 \rightarrow {}^7F_2$ transition following excitation at 589.4 nm. The magnitudes of the g_{em} values were only slightly different for the two isomers with the form and sequence for the observed bands being the same (Figure 5.14).

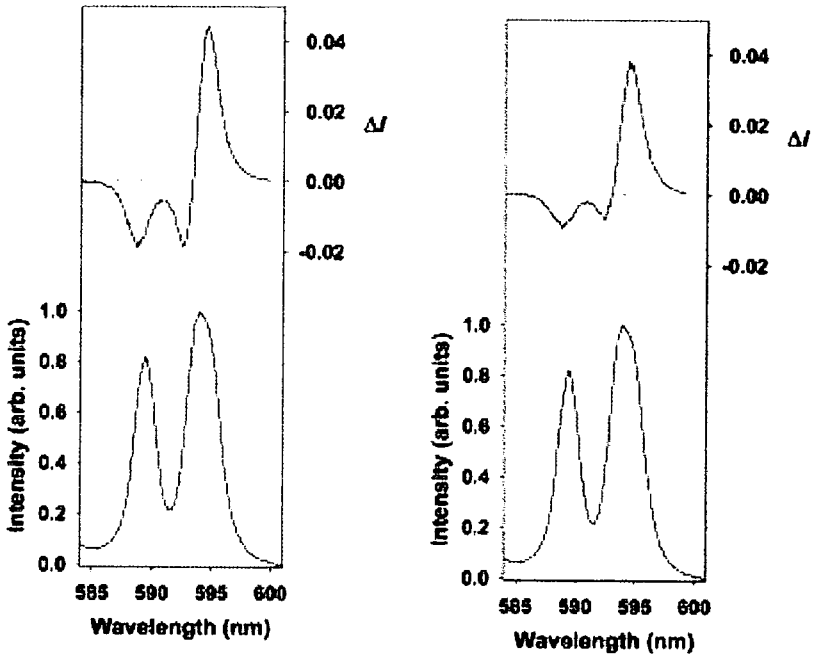

Figure 5.13: Emission (lower) and circularly polarised emission (upper) spectra showing the MD-allowed ΔJ = 1 transitions for (S)-[Eu-(EOB-DTPA)]$^{2-}$ for the major (left) and minor isomer (right) (10 mM complex, pH 7.5, 9°C, D_2O, λ_{exc} = 589.4 nm).

The magnitude of the g_{em} values was only slightly different for the 2 isomers with the form and sign sequence for the observed bonds being the same. Thus, $g_{em}^{594} = +0.10(\pm 0.01)$ in each case, whereas $g_{em}^{588} = -0.04$ (major) and -0.02 (minor) and $g_{em}^{593} = -0.05$ (major) and -0.02 (minor).

For the electric dipole ΔJ =2 transition, the CPL spectra were similar, with $g_{em}^{616} = -0.10(\pm 0.01)$ and -0.08 with $g_{em}^{622} = +0.06(\pm 0.01)$ for each isomer (Figure 5.14).

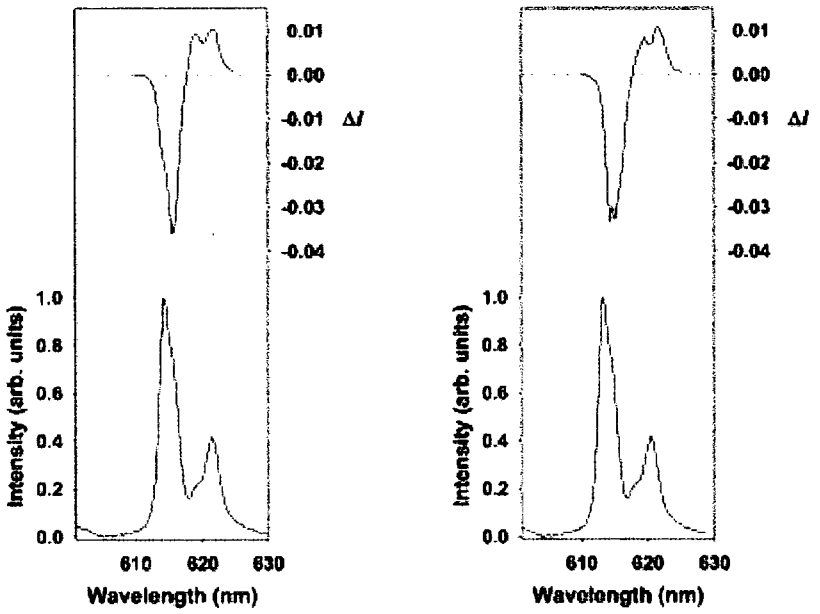

Figure 5.14: Emission (lower) and circularly polarised emission (upper) spectra showing the ED-allowed ΔJ=2 transitions for (S)-EOB-DTPA, for the major (left) and minor isomers (right) (10 mM complex, pH 7.5, 9°C, D_2O, λ_{exc} = 589.4 nm).

5.9 Conclusions

It can be concluded that the europium (III) complex of (S)-EOB-DTPA, **[EuL^{14}]** exists in solution as two isomers, which are in slow exchange at ambient pH and temperature on the NMR timescales. The similarity in the paramagnetic shifted NMR spectrum implies an identical coordination environment for the two isomeric species i.e. each has the same coordination number geometry, with the same donor arm layout. However, it was apparent from variable temperature NMR experiments that the minor isomer differed in intermolecular exchange dynamics from the major isomer. The similar CPL spectra of each isomer provided compelling evidence that each of the isomers possessed the same time-averaged helicity about the principle axis around the metal centre. Otherwise, more significant differences in their emission dissymmetry factors and in their sign and sign sequence (Λ and Δ), for the observed bands in the magnetic-dipole allowed ΔJ=1 manifold, i.e. a -/- to + sequence would have been observed.

It is concluded that each of the isomers for the (S) complex differs only in its configuration at the central nitrogen. This is consistent with the temperature and pH dependence of their rate of interconversion. The overall helicity for each isomer

is suggested to be Λ. Prior CPL studies quoted in the literature, examining several Λ and Δ Eu analogues of chiral lanthanide complexes based upon a 1,4,7,10 tetraazacyclododecane backbone, have shown that a Δ-complex is characterised by the +/+ to - sequence in the ΔJ=1 transitions of the circularly polarised light emission spectra. For these examples, the absolute configuration was also independently determined from other techniques such as X-ray crystallography.

Parker *et al* noted this behaviour for several europium complexes, including the C-4 symmetric cationic tetraamide complex **[Eu3a]**$^{3+}$ (Figure 5.15), where the predominant (Δ *-λλλλ)* isomer (≥90%), is a mono-capped square antiprismatic structure with an S configuration at the carbon. This was an ideal system to study as the complex obviously exists as one isomer in solution and its exchange dynamics had already been clearly defined. CPL behaviour and emission dissymmetry values for **[Eu3a]**$^{3+}$ were compared with other europium complexes, including **[Eu4]**$^{3+}$ (SSS), which lacks C_n symmetry.[142]

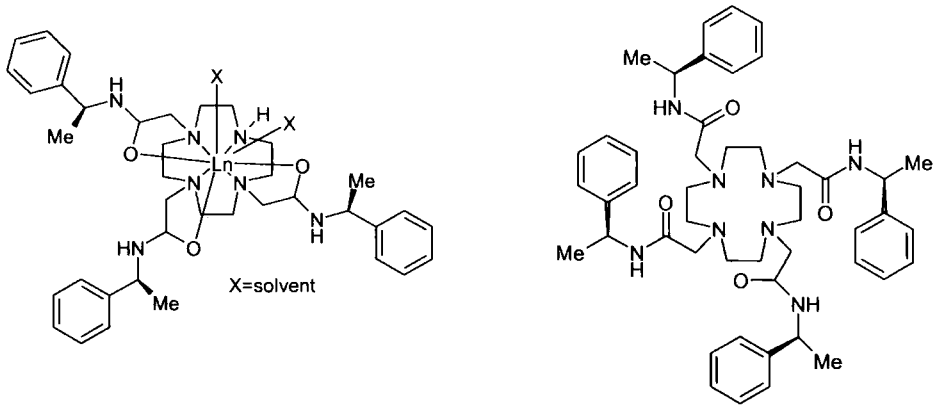

Figure 5.15: Chemical Structures of [Eu3a]$^{3+}$ and [Eu4]$^{3+}$ respectively

The spectrum shows the adjacent positive and negative CPL bands observed for the magnetic-dipole allowed ΔJ=1 transition at 588 and 594 nm for the (SSSS)-**[Eu3a]**$^{3+}$ and (SSS)-**[Eu4a]**$^{3+}$ (Figure 5.16).

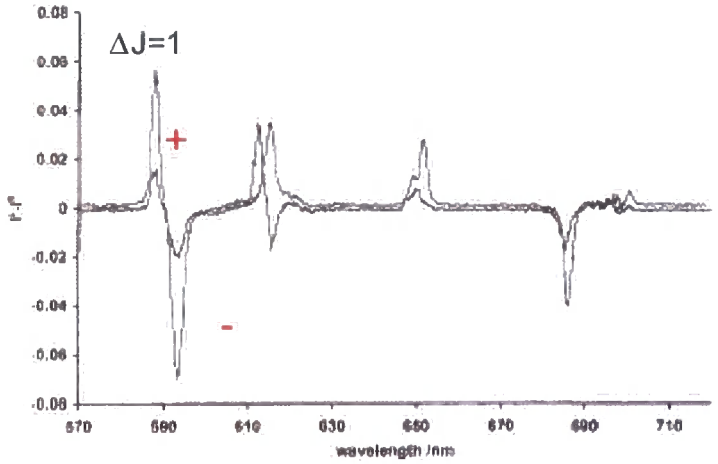

Figure 5.16 : Circualrly polarised emission spectra for (SSSS)-[Eu3a]$^{3+}$ and (SSS)-[Eu4]$^{3+}$ in water (1 mM complex, 295 K, λ_{exc} = 255 nm.

The spectrum was compared to that obtained for the isomeric (RR) diamide complex, where the complex shows mirror image behaviour, hence Λ helicity around the metal centre, corresponding to a reverse for the adjacent bands of the ΔJ=1 transition at 588 and 594 nm (Figure 5.17).

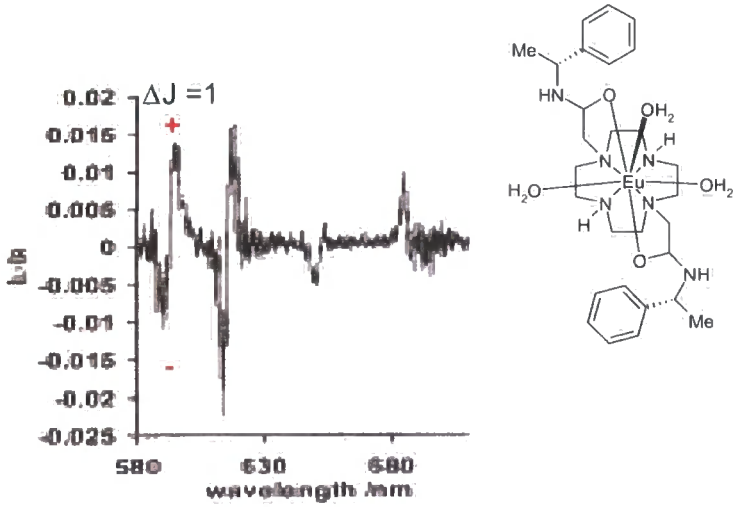

Figure 5.17: Circularly polarised luminescence spectra for trans-(RR)-[Eu6]$^{3+}$ in MeCN solution (1 mM complex, 295 K, λ_{ece} 255 nm).

Thus, it can be concluded that the two isomers existing in solution were of Λ helicity about the Eu-OH_2 vector.

5.10 Protein Binding Studies

Magnevist (gadopentetate dimeglumine $[Gd(DTPA)]^{2-}$) and other extracellular agents rapidly distribute in the vascular and interstitial space but they do not cross plasma membranes. Their hepatocellular uptake and biliary excretion are negligible. Targeting the hepatocytes is an effective approach for imaging the liver and there are several compounds with different magnetic properties currently in clinical trials, such as $[Gd\text{-}(EOB\text{-}DTPA)(H_2O)]^{2-}$, which has been discussed throughout this chapter.

$Gd(BOPTA)^{2-}]$, (international non-proprietary name: gadobenate) is also a promising candidate for hepatocyte imaging. Similarly, to $[Gd\text{-}(EOB\text{-}DTPA)(H_2O)]^{2-}$, the contrast agent is a lipophilic analogue of DTPA, incorporating one aromatic side chain arm.[86]

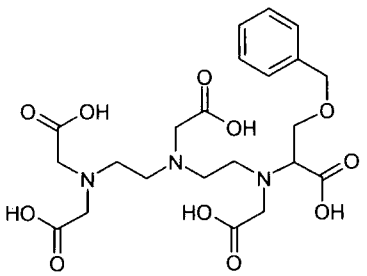

Figure 5.18: Chemical structure of BOPTA.

Relaxivity studies for the gadolinium complexes of both EOB-DTPA and BOPTA show that the relaxivity of these compounds is higher than expected when compared to the values obtained for the parent compound DTPA. This has been attributed to a reduced distance between the central gadolinium (III) ion and the inner sphere water protons (approximately 0.29 nm), compared to the value reported for $[Gd(DTPA)]^{2-}$ of 0.31 nm. The species are both reported to bind weakly *in vivo* with human serum albumin, both being relatively biochemically passive, so that toxicity associated with their binding is not a significant issue. However, side effects of hepatobiliary agents in humans have been reported for $[Gd(BOPTA)^{2-}]$, whereas $[Gd\text{-}(EOB\text{-}DTPA)(H_2O)]^{2-}$, has so far been found to be a safe contrast agent in the patients studied.[135]

$[Gd\text{-}(EOB\text{-}DTPA)(H_2O)]^{2-}$ exhibits a T_1 relaxivity as measured in water at 0.47 Tesla of 4.9 $mM^{-1}s^{-1}$, compared to gadopentetate dimeglumine $[Gd\text{-}(DTPA)]^{2-}$ with a relaxivity value of 3.7 $mM^{-1}s^{-1}$. However, a much higher T_1 value of 8.2 $mM^{-1}s^{-1}$ is exhibited for $[Gd\text{-}(EOB\text{-}DTPA)(H_2O)]^{2-}$ in the presence of human serum whereas the relaxivity in human serum for $[Gd(DTPA)]^{2-}$ is 5.0 $mM^{-1}s^{-1}$.[36] Hence, a greater degree of protein binding, creating an increase in molecular weight, hence an increased τ_R effect, is exhibited by $[Gd\text{-}(EOB\text{-}DTPA)(H_2O)]^{2-}$ compared to $[Gd\text{-}(DTPA)]^{2-}$. $[Gd(BOPTA)]^{2-}$ is also found to bind moderately to human serum albumin.[8]

The BOPTA ligand (4-carboxy-5,8,11-tris(carboxymethyl)-1-phenyl-2-oxa-5,8,11-triazatridecan-13-oic acid) was kindly donated by Bracco SpA, Italy. The homogeneity of the ligand sample was confirmed by ^1H and ^{13}C NMR. Gadolinium (III) complexes of BOPTA and EOB-DTPA were examined in protein binding studies, allowing a comparison with earlier work (Chapter 2) and with the literature. The protein binding interaction of each of the gadolinium complexes was assessed by measuring the proton relaxation rates at 60 MHz, 37°C, in the presence of water and then titrating the paramagnetic solution with increasing concentrations of human serum albumin.

The protein binding curve for the gadolinium complex of $[Gd\text{-}(EOB\text{-}DTPA)(H_2O)]^{2-}$ is shown in Figure 5.19.

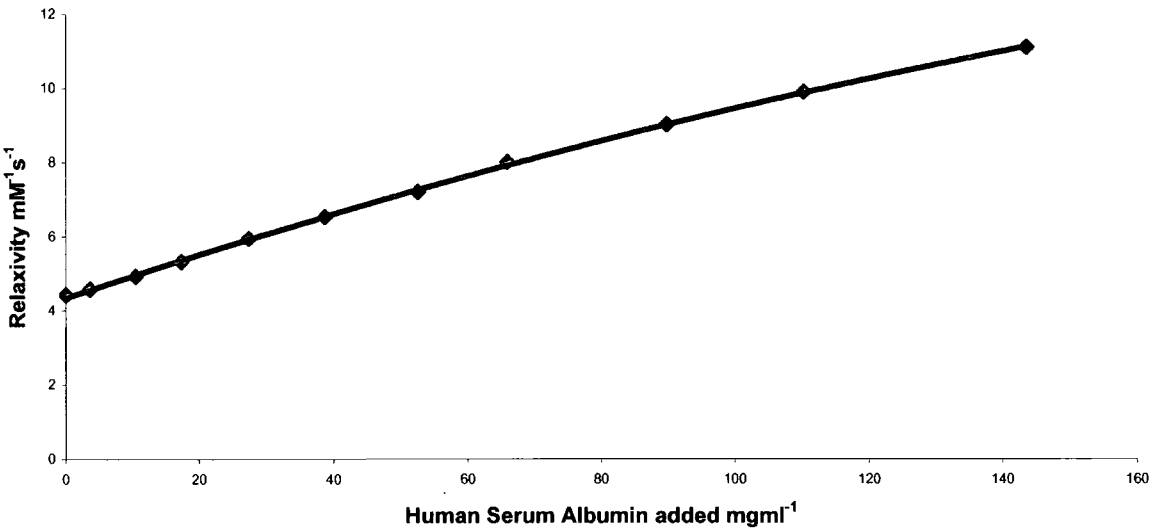

Figure 5.19: Increase in relaxivity of [Gd-(EOB-DTPA)(H_2O)]$^{2-}$] with increasing HSA concentration (60 MHz, 37°C).

The relaxivity values of the free complexes prior to titration with serum albumin are shown in table 5.1.

Complex	Relaxivity free complex	Relaxivity Human serum
[Gd-(EOB-DTPA)(H_2O)]$^{2-}$	4.41	6.50
[Gd-(BOPTA)(H_2O)]$^{2-}$	4.18	5.76

Table 5:1: Relaxivity values obtained for [Gd-(EOB-DTPA)]$^{2-}$ and [Gd-(BOPTA)]$^{2-}$ as the free complexes and as HSA adducts (60 MHz, 37°C)

The results show that there is a weak interaction for each of the complexes with human serum albumin especially with respect to the parent compound [Gd(DTPA)]$^{2-}$. The binding of [Gd-(EOB-DTPA)(H_2O)]$^{2-}$ with serum albumin is of slightly higher affinity to the protein than that of [Gd-(BOPTA)(H_2O)]$^{2-}$. The modest increases revealed here for these commerically important complexes may now be compared to those obtained for the complexes examined in detail in Chapters 2 and 4.

Conclusions and Suggestions for further work

Although it was hoped that heptadentate ligands based upon aDO3A, incorporating aromatic substituents, capable of binding to serum albumin may result in contrast agents with very high relaxivities, these studies in this thesis have shown the relaxivity enhancements were not as large as hoped for. The complex, $[Gd(aDO3A)]^{3-}$ was not found to bind endogenous anions, such as carbonate, phosphate and lactate at physiological pH. However, addition of hydrophobic substituents on the ring nitrogen atom, producing a variety of tetrasubstituted species, results in complexes with increased affinities towards anions. It may be possible to selectively increase the affinity towards serum albumin, yet prevent the binding of anions following an increased hydrogen bonding network based on an aDO2A based system (Figure 0.1).

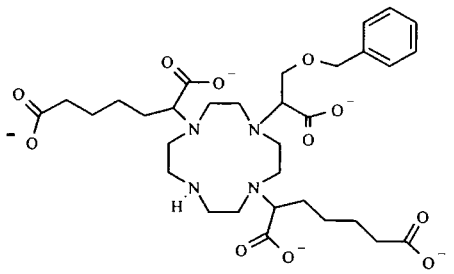

Figure 0.1: Schematic diagram of a putative aDO2A based system

The phosphonate derivative of the aDO3A ligand was recognised as possessing a higher negative peripheral charge in the lanthanide (III) complex, which was anticipated to inhibit the binding of anions. The gadolinium (III) complex was found to be a di-aqua species with similar relaxivities in the pH range 3.5 to 6.0. Above pH 6, carbonate and phosphate were found to compete with inner sphere water molecules. The problems associated with oligomerisation and the time dependence of pH reversibility, rendered this compound unsuitable for *in vivo* use. The high relaxivities displayed in the presence of serum solutions did suggest that suitably derivatised compounds may yet be suitable for use as contrast agents. Therefore, this idea may be pursued further by the synthesis and characterisation of the compound depicted in Figure 0.2, following the substitution of the ethyl groups

of the peripheral phosphonate esters by various *R* groups.

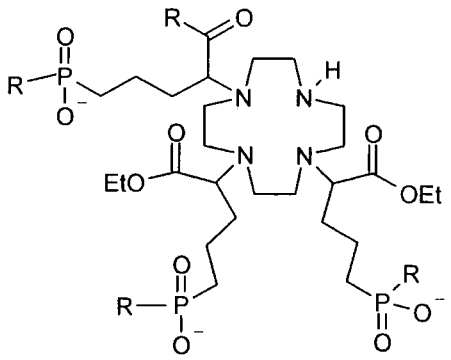

Figure 0.2: Chemical structure of a putative phosphonate derivative

In addition, work focused on the synthesis of aDO3A type carboxylate ligands incorporating peripheral amino acid groups should be pursued. These can be more easily functionalised, for example, with aromatic substituents capable of protein binding, whilst retaining the inhibition characteristics towards endogenous anions. An example of such a system is given below (Figure 0.3), in which the N substituent may be perturbed.

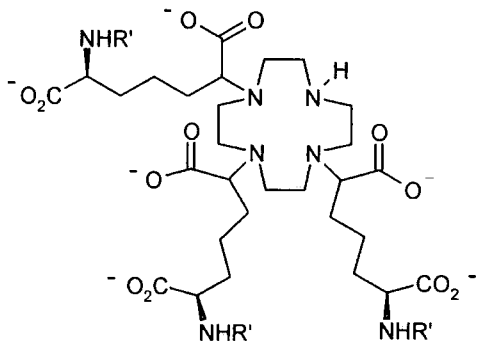

Figure 3: Chemical structure of a possible target aDO3A based ligand incorporating amino acid groups

Chapter 6

Experimental

6 Experimental

6.1 Synthetic Procedures and Characterisation

Reactions requiring anhydrous conditions were carried out using Schlenk-line techniques under an atmosphere of dry argon. Solvents were dried from an appropriate drying agent when required and water was purified by the 'Purite$_{STILL}$ plus' system with a conductivity value of ≤ 0.04 μScm^{-1}. Reagents were used as received from suppliers unless otherwise stated.

Fluorescent silica plates (254 nm) were used for thin layer chromatography (Merck Art 5554) and visualised using UV (254 nm) or iodine staining. Flash column chromatography was carried out using silica purchased from Merck (silica gel 60, 230-400 mesh). Ion exchange chromatography was performed using strong cation exchange resin Dowex 50W x 4-200 or weakly acidic carboxylic acid cation exchange resin Amberlite IRC-50.

NMR spectra were acquired using a Varian Mercury 200 spectrometer operating at 199.99 MHz (^{1}H), 50.29 MHz (^{13}C), 80.95 MHz (^{31}P), or a Varian Unity 300 spectrometer at 299.91 MHz (^{1}H) and 75.41 MHz (^{13}C) or a Varian Mercury 400 spectrometer at 399.97 MHz (^{1}H) and 50.58 MHz (^{13}C) or a Varian Inova 500 spectrometer at 499.87 MHz (^{1}H) and 125.71 (^{13}C). Spectra were referenced internally to the residual proton-solvent resonances and are reported relative to TMS. Chemical shifts are given in values of ppm with coupling constants in Hz. Splitting patterns are described as singlet (s), doublet (d), triplet (t), quartet (q), or multiplet (m). Variable temperature ^{1}H NMR studies and two dimensional spectra were recorded on a Varian Inova 500.

Electrospray mass spectra were acquired using a VG platform (II) spectrometer (Fisons instruments), operating in positive or negative ion mode with methanol used as a carrier solvent, typically using a cone voltage of 60 V and a source temperature of 110°C. Accurate mass measurements were recorded at the University of Durham using a Micromass LCT at 5000 resolution using sodium

iodide as a reference source.

I.R spectra were recorded on a Perkin-Elmer FT-IR 1720X spectrometer with GRAMS Analyst operating software; Melting points were determined on a Reichert-Köfler block melting point apparatus and are uncorrected. Combustion analysis was preformed using an Exeter Analytical Inc CE-440 elemental analyser.

6.2 Relaxivity Measurements

Longitudinal proton relaxation times were measured at 65 MHz using a custom built 65.6 MHz Varian spectrometer operating at 295 K or at 60 MHz using a Bruker Minispec mq 60 NMR analyser, operating at 310 K; both operated using an inversion recovery technique. The concentration of gadolinium in the sample was typically in the range of 0.1-0.5 mM, measured by accurately digesting the complex in nitric acid (5 M) for a period of time ranging from 18 hours to approximately 48 hours. The relaxation rate of the digested sample was measured and the concentration determined using equations 2.2-2.4 (Chapter 2).

Variable temperature proton-solvent longitudinal relaxation times were measured in the range of 0.01 to 20 MHz in Durham on a Stelar Spinmaster-FFC 2000 Fast Field Cycling NMR relaxometer (Stelar, Mede (PV), Italy) by means of the inversion recovery technique (thirty two experiments, four scans). The reproducibility of T_1 measurements was within 1%. The temperature was controlled by a Stelar VTC 90 airflow heater equipped with copper constantan thermocouple: the actual temperature in the probe head was measured with a Fluke 53 k/j digital thermometer with an uncertainty of 0.5 K.

6.3 Photophysical Measurements

pH Measurements were made using a Jenway 3320 pH meter (fitted with a BDH glass and combination electrode microsampler) calibrated using pH 4, 7, and 10 buffer solutions.

Ultraviolet absorbance spectra were recorded using a Perkin Elmer Lambda 900

UV/VIS/NIR spectrometer operating UV WinLab L800/L900 software. Samples were contained in quartz cuvettes with a path length of 1 cm. All spectra were acquired with respect to a purite water reference measured in a matched cell.

Luminescence spectra were recorded using a S.A. Fluorolog 3-11 system operating using DataMax software. Quartz fluorescence cuvettes were employed with a path length of 1cm. Second order diffraction effects were obviated as a result of using a cut-off filter to remove the scattered light before it enters the emission monochromator.

Excited state lifetimes were measured using a Perkin Elmer LS-55 spectrometer. Measurements were made following excitation of the sample by a short pulse of light (348 nm) followed by monitoring the integrated intensity of light (620 nm for europium) emitted during a fixed gate time, t_g, a delay time, t_d, later. At least 20 delay times were used covering 3 or more lifetimes. A gate time of 0.1 ms was used, and the excitation and emission slits were set to bandpass values of 2.5 and 15 nm respectively. The obtained decay curves were fitted using Microcal Origin.

6.4 Chapter 2 Experimental

6.4.1 Ligand Synthesis

Dimethyl 2-bromo-adipate (1)[38]

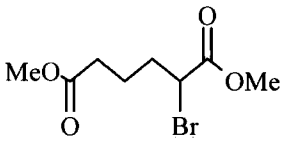

A solution of monomethyladipic acid (21 g, 131 mmol) in thionyl chloride (38 ml) and carbon tetrachloride (60 ml) was heated to 65°C for 40 minutes. N-Bromosuccinimide (27.8 g, 157 mmol), carbon tetrachloride (50 ml) and hydrogen bromide (5 drops) were then added and the resulting orange solution was heated at 85°C for 2 hours. The resulting brown solution was cooled with an ice bath and quenched with methanol (80 ml). The suspension which formed was stirred

overnight. The succinimide precipitate was removed by filtration and washed with methanol. The methanol was removed under reduced pressure and the resulting brown oil was dissolved in dichloromethane (150 ml), washed successively with water (100 ml), saturated aqueous sodium hydrogen carbonate solution (100 ml), and water (100 ml). The organic phase was dried (Na_2SO_4), filtered and concentrated under reduced pressure to yield a pale purple oil (42.3 g). Fractional distillation (125-126°C, 0.1 mm Hg) yielded the desired product (25.1 g, 69%). ^1H NMR (250 MHz, $CDCl_3$) δ_H: 1.64 (2H, m, $C\underline{H}_2CH_2CHBr$), 2.05 (2H, m, CH_2CHBr), 2.34 (2H, bt, J 7.2, $C\underline{H}_2CO_2CH_3$), 3.66 (3H, s, $CHBrCO_2CH_3$), 3.77 (3H, s, $CH_2CO_2CH_3$), 4.22 (1H, dd J 6.6, 7.9, CHBr); ^{13}C NMR (62.9 MHz, $CDCl_3$) δ_C: 22.41 (CH_2CH_2CHBr), 32.79 ($CH_2CO_2CH_3$), 33.88 (CH_2CHBr), 44.91 (CHBr), 51.42 (CH_2COCH_3), 52.76 ($CHBrCO_2CH_3$), 169.79 ($CH_2CO_2CH_3$), 172.99 ($CHBrCO_2CH_3$); m/z (ES^+): 528.7 (64%, $2MNa^+$), 276.8 (100%, MNa^+).

1,4,7,-Tris-[(4'-methoxycarbonyl)-1'methoxycarbonylbutyl]-1,4,7,10,-tetraazacyclododecane (2)[38]

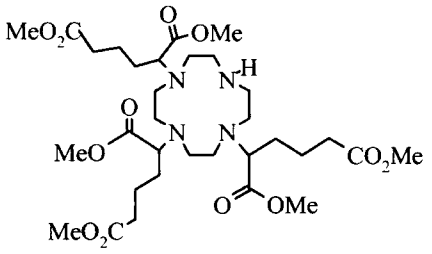

1,4,7,10,-Tetraazacyclododecane (1.5 g, 8.7 mmol), α- bromo dimethyl adipate **(1)** (6.4 g, 25.3 mmol) and potassium carbonate (2.7 g, 25 mmol) were mixed in dry acetonitrile (15 ml) and stirred under argon at 60°C for 36 hours. The solids were removed by filtration and solvent removed under reduced pressure. The product was purified using flash column chromatography on silica [gradient elution: 70/30 v/v DCM/THF to 10% MeOH-65% DCM-25% THF] yielding a dark yellow oil (1.52 g, 25%). ^1H NMR (300 MHz, $CDCl_3$) δ_H: 1.55-1.90 (18H, br, CH_2), 2.35-2.62 (16H, br, NCH_2), 2.62-3.27 (3H, br, CH), 3.65-3.70 (18H, s, CO_2CH_3), ^{13}C NMR (62.9 MHz, $CDCl_3$) δ_C: 21.0, 30.0, 33.2, 46.2, 51.0, 51.3, 51.5, 59.0, 63.5, 170.9 (CO_2) 173.5, (br, aliphatic CO),; m/z (ES^+) 689.5 (100%, MH^+); R_f = 0.34 (SiO_2; THF: DCM: MeOH

6:3:1); IR (thin film) ν_{max} (cm^{-1}): 2919, 2850, 1729 (CO stretch) 1460, 1266, 1178, 918, 825.

1-2'-(4-Tert-butyl-benzyl)-4,7,10-tris-[(4'methoxycarbonyl)-1'-methoxycarbonylbutyl-1,4,7,10-tetraazacyclododecane (3)

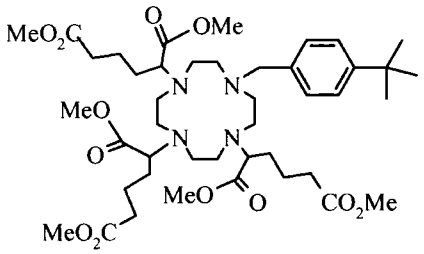

1,4,7,-Tris-[(4'-methoxycarbonyl)-1'methoxycarbonylbutyl]-1,4,7,10,-tetraazacyclododecane **(2)** (360 mg, 0.52 mmol) was dissolved in dry acetonitrile (5 ml). 4-(Tert-butyl) benzylbromide (118.7 mg, 0.52 mmol) and caesium carbonate (170 mg, 0.52 mmol) were added. The resulting mixture was stirred overnight at 60°C under argon. The solids were removed by filtration and the solvent removed under reduced pressure to yield a pale brown oil. The residue was purified by flash column chromatography on silica [gradient elution-100% DCM to 10% MeOH-90% DCM, R_f=0.42 (95% DCM- 5% MeOH)] producing a yellow oil (290 mg, 66%). ^1H NMR (200 MHz, $CDCl_3$) δ_H: 1.29 (9H, s, $(CH_3)_3C$), 1.55-1.90 (18H, br, CH_2), 2.42-2.35 (16H, br, NCH_2), 2.62-3.27 (3H, br, CH), 3.65-3.70 (18H, s, CO_2CH_3), 7.33 (2H, d, ArH, J8.4 Hz), 7.45 (2H, d, ArH, J 8.4 Hz), m/z (ES^+) 834 (100%, M^+) , 835 (25%, MH^+); Accurate Mass Found: 835.5109 (MH^+), $C_{43}H_{71}N_4O_{12}$ requires 835.5068.

2-(4-Tert-butyl-benzyloxy)-ethanol (4)

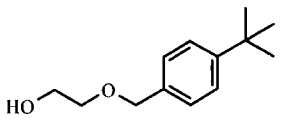

4-Tert-butyl benzyl bromide (11.0 g, 49.1 mmol), ethylene glycol (30.48 g, 0.49 mol), sodium hydroxide (1.96 g, 49.1 mmol) and tetrapropylammonium bromide (55 mg, 0.21 mmol) were mixed in THF (150 ml), and the mixture was boiled under reflux for 18 hours. The solvent was removed under reduced pressure and the residue

washed with water (25 ml), ether (2 x 50 ml) and chloroform (25 ml). The combined organic extracts were dried and the solvent removed under reduced pressure. Column chromatography on silica [gradient elution; hexane to 20% methanol-hexane, R_f=0.16 (hexane)] gave a yellow oil (7.68 g, 75%). ^{1}H NMR (200 MHz, $CDCl_3$) δ_H: 1.32 (9H, s, $(CH_3)_3C$), 2.28 (1H, bs, OH), 3.58 (2H, t, CH_2CH_2OH, J 4.5Hz), 3.74 (2H, t, CH_2OH, J 4.5 Hz), 4.53 (2H, s, ^{t}Bu-C_6H_4-CH_2), 7.26-7.30 (2H, d, ArH, J 8.4 Hz), 7.36-7.41 (2H, d, ArH, J 8.4 Hz); ^{13}C NMR (69.2 MHz, $CDCl_3$) δ_C: 31.13, 34.52, 61.87, 71.30, 73.09, 125.38, 127.70, 134.87, 150.84; m/z (ES^+) 231.0 (100%, MNa^+), 439.3 ($2MNa^+$); Accurate mass found 231.1357, $C_{13}H_{20}O_2Na$ requires 231.1361.

2-(4-Methoxy-benzyloxy)-ethanol (5)

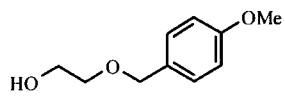

2-(4-Methoxy-benzyloxy)-ethanol was synthesized by a similar method to that used for (4), using 4-methoxybenzyl chloride (7.83 g, 50 mmol), ethylene glycol (31.04 g, 0.5 mol), sodium hydroxide (2.00 g, 50 mmol), tetrapropylammonium bromide (56 mg, 0.21 mmol) and THF (150 ml) to yield a yellow oil (6.67 g, 73%).^{1}H NMR (200 MHz, $CDCl_3$) δ_H: 2.06 (1H, bs, OH), 3.58 (2H, t, CH_2CH_2OH , J 5.2Hz,), 3.71 (2H, t, CH_2OH, J 3.4Hz), 3.80 (3H, s, CH_3O), 4.49 (2H, s, C_6H_4-C H_2), 6.86-6.90 (2H, d, ArH, J 8.5Hz), 7.24-7.29 (2H, d, ArH, J 8.5 Hz), ^{13}C NMR (100.6 MHz, $CDCl_3$) δ_C: 55.50 (OCH_3), 62.14, 71.29, 73.20, 114.09, 129.71, 130.25, 159.54; m/z (ES^+) 204.9 (100%, MNa^+), 387.0 (60% $2MNa^+$); Accurate mass found 205.0859, $C_{10}H_{14}O_3Na$ requires 205.0865.

2-[4-(1,1-Dimethylethyl) phenyl) methoxy]-2ethyl p-toulene sulphonate (6)

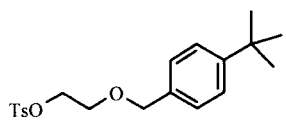

A solution of 2-(4-tert-butyl-benzyloxy)-ethanol **(4)** (1.04 g, 5 mmol) in pyridine (20 ml) was cooled to <0°C under argon. p-Toluene-sulfonyl chloride (0.935 g, 5 mmol)

was added in five equal parts and the solution maintained below 0 °C for 24 hours. The reaction mixture was poured onto crushed ice (150 g) and stirred until fully melted. The solid was removed by filtration and washed with water to give a white solid (1.36 g, 75%). ^{1}H NMR (250 MHz, $CDCl_3$) δ_H: 1.31 (9H, s, $(CH_3)_3C$), 2.43 (3H, s, CH_3), 3.65 (2H, t, CH_2CH_2OTs, J 4.8 Hz), 4.18 (2H, t, CH_2-tosyl, J 4.8 Hz), 4.45 (2H, s, ^{t}Bu-C_6H_4-CH_2), 7.18-7.21 (2H, d, $CH_3C(CH)_2$, J 8.5 Hz), 7.33-7.36 (4H, dt, ^{t}Bu-ArH), 7.79 (2H, d, tosyl ArH, J 6.6 Hz); ^{13}C NMR (62.9 MHz, $CDCl_3$) δ_C: 21.61, 31.31, 34.51, 67.39, 69.27, 73.03, 125.31, 127.55, 127.96, 129.76, 133.02, 134.47, 144.70, 150.81; m/z (ES^+) 385.1 (90%, MNa^+), 747.3 (50%, $2MNa^+$); Elemental Analysis Found C% 65.94, H% 7.24, $C_{20}H_{26}O_4S$ requires C% 66.27, H% 7.23; Mp: 45-46 °C.

2-[(4-Methoxyphenyl)methoxy]-4-methyl benzenesulphonate (7)

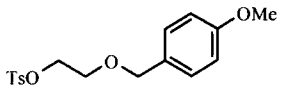

Toulene-4-sulfonic acid 2-(4-methoxy-benyloxy)-ethyl-ester **(7)** was synthesised using a similar method to that used for (6), using 2-(4-methoxy-benzyloxy)-ethanol (5) (0.911 g, 5 mmol), p-toluene-sulfonyl chloride (1.9 g, 10 mmol) and pyridine (18 ml) to yield a white solid (1.20 g, 72%). ^{1}H NMR (200 MHz, $CDCl_3$) δ_H: 2.43 (3H, s, CH_3-C_6H_4), 3.62 (2H, t, CH_2CH_2OTs , J 4.8 Hz), 3.80 (3H, s, OCH_3), 4.17 (2H, t, CH_2OTs, J 4.8 Hz), 4.41 (2H, s, CH_3O-C_6H_4-CH_2), 6.85 (2H, d, CH_3OArH, J 8.6 Hz), 7.18 (2H, d, CH_3CCH, J 8.4 Hz), 7.30 (2H, d, CH_3O-ArH, J 8.4 Hz), 7.78 (2H, d, tosyl-ArH, J 8.4 Hz), m/z (ES^+) 358.9 (85%, MNa^+), 695.1 (25%, $2MNa^+$); Elemental Analysis: Found C% 60.78, H% 6.06; $C_{17}H_{20}O_5S$ requires C% 60.71, H% 5.99; Mp: 44-45 °C

1-[2'-(4-Tert-butyl-benzyloxy)-ethyl]-4,7,10-tris-[(4'-methoxycarbonyl)-1'-methoxycarbonylbutyl-1,4,7,10-tetraazacyclododecane (8)

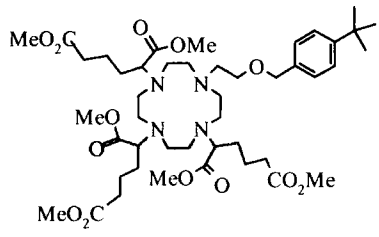

The amine **(2)** (160 mg, 0.233 mmol), the tosylate **(6)** (84 mg, 0.233 mmol) and caesium carbonate (75.6 mg, 0.233 mmol) were mixed in acetonitrile (4 ml) under argon and the mixture was boiled under reflux for 4 hours. The solids were removed by filtration and the residue purified by flash column chromatography on silica [gradient elution; DCM to 10% MeOH-DCM, R_f =0.2 (DCM)] to yield a dark brown oil (74 mg, 34 %). ^{1}H NMR (200 MHz, $CDCl_3$) δ_H: 1.31 (9H, s, $(CH_3)_3C$), 1.55-1.85 (18H, br, CH_2), 2.64-2.29 (16H, br, NCH_2), 3.30-3.20 (3H, br, CH), 3.65 (18H, s, CO_2CH_3), 3.78 (2H, t, NCH_2CH_2O, J 4.8 Hz), 4.18 (2H, t, NCH_2CH_2O, J 4.8 Hz), 4.48 (2H, s, C_6H_4-CH_2), 7.23 (2H, d, ArH, J 8.2 Hz), 7.32 (2H, d, ArH, J 8.2 Hz); m/z (ES^+) 879.7 (100%, M^+); Accurate mass found: 879.5329 (MH^+), $C_{45}H_{74}N_4O_{13}$ requires 879.5330.

1-[2'-(4-Methoxy-benzyloxy)-ethyl]-4,7,10-tris-[(4'-methoxycarbonyl)-1'-methoxycarbonylbutyl-1,4,7,10-tetraazacyclododecane (9)

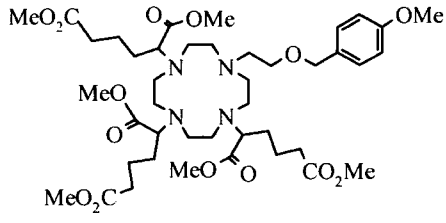

Compound **(9)** was synthesised by a similar method to that of (8), using **(2)** (258mg, 0.37mmol), **(7)** (120mg, 0.37mmol), caesium carbonate (122mg, 0.37mmol) and acetonitrile (5 ml) to yield a dark brown oil (92.6 mg, 29%). ^{1}H NMR (200 MHz, $CDCl_3$) δ_H: 1.58-1.85 (br, 18H, CH_2), 2.30-2.55 (br, 16H, NCH_2), 3.20-3.40 (br, 3H, CH), 3.40-3.65 (br, 18H, CO_2CH_3), 3.61 (t, J=6.2Hz, 2H, NCH_2CH_2O), 3.74 (s, 3H, OCH_3), 4.40 (t, J=6.2Hz, 2H, NCH_2CH_20), 4.45 (s, 2H, C_6H_4-CH_2, 6.84 (d, J=8.6Hz, 2H, meta ArH), 7.22 (d, J=8.6Hz, 2H, ortho ArH), m/z (ES^+) 853.6 (100%, M^+); Accurate mass found: 853.4810, $C_{42}H_{68}N_4O_{14}$ requires 853.4808.

1-[2'-(4-Tert-butyl-benzyl)-4,7,10-tris-[(4'carbonxy)-1'-carbonylbutyl]-1,4,7,10-tetraazacyclododecane **[L^1]**

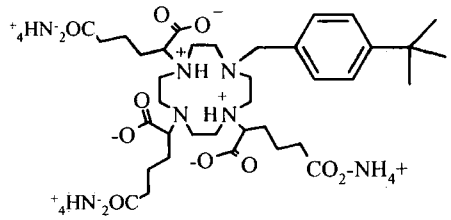

The hexaester **(3)**, (290 mg, 0.35 mmol) was suspended in an aqueous solution of potassium hydroxide (6 M, 5 ml). The suspension was heated at 80°C for 18 hours and passed through a strong cationic exchange resin (Dowex 50W), eluting with 12% ammonia solution. The fractions were collected and removed under reduced pressure to yield the ligand as the tri-ammonium salt, as a light brown solid (150 mg). This was used directly in metal complexation without further purification, having checked that the methyl esters had hydrolysed completely by proton NMR. ^{1}H NMR (200 MHz, D_2O) δ_H: 1.29 (9H, s, $(Me)_3C$), 1.91–1.64 (18H, br, CH_2), 2.27-2.12 (16H, br, NCH_2), 7.36 (2H, d, ArH, J 8.4 Hz), 7.50 (2H, d, ArH, J 8.4 Hz).

1-[2'-(4-Tert-butyl-benzyloxy)-ethyl]-4,7,10-tris-[(4'-carboxy)-1'-carboxylbutyl]-1,4,7,10-tetraazacyclododecane **[L^2]**

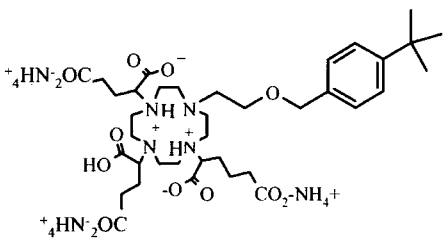

The hexaester **(8)**, (80 mg, 0.09 mmol) was suspended in an aqueous solution of potassium hydroxide (6M, 5 ml). The suspension was heated at 80°C for 18 hours and passed through a strong cationic exchange resin (Dowex 50W), eluting with 12% ammonia solution. The fractions were collected and removed under reduced pressure to yield the ligand as the tri-ammonium salt, as a colourless solid (25 mg, 29%). This was used directly in metal complexation without further purification, having checked that the methyl esters had hydrolysed by proton NMR. ^{1}H NMR (200 MHz, D_2O) δ_H: 1.19 (9H, s, $(CH_3)_3C$), 1.89-1.5 (18H, br, CH_2), 2.00-2.39 (16H, br, NCH_2), 3.20-3.41 (3H, br, CH), 3.87 (2H, t, NCH_2CH_2O, J 7.4 Hz), 4.37 (2H, s, C_6H_4-CH_2), 4.44 (2H, t, NCH_2CH_2O, J 7.4 Hz), 7.20 (2H, d, ArH, J 8 Hz), 7.49 (2H, d, ArH, J 8.0 Hz).

1-[2`-(4-Methoxy-benzyloxy)-ethyl]-4,7,10-tris-[(4`-carboxy)-1`-carboxylbutyl]-1,4,7,10-tetraazacyclododecane **[L^3]**

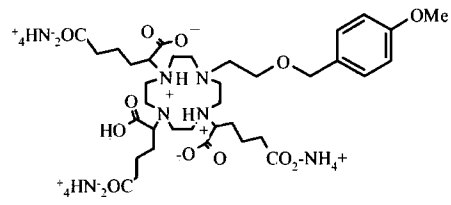

The hexaester **(9)**, (92.6 mg, 0.11 mmol) was suspended in an aqueous solution of potassium hydroxide (6M, 5 ml). The suspension was heated at 80°C for 18 hours and passed through a strong cationic exchange resin (Dowex 50 W), eluting with 12% ammonia solution. The fractions were collected and removed under reduced pressure to yield the ligand as the tri-ammonium salt, as a colourless solid (40.7 mg, 47%). This was used directly in metal complexation without further purification, having checked that the methyl esters had hydrolysed completely. ^{1}H NMR (D_2O, 200 MHz) δ_H: 1.51-1.99 (18H, br, CH_2), 2.00-2.50 (16H, br, NCH_2), 3.20-3.44 (3H, br, CH), 3.63 (2H, t, NCH_2CH_2, J 6.2 Hz), 3.74 (3H, s, OCH_3), 4.39 (2H, t, NCH_2CH_2O, J 5.8 Hz), 4.43 (2H, s, C_6H_4-CH_2), 6.99 (2H, d, ArH, J 8.1 Hz), 7.37 (2H, d, ArH, J 8.4 Hz).

2-(3,5-Dimethyl-phenoxy)-ethanol (10)

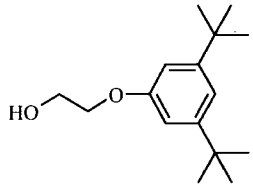

3,5 Di-(tertbutyl) phenol (11.1 g, 53.4 mmol), bromoethanol (3.8 ml, 53.4 mmol) and potassium carbonate (7.4 g, 53.4 mmol) were dissolved in acetonitrile (40 ml) and the mixture boiled under reflux for approximately 18 hours. The solid precipitate that formed was filtered and washed using dichloromethane (10 ml), which was removed under reduced pressure to yield a white, crystalline solid. The solid residue was dissolved into dichloromethane (3 ml) and purified by column chromatography using silica, to yield a pale yellow, oily liquid (4.8 g, 36%);

[gradient elution DCM 100% - 95% DCM-5% MeOH, TLC conditions 97% DCM-3% MeOH, R_f = 0.36]. ^{1}H NMR (200 MHz, CDCl3) δ_H: 1.53 (18H, s, $(CH_3)_3$), 2.27 (1H, br, OH), 4.17 (2H, dd, CH_2, J 8.6 Hz), 4.32 (2H, dd, CH_2, J 8.6 Hz), 6.99 (2H, d, ArH, J 1.6 Hz), 7.27 (1H, t, ArH, J 1.6 Hz); ^{13}C NMR ($CDCl_3$, 125.6 MHz) δ_C: 31.3 (CH_3), 34.9 ($C(CH_3)_3$), 64.5 (CH_2), 68.9 (CH_2), 108.8 (Ar CH), 115.2 (Ar CH), 152.2 ($\underline{C}(CH_3)_3$), 158.1 ($\underline{C}OH$); m/z (ES^+) 250.1 (20%, MH^+), 273.2 (100%, MNa^+), 523.4 (85%, $2MNa^+$); Accurate mass found 273.1839, $C_{16}H_{26}O_2Na$ requires 273.1831.

(2-(3,5-Dimethyl-phenoxy)-ethyl-p-toluenesulphonate (11)

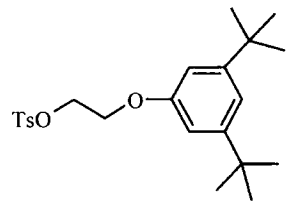

Compound **(10)** (1.08 g, 40.0 mmol) was dissolved in pyridine (20 ml) and cooled to 0°C under an argon atmosphere. p- Toluenesulfonyl chloride (1.02 g, 50.0 mmol) was added in five equal portions and the solution was maintained below 0°C for 24 hours. The resulting orange solution was poured onto crushed ice (150 g) and stirred until the ice had fully melted. The precipitate which formed was removed by filtration, and washed with water to give a white solid (1.33 g, 76%). ^{1}H NMR (200 MHz, $CDCl_3$) δ_H: 1.29 (18H, s, $(CH_3)_3$), 2.44 (3H, s, CH_3), 4.16 (2H, m, CH_2), 4.37 (2H, m, CH_2), 6.64 (2H, d, ArH), 7.02 (1H, t, ArH, J 1.4 Hz), 7.40 (2H, d, Ar-H-tosylate), 7.82 (2H, d, Ar-H-tosylate, J 8.2 Hz); ^{13}C NMR (125.7 MHz, $CDCl_3$) δ_C: 21.6 (CH_3), 31.4 ($CH_3)_3$), 34.9 ($C(CH_3)_3$), 65.3 (O-CH_2), 68.3 (O-CH_2), 115.6 (CH), 108.9 (CH), 128.1 (CH), 129.8 (CH), 132.9 (C-CH_3), 144.8 (C-S), 152.3 (CH), 157.6 (Ar$\underline{C}$OC); m/z (ES^+) 427.4 (80%, MNa^+), 831.4 (45%, $2MNa^+$); TLC Analysis 100% DCM R_f = 0.81; Mp: 98-99°C; Elemental Analysis: Calculated C = 68.28 %, H = 7.97 %, Measured C = 68.24 %, H = 8.00 %.

1-2-[(3,5-Dimethyl-phenoxy)-ethyl]-4,7,10-tris-[(4'ethoxycarbonyl)-1'-methoxycarbonylbutyl-1,4,7,10-tetraazacyclododecane (12)

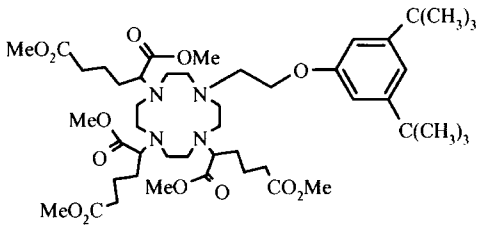

The amine **(2)** (240 mg, 0.35 mmol), the tosylate **(11)** (140 mg, 0.35 mmol) and caesium carbonate (114 mg, 0.35 mmol) were suspended in acetonitrile (5 ml) and the mixture was heated under reflux, under an atmosphere of argon for approximately 4 hours. The solids were removed by filtration and the residue purified by flash column chromatography on silica. [gradient elution; 100% DCM-95% DCM/ 5% MeOH] to yield a yellow oil (140 mg, 43%). ^{1}H NMR (500 MHz, $CDCl_3$,) δ_H: 1.29 (18H, s, $C(CH_3)_3$), 1.45-2.20 (18H, br, CH_2), 2.31-3.09 (16H, br, NCH_2), 3.63-3.66 (18H, s, CO_2CH_3), 4.23 (4H, br m, CH_2), 6.73 (2H, d, ArH), 7.17 (1H, t, ArH); m/z (ES^+) 921.6 (100%, M^+), 922.8 (75%, MH^+), 943.5 (25%, MNa^+).

***1-2-[(3,5-Dimethyl-phenoxy)-ethyl]-4,7,10-tris-[(4'carboxy)-1'-carbonylbutyl-1,4,7,10-tetraazacyclododecane* [L^4]**

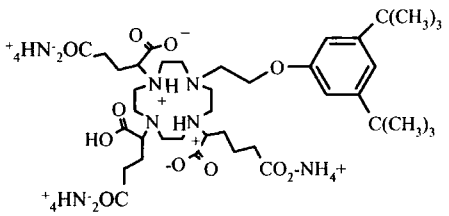

The hexaester **(12)** (140 mg, 0.151 mmol) was suspended in an aqueous solution of potassium hydroxide (6 M, 5 ml). The suspension was heated at 80°C for 18 hours and passed through a strong cationic exchange resin (Dowex 50W), eluting with 12% ammonia solution. The UV active fractions were collected and solvent was removed under reduced pressure, yielding the ligand as the tri-ammonium salt, which was an off-white crystalline solid. That hydrolysis was complete was confirmed using ^{1}H NMR and the ligand was used directly in metal

complexation without further purification (153 mg, 46%). ^{1}H NMR (200 MHz, D_2O) δ_H: 1.28 (18H, s, $C(CH_3)_3$), 1.45-1.89 (18H, br, CH_2), 2.15-2.91 (16H, br, NCH_2), 4.22 (4H, br m, CH_2), 6.90 (2H, m, ArH), 7.19 (1H, br, ArH).

1-(4-Benzyloxybenzyl]-4,7,10-tris-[(4'methoxycarbonyl)-1'-methoxycarbonylbutyl-1,4,7,10-tetraazacyclododecane (13)

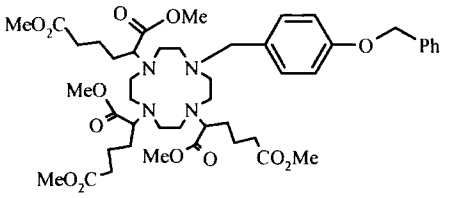

The amine **(2)** (266 mg, 39 mmol) and 4-benzyloxybenzyl chloride (89 mg, 39 mmol) and caesium carbonate (125 mg, 39 mmol) were suspended into acetonitrile (5 ml) and the mixture boiled under reflux overnight, under argon. The solids were removed by filtration and the residue purified by flash column chromatography on silica [gradient elution; 100 % DCM-5 % MeOH-DCM, R_f = 0.31], to yield a yellow oil (52 mg, 15%). ^{1}H NMR (400 MHz, $CDCl_3$) δ_H: 1.40-1.99 (18H, br, CH_2), 2.48-2.89 (16H, br, NCH_2), 2.91-3.45 (3H, br, CH), 3.55-3.61 (18H, m, CO_2CH_3), 4.99 (2H, m, CH_2O), 5.22 (2H, s, CH_2N), 6.81-6.90 (3H, m, ArH), 7.06-7.14 (2H, m, ArH), 7.31-7.37 (4H, m, ArH); m/z (ES^+) 885.4 (100%, M^+), 886.5 (75%, MH^+), 907.2 (50%, MNa^+).

1-(4-Benzyloxybenzyl]-4,7,10-tris-[(4'carbonxy)-1'-carbonylbutyl-1,4,7,10-tetraazacyclododecane [L^5]

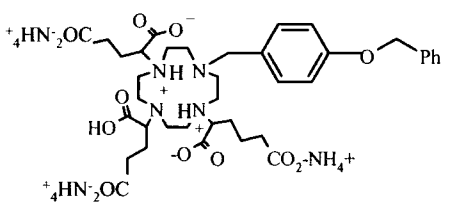

The hexaester **(13)** (52 mg, 58.8 mmol) was suspended in an aqueous solution of potassium hydroxide (6 M, 5 ml). The suspension was heated at 80°C for 18 hours and passed through a strong cationic exchange resin (Dowex 50W), eluting with

12% ammonia solution. The UV active fractions were collected and solvent was removed under reduced pressure, yielding the ligand as the tri-ammonium salt which was an off white crystalline solid (22mg, 47%). That ester hydrolysis was complete was confirmed by ^{1}H NMR and the ligand was then used directly for metal complexation without further purification. ^{1}H NMR (300 MHz, D_2O) δ_H: 1.35-1.98 (18H, br m, CH_2), 2.23-2.91 (16H, br, NCH_2), 4.84 (2H, br, CH_2O), 4.99 (2H, m, CH_2), 6.75 (3H, br, ArH), 7.16 (2H, br, ArH), 7.41 (4H, br, ArH).

9H-Fluorene-9-p-toluenesulfonatomethyl (14)

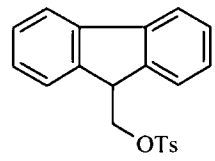

9-Fluorene methanol (1.03 g, 5.1 mmol) was dissolved in anhydrous pyridine (15 ml) and cooled to 0°C whilst stirring under an argon atmosphere. Para-toluene sulphonyl chloride (0.96 g, 5.1 mmol) was added slowly in several, small portions. The solution was stirred until all solid material had fully dissolved. The straw coloured solution was then cooled to -5°C for approximately 18 hours. The cooled solution was poured directly onto crushed ice (100 g) and stirred until fully melted; the white solid precipitate that formed was filtered, washed using purite water and dried under vacuum, to yield an off- white coloured solid. NMR analysis confirmed the presence of the starting alcohol, so the compound was recrysallised using a chloroform and petroleum ether mixture, producing a white crystalline solid (1.43g, 78%). ^{1}H NMR (500 MHz, $CDCl_3$) δ_H: 2.44 (3H, s, tosyl CH_3), 4.27 (3H, m, CH, & CH_2-fm), 7.28-7.32 (4H, m, fm ArH), 7.39-7.42 (2H, dd, tosyl ArH, J 8Hz), 7.54-7.56 (2H, dd, tosyl ArH, J 8 Hz), 7.74-7.78 (4H, m, fm ArH); ^{13}C NMR (125.7 MHz, $CDCl_3$) δ_C: 21.90 (CH_3), 46.93 (CH,[fm]), 72.13 (CH_2,[fm]), 120.34, 125.43, 127.47, 128.18 (CH, fm ArC), 128.34, 130.14 (CH, tosyl ArC), 133.01, 141.59, 142.72 & 145.15 (q, ArCH); TLC analysis (SiO_2, DCM) R_f = 0.65; m/z (ES$^+$) 373.1 (100%, MNa^+), 723.2 ($2MNa^+$); Elemental analysis: Calculated C% 71.77; H% 5.45, Found: C% 71.99, H% 5.19.

2-(9H-Fluoren-9-yl)-ethanol (15)

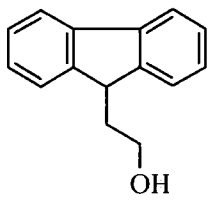

9-Fluorene-acetic acid (200 mg, 0.90 mmol) was dissolved into dry tetrahydrofuran (2 ml) and stirred under argon at -40°C. Borane-THF solution (490 µL, 1.0 mmol) was added dropwise and the resulting mixture was stirred at room temperature for approximately 18 hours. The clear solution was cooled to 0°C and quenched using methanol (5 ml). The solution was stirred for a further 2 hours under an argon atmosphere. The reaction mixture was then treated with diethyl ether (20 ml) and washed successively with water, saturated aqueous sodium carbonate solution and water. The organic layer was dried ($MgSO_4$), and the organic solvent removed under reduced pressure, to yield a white solid (80 mg, 42%). ^1H NMR (400 MHz, $CDCl_3$) δ_H: 1.25-1.30 (1H, br, OH), 2.29-2.34 (2H, q, CH_2, J 6.8 Hz), 3.59-3.62 (2H, t, CH2, J 6.8 Hz), 4.13-4.16 (1H, t, CH, J 5.6 Hz), 7.32-7.84 (4H, m, ArH), 7.54-7.56 (4H, dd, ArH, J 7.6 Hz); ^{13}C NMR (125.7 MHz, $CDCl_3$) δ_C: 35.99, 46.86 (CH_2), 60.52 (CH), 120.28, 124.72, 127.29, 127.44 (ArC), 141.23, 147.07 (q, C); m/z (ES^+) 233.0 (70%, MNa^+); Elemental analysis found C% 80.20, H% 6.99 $C_{15}H_{14}O$. 4/5 H_2O requires C% 80.18, H% 6.99.

9H-fluorene-9-p-toluenesulfonatoethyl (16)

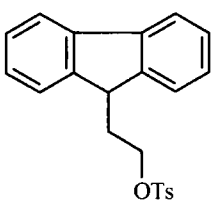

2-(9H-Fluoren-9-yl)-ethanol **(15)** (35 mg, 0.167 mmol) was dissolved into anhydrous pyridine (10 ml) and stirred under argon at 0 °C. p-Toluene sulphonyl chloride (32 mg, 0.167 mmol) was added slowly in two equal parts. The solution was stirred until solids were fully dissolved maintaining a temperature of 0°C, then cooled to -5°C for approximately 18 hours. The orange coloured solution was poured directly

onto crushed ice (100 g) and stirred until the ice had fully melted. The white solid precipitate that formed was filtered, washed using distilled water and dried over P_2O_5 under vacuum, to yield a white solid. ^1H NMR ($CDCl_3$, 400 MHz) δ_H: 2.21-2.26 (2H, q, CH_2, J 6.4 Hz), 3.91-3.99 (3H, m, CH_2 & CH), 7.19-7.28 (8H, m, ArH), 7.62-7.63 (2H, d, ArH tosyl, J 8 Hz), 7.65-7.66 (2H, d, ArH tosyl); ^{13}C NMR ($CDCl_3$, 100.6 MHz) δ_C: 21.62 (CH_3), 32.35 (CH_2), 43.68 (CH_2), 67.75 (CH), 120.03, 124.29, 127.09, 127.90 (CH-fm ArC), 128.90, 129.80 (CH tosyl ArC), 145.69, 140.89, 134.70, 133.05 (q, ArC); m/z (ES^+) 387.1 (50%, MNa^+).

1-2'-(9-Propyl-9H-fluorene)-4,7,10-tris-[(4'methoxycarbonyl)-1'-methoxycarbonylbutyl-1,4,7,10-tetraazacyclododecane (17)

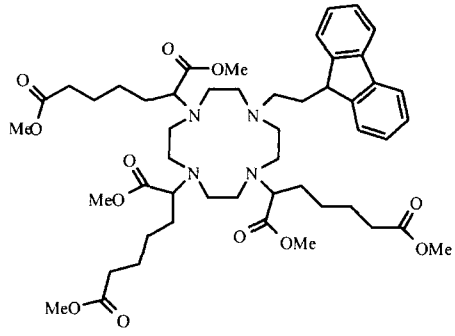

9H-fluorene-9-p-toluenesulfonatoethyl **(16)** (295 mg, 0.80 mmol) was dissolved in dry acetonitrile (5 ml). 1,4,7,-Tris-[(4`-methoxycarbonyl)-1`methoxycarbonylbutyl]-1,4,7,10,-tetraazacyclododecane **(2)** (280 mg, 0.41 mmol) and caesium carbonate (264 mg, 0.81 mmol) were then added. The resulting mixture was heated under reflux for approximately 36 hours under an argon atmosphere. The solid residues were removed by filtration and washed with dichloromethane (20 ml). The organic solvent was removed by reduced pressure, to yield a crude, brown oily product (295 mg). The required product was purified by flash chromatography on silica [100% DCM- 95% DCM- 5% MeOH]. The fractions were collected and solvent removed by reduced pressure to yield a brown oily product (75 mg, 21%). ^1H NMR (300 MHz, $CDCl_3$) δ_H: 1.41-1.77 (16H, br m, CH_2), 2.26-2.33 (6H, br m, CH_2), 2.41-3.10 (12H, br m, CH_2), 3.42-3.48 (3H, br, CH), 3.68 (21H, m, CO_2CH_3 & CH_2 & CH), 7.34-7.67 (8H, br m, ArH); m/z (ES^+) 881.3 (100%, MH), 463.5 (48%, ½MNa^+); TLC

[SiO_2 DCM- 95% DCM- 5% MeOH] R_f = 0.35.

1-2'-(9-Propyl-9H-fluorene)-4,7,10-tris-[(4'carboxy)-1'-carbonylbutyl-1,4,7,10-tetraazacyclododecane **[L^6]**

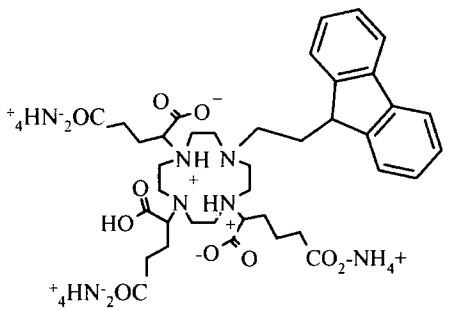

The hexaester **(17)** (74 mg, 0.084 mmol) was dissolved into lithium hydroxide solution (1 M, 10 ml), and the solution was heated under reflux for approximately 72 hours. The resulting milky white solution was neutralized to pH 6.5 prior to ion exchange using hydrochloric acid (0.1M). The product was loaded on a strong cation exchange column (Dowex -50) and washed using Purite water pH 6. The product was eluted from the column using 12% ammonia solution, which was removed from the compound by reduced pressure, yielding the ligand as the tri-ammonium salt, a white crystalline solid. That ester hydrolysis was complete was confirmed using ^1H NMR and the ligand was used directly for metal complexation without further purification (36 mg, 49%). As the synthetic pathway is analogous for the C_2 and the C_1 appended aDO3A ligand system **[L^6]** and **[L^7]** respectively; the synthetic details will only be described for the C_2 variant.

1-2'-(N-Ethyl-acridone),4,7,10-tris[(4'methoxycarbonyl)-1'-methoxy carbonylbutyl (18)

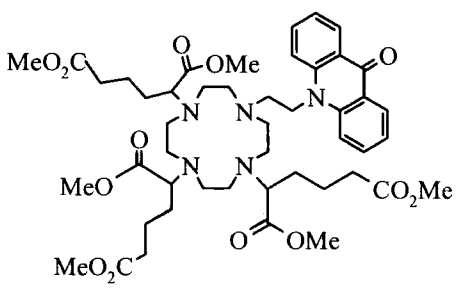

Mono-substituted N-acridoneethyl 1,4,7,10-tetraazacyclododecane (215 mg, 0.55 mmol) was donated by Y. Bretonnèire, University of Durham. The compound was dissolved into dry acetonitrile (5 ml). Dimethyl 2-bromo adipate **(1)** (425 mg, 1.67 mmol) and caesium carbonate (547 mg, 1.67 mmol) were added. The resulting mixture was heated under reflux for approximately 96 hours. The solids were removed by filtration and washed with acetonitrile, the solution being concentrated by reduced pressure to yield a brown crude mixture. The required product was purified by flash column chromatography on silica [SiO_2, DCM→3% MeOH in DCM] (67 mg, 13%). ^{1}H NMR ($CDCl_3$, 500 MHz) δ_H: 1.57-1.82 (16H, br, CH_2), 2.28-3.12 (19H, br, NCH_2 x 16H & CH x 3H), 3.59-3.72 (20H, br, CO_2CH_3 x 18H & CH_2), 4.51 (2H, br, CH_2), 7.33 (2H, m, ArH), 7.59 (1H, br, ArH), 7.78 (3H, m, ArH), 8.59 (2H, dd, ArH, J 7 Hz); ^{13}C NMR partial assignment ($CDCl_3$, 125.6 MHz) δ_C: 19.79, 20.93, (CH), 25.63, 29.96, 31.28 (CH_2), 33.54, 33.81 (NCH_2), 51.81 (OCH_3), 121.83, 128.48, 134.58 (ArC), 173.87 (C=O); m/z (ES^+) 976.3 (100%, MCu^+); A suitable accurate mass could not be obtained for this compound.

***1-2'-(N-ethyl-acridone),4,7,10-tris[(4'carboxy)-1'-carbonylbutyl* [L^8]**

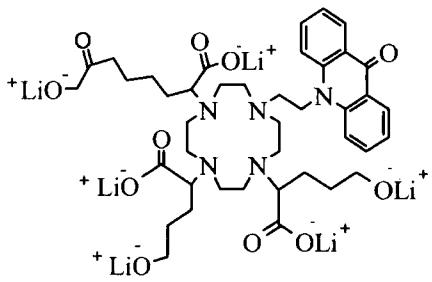

A suspension of **(18)** (60 mg, 0.065 mmol) and lithium hydroxide (54 mg) in water (1 ml) was left stirring at room temperature for 24 hours. The hydrolysis of the methyl esters was monitored by ^{1}H NMR. The ligand was complexed in *situ*. ^{1}H NMR was used to confirm all methyl esters were hydrolysed. ^{1}H NMR (200 MHz, D_2O) δ_H: 1.41-3.01 (37 H, br, CH_2's and NCH_2's), 7.51-8.70 (8H, br, ArH).

Methyl-3-benzyloxy-2-chloro-propionate (19)

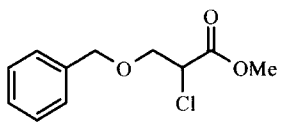

The potassium salt of 3-benzyloxy-2-chloro-propionic acid (0.53 g, 2.097 mol), was dried thoroughly and then dissolved in dry methanol (10 ml). Acetyl chloride (0.2 ml) was added and the resulting mixture was heated under reflux under an argon atmosphere for 18 hours. The solution was cooled to room temperature and dissolved into diethyl ether (30 ml). The organic phase was washed successively using water (20 ml) sodium bicarbonate solution (pH 8.5, 20 ml) and water (20 ml). The organic phase was dried (Mg_2SO_4), and the organic solvent removed at reduced pressure to yield a transparent oily product (0.50 g, 87%). ^1H NMR ($CDCl_3$, 500 MHz) δ_H: 7.23-7.28 (5H, m, ArH), 4.52 (2H, s, CH_2Ar), 4.34-4.37 (1H, t, CH, J 6 Hz), 3.71-3.74 (4H, m, OCH_3 & CH); ^{13}C NMR ($CDCl_3$, 125.7 MHz) δ_C: 53.39 (OCH_3), 54.79 (C*), 71.16 (CH_2C*), 73.82 (Ar-CH_2), 128.03, 128.25, 128.77 (ArCH), 137.54 (q, C), 168.89 (C=O); m/z (ES^+) 251.0 (100%, MNa^+), 267.7 (48%, MK^+); Accurate mass found 251.0457, $C_{11}H_{13}O_3ClNa$ requires 251.0451.

1-3'-(Benzyloxy-propionic acid methyl ester)-4,7,-di-[4' (methoxycarbonyl)-1' - methoxycarbonylbutyl]-1,4,7,10-tetraazacyclododecane (20)

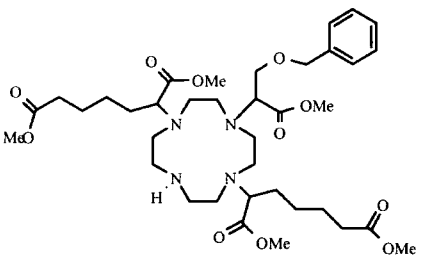

Methyl-3-benzyloxy-2-chloro-propionate (19) (118 mg, 0.474 mol) and 1,7-bis-[(4`methoxycarbonyl)-1`-methoxycarbonylbutyl-1,4,7,10-tetraazacyclododecane, (245 mg, 0.474 mol) were suspended in dry acetonitrile (5 mL). Caesium carbonate (154 mg, 0.474 mol) was added and the resulting mixture heated under reflux under an argon atmosphere for approximately 48 hours. The solid residue was filtered and washed using dichloromethane. The combined organic washings were evaporated under reduced pressure yielding a crude brown oily product (270 mg). The required product was purified by flash chromatography on silica [100% DCM-95% DCM- 5% MeOH]. The fractions were collected and solvent removed at reduced pressure to yield a brown oily product (22 mg, 6%). ^1H NMR ($CDCl_3$, 400

MHz) δ_H: 1.44-1.68 (30H, br, CH_2), 2.36-3.07 (16H, br, NCH_2), 3.67 (17H, br s, OCH_3 & CH_2), 4.12 (2H, br, CH_2), 7.32 (5H, br, ArH); m/z 751.4 (50%, MH^+), 790.3 (10%, MK^+); Accurate mass Found 751.4542 $C_{38}H_{63}N_4O_{11}$ requires 751.4493.

6.5 Complex Synthesis

The gadolinium and europium lanthanide complexes were all synthesised by a general method. The hydrolysed ligand was suspended into a solution of methanol/ water (1:1) (4 ml) and the lanthanide chloride or acetate hexahydrate added in a 1:1 ratio. The pH was adjusted to using sodium hydroxide solution (0.1 M) and the mixture heated at 90°C for 18 hours. The solution was then cooled, the pH raised to 10 and the solution filtered through a 0.45 μm filter to remove any excess lanthanide as the insoluble $Ln(OH)_3$. The pH was then lowered and the solution lyophilised to give the desired complex as an off-white crystalline solid.

{1-[2'-(4-Tert-butyl-benzyl)-4,7,10-tris-[(4'carboxy)-1'-carboxylbutyl-1,4,7,10-tetraazacyclododecane} Gadoliniate **$[GdL^1]^{3-}$**

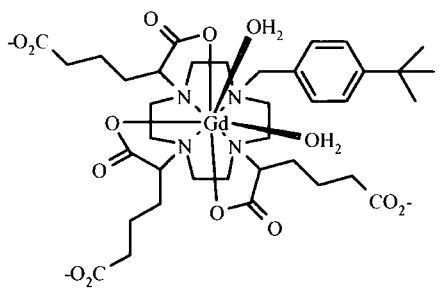

r_{1p} = 8.7 $mM^{-1}s^{-1}$ (65 MHz, 295 K, pH 5.7); MALDI-TOF: 938.3.

{1-[2'-(4-Tert-butyl-benzyl)-4,7,10-tris-[(4'carboxy)-1'-carboxylbutyl-1,4,7,10-tetraazacyclododecane} Europiate **$[EuL^1]^{3-}$**

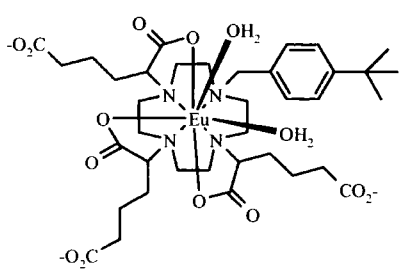

^{1}H NMR (200 MHz, D_2O): The ^{1}H spectrum was exchanged broadened.

{1-[2'-(4-Tert-butyl-benzyloxy)-ethyl]-4,7,10-tris-[(4'carboxy)-1'-carboxybutyl-1,4,7,10-tetraazacyclododecane} Gadoliniate **[GdL^2]$^{3-}$**

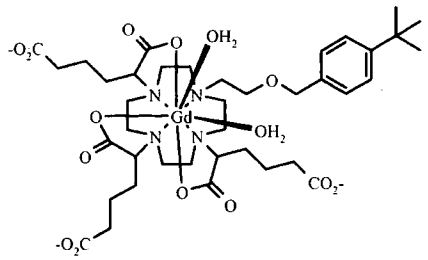

r_{1p}: 10.2 mM^{-1} s^{-1} (65 MHz, 295 K, pH 5.3); m/z (ES^-) 947 [M^-].

{1-[2'-(4-Tert-butyl-benzyloxy)-4,7,10-tris-[(4'carboxy)-1'-carboxylbutyl-1,4,7,10-tetraazacyclododecane} Europiate **[EuL^2]$^{3-}$**

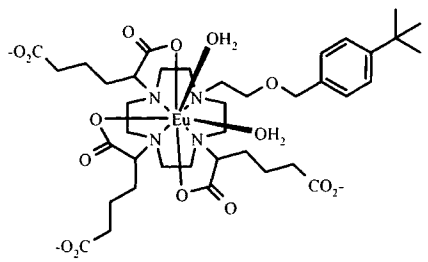

^{1}H NMR (200 MHz, D_2O): The spectrum was exchanged broadened; m/z (ES^-) 943 [M^-]

{1-[2'-(4-Methoxy-benzyloxy)-ethyl]-4,7,10-tris-[(4'carboxy)-1'-carboxybutyl-1,4,7,10-tetraazacyclododecane} Gadoliniate **[GdL^3]$^{3-}$**

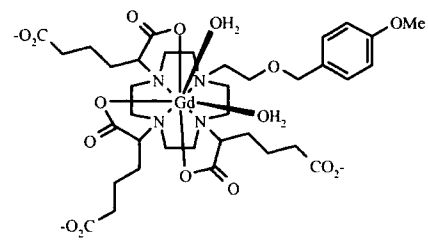

r_{1p} = 9.0 $mM^{-1}s^{-1}$ (65 MHz, 295 K, pH 5.7)

{1-[2'-(4-Methoxy-benzyloxy)-4,7,10-tris-[(4'carboxy)-1'-carboxylbutyl-1,4,7,10-tetraazacyclododecane} Europiate **[EuL^3]$^{3-}$**

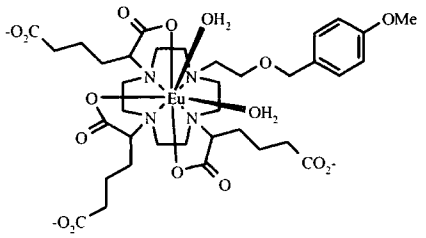

^{1}H NMR (200 MHz, D_2O): The spectrum was exchanged broadened

1-2-[(3,5-Dimethyl-phenoxy)-ethyl]-4,7,10-tris-[(4'ethoxycarbonyl)-1'-methoxycarbonylbutyl-1,4,7,10-tetraazacyclododecane} Gadoliniate **[GdL^4]$^{3-}$**

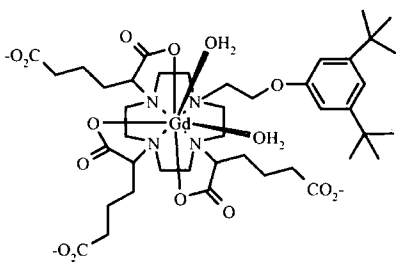

r_{1p} = 6.9 $mM^{-1}s^{-1}$ (65 MHz, 295 K, pH 5.7); MALDI-TOF: 994.1

1-(4-Benzyloxybenzyl]-4,7,10-tris-[(4'carboxy)-1'-carbonylbutyl-1,4,7,10-tetraazacyclododecane gadoliniate **[GdL^5]$^{3-}$**

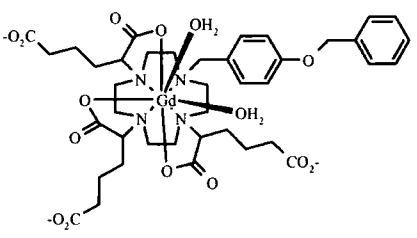

r_{1p} = 9.6 $mM^{-1}s^{-1}$ (65 MHz, 295 K, pH 5.7); MALDI-TOF: 991.1

1-2'-(9-Propyl-9H-fluorene)-4,7,10-tris-[(4'carboxy)-1'-carbonylbutyl-1,4,7,10-tetraazacyclododecane gadoliniate **[GdL^6]$^{3-}$**

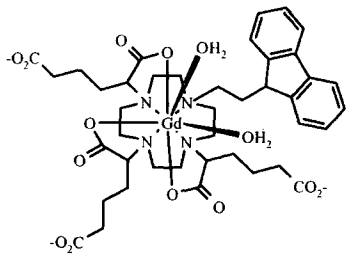

r_{1p} = 7.9 $mM^{-1}s^{-1}$ (60 MHz, 310 K, pH 6.0)

1-2'-(9-methyl-9H-fluorene)-4,7,10-tris-[(4'carboxy)-1'-carbonylbutyl-1,4,7,10-tetraazacyclododecane gadoliniate **[GdL^7]$^{3-}$**

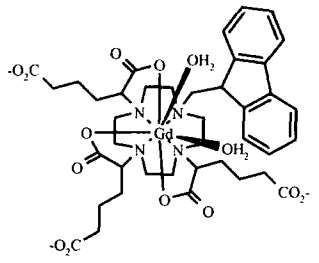

r_{1p} = 3.9 $mM^{-1}s^{-1}$ (60 MHz, 310 K, pH 5.8)

1-2'-(N-ethyl-acridone),4,7,10-tris[(4'methoxycarbonyl)-1'-carbonylbutyl-1,4,7,10-tetraazacyclododecane gadoliniate **[GdL^8]$^{3-}$**

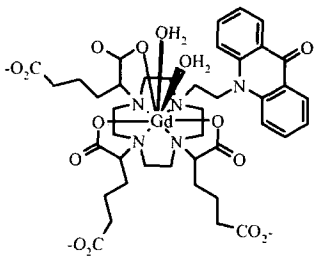

r_{1p} = 7.1 $mM^{-1}s^{-1}$ (60 MHz, 310 K, pH 6.0)

1-2'-(N-ethyl-acridone),4,7,10-tris[(4'methoxycarbonyl)-1'-carbonylbutyl-1,4,7,10-tetraazacyclododecane europiate **$[EuL^8]^{3-}$**

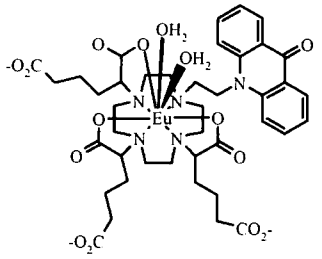

^1H NMR (300 MHz, D_2O): The spectrum was exchanged broadened

6.6 Chapter 3 Experimental

6.6.1 Ligand Synthesis

tert-Butyl-5-(diethoxy-phosphonyl)-pentanoate (21)

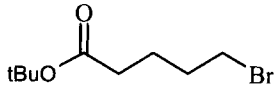

5-Bromovaleric acid (10.36 g, 0.057 mol) was dissolved in dichloromethane (50 ml), oxalyl chloride (25 ml, 0.286 mol) was added and the resulting yellow solution was stirred at room temperature for 3 hours. Excess acid chloride was removed by simple distillation and the product was washed using dichloromethane (4 x 50 ml). The product was then cooled to -78°C and a mixture consisting of pyridine (4.6 ml, 0.057 mol), and t-butyl alcohol (6.4 ml, 0.069 mol) in dichloromethane (5 ml) was slowly added dropwise. The reaction mixture was allowed to warm to room temperature whilst stirring overnight under an argon atmosphere. The crude product was purified using flash column chromatography to remove any white, pyridinium salts (SiO_2, 10% ethyl acetate in hexane → 50% ethyl acetate in hexane), to yield the desired product as a yellow oil (12.3 g, 91%). ^1H NMR (400 MHz, $CDCl_3$) δ_H: 1.31 (9H, s, $C(C\underline{H}_3)_3$), 1.66 (2H, m, CH_2), 1.82 (2H, m, CH_2), 2.18 (2H, t, $C\underline{H}_2CO$, J 7.7 Hz), 3.34 (2H, t, $C\underline{H}_2Br$, J 6.8 Hz); ^{13}C NMR (100.6 MHz, $CDCl_3$) δ_C:

23.74 (CH_2), 28.19 (CH_3), 32.11 (CH_2), 33.25 ($C\underline{H}_2Br$), 34.56 (CH_2CO), 80.23 (q, C), 172.40 (C=O); m/z (ES^+): 259.0 (100%, $^{79}Br\ MNa^+$), 261.1 (100%, $^{81}Br\ MNa^+$); Accurate mass Found 258.0213, $C_9H_{16}O_2BrNa$ requires 258.0231.

Tert-butyl-5-(diethoxy-phosphonyl)-pentanoate (22)

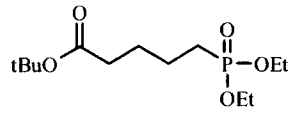

Compound **(21)** (7.16 g, 0.024 mol) was dissolved in triethylphosphite and heated under reflux for 18 hours under an argon atmosphere. The crude product was distilled under pressure (78°C, 1.0 mmHg) to yield the desired product as a transparent oil (6.31 g, 83%). ^1H NMR (400 MHz, $CDCl_3$) δ_H: 1.22 (6H, t, $OCH_2C\underline{H}_3$, J 7.2 Hz), 1.33 (9H, s, $C(CH_3)_3$), 1.53 (6H, m, CH_2), 2.12 (2H, t, $C\underline{H}_2CO$, J 7.6 Hz), 3.98 (4H, m, $C\underline{H}_2OP$); ^{13}C NMR (125.6 MHz, $CDCl_3$) δ_C: 16.61 ($POCH_2CH_3$), 24.14 (CH_2), 25.86 (CH_2), 26.29 (CH_2), 27.97 ($C(\underline{C}H_3)_3$), 35.06 ($\underline{C}H_2CO$), 61.53 ($PO\underline{C}H_2$, J_{CP} 6.5 Hz), 80.21 (q, C), 176.6 (C=O); ^{31}P NMR (80.9 MHz, $CDCl_3$) δ_P: 32.9; m/z (ES^+): 295.2 (10%, M^+), 317.2 (100%, MNa^+), 611.4 ($2MNa^+$); Accurate Mass Found 317.1525, $C_{13}H_{27}O_5PNa$ requires 317.1494.

5-(Diethoxy-phosphonyl)-pentanoic acid (23)

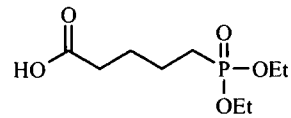

Compound **(22)** (1.0 g, 0.003 mmol) was suspended in trifluoroacetic acid (1 ml) and dichloromethane (3 ml). The resulting solution was stirred under argon at room temperature overnight. The mixture was concentrated by reduced pressure and the residue washed using dichloromethane (3 x 10 ml). ^1H NMR (400 MHz, $CDCl_3$) δ_H: 1.28 (6H, t, $CH_2C\underline{H}_3$, J 7 Hz), 1.71 (6H, m, CH_2), 2.42 (2H, t, CH_2CO, J 7 Hz), 4.16 (4H, m, CH_2PO), 12.56 (1H, s, OH); ^{13}C NMR (100.6 MHz, $CDCl_3$) δ_C: 16.41 (CH_3), 21.75 (CH_2), 24.72 (CH_2), 25.46 (CH_2), 35.55 (CH_2CO), 63.01 ($PO\underline{C}H_2CH_3$), 179.77

(C=O); ^{31}P NMR (80.9 MHz, $CDCl_3$) δ_P: 33.5 (P=O); m/z (ES$^-$): 237.1 (10%, M$^-$); Accurate Mass Found 237.0905, $C_9H_{18}O_5P$ requires 237.0892.

(±) Ethyl-2-bromo-5-(diethoxy-phosphonyl)-pentanoate (24)

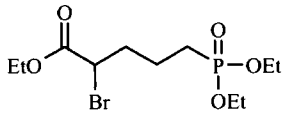

Compound **(23)** (6.01 g, 0.025 mmol) was dissolved in thionyl chloride (10 ml) and heated under reflux for approximately 1 hour. Liquid bromine (4.01g, 0.025 mmol) was carefully added and the resulting brown solution was heated under reflux, under an argon atmosphere overnight. The reaction mixture was cooled in an ice bath and then added drop-wise to a cooled solution of anhydrous ethanol. The resulting yellow solution was stirred under argon for approximately 30 minutes. The solution was poured onto crushed ice (100 g) and stirred until fully melted. The desired product was then extracted using diethyl ether (3 x 50 ml). The organic phase was dried over $MgSO_4$ and solvent removed under reduced pressure to yield a yellow oily product (6.12g, 83%). ^1H NMR (500 MHz, $CDCl_3$) δ_H: 1.04 (6H, t, ($POCH_2C\underline{H}_3$), J 8.5 Hz), 1.13 (3H, m, $CH_2C\underline{H}_3$), 1.79 (4H, m, CH_2), 2.12 (CH_2CO), 3.90 (4H, m, $POC\underline{H}_2CH_3$), 4.04 (3H, m, $OCOC\underline{H}_2CH_3$ & $C\underline{H}Br$); ^{13}C NMR (125.6 MHz, $CDCl_3$) δ_C: 13.90 (CH_3), 16.33 (CH_3, $J_{C\text{-}P}$ 5.7), 20.34 (CH_2), 23.88-25.01 (CH_2, J_{CP} 141), 35.10 ($\underline{C}H_2CHBr$), 45.32 (CHBr), 62.20 ($CH_3\underline{C}H_2OCO$), 62.22 ($CH_3\underline{C}H_2OP$), 169.60 (C=O); ^{31}P NMR (80.9 MHz, $CDCl_3$) δ_P: 32.5; m/z (ES$^+$): 345.1 (100%, ^{79}Br M$^+$), 347.2 (100%, ^{81}Br M$^+$), 367.2 (20%, MNa$^+$), Accurate Mass Found 345.0461, $C_{11}H_{23}O_5PBr$ requires 345.0466.

1,4,7-tris-Trifluoromethyl carbonyl-1,4,7,10-tetraazacyclododecane (25)[125]

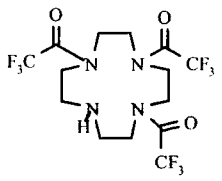

1,4,7,10-Tetraazacyclododecane (1.01 g, 5.87 mmol) and triethylamine (0.8 ml, 6.98 mmol) were dissolved into anhydrous methanol and cooled to -0°C. Ethyl trifluoroacetate (3.30 g, 0.023 mmol) was added dropwise over a 30 minute period, the mixture was left stirring under an argon atmosphere for approximately 4 hours, and the temperature was allowed to increase to room temperature. The solvent was removed by reduced pressure to yield a crude yellow product, which was purified by flash column chromatography (SiO_2, 1% MeOH in DCM → 3% MeOH in DCM) (1.9 g, 70%). R_f (SiO_2, 100 EtOAc = 0.295) ^1H NMR (400 MHz, $CDCl_3$) δ_H: 1.49 (1H, br s, NH), 2.87 (4H, m, NCH_2), 3.52-3.65 (8H, m, NCH_2), 3.85 (4H, m, NCH_2); ^{13}C NMR (100.6 MHz, $CDCl_3$) δ_C: 20.93 (CH_2), 46.91-52.81 (m, $N\underline{C}H_2$), 116.44 (q, CF_3, J_{C-F} ~ 278 Hz, further split due to conformers), 156.78-158.22 (m, C=O, existence of conformers and long range C-F coupling); m/z (ES^+) 483.3 (100%, MNa^+), 943.1 (75% $2MNa^+$).

1,t-Butoxycarbonyl-4,7,10-tris-trifluoromethylcarbonyl-1,4,7,10-tetraazacyclododecane (26)

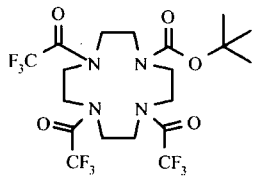

1,4,7-tris-trifluoromethyl carbonyl-1,4,7,10-tetraazacyclododecane **(25)** (1.86 g, 4.0 mmol) was dissolved into dry methanol (20 ml), di-tert-butyl-dicarbonate (1.02 g, 4.7 mmol) was added and the resulting mixture was left stirring at room temperature, under an argon atmosphere, for approximately 5 hours. The solvent was removed under reduced pressure to yield an oily crude product. The desired product was purified by flash column chromatography (SiO_2, DCM → 2% EtOAc in DCM), as a colourless oil (1.35 g, 57%), R_f (10% EtOAc in DCM = 0.54). ^1H NMR (400 MHz, $CDCl_3$) δ_H: 1.33 (9H, s, $C(CH_3)_3$), 3.34-3.73 (16H, m, NCH_2); ^{13}C NMR (100.6 MHz, $CDCl_3$) δ_C: 20.62 (CH_2), 27.98 ($C(\underline{C}H_3)_3$), 48.54-50.70 (m, $N\underline{C}H_2$), 81.04 ($\underline{C}(CH_3)_3$), 116.03 (q, CF_3, J_{C-F} ~ 287 Hz, further split due to conformers), 156.67-158.70 (m, C=O, existence of conformers and long range C-F coupling); (m/z (ES^+)

583.3 (100%, MNa^+); Accurate Mass found 583.1617, $C_{19}H_{25}O_5N_4F_9Na$ requires 583.1579.

1, 4, 7,10-Tetraazacyclododecane-1-t-Butoxycarbonyl (27)

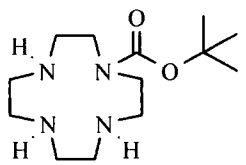

1,t-Butoxycarbonyl-4,7,10-tris-trifluoromethylcarbonyl-1,4,7,10-tetraazacyclododecane **(26)** (1.35 g, 2.31 mmol) was dissolved in methanol (20 ml) and water (5 ml), potassium hydroxide solution (1 ml, 2M) was added and the resulting mixture was stirred at room temperature for approximately 3 hours. The product was concentrated under reduced pressure to yield a pale yellow oil. The product was suspended into dichloromethane (50 ml) and washed successively with saturated $NaHCO_3$ solution (10 ml) followed by saturated NaCl solution (10 ml). The organic layer was dried over K_2CO_3 and solvent removed by reduced pressure. ^1H NMR (400 MHz, $CDCl_3$) δ_H: 1.21 (9H, s, $C(C\underline{H}_3)_3$), 2.45 (4H, br m, NCH_2), 2.56 (8H, br m, NCH_2), 3.17 (4H, br m, NCH_2), 3.37 (1H, br s, NH); ^{13}C NMR (100.6 MHz, $CDCl_3$) δ_C: 28.29 ($C(CH_3)_3$), 46.46 (NCH_2), 48.06 (NCH_2), 48.56 (NCH_2), 48.68 (NCH_2), 48.94 (NCH_2), 79.38 (q, $C(CH_3)_3$), 156.38 (C=O); m/z (ES^+) 295.1 (100%, MNa^+), Accurate Mass Found 273.2302, $C_{13}H_{29}O_2N_4$ requires 273.2291.

1-t-Butoxycarbonyl-4,7,10-tris-[2-ethyl-5-(diethoxy-phosphonyl)-pentanoate-1,4,7,10-tetraazacyclododecane (28)

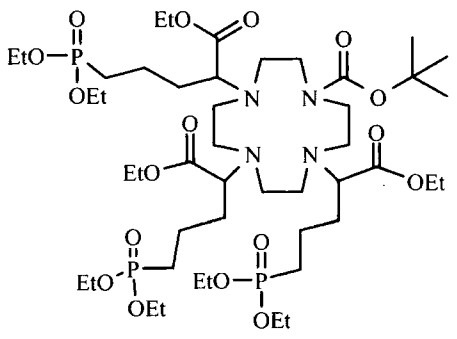

1, 4, 7, 10-Tetraazacyclododecane-1-t-Butoxycarbonyl **(27)** (170 mg, 0.649 mol) was suspended in dry acetonitrile, then **(24)** (738 mg, 2.271 mol) and caesium carbonate (738 mg, 2.271 mol) were added. The resulting mixture was heated under reflux whilst stirring under an inert atmosphere for approximately 72 hours. The particulate matter was removed by filtration, the solution then being concentrated at reduced pressure. The crude mixture was purified by flash column chromatography (SiO_2, DCM → 3% MeOH in DCM R_f =0.62), to yield the required product as a brown oil (150 mg, 22%). ^1H NMR (500 MHz, $CDCl_3$) δ_H: 1.24-1.31 (27H, m, 18H $POCH_2C\underline{H}_3$ & 9H $COCH_2C\underline{H}_3$), 1.43 (9H, s, $C(CH_3)_3$), 1.74-1.77 (34H, m, 16H NCH_2 & 18H CH_2's), 4.07 (21H, m, 12H $POC\underline{H}_2CH_3$ & 6H $COC\underline{H}_2CH_3$ & 3H $C\underline{H}$); ^{13}C NMR (125.6 MHz, $CDCl_3$) δ_C: 13.17 (CH_3), 15.46 (CH_3 J_{CP}= 3.8 Hz), 17.21 (CH_2), 23.75 (CH_2), 24.82 (CH_2), 27.42 ($C(\underline{C}H_3)_3$), 33.76 (CH_2), 60.48-60.53 (m, $POCH_2CH_3$, existence of long range CP coupling and isomers, J_{CP} = 6.2 Hz); ^{31}P NMR (80.9 MHz, $CDCl_3$) δ_P: 31.8 - 32.7 m/z (ES^+) 1087.4 (10%, MNa^+), 1127.4 (50%, MCu^+); Accurate Mass Found 1087.555, $C_{46}H_{91}O_{17}N_4P_3Na$ requires 1087.549.

1,4,7-Tris-[ethyl-5-(diethoxy-phosphonyl)-pentanoate-1,4,7,10-tetraazacyclododecane (29)

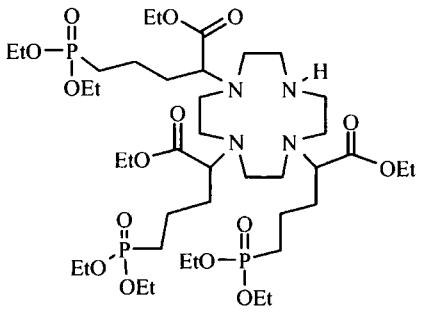

1,4,7,10-Tetraazacyclododecane-1-t-Butoxycarbonyl-4,7,10-tris-[2-ethyl-5-(diethoxy-phosphonyl)-pentanoate-1,4,7,10-tetraazacyclododecane (28) (154 mg, 0.145 mmol) was thoroughly dried then suspended in trifluoroacetic acid (2 ml) and dichloromethane (2 ml). The resulting mixture was stirred overnight under an argon atmosphere. The residual acid chloride was removed at reduced pressure and washing using dichloromethane (3 x 2 ml), to yield the product as a brown oil (120.2 mg, 89%). ^1H NMR (400 MHz, $CDCl_3$) δ_H: 1.19-1.28 (27H, br m, 18 x

$POCH_2\underline{CH}_3$ & 9 x $COCH_2\underline{CH}_3$), 1.64-2.34 (38H, br m, 16 x $NC\underline{H}_2$ & 21 x $C\underline{H}_2$ & $NC\underline{H}$), 4.03-4.14 (21H, 12 x $POC\underline{H}_2CH_3$ & 6 x $COC\underline{H}_2CH_3$ & 3 x $C\underline{H}$), ^{31}P NMR (80.9 MHz, $CDCl_3$) δ_P: 32.9 (s, $\underline{P}OCH_2CH_3$); m/z (ES^+) 965.3 (10%, MH^+), 1003.2 (100%, MK^+), 1027.2 (10%, MCu^+); Accurate mass Found 965.5210, $C_{41}H_{84}O_{15}N_4P_3$ requires 965.5146.

1,4,7-Tris-(di-phosphonyl)-pentanoate-1,4,7,10-Tetraazacyclododecane [L⁹]

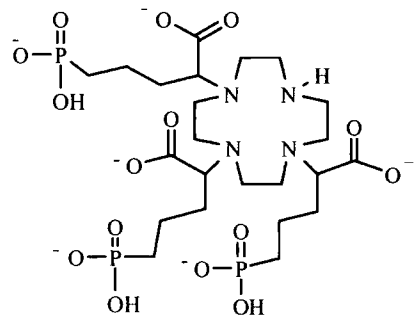

1,4,7-Tris-[2-ethyl-5-(diethoxy-phosphonyl)-pentanoate-1,4,7,10-tetraazacyclododecane **(29)** (90 mg, 0.093 mmol) was suspended into hydrogen bromide solution in acetic acid (5 ml). The resulting mixture was heated under reflux at 90°C for eighteen hours. The solution was allowed to cool to room temperature and was then added dropwise to a cooled solution of diethyl ether. The product was insoluble in ether and formed a yellow oily precipitate. The product was concentrated at reduced pressure. Toluene was added (5 x 10 ml) which was also removed at reduced pressure in an attempt to remove any remaining acetic acid. ^1H NMR (200 MHz, D_2O) δ_H: 1.64-1.93 (18H, br m, $C\underline{H}_2$), 2.52-3.58 (16H br m, NCH_2), 3.92 4.32 (3H, m, $NC\underline{H}$), ^{31}P NMR (D_2O, 80.9 MHz) δ_P: 31.7 - 33.0 (s, $\underline{P}OCH_2CH_3$).

6.6 Complex Synthesis

1,4,7-Tris-5-(di-phosphonyl)-pentanoate-1,4,7,10-Tetraazacyclododecane **$[GdL^9]^{3-}$**

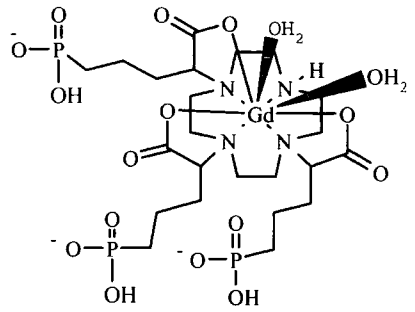

1,4,7-Tris-5-(di-phosphonyl)-pentanoate-1,4,7,10-Tetraazacyclododecane (33 mg, 0.047 mmol) was dissolved into water (2 ml). The pH of the acidic solution was adjusted to pH 5.5 using sodium hydroxide solution (0.1 M). Gadolinium(III) chloride hexahydrate (17 mg, 0.047 mmol) was added, the pH being re-adjusted to pH 5.5. The resulting brown solution was heated under reflux for 18 hours. The cloudy brown solution was allowed to cool to room temperature and was centrifuged to remove any particulate matter. The filtrate was collected and the pH of the solution increased to pH 10 using sodium hydroxide solution (0.1 M) for approximately 20 minutes. The solution was filtered through a 0.45 μm syringe filter to remove any free gadolinium hydroxide precipitate. The pH was then lowered to pH 5.5 using hydrochloric acid (0.1 M). The solution was lyophilised to yield a white solid. (22 mg, 55%). Relaxivity value for $[GdL^9]^{3-}$ 7.3 $mM^{-1}s^{-1}$ (pH 6.8, 310 K, 60 MHz).

6.7 Chapter 4 Experimental

6.7.1 Ligand Synthesis

Diethyl-pyridine-2,6-dicarboxylate (30)

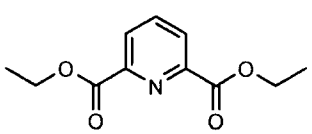

2,6 Pyridine carboxylic acid (10.2 g, 0.062 mol) was dried under vacuum and then

suspended into dry ethanol (20 ml). Concentrated sulphuric acid was added (0.8 ml) and the resulting white mixture was heated under reflux for approximately 18 hours. The transparent reaction mixture was cooled and quenched using excess sodium hydrogen carbonate and stirred for approximately 30 minutes. The solvent was evaporated at reduced pressure producing a white solid, which was then suspended into dichloromethane (40 ml) and washed successively with water, saturated sodium hydrogen carbonate solution and water. The organic phase was dried using $MgSO_4$ and solvent removed at reduced pressure to yield a white, crystalline solid (7.88 g, 58 %). ^1H NMR (400 MHz, $CDCl_3$) δ_H: 1.39 (6H, t, $C\underline{H}_3$, J 7.2 Hz), 4.43 (4H, q, $C\underline{H}_2CH_3$, J 7.2 Hz), 7.96 (1H, t, H_4, J 7.2 Hz), 8.23 (2H, d, H_3 & H_5, J 7.2 Hz); ^{13}C NMR (100.6 MHz, $CDCl_3$) δ_C: 14.16 (2 CH_3), 62.23 (2 CH_2), 127.76 (C4), 138.16 (C_3 & C_5), 148.63 (q, C_2 & C_6), 164.57 (C=O); m/z (ES^+) 246.1 (50%, MNa^+), 469.0 (100%, $2MNa^+$).

6-Hydroxymethyl-pyridine-2-carboxylic acid ethyl ester*[130]*(31)

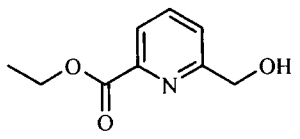

Sodium borohydride (0.73 g, 0.019 mmol) was added to a solution of **(30)** (7.15 g, 0.032) in dry ethanol (100 ml). The resulting white suspension was heated under reflux for approximately 18 hours under an argon atmosphere. The reaction mixture was allowed to cool to room temperature and quenched with water (80 ml). The solvent was then evaporated at reduced pressure to approximately 30 ml, which was then extracted using chloroform (3 x 80 ml). The organic fractions were collected and dried using sodium sulphate, and organic solvent removed at reduced pressure to yield a white solid (3.50 g, 60%). ^1H NMR (400 MHz, $CDCl_3$) δ_H: 1.35 (3H, t, CH_3, J 7.2 Hz), 3.76 (1H, brs, OH), 4.38 (2H, q, CH_2CH_3, J 7.2 Hz), 4.79 (2H, s, CH_2OH), 7.46 (1H, d, H_5, J 7.6 Hz), 7.76 (1H, t, H_4, J 7.6 Hz), 7.94 (1H, d, H_3, J 7.6 Hz); m/z (ES^+) 204.1 (100%, MNa^+).

***6-Azomethyl-pyridine-2-carboxylic acid ethyl ester*[130] (32)**

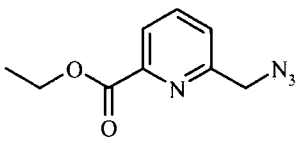

Methanesulfonyl chloride (3.37 g, 19.34 mmol) was added to a stirred suspension of **(31)** (3.50 g, 19.34 mmol) and triethylamine (1.96 g, 19.34 mmol) in dry toluene (50 ml), which was cooled in an ice bath. The reaction mixture was gradually allowed to warm to room temperature whilst stirring under argon for approximately 6 hours. Tetrabutylammonium bromide (0.65 g, 154.7 mmol) and water (35 ml) were added and the resulting orange mixture was heated under reflux overnight under an argon atmosphere. The mixture was cooled to room temperature and the organic phase separated. The aqueous phase was extracted with toluene (4 x 100 ml), the organic residues were collected, dried using sodium sulphate, filtered and concentrated at reduced pressure to yield a brown oil. The crude product was purified by flash column chromatography (SiO_2, EtOAc) to yield a pale yellow oil (3.46 g, 87%). ^1H NMR (400 MHz, $CDCl_3$) δ_H: 1.27 (3H, t, CH_3, J 7 Hz), 4.34 (2H, q, $C\underline{H}_2CH_3$, J 7 Hz), 4.47 (2H, s, $C\underline{H}_2N_3$), 7.47 (1H, d, H_3, J 7.6 Hz), 7.79 (1H, t, H_4, J 7.6 Hz), 7.95 (1H, d, H_5, J 7,6 Hz); ^{13}C NMR (100.6 MHz, $CDCl_3$) δ_C: 14.10 (CH_3), 55.25 (CH_2N_3), 61.80 (CH_2CH_3), 124.07 (C_3), 124.88 (C_5), 137. 94 (C_4), 148.03 (q, C_6), 156.29 (q, C_2), 164.70 (C=O); m/z (ES^+) 229.1 (100%, MNa^+).

6-tert-Butoxycarbonylamino-methyl-pyridine-2-carboxylic acid ethyl ester (33) [130]

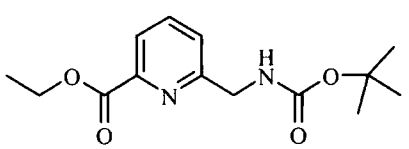

Compound **(32)** (3.46 g, 16.79 mmol) was dissolved in ethyl acetate (35 ml), BOC anhydride (4.39 g, 20.15 mmol) and 10% palladium on carbon (0.37 g) were added. The resulting black suspension was stirred under hydrogen (40 psi) on a Parr

hydrogenator for 18 hours at room temperature. The reaction mixture was filtered through a bed of celite and washed thoroughly with copious amounts of ethyl acetate. The resulting solution was concentrated under reduced pressure. The product was purified by flash column chromatography (SiO_2, EtOAc) to give the desired product as a yellow oil (4.05 g, 86%). ^{1}H NMR (400 MHz, $CDCl_3$) δ_H: 1.36 (9H, s, $C(C\underline{H}_3)_3$), 4.40 (2H, q, $C\underline{H}_2CH_3$, J 6.8 Hz), 4.46 (2H, d, $C\underline{H}_2NH$, J 5.6 Hz), 7.43 (1H, d, H_5, J 8 Hz), 7.74 (1H, t, H_4, J 7.6 Hz), 7.93 (1H, d, H_3, J 7.2 Hz); m/z (ES^+) 303.1 (100%, MNa^+).

[6-(3-Hydroxy-propylcarbamoyl)-pyridine-2-ylmethyl]-carbamic tert-butyl ester (34)[130]

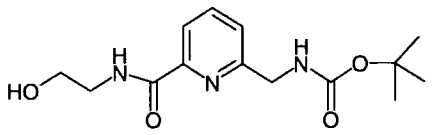

A pale yellow solution of **(33)** (5.05 g, 18.04 mmol) in ethanolamine (5 ml) and methanol (3ml) was stirred at room temperature for 49 hours. The solvent was removed using a Kügelrohr apparatus, and the solution was washed using another quantity of methanol (2 ml), which was removed by the same process, to yield the desired product as a clear, colourless oil (3.34 g, 58%). ^{1}H NMR (400 MHz, $CDCl_3$) δ_H: 1.34 (9H, s, *t*-Bu), 3.53 (2H, q, $NHC\underline{H}_2CH_2$, J 5.2 Hz), 3.57 (2H, t, $HOC\underline{H}_2CH_2$, J 5.2 Hz), 4.31 (2H, d, $ArCH_2NH$, J 5.6 Hz), 5.81 (1H, br s, NH), 7.30 (1H, d, H_3, J 7.6 Hz), 7.66 (1H, t, H_4, J 7.8 Hz), 7.87 (1H, d, H_5, J 7.6 Hz), 8.42 (1H, br s, NH); m/z (ES^+): 318.2 (100%, MNa^+).

6-(2-Bromo-ethylcarbamoyl)-pyridin-2-ylmethyl]-carbamic acid tert-butyl ester[130] (35)

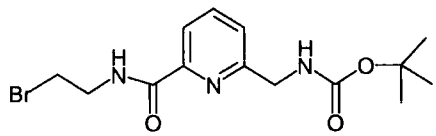

(34) (3.34 g, 11.32 mmol) was dried thoroughly under reduced pressure. The oily product was dissolved in dichloromethane (4 ml), triphenylphosphine (4.45 g, 16.98

mmol) was added and the mixture cooled in an ice bath. Carbon tetrabromide (4.67 g, 14.13 mmol) was then added and the resulting yellow solution was gradually warmed to room temperature whilst stirring under argon overnight. The resulting red solution was concentrated under reduced pressure and purified by flash column chromatography (SiO_2, EtOAc) to produce a clear colourless oil (2.33 g, 58%). ^{1}H NMR (400 MHz, $CDCl_3$) δ_H: 1.43 (9H, s, *t*-Bu), 3.58 (2H, t, $HOC\underline{H}_2CH_2N$, J 6 Hz), 3.88 (2H, q, $NHC\underline{H}_2CH_2$, J 6 Hz), 4.49 (2H, d, $ArC\underline{H}_2NH$, J 5.6 Hz), 5.32 (1H, br s, NH), 7.45 (1H, d, H_3, J 7.5 Hz), 7.84 (1H, t, H_4, J 7.8), 8.08 (1H, d, H_5, J 7.6 Hz), 8.45 (1H, br s, NH); ^{13}C NMR (75.4 MHz, $CDCl_3$): δ_C 28.50 ($C(\underline{C}H_3)_3$), 32.07 (CH_2), 41.17 (CH_2), 45.74 (CH_2), 120.97 (C_4), 124.38 (q, C_2), 138.25 (C_3), 148.92 (C_5), 156.12 (q, C_6), 157.16 (C=O), 164.35 (C=O); m/z (ES^+): 380.1 (100%, ^{79}Br MNa^+), 382.0 (85%, ^{81}Br MNa^+).

{6-[2-(1,4,7,10-Tetraaza-cyclododec-yl)-ethylcarbamoyl]-pyridin-2-ylmethyl}-carbamic acid tert-butyl ester*[130] *(36)

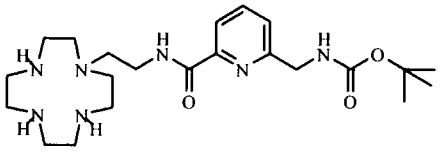

Under an argon atmosphere, a solution of **(35)** (1.71 g, 3.271 mmol) in dry chloroform (75 ml) was slowly added dropwise to a solution of cyclen (1.79 g, 10.41 mmol) in dry chloroform (100 ml). The resulting clear solution was stirred at room temperature for approximately 72 hours. The solution was concentrated at reduced pressure and the resulting yellow oil was dissolved into dichloromethane (60 ml). The organic phase was washed with water (4 x 60 ml), dried using potassium carbonate and concentrated at reduced pressure to yield a clear oil (1.07 g, 91%). ^{1}H NMR (400 MHz, $CDCl_3$) δ_H: 1.41 (9H, s, $C(CH_3)_3$), 2.49-2.64 (18H, m, 8 ring CH_2 & $NHCH_2C\underline{H}_2$), 3.50 (2H, q, $NHC\underline{H}_2CH_2$, J 5.4 Hz), 4.30 (2H, d, $ArC\underline{H}_2NH$, J 5.6 Hz), 7.32 (1H, d, H_3, J 7.6 Hz), 7.71 (1H, t, H_4, J 7.6 Hz), 7.97 (1H, d, H_5, J 7.6 Hz), 8.01 (1H, br, NH), 8.35 (1H, br, NH); ^{13}C NMR (100.6 MHz, $CDCl_3$) δ_C: 24.48 ($C(\underline{C}H_3)_3$), 37.76 (CH_2), 44.67 (CH_2), 45.60 (CH_2), 46.43 (CH_2), 51.81 (CH_2), 54.42 (CH_2), 78.92

(C(CH$_3$)$_3$), 120.41 (C$_4$), 124.40 (C$_2$), 137.84 (C$_3$), 149.63 (C$_5$), 157.14 (q, C$_6$), 164.19 (C=O); m/z (ES$^+$): 450.4 (100%, M$^+$), 473.6 (10%, MNa$^+$).

1,4,7-Tris-[(4'-methoxycarbonyl)-1'methoxycarbonylbutyl]-{6-[2-(1,4,7,10-tetraaza-cyclododec-yl)-ethylcarbomoyl]-pyridin-2-ylmethyl}-carbamic acid tert-butyl ester[130] (37)

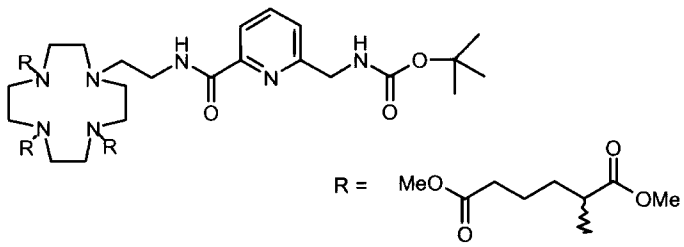

Under anhydrous conditions and an argon atmosphere, a stirred suspension of **(36)** (31 mg, 0.068 mmol), dimethyl-α-bromoadipate **(1)** (52.3 mg, 0.206 mmol) and caesium carbonate (68 mg, 0.206 mmol) in dry acetonitrile (5 ml) was heated at reflux for 10 days. The reaction mixture was cooled to room temperature and filtered to remove the inorganic solids; evaporation of the solvent yielded a brown oil which was purified by gradient elution column chromatography (SiO_2, 1% MeOH in DCM → 5% MeOH in DCM). The desired product was obtained as a yellow oil (42 mg, 64%). R_f = 0.23 (SiO_2, 10% MeOH in DCM); ^{1}H NMR (400 MHz, $CDCl_3$) δ_H: 1.39 (9H, s, *t*-Bu), 1.55-2.85 (39H, m, 16H NC$\underline{H}_2$ & 3 NC$\underline{H}_2$, 18H C$\underline{H}_2$ & 2 NHC$\underline{H}_2$CH$_2$), 3.13-3.70 (20H, m, 18H OC$\underline{H}_3$ & 2H NHCH$_2$C$\underline{H}_2$), 4.47 (2H, s, CH$_2$Ar), 7.43 (1H, d, H$_3$, J 6.6 Hz), 7.79 (1H, t, H$_4$, J 7.5 Hz), 7.98 (1H, d, H$_5$, J 7.2 Hz), 8.24 (1H, br, NH); m/z (ES$^+$) 966.4 (100%, MH$^+$), 988.4 (30%, MNa$^+$).

1,4,7-Tris-[4'-methoxycarbonyl)-1'methoxycarbonylbutyl]-{6-[2-(1,4,7,10-tetraazacyclododecyl)-ethylcarbamoyl]-pyridin-2-ylmethyl}-amine[130] (38)

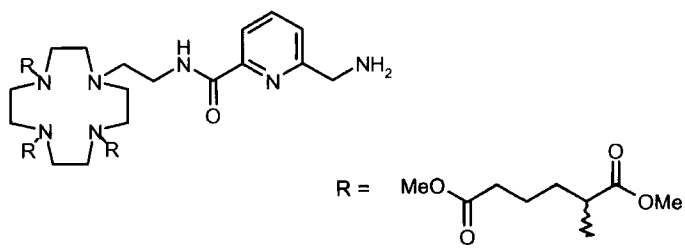

Under an argon atmosphere, a solution of **(37)** (141 mg, 0.146 mmol) in trifluoroacetic acid (2 ml) was left stirring at room temperature for approximately 18 hours. The solvent was then removed under reduced pressure and the resulting brown oil was re-dissolved in dichloromethane (2 ml) and the solvent evaporated under reduced pressure. This process was repeated three times to remove the residual TFA. ^{1}H NMR (400 MHz, $CDCl_3$) δ_H: 1.56-3.52 (41H, br m, CH_2's), 3.60 (18H, br m, OCH_3), 4.43 (2H, s, NH_2CH_2Ph), 7.44 (1H, d, H_3, J 7.6 Hz), 7.87 (1H, t, H_4, J 8 Hz), 8.05 (1H, d, H_5, J 7.2 Hz), 8.60 (1H, br s, NH); m/z (ES^+) 434.1 (100%, MH^{2+}), 866.4 (20%, MH^+).

***1,4,7-Tris-[4'carbonyl)-1'carbonylbutyl]-{6-[2-(1,4,7,10-tetraazacyclododecyl)-ethylcarbamoyl]-pyridin-2-ylmethyl}-amine*[130] [L[10]]**

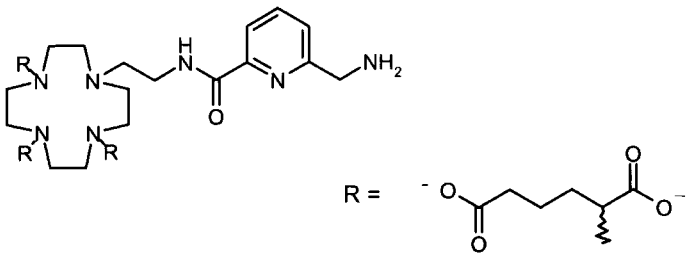

A suspension of **(43)** (46 mg, 0.053 mmol) and lithium hydroxide (103 mg, 2.466 mmol) were dissolved into D_2O (1.5 ml), the resulting mixture agitated at room temperature for 19 hours. The reaction was monitored by ^{1}H NMR and the hydrolysed product was complexed without further purification. ^{1}H NMR (400 MHz, D_2O) δ_H: 1.20-3,67 (43H, br, CH_2), 7.60 (1H, d, H_3), 7.97 (2H, br m, H_4 & H_5).

1,4,7,-Tris-[(4'-methoxycarbonyl)-1'methoxycarbonylbutyl]-{6-[2-(1,4,7,10-tetraaza-cyclododec-yl)-ethylcarbamoyl]-pyridin-2-ylmethyl}-trimethylsulfonamide (39)

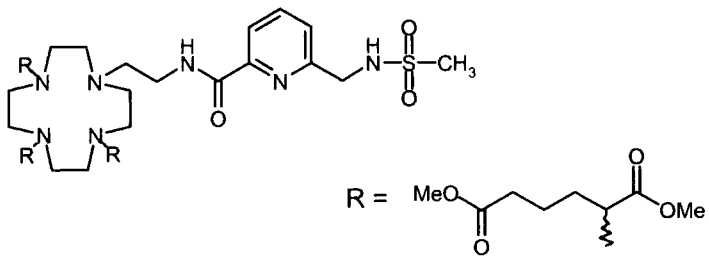

Compound **(38)** (110 mg, 0.127 mmol) was dried thoroughly under reduced

pressure. The flask was flushed with argon and the compound suspended into dichloromethane (2 ml), which was then cooled to -40 °C in an ice bath. Methane sulphonyl chloride (44 mg, 0.386 mmol) and triethylamine (29.9 mg, 0.508 mmol) were added. The resulting mixture was allowed to warm up to room temperature whilst gradually stirring under an argon atmosphere for approximately 18 hours. The product was purified by flash column chromatography (SiO2, 8% MeOH in DCM), to yield the required product as a yellow oil. (40 mg, 33%). ^{1}H NMR (500 MHz, $CDCl_3$) δ_H: 1.24 (3H, s, CH_3), 1.61-2.97 (41H, br m, CH_2s), 3.66 (18H, s, OCH_3), 4.46 (2H, $NHCH_2Ph$), 7.34 (1H, d, H_3, J 7.5 Hz), 7.79 (1H, t, H_4, J 7.5 Hz), 8.01 (1H, d, H_5, J 8 Hz); ^{13}C NMR ($CDCl_3$, 125.6 MHz) δ_C: 21.30 (CH_3), 26.74 (CH_2), 28.68 (CH_2), 32.46 (CH_2), 39.37 (CH_2), 46.19 ($NH\underline{C}H_2Ph$), 50.65 (OCH_3), 119.82 (C_3), 123.26 (C_5), 136.93 (C_4), 148.07 (C_2), 154.50 (q, C_6), 164.44 (C=O), 172.55 (C=O); m/z (ES^+) 944.4 (100%, M^+), 967.2 (15%, MNa^+); Accurate mass Found 944.4707, $C_{42}H_{70}O_{15}N_7S$ requires 944.4651.

1,4,7,-Tris-[(4'-carbonxy)-1'carbonylbutyl]-{6-[2-(1,4,7,10-tetraaza-cyclododec-yl)-ethylcarbamoyl]-pyridin-2-ylmethyl}-trimethylsulfonamide [L^{11}]

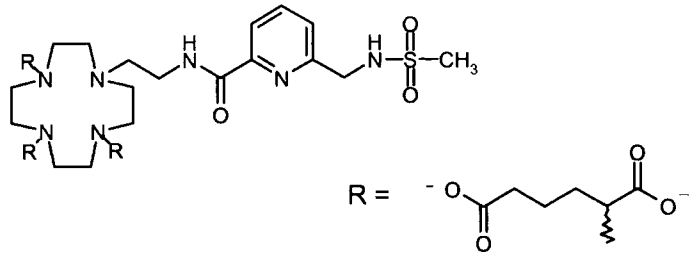

A suspension of **(39)** (39 mg, 0.041 mmol) and lithium hydroxide (79 mg, 1.900 mmol) in water (1.5 ml) was agitated at room temperature for 24 hours. The reaction was monitored by ^{1}H NMR and the hydrolysed compound complexed without any further purification. ^{1}H NMR (200 MHz, D_2O) δ_H: 1.61-3.63 (46H, br m, CH_2 & CH_3), 7.72 (1H, br d, H_3), 7.97 (2H, br m, H_4 & H_5).

Pyridine-2-carboxylic acid (2-hydroxyethyl)-amide^{ref} (40)

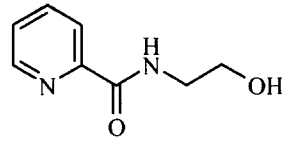

Picolinic ethyl ester (900 mg, 5.96 mmol) and ethanolamine (5 ml) were stirred together under argon for 24 hours. The ethanolamine solution was removed by distillation under reduced pressure using Kugelrohr apparatus to yield a yellow oil (700 mg, 66%). ^{1}H NMR ($CDCl_3$, 200 MHz) δ_H: 3.59 (1H, br, OH) 3.63 (2H, q, $C\underline{H}_2NH$, J 5.6 Hz), 3.81 (2H, t, $C\underline{H}_2OH$, J 5.2 Hz), 7.39 (1H, t, H_5, J 6 Hz), 7.80 (1H, t, H_4, J 7.6 Hz) 8.14 (1H, d, H_3, J 5.8 Hz), 8.48 (1H, br s, NH), 8.52 (1H, d, H_6, J 4.6 Hz); m/z (ES$^+$) 167.0 (70%, MH$^+$), 189.0 (100%, MNa$^+$).

Pyridine-2-carboxylic acid (2-bromoethyl)-amide[130] (41)

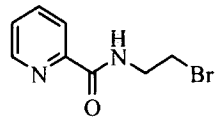

Compound **(40)** (1.30 g, 7.83 mmol) was dried thoroughly under vacuum and then suspended into dichloromethane (10 ml). Triphenylphosphine (3.1 g, 11.75 mmol) was added portion-wise to the stirred solution and cooled in an ice salt bath. Carbon tetrabromide (3.24 g, 9.78 mmol) was added and the mixture left to gradually warm up overnight whilst stirring under argon. The resulting red solution was concentrated by reduced pressure and purified by flash column chromatography (SiO_2, EtO_2Ac) to isolate the product as a white solid (1.38 g, 72%). ^{1}H NMR (400 MHz, $CDCl_3$) δ_H: 3.50 (2H, t, $C\underline{H}_2Br$, J 6 Hz), 3.82 (2H, q, $C\underline{H}_2NH$, J 6 Hz), 7.35 (1H, t, H_5, J 6.4 Hz), 7.75 (1H, t, H_4, J 5.8Hz), 8.16 (1H, d, H_3, J 6.8 Hz), 8.49 (2H, br, H_6 & NH); ^{13}C NMR (100.6 MHz, $CDCl_3$) δ_C: 31.75 (CH_2), 41.14 (CH_2), 122.19 (C_3), 126.12 (C_5), 137.32 (C_4), 148.16 (C_6), 149.46 (q, C_2), 164.42 (C=O); m/z (ES$^+$) 228.9 (10%, M$^+$), 251.0 (100%, ^{79}Br MNa$^+$), 253.0 (100%, ^{81}Br MNa$^+$).

Pyridine-2-carboxylic acid [2-(1,4,7,10 tetraazacyclododec-1-yl)-ethyl]-amide (42)

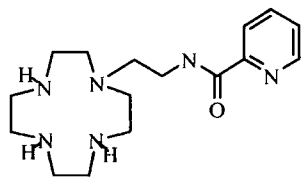

Under an argon atmosphere, a solution of **(41)** (228 mg, 0.247 mmol) in anhydrous

chloroform (120 ml) was slowly added dropwise to a solution of cyclen (128 mg, 0.744 mmol) in dry chloroform (100 ml). The resulting clear solution was stirred at room temperature for 48 hours. The solution was then concentrated to approximately 100 ml and washed with water (4 x 60 ml). The organic residues were collected, dried using potassium carbonate and concentrated at reduced pressure to give the desired product as a pale yellow oil (140 mg, 56%). ^{1}H NMR (400 MHz, $CDCl_3$) δ_H: 2.46-2.74 (21H, br m, 8 x CH_2, 3 x NC<u>H</u> & $NCH_2C\underline{H}_2$), 3.52 (2H, q, $NHC\underline{H}_2CH_2$), 7.29 (1H, br d, H_3), 7.72 (1H, t, H_4, J), 8.08 (1H, d, H_5, J 7.6 Hz), 8.39 (1H, br s, NH); ^{13}C NMR (50.3 MHz, $CDCl_3$) δ_C: 37.3 (CH_2), 45.6 (CH_2), 46.5 (CH_2), 47.4 (CH_2), 51.8 (CH_2), 53.9 (CH_2), 122.37 (C_3), 126.13 (C_5), 137.36 (C_4), 148.07 (C_2), 150.32 (C_6, q), 164.39 (C=O); m/z (ES$^+$) 321.3 (100%, M$^+$), 383.2 (15%, MCu^{2+}); Accurate mass $C_{16}H_{29}N_6O$ requires 321.2403 Found 321.2406.

1,4,7-Tris-[(4'-methoxycarbonyl)-1'methoxycarbonylbutyl]-{6-[2-(1,4,7,10-tetraaza-cyclododec-yl)-ethyl-pyridine-2-carboxylic acid cyclododec-1-yl)-ethyl]-amide (43)

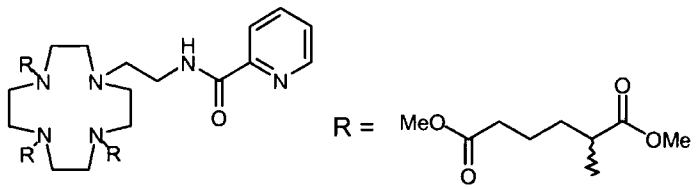

Under anhydrous conditions and an argon atmosphere, a stirred suspension of **(42)** (114 mg, 0.356 mmol) was dissolved into dry acetonitrile (5 ml). Caesium carbonate (347 mg, 1.069 mmol) and dimethyl-α-bromo adipate (270 mg, 1.069 mmol) were added. The resulting mixture was heated under reflux for 11 days. The reaction mixture was cooled to room temperature and filtered to remove the inorganic solids; evaporation of the solvent yielded a brown oil which was purified by gradient elution column chromatography (SiO_2, 1% MeOH in DCM → 8% MeOH in DCM), to yield the desired product as a yellow oil (140 mg,). R_f = 0.49 (SiO_2, 10% MeOH in DCM); ^{1}H NMR (400 MHz, $CDCl_3$) δ_H: 1.58-3.28 (41H, br m, CH_2) 3.62 (20H, br m, CO_2CH_3 & $C\underline{H}_2CH_2NH$), 3.97 (2H, s, $CH_2C\underline{H}_2NH$), 7.41 (1H, br d, H_3), 7.81 (1H, t, H_4, J 7.6 Hz), 8.14 (1H, br s, NH), 8.56 (1H, d, H_5, J 7.6 Hz); ^{13}C NMR (50.3 MHz, $CDCl_3$) δ_C: partial assignment (ring resonances are exchange broadened

at 295 K and 200 to 500 MHz) 22.3 (CH_3), 38.8 (CH_2), 50.2 (CH_2), 122.3 (C_5), 137.4 (C_4), 172.8 (C=O); m/z (ES^+) 837.4 (15%, M^+), 859.4 (10%, MNa^+); Accurate Mass Found 837.4536, $C_{40}H_{65}N_6O_{13}$ requires 837.4610.

1,4,7-Tris-[(4'-carbonyl)-1'carbonylbutyl]-{6-[2-(1,4,7,10-Tetraaza-cyclododec-yl)-ethyl-pyridine-2-carboxylic acid cyclododec-1-yl)-ethyl]-amide **[L^{12}]**

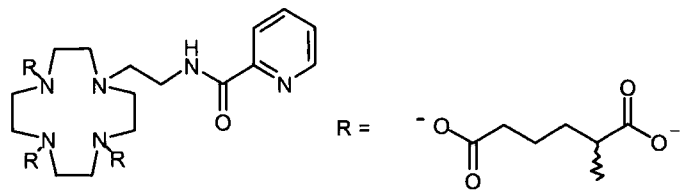

A suspension of **(42)** (66 mg, 0.079 mmol) and lithium hydroxide (50 mg, 1.210 mmol) in D_2O (1 ml) was agitated at room temperature for approximately 18 hours. The reaction mixture was monitored by ^1H NMR. The hydrolysed product was used for complexation without further purification. ^1H NMR (200 MHz, D_2O) δ_H: 1.29-3.49 (41H, br m, CH_2's), 7.43 (1H, br d, H_3), 7.83 (1H, br t, H_4), 8.44 (1H, br d, H_5).

1,4,7,-Tris-[(4'-methoxycarbonyl)-1'methoxycarbonylbutyl]-{6-[2-(1,4,7,10-tetraaza-cyclododec-yl)-ethylcarbamoyl]-pyridin-2-ylmethyl}-trifluoromethanesulfonamide[130] (44)

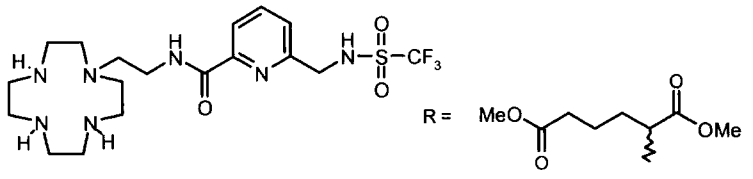

Under anhydrous conditions and an argon atmosphere, trifluoromethanesulphonyl chloride (0.039 ml, 0.361 mmol) was added to a stirred solution of **(38)** (157 mg, 0.181 mmol) in dichloromethane (1 ml) and triethylamine (0.029 ml, 0.361 mmol) which had been cooled to -40°C. The solution was stirred for 18 hours and warmed gradually to room temperature. The solvent was removed by reduced pressure to yield a crude brown mixture. This was re-dissolved in DCM (20 ml) and washed using water to remove excess triethylamine. The organic layer was dried over

$MgSO_4$ and solvent removed by reduced pressure to yield a brown oily product. The product was purified by flash column chromatography (SiO_2, 100% DCM → 6% MeOH in DCM) (83 mg, 23%). ^1H NMR (400 MHz, $CDCl_3$) δ_H: 1.57-2.98 (44H, br m, CH_2s, NCH_2s & NCH), 3.57 (18 H, m, OCH_3), 3.94 (2H, s, $ArCH_2NH$),7.35 (1H, d, H_3, J 7.4), 7.49 (1H, d, impurity), 7.80 (1H, br m, H_4 plus impurity), 8.01 (1H, br m, H_5 plus impurity), ^{19}F NMR (282 MHz, $CDCl_3$) δ_F: -78.14 (s, CF_3); m/z (ES^+) 998.1 (33%,MH^+), 982.3 (45%, MH^+ - Me). Attempts were made to separate the product from its major impurity by reverse phase HPLC but this was unsuccessful.

1,4,7,-Tris-[(4'-carbonxy)-1'carbonylbutyl]-{6-[2-(1,4,7,10-tetraaza-cyclododec-yl)-ethylcarbamoyl]-pyridin-2-ylmethyl}-trifluoromethanesulfonamide[130] [L13]

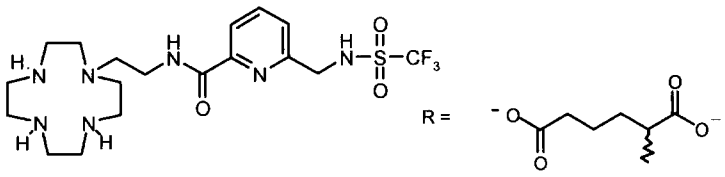

A suspension of (44) (66 mg, 0.067 mmol) and lithium hydroxide (2 ml, 3 M) was stirred at room temperature for approximately 189 hours. That hydrolysis was complete was assessed by ^1H NMR. The hydrolysed product was the complexed without further purification. ^1H NMR (400 MHz, D_2O) δ_H: 1.57-2.78 (44H, br m, CH_2 NCH_2 & CH), 3.69 (2H, br m, CH_2), 7.60 (1H, br d, H_3), 7.71 (1H, br d, impurity), 7.95 (1H, br m, H_4 plus impurity), 8.01 (1H, br m, H_5 plus impurity).

6.8 Complex Synthesis

The gadolinium complexes were all synthesised using a general method. The hydrolysed ligand was suspended into a solution of methanol/ water (1:1) (4 ml) and the lanthanide chloride or acetate hexahydrate added in a 1:1 ratio. The pH was adjusted by using sodium hydroxide solution (0.1 M) and the mixture heated at 90°C for 18 hours. The solution was then cooled, the pH raised to 10 and the solution filtered through a 0.45 μm filter to remove any excess lanthanide as the insoluble $Ln(OH)_3$. The pH was then lowered and the solution lyophilised to give the desired complex as an off-white crystalline solid.

1,4,7-Tris-[4'carbonyl)-1'carbonylbutyl]-{6-[2-(1,4,7,10-tetraazacyclododecyl)-ethylcarbamoyl]-pyridin-2-ylmethyl}-amine-Gadoliniate **[GdL[10]]$^{3-}$**

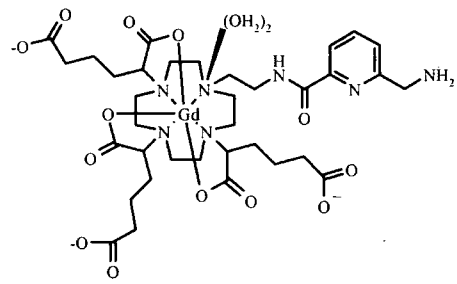

r_{1p} = 9.87 $mM^{-1}s^{-1}$ (60 MHz, pH 5.8, 310 K); MALDI-TOF: 935.9

1,4,7,-Tris-[(4'-carbonxy)-1'carbonylbutyl]-{6-[2-(1,4,7,10-tetraaza-cyclododec-yl)-ethylcarbamoyl]-pyridin-2-ylmethyl}-trimethylsulfonamide-Gadoliniate [GdL[11]]$^{3-}$

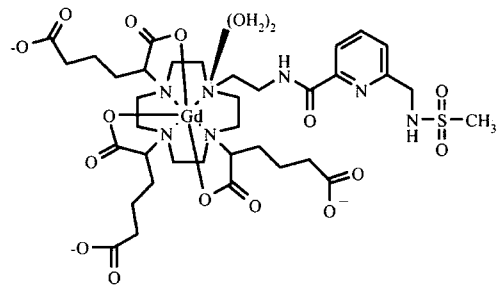

r_{1p} = 7.90 $mM^{-1}s^{-1}$ (60 MHz, pH 5.8, 310 K); MALDI-TOF: 1013.02

1,4,7-Tris-[(4'-carbonyl)-1'carbonylbutyl]-{6-[2-(1,4,7,10-Tetraaza-cyclododec-yl)-ethyl-pyridine-2-carboxylic-acid-cyclododec-1-yl)-ethyl]-amide-Gadoliniate **[GdL[12]]$^{3-}$**

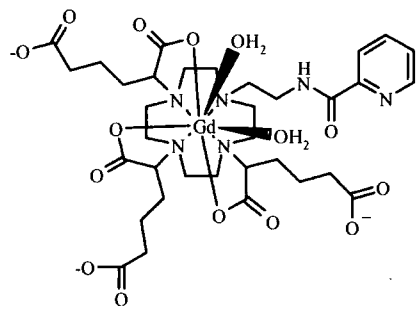

r_{1p}: 7.80 $mM^{-1}s^{-1}$ (60 MHz, pH 5.6, 310 K); MALDI-TOF

6.9 Chapter 5 Experimental

Disodium-S-[4-(4-Ethoxybenzyl)-3,6,9-tris[(carboxy-κO)methyl]-3,6,9-triazaundecandioata)(5-)-κ^3N^3,N^6,N^9, κ^2O^1, O^{11}] europiate-(2-) (Europium-EOB-DTPA) [EuL^{14}].

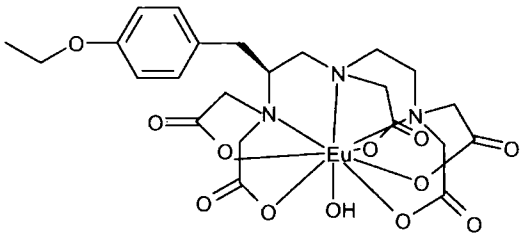

(S)-EOB-DTPA (100 mg, 0.177 mol) and europium chloride hexahydrate were suspended in a mixture of water-methanol (2 ml, 50/50 v/v), and the pH of solution was adjusted to 5.5. The resulting mixture was heated under reflux for 1 hour. The mixture was allowed to cool to room temperature, and the solid colloidal waste was removed by filtration through a 0.45 μm syringe filter. The pH of the filtrate was increased to 7 using sodium hydroxide solution (0.1 M). The solution was concentrated by reduced pressure to a volume of approximately 1 ml. This solution was then dropped onto ethanol (5 ml); the resulting white precipitate was heated under reflux for two hours, then cooled to room temperature. The turbid solution was centrifuged, supernatant solution was discarded and the white solid washed with cold dry ethanol and dried under reduced pressure. NMR analysis confirmed the presence of free europium (III) salts. The solid was dissolved in water (5 ml) and the pH increased to 10.0 using sodium hydroxide solution (0.1 M) for 30 minutes. The solid colloidal waste was then removed by filtration through 0.45 μm filter. The pH of the resulting clear solution was decreased to 5.5 using hydrochloric acid (0.1 M). The solvent was removed under reduced pressure to yield a white solid product (58 mg, 50%). Semi- preparative HPLC: Hypersil ODS 5 μm, column length 25 cm, diameter 16 mm; mobile phase, 2.5 g of NH_4HCO_3 in 940 ml of distilled water and 60 ml of CH_3CN at 295 K; flow rate 10 ml min-1. t_R (major isomer): 15.6 min; 19. 7 min (minor isomer). m/z (ES^-) 674 (^{151}EuLH), 676 (^{153}EuLH),

386.8, 387.8 (doubly charged). IR (KBr, cm-1) 3440, 2990, 2980, 2920, 1607, 1509, 1476, 1401, 1325, 1276, 1241, 1182, 1115, 1089, 991, 973, 926. ^{1}H NMR (200 MHz, D_2O, pD 6.0 major isomer, Figure 5. 8 Chapter 5 for numbering scheme): 29.1 (1H, brs, H8ax), 28.0 (1H, brs, H5ax), 13.8 (1H, brs, H8eq), 10.9 (2H, s, H17), 8.9 (2H, s, H18), 6.8 (1H, s, Heq), 5.6 (1H, s, H5eq), 5.3 (1H, s, H14), 5.1 (2H, s, H15), 2.2 (3H, brs, CH3), -0.9 (3H, brs, H4ax, H'ac-2, H'ac-1), -2.7 (1H, brs, H'14), -7.7 (1H, brs, H'ac-3), -8.1 (1H, brs, Hac-2), -10.0 (1H, brs, H'ac-4), -10.5 (1H, brs, Hac-3), -11.1 (1H, brs, Hac-4), -13.9 and -14.0 (2H, brs, Hac-1 + H'ac-5), -16.8 (1H, brs, Hac-5).

References

1. P. Caravan, J.J. Ellison, T.J. McMurry, R.B. Lauffer, *Chem.Rev.*, **1999**, 99, 2293-2352.

2. R. B. Lauffer, *Chem. Rev.*, **1987**, 87, 901-927.

3. A. E. Merbach, E. Tóth, *The Chemistry of Contrast Agents in Medical Magnetic Resonance Imaging*, Wiley, New York, 2001.

4. S. Aime, M. Botta, M. Fasano, E. Terreno, *Chem. Soc. Rev.*, **1998**, 27, 19-29.

5. M. Woods, Z. Kovacs, S. Zhang, A. D. Sherry, *Angew. Chem. Int. Ed.*, **2003**, 5889-5892.

6. A. Bianchi, L. Calabi, F. Corana, S. Fontana, P. Losi, A. Maiocchi, L. Paleari, B. Valtancoli, *Coordination. Chem. Rev.*, **2000**, 204, 309-393.

7. S. Aime, L. Barbero, M. Botta, *Mag. Resn. Imag.*, **1991**, 9, 843-847.

8. W. Krause, *Topics in Current Chemistry, Contrast Agents I – Magnetic Resonance Imaging*, Vol. 221, Springer, Berlin, 2002.

9. . E. Tóth, L. Burai, A. E. Merbach, *Coordination.Chem. Rev.*, **2001**, 216-217, 363-382.

10. Y. Okuhata, *Ad. Drug Delivery Review*, **1999**, 37, 121-137.

11. D. Dischino, E. J. Delaney, J. E. Emswiler, G. T. Gaughan, J. S. Prasad, S. K. Srivasta, M. Tweedle, *Inorg. Chem.*, **1991**, 30, 1265-1269.

12. X. Zhang, C. A. Chang, H. G. Brittain, J. M. Garrison, J. Telser, M. F. Tweedle, *Inorg. Chem.*, **1992**, 31, 5597-5600.

13. J. Platzek, P. Blaszkiewicz, H. Gries, P. Luger, G. Michl, A. Müller-Fahrnow, B. Radüchel D. Sülzle, *Inorg. Chem.*, **1997**, 36, 6086-6093.

14. S. I. Kang, R. S. Ranganathan, J. E. Emswiler, K. Kumar, J. Z. Gougoutas, M. F. Malley, M. F. Tweddle, *Inorg. Chem.*, **1993**, 32, 2912-2918.

15. S. Aime, A. Barge, M. Botta, J. A. K. Howard, R. Kataky, K. P. Lowe, J. M. Moloney, D. Parker, A. S. deSousa, *Chem. Commun.*, **1999**, 1047- 1048.

16. J. I. Bruce, R. S. Dickins, L. J. Govenlock, T. Gunnlaugsson, S. Lopinski, M. P. Lowe, D. Parker, R. D. Peacock, J. J. B. Perry, S. Aime, M. Botta, *J. Am. Chem. Soc.*, **2000**, 122, 9674-9684.

17. R. M. Supkowski, W. D. Horrocks, J. *Inorg. Chem.*, **1999**, 38, 5616-5619.

18. R. S. Dickins, T. Gunnlaugsson, D. Parker, R. D. Peacock, *Chem. Commun.*, **1998**, 1643-1644.

19. S. Aime, E. Gianolio, E. Terreno, G. B. Giovenzana, R. Pagliarin, M. Sisti, G Palmisano, M. Botta, M. P. Lowe, D. Parker, *SBIC*, **2000**, 5, 488-497.

20. S. Aime, M. Botta, S. G.Crich, G. Giovenzana, G. Jommi, R. Pagliarin, M. Sisti, *J. Chem. Soc., Chem. Commun.*, **1995**, 1885-1886.

21. H. Stetter, W. Frank, R. Mertens, *Tetrahedron*, **1981**, 37, 767-772.

22. S. Aime, M. Botta, S. G. Crich, G. B. Giovenzana, G. Jommi, R. Pagliarin, M. Sisti, *Inorg. Chem.*, **1997,** 36, 2992-3000.

23. W. D. Kim, G. E. Kiefer, F. Maton, K. McMillan, R. N. Muller, A. D. Sherry, *Inorg. Chem.*, **1995,** 34, 2233-2243.

24. R. Hovland, C. Gløgard, A. J.Aasen, J. Klaveness, *Org. Biomol. Chem.*, **2003,** 1, 644-647.

25. S. Aime, M. Botta, S. G. Crich, G. Giovenzana, R. Pagliarin, M. Sisti, E. Terreno, Magn. *Reson. Chem.*, **1998,** 36, S200-S209.

26. S. Aime, M. Botta, L. Frullano, S. G. Crich, G. Giovenzana, R. Pagliarin, G. Palmisano, F. R. Sirtori, M. Sisti, *J. Med. Chem.*, **2000,** 43, 4017-4024.

27. Y. Bretonnière, M. Mazzanti, J. Pécaut, F. A. Dunand, A. E. Merbach, *Chem. Commun.*, **2001,** 621-622.

28. J. Xu, S. J. Franklin, D. W. Whisenhunt, K. N. Raymond, *J. Am. Chem. Soc.*, **1995,** 117, 7245-7246.

29. D. M. J. Doble, M. Melchior, B. O'Sullivan, C. Siering, J. Xu, V.C. Pierre, K. N. Raymond, *Inorg. Chem.* **2003,** 42, 4930-4937.

30. K. Micskei, L. Helm, E. Brucher, A.E. Merbach, *Inorg. Chem*, **1993**, 32, 3844-3850.

31. S. M. Cohen, J. Xu, E. Radkov, K. N. Raymond, M. Botta, A. Barge, S. Aime, *Inorg. Chem.*, **2000**, 39, 5747-5756.

32. D. M. J. Doble, M. Melchior, B. O'Sullivan, C. Siering, J. Xu, V. C. Pierre, K. N. Raymond, *Inorg. Chem.*, **2003**, 42, 4930-4937.

33. S. Hajela, M. Botta, S. Giraudo, J. Xu, K. N. Raymond, S. Aime, *J. Am. Chem. Soc.*, **2000**, 122, 11228-11229.

34. D. M. J. Doble, M. Botta, J. Wang, S. Aime, A. Barge, K. N. Raymond, *J. Am. Chem. Soc.*, **2001,** 123, 10758-10759.

35. S. Aime, A. Barge, M. Botta, J. A. K. Howard, R. Kataky, M. P. Lowe, J. M. Moloney, D. Parker, A. S. DeSousa, *Chem. Commun.*, **1999,** 1047-1048.

36. S. Aime, M. Botta, S. G. Crich, G. B. Giovenzana, R. Pagliarin, M. Piccinini, M. Sisti, E. Terreno, *J. Bio. Inorg. Chem.*, **1997,** 2, 70-479.

37. D. Messeri, M. P. Lowe, D. Parker, M. Botta, *Chem. Commun.*, **2001,** 2742-2743.

38. D. Messeri, Ph. D. Thesis, Targeted and High Relaxivity Contrast Agents, University of Durham, 2002.

39. A. Borel, L. Helm, A. E. Merbach, *Chem. Eur. J.*, **2001,** 7, 600-610.

40. C. J. Broan, E. Cole, K. J. Jankowski, D. Parker, K. Pulukkody, B. A. Boyce, N. R. A. Beeley, K. Millar, A. T. Millican, *Synthesis*, **1992**, 63-68.

41. J. W. Chen, R. L. Belford, R. B. Clarkson, *J. Phys. Chem.*, **1996**, 100, 8093.

42. P. Lebduskova, J. Kotek, P. Hermann, L. V. Elst, R. N. Muller, I. Lukes, J. A. Peters, *Bioconjugate Chem.* **2004,** 15, 881-889.

43. X. Li, S. Zhang, P. Zhao, Z. Kovacs, A. D. J. Sherry, *Inorg. Chem.*, **2001**, 40, 6572-6579.

44. J. Ren, A. D. J. Sherry, *J. Magn. Reson.*, **1996**, B111, 178-186.

45. I. Lazar, A. D. Sherry, R. Ramasamy, E. Brucher, R. Kiraly, *Inorg. Chem*, **1991**, 30, 5016-5019.

46. J. Rohovec, P. Vojtišek, P. Hermann, J. Ludvik, I. Lukeš, *J. Chem. Soc., Dalton Trans.*, **2000**, 141-148.

47. S. Aime, L. Frullano, S. G. Crich, *Angew. Chem. Int. Ed.*, **2002**, 41, 1017-1019.

48. K. P. Pulukkody, T. J. Norman, D. Parker, L. Royle, C. J. Broan, *J. Chem. Soc. Perkin Trans.*, **1993**, 605-620.

49. S. Aime, A. S. Batsanov, M. Botta, R. S. Dickins, S. Faulkner, C. E. Foster, A. Harrison, J. A. K. Howard, J. M. Moloney, T. J. Norman, D. Parker, L. Royle, J. A. G. Williams, J. *Chem. Soc., Dalton Trans.*, **1997**, 3623-3636.

50. L. Burai, R. Király, I. Lázár, E. Brücher, *Eur. J. Inorg. Chem.*, **2001**, 813-820.

51. S. Aime, A. S. Batsanov, M. Botta, R. S. Dickins, S. Faulkner, C. E. Foster, A. Harrison, J. A. K. Howard, J. M. Moloney, T. J. Norman, D. Parker, L. Royle, J. A. G. Williams, J. *Chem. Soc., Dalton Trans.*, **1997**, 3623-3636.

52. C.Bianchini, G. Giambastiani, F. Laschi, P. Mariani, A. Vacca, F. Vizza, P. Zanello, *Org. Biomol. Chem.*, **2003**, 1, 879-886.

53. J. Kotek, P. Lebdušková, P. Hermann, L. V. Elst, R. N. Muller, C. F. G. C. Geraldes, T. Maschmeyer, I. Lukes, J. A. Peters, *Chem. Eur. J.*, **2003**, 9, 5899-5915.

54. L. V. Elst, S. Laurent, H. M. Bintoma, R. N. Muller, *Mag. Res. Mat. Physics Biology Medicine*, **2001**, 12, 135-140.

55. E. Tóth, D. Pubanz, S. Vauthey, L. Helm, A. E. Merbach, *Chem. Eur. J.*, **1996**, 2, 1606-1615.

56. H. Kobayashi, S. Kawamoto, R. A. Star, T. A. Waldmann, M. W. Brechbiel, P. L. Choyke, *Bioconjugate Chem.*, **2003**, 14, 1044-1047.

57. L. Lattuada, G. Lux, *Tetrahedron Letters*, **2003**, 44, 3893-3895.

58. P. Lebduskova, J. Kotek, P. Hermann, L. V. Elst, R. N. Muller, I. Lukes, J. A. Peters, *Bioconjugate Chem.*, **2004**, 15, 881-889.

59. T. N. Parac-Vogt, K. Kimpe, K. Binnemans, *Journals of Alloys and Compounds*, **2004**, 374, 325-329.

60. N. Fatin-Rouge, E. Tóth, R. Meuli, J. G. Bünzli, *Journal of Alloys and Compounds*, **2004**, 298-302.

61. S. W. A. Bligh, A. H. M. S. Chowdhury, D. Kennedy, C. Luchinat, G. Parigi, *Magn. Res. Med.*, **1999**, 41, 767-773.

62. E. Tóth, F. Connac, L. Helm, K. Adzamli, A. E. Merbach, *JBIC*, **1998**, 3, 606-613.

63. F. A. Dunand, A. Borel, A. E. Merbach, *J. Am.Chem. Soc.*, **2002**, 124, 710-716.

64. S. Aime, M. Botta, M. Fasano, E. Terreno, *Acc. Chem. Res.*, **1999,** 32, 941-949.

65. U. Cosentino, D. Pitea, G. Moro, V. Barone, A. Villa, R. N. Muller, F. Botteman, *Theor. Chem. Acc.*, **2004,** 111, 204-209.

66. E. Tóth, S. Vauthey, D. Pubanz, A. E. Merbach, *Inorg. Chem.*, **1996,** 35, 3375-3379.

67. E. Tóth, O. M. Ni Dhubhghaill, G. Besson, L. Helm, A. E. Merbach, *Magn. Reson. Chem.*, **1999,** 37, 701-708.

68. K. Micskei, L. Helm, E. Brücher, A. E. Merbach, *Inorg. Chem.*, **1993,** 32, 3844-3850.

69. M. P. Lowe, *Aust. J. Chem.*, **2002,** 55, 551-556.

70. D. Parker, *Chem. Soc. Rev.*, **2004**, 33, 156-65.

71. S. Laurent, F. Botteman, L. V. Elst, R. N. Muller, *Magma,* **2004,** 16, 235-245.

72. R. Ruloff, E. Tóth, R. Scopelliti, R. Tripier, H. Handel, A. E. Merbach, *Chem. Commun.*, **2002,** 2630-2631.

73. S. Aime, M. Botta, J. I. Bruce, V. Mainero, D. Parker, E. Terreno, *Chem. Commun.*, **2001,** 115-116.

74. A. Barge, M. Botta, D. Parker, H. Puschmann, *Chem. Commun.*, **2003,** 1386-1387.

75. E. Tóth, F, Connac, L. Helm, K. Adzamli, A. E. Merbach, *J. Bio. Inorg. Chem.*, **1998,** 3, 606-613.

76. S. Zhang, K. Wu, A. D. Sherry, *Angew Chem. Int. Ed.*, **1999,** 38, 3192-3194.

77. M. Woods, G. E. Kiefer, S. Bott, A. Castillo-Muzquiz, C. Eshelbrenner, L. Michaudet, K. McMillan, S. D. K. Mudigunda, D. Ogrin, G. Tircsó, S. Zhang, P. Zhao, A. D. Sherry, *J. Am. Chem. Soc.*, **2004,** 126, 9248-9256.

78. M. P. Lowe, D. Parker, O Reany, S. Aime, M. Botta, G. Gastellano, E. Gianolio, R. Pagliarin, *J. Am. Chem. Soc.*, **2001,** 123, 7601-7609.

79. N. Raghunand, C. Howison, A.D. Sherry, S. Zhang, J. Gillies, *Mag. Res. Med.* **2003,** 49, 249-257.

80. S. Aime, E. Gianolio, E. Terreno, M. Botta, *Angew. Chem. Int. Ed.*, **2000,** 39, 747-750.

81. W. Li, S. E. Fraser, T. J. Meade, *J. Am. Chem. Soc.*, **1999,** 121, 1413-1414.

82. K. Hanaoka, K. Kikuchi, Y. Urano, T. Nagano, *J. Chem. Soc.*, **2001**, 2, 1840-1843.

83. T. J. McMurry, A. L. Nivorozhkin, A. F. Kolodziej, P. Caravan, M. T. Greenfield, R. B. Lauffer, *Angew. Chem. Ind. Ed.*, **2001,** 40, 2903-2906.

84. R. A. Moats, S. E. Fraser, T. J. Meade, *Angew Chem. Int. Ed. Engl.*, **1997,** 36, 726-728.

85. L. Pascolo, F. Cupelli, P. L. Anelli, V. Lorusso, M. Visigalli, F. Uggeri, C. Tiribelli, *Biochemical & Biophysical Res. Comm.*, **1999,** *257, 746-752.*

86. F. Uggeri, S. Aime, P. L. Anelli, M. Botta, M. Brocchetta, C. De Haën, G. Ermondi, M. Grandi, P. Paoli, *Inorg. Chem*, 34, **1995**, 633-642.

87. H. Schmitt-Willich, M. Brehm, C. L. J. Ewers, G. Michl, A. Müller-Fahrnow, O. Petrov, J. Platzek, B. Radüchel, D. Sülzle, *Inorg. Chem.*, **1999**, 3, 1134-1144.

88. M. A. Schiffler, *Biomaterials Seminar*, **2001**, 1, 1-7.

89. F. M. Cavagna, M. Daprà, P. M. Castelli, F. Maggioni, M. A. Kirchin, *Eur. Radiol*, **1997**, 7, (suppl. 5), S222-224.

90. T. Zhang, A. Matsumura, T. Yamamoto, F. Yoshida, T. Nose, N. Shimojo, *Am. J. Neuroradiol*, **2002**, 23, 15-18.

91. G. Bombieri, R. Artali, *J. Alloys and Compounds*, **2002**, 344, 9-16.

92. T. Peters, All about Albumin: biochemistry, genetics and medical applications, Academic Press, San Diego, 1996.

93. S. Curry, H. Mandelkow, P. Brick, N. Franks, *Nature Structural Biology*, **1998**, 5, 9, 827-835.

94. X. M. He, D. C. Carter, *Nature*, **1992**, 209-215.

95. S. Curry, P. Brick, N. P. Franks, *Biochimica et Biophysica Acta*, **1999**, 131-140.

96. I. Petitpas, A. A. Bhattacharya, S. Twine, M. East, S. Curry, *J. Biochem.*, **2001**, 276, 22804-22809.

97. S. Baroni, M. Mattu, A. Vannini, R. Cipollone, S. Aime, P. Ascenzi, M. Fasano, *Eur. J. Biochem*, **2001**, 265, 6214-6220.

98. A. Sułkowska, *J. Molecular Structure*, **2002**, 227-232.

99. M. Botta, S. Quici, G. Pozzi, G. Marzanni, R. Pagliarin, S. Barra, S. G. Crich, *Org. Biomol. Chem.*, **2004**, 2, 570-577.

100. S. Aime, M. Botto, M. Fasano, S. G. Crich, E. Terreno, *SBIC*, **1996**, 1, 312-319.

101. P. Caravan, N. J. Cloutier, M. T. Greenfield, S. A. McDermid, S. U. Dunham, J. W. M. Bulte, J. C. Amedio, Jr., R. J. Looby, R. M. Supkowski, W. D. Horrocks, T. J. McMurry, R. B. Lauffer, *J.* Am. *Chem. Soc.*, **2002**, 124, 3152-3162.

102. P. Caravan, C. Commuzzi, W. Crooks, T. J. McMurry, G. R. Choppin, S. R. Woulfe, *Inorg. Chem.*, **2001**, 40, 2170-2176.

103. K. Adzamli, D. A. Yablonskiy, M. R. Chicoine, E. K. Won, K. P. Galen, M. C. Zahner, T. A. Woolsey, J. J. H. Ackerman, *Mag. Reson. Med*, **2003**, 49, 586-590.

104. K. Adzamli, M. Spiller, S. Koenig, *Acad Radiol*, **2002**, 9 (suppl 1), S11-S16.

105. K. Adzamli, L. V. Elst, S.Laurent, R. N. Muller, *Mag. Res. Mat. Phy. Bio. Med.*, **2001**, 12, 92-95.

106. S. Aime, M. Chiaussa, G. Digilio, E. Gianolio, E. Terreno, *Bio. Inorg. Chem.*, **1999**, 4, 766-774.

107. P. Caravan, M. T. Greenfield, X. Li, A. D. Sherry, *Inorg. Chem.*, **2001,** 40, 6580-6587.

108. D. Parker, J.A.G. Williams, *Metal Ions in Biological Systems - The Lanthanides and their interrelations with Biosystems, Volume 40, Eds. A. Sigel, H. Sigel,* Marcel Dekker, New York. 2003.

109. D. Parker, J. A. G. Williams, *J. Chem. Soc. Dalton Trans,* **1996,** 3613-3628.

110. D. Parker, *Coord. Chem. Rev.*, **2000**, 205, 109-130.

111. A. Beeby, I. M. Clarkson, R. S. Dickins, S. Faulkner, D. Parker, L. Royle, A. S. de Sousa, J. A. G. Williams, M. Woods, *J. Chem. Soc, Perkin Trans. 2*, **1999**, 493-503.

112. M. P. Lowe, D. Parker, *Chem. Commun.* **2000,** 707-708.

113. W. D. Horrocks, Jr., D. R. Sudnick, *J. Am. Chem. Soc.*, **1979,** 101, 334-340.

114. M. V. Rekharsky, Y. Inove, *Chem. Rev*, **1998**, 1875-1917.

115. S. Aime, M. Botta, L. Frullano, S. G. Crich,G. B. Giovenzana, R. Pagliarin, G. Palmisano, M.Sisti, *Eur. J. Chem*, **1999**, 5, 4, 1253-1260.

116. A. A. Bogdanov Jr, K. Licha, Molecular Imaging: An Essential Tool in Preclinical Research, Diagnostic Imaging, and Therapy, Ernst Schering Reasearch Foundation, Springer, New York, 2005.

117. Y. Bretonniere, M. J. Cann, D. Parker, R. Slater, *Org. Biomol. Chem.*, **2004**, 2 (11), 1624-1632.

118. P. Atkinson, Y. Bretonniere, D. Parker, *Chem. Commun.*, **2004**, 4, 438-439.

119. F. Uggeri, S. Aime, P. L. Anelli, M. Botta, M. Brocchetta, C. De Haën, G. Ermondi, M. Grandi, P. Paoli, *Inorg. Chem*, 34, **1995**, 633-642.

120. T. I. Richardson, S. D. Rychnovsky, *J. Am. Chem. Soc*, **1997**, 119, 12360-12361.

121. U. Schmidt, C. Braun, H. Sutoris, *Synthesis*, **1996**, 223-229.

122. P. Y. Bruice, *Organic Chemistry*, 3rd Edition, Prentice Hall Inc., 2001, 786-787.

123. A. K.Bhattacharya, G. Thyagarajan, *Chem. Rev.*, **1981**, 81, 415-430.

124. J. March, Advanced Organic Chemistry - Reactions, Mechanisms and Structure, 3rd Edition, John Wiley and Sons, New York, 530-531.

125. W. Yang, C. M. Giandomenico, M. Sartori, D. A. Moore, *Tetrahedron Letters*, **2003**, 44, 2481-2483.

126. T.J. Norman, Ph. D Thesis, Radioimmunotherapy with Yttrium Macrocylces, University of Durham, September 1994.

127. D. Parker, R. S. Dickins, H. Puschmann, C. Crossland, J. A. K. Howard, *Chem. Rev.*, **2002**, 102, 1977-2010.

128. A. J. Stewart, C. A. Blindauer, S. Berezenko, D. Sleep, P. J. Sadler, *PNAS*, **2003**, 7, 1-, 3701-3706.

129. J. Masuoka, J. Hegenauer, B. R. Van Dyke, P. Saltman, *J. Biol. Chem.*, **1993**, 21533-21537.

130. A. Congreve, Responsive Lanthanide Complexes for Metal Ion Sensing, Ph. D. Thesis, University of Durham, 2004.

131. C. A. Hunter, D. H. Purvis, *Angew. Chem. Int. Ed.*, **1992**, 31, 6, 792-795.

132. A. Congreve, R. Kataky, M. Knell, D. Parker, H. Puschmann, K. Senanayake, L. Wylie, *New J. Chem.*, **2003**, 27, 98-106.

133. R. Lencioni, D. Cioni, L, Crocetti, C. D. Pina, C. Bartolozzi, *Journal of Hepatology.*, **2004**, 40, 162-171.

134. K. P. Pulukkody, T. Norman, D. Parker, L. Royle, *J. Chem. Soc. Perkin Trans*, **1993**, 605-612.

135. P. Reimer, E. J. Rummeny, H. E. Daldrup, T. Hesse, T. Balzer, B. Tombach, P. E. Peters, *Eur. Radiol.*, **1997**, 7, 275-280.

136. P. Reimer, E. J. Rummeny, K. Shamsi, T. Balzer, H. E. Daldrup, B. Tanbach, T. Hesse, T. Berns, P. E. Peters, *Radiology*, 1996, 199, 177-183.

137. N. C. Thompson, D. Parker, H. Schmitt-Willich, D. Sülzle, G. Muller, J. P. Riehl, *Dalton Trans.*, **2004**, 1892-1895.

138. E. N. Rizkalla, G. R. Choppin, *Inorg. Chem*, **1993**, 32, 582-586.

139. L. V. Elst, F.Chapelle, S. Laurent, R. N. Muller, *J. Biol. Inorg. Chem.*, **2001**, 6, 196-200.

140. H. Schmitt-Willich, M. Brehm, C. L. J. Ewers, G. Michl, A. Müller-Fahrnow, O. Petrov, J. Platzek, B. Radüchel, D. Sülzle, *Inorg. Chem.*, **1999**, 38, 1134-1144.

141. J. P. Riehl, F. S. Richardson, *Methods Enzymol.*, **1993**, 226, 539.

142. J. I. Bruce, D. Parker, S. Lopinski, R. D. Peacock, *Chirality.*, **2002**, 14, 562-567.

143. S. Aime, M. Botta, G. Ermondi, *Inorg. Chem.*, **1992**, 31, 4291-4299.

144. S. Hoeft, K. Roth, *Chem. Ber.*, **1993**, 126, 869-873.

145. S. Aime, A. Barge, J. I. Bruce, M. Botta, J. A. K. Howard, J. M. Moloney, D. Parker, A. S. de Sousa, M. Woods, *J. Am. Chem. Soc.*, **1999**, 121, 5762-5771.

146. *Circular Dichroism - Principles and Applications*, Eds. N. Berova, K. Nakanishi, R. W. Woody, Wiley-VCH, New York, **2000**.

147. G. Bobba, Interaction of Chiral Lanthanide Complexes with Nucleic Acids, Ph.D. Thesis, University of Durham, 2002.

148. S. D. Belair, C. L. Maupin, M. W. Logue, J. P. Riehl, *J. Luminescence.*, **2000**, 86, 61-66.

149. G. Bobba, R. S. Dickins, S. D. Kean, C. E. Mathieu, D. Parker, R. D. Peacock, G. Siligardi, M. J. Smith, J. A. G. Williams, C. F. G. C. Geraldes, *J. Chem Soc., Perkin Trans. 2.*, **2001**, 1729-1737.

150. L. Govenlock, J. A. K. Howard, J. M. Moloney, D. Parker, R. D. Peacock, G. Siligardi, *J. Chem. Soc, Perkin Trans. 2.*, **1999**, 2415-2418.

151. J. P. Riehl, F. S. Richardson, *Chem. Rev.*, **1986**, 86, 1-16.

152. H. G. Brittain, *Chirality.*, **1996**, 8, 357-363.

Appendix

Lecture Courses Attended 2001/2002

Fluorine Chemistry

Separation Methods

Supramolecular Chemistry

Practical Spectroscopy

Conferences Attended

RSC Dalton Division, Coordination Chemistry in Action, University of Edinburgh, 6th November 2002.

RSC UK Macrocycles and Supramolecular Chemistry Group Meeting, University of York, 18-19th December 2002.

RSC Perkin Group Meeting, University of York, 8th April 2002.

Biomolecular Probes Mini-Symposium, University of Durham, 16th January 2003.

Seminars Attended

2001

October 9 Dr Roy S Lehrle, Birmingham
Forensics, Fakes and Failures

October 30 Professor Steve Howdle, Nottingham University
A thousand and one uses for CO_2 - from coffee to concrete to bone

October 31 Dr Colin Raston, School of Chemistry, Uni. of Leeds
Towards benign supramolecular chemistry: synthesis - self organization

November 6 Dr Cliff Ludman, Durham University
Explosions - a demonstration lecture

November 14 Professor John Goodby, Department of Chemistry, University of Hull

Supermolecular liquid crystals - multipodes and dendrimers

November 21 Dr Roy Copely, GlaxoSmithKline
Crystallography in the Pharmaceutical Industry

December 5 Dr Mike Eaton, Celltech
Drugs of the Future

2002

January 22 Dr Ian Fallis, University of Cardiff
Size is Everything

January 29 Dr Paul Monks, University of Leicester
Ozone - the good, the bad and the ugly

January 30 Dr Peter Hore, PCL, University of Oxford
Chemistry in a spin: effects of magnetic fields on chemical reactions

February 13 Dr Helen Aspinall, Department of Chemistry, University of Liverpool
Defining effective chiral binding sites at lanthanides

February 26 Dr Mike Griffin, Forensic Science Service, Metropolitan Police
Smack, Crack, Speed and Weed: A forensic chemists tale

March 12 Professor David Williams, Cardiff
Beer and Health: 7000 years of history

May 8 Professor Paul Madden, PCL, University of Oxford
Covalent Effects in "Ionic" Systems

October 8 Dr Stella Peace, Unilever

The Chemistry Behind your Cuppa

October 15 Professor Mike Zaworotko from the University of South Florida
Suparamolecular Synthesis of Functional Molecules & Materials

November 12 Dr Dave Alker, Pfizer
The Discovery of a New Medicine

November 13 Professor Geoffrey Lawrance, Newcastle University, Australia
Designer Ligands: Macrocyclic and alicyclic moleculas for metal complexation and biocatalysis

December 3 Dr Ian Sage, Qinetiq
Tough Plastics for a tough world

2003

January 22 Dr David Procter, Department of Chemistry, University of Glasgow
New Strategies and Methods for Organic Synthesis

February 11 Dr John Emsley, University of Cambridge
False Alarms: Chemistry & the Media

February 19 Professor Tony Ryan, Department of Chemistry, University. of Sheffield
Introducing Soft Nanotechnology

March 4 Professor Richard Taylor, University of York
Adventures in Natural Product Synthesis"

October 15 Professor Huw Davies, Department of Chemistry, University of Buffalo
Applications of Catalytic Asymmetric C-H Activation to Synthesis

October 21	Dr Roger Newton, Maybridge plc The Pharmaceutical Industry - Does it have a Future?
October 28	Dr Dave Alker, Pfizer Careers in the Pharmaceutical Industry
December 2	Dr Bill MacDonald, DuPont 'Flexible Electronics - What's it all About?!
January 28	Dr Lesley Yellowlees, Department of Chemistry, Edinburgh University Electrochemical and spectroelectrochemical studies of transition metals
February 11	Professor D Parker FRS, Department of Chemistry, University of Durham Chiral Lanthanide Complexes: Structure, dynamics and function
February 17	Professor A P De Silva, Queens University of Belfast Designer Molecules for Photonic Signalling
March 16	Dr Chris Clarke, Unilever The Science Of Ice Cream
July 2	Professor Sir Harry Kroto, Nobel Laureate in Chemistry (1996) 2010: a NanoSpace Odyssey

Publications

NMR and chiroptical examination of the diastereoisomers of (S)-Eu-EOB-DTPA. N. C. Thompson, D. Parker, H. Schmitt-Willich, D. Sülzle, G. Muller, J. P. Riehl, *Dalton Trans.*, **2004**, 1892-1895.